

TECHNISCHE UNIVERSITÄT MÜNCHEN

Lehrstuhl für Ernährungsmedizin

Molecular and functional analysis of the cross-talk
between human preadipocytes, adipocytes and
endothelial cells *in vitro*

Isabelle Mack

Vollständiger Abdruck der von der Fakultät Wissenschaftszentrum Weihenstephan für Ernährung, Landnutzung und Umwelt der Technischen Universität München zur Erlangung des akademischen Grades eines

Doktors der Naturwissenschaften

genehmigten Dissertation.

Vorsitzender: Univ.-Prof. Dr. M. Klingenspor

Prüfer der Dissertation:

1. Univ.-Prof. Dr. J. J. Hauner
2. Univ.-Prof. Dr. H. Daniel

Die Dissertation wurde am 02.08.2010 bei der Technischen Universität München eingereicht und durch die Fakultät Wissenschaftszentrum Weihenstephan für Ernährung, Landnutzung und Umwelt am 03.01.2011 angenommen.

Table of contents

1	INTRODUCTION.....	1
1.1	Obesity	1
1.1.1	Prevalence of obesity.....	2
1.1.2	Obesity-associated diseases	2
1.1.3	Obesity as an inflammatory state	4
1.2	Adipose Tissue	5
1.2.1	Adipose tissue function	5
1.2.2	WAT secretory function	6
1.2.2.1	Leptin.....	7
1.2.2.2	Adiponectin.....	7
1.2.2.3	IL-6.....	8
1.2.2.4	Vascular endothelial growth factor (VEGF).....	8
1.2.2.5	Chemokines.....	9
1.2.3	WAT morphology	9
1.2.4	WAT growth and vasculature	10
1.2.4.1	Blood vessels, endothelial cells and endothelial dysfunction	10
1.2.4.2	WAT growth	11
1.2.4.3	Adipogenesis	11
1.2.4.4	WAT vasculature.....	12
1.2.5	WAT blood flow	13
1.2.6	WAT hypoxia.....	14
1.2.7	WAT immune cell infiltration.....	16
1.2.7.1	Mechanisms of leukocyte infiltration in tissues – Extravasation.....	19
1.2.8	Study of adipose tissue and adipocytes	22
1.2.9	Study of endothelial cells <i>in vitro</i>	24
1.2.10	Study of cross-talk between cell types	25
1.3	Aim of the study.....	27
2	MATERIALS AND METHODS.....	29
2.1	Cell Culture.....	29
2.1.1	Primary cell culture and size fractionation of human mature adipocytes	29
2.1.1.1	Reagents.....	29
2.1.1.2	Theoretical Background and Method	29
2.1.2	SGBS cell culture	30
2.1.2.1	Reagents.....	30
2.1.2.2	Theoretical Background and Method	31
2.1.3	HMEC-1 cell culture	32
2.1.3.1	Reagents.....	32
2.1.3.2	Theoretical Background and Method	33
2.1.4	U937 cell culture	33
2.1.4.1	Reagents.....	33
2.1.4.2	Theoretical Background and Method	33

2.1.5	Coculture between CM of SGBS cells and HMEC-1 cells	34
2.1.6	Coculture and monocyte-endothelial cell-cell adhesion assay	34
2.1.6.1	Theoretical Background.....	34
2.1.6.2	Reagents.....	35
2.1.6.3	Method.....	35
2.2	Cell surface expression analysis by cell-ELISA.....	36
2.2.1	Theoretical Background.....	36
2.2.2	Reagents.....	36
2.2.3	Method.....	37
2.3	Proliferation assay	38
2.3.1	Theoretical Background.....	38
2.3.2	Reagents.....	38
2.3.3	Method.....	38
2.4	RNA extraction, DNase I treatment and RNA integrity check.....	39
2.4.1	Reagents.....	39
2.4.2	Theoretical Background and Method	39
2.5	Reverse transcription (RT), polymerase chain reaction (PCR) and quantitative real-time PCR (qRT-PCR)	40
2.5.1	Theoretical background	40
2.5.1.1	SYBR® Green.....	41
2.5.1.2	TaqMan®	42
2.5.1.3	Primer design	42
2.5.2	RT.....	42
2.5.2.1	Reagents.....	42
2.5.2.2	Method.....	42
2.5.3	PCR.....	43
2.5.3.1	Reagents.....	43
2.5.3.2	Method.....	43
2.5.4	qRT-PCR	44
2.5.4.1	Reagents.....	44
2.5.4.2	Method.....	44
2.6	Measurement of adipokines in CM.....	45
2.6.1	Theoretical Background.....	45
2.6.1.1	ELISA	45
2.6.1.2	Multiplex bead-based Luminex® assays	46
2.6.2	Reagents.....	46
2.6.3	Method.....	46
2.7	Protein determination.....	47
2.7.1	Bicinchoninic acid (BCA) method	47
2.7.1.1	Reagents.....	47
2.7.1.2	Theoretical Background and Method	47
2.7.2	Modified Bradford method	47
2.7.2.1	Theoretical Background.....	47
2.7.2.2	Reagents.....	48

2.7.2.3	Method.....	48
2.7.3	Amido Black method.....	48
2.7.3.1	Reagents.....	48
2.7.3.2	Theoretical Background and Method.....	48
2.8	SDS-Polyacrylamide electrophoresis (SDS-PAGE) and Western blot analysis.....	49
2.8.1	Theoretical Background.....	49
2.8.2	Reagents.....	50
2.8.3	Method.....	51
2.9	Methods to monitor adipocyte differentiation.....	52
2.9.1	Glycerinphosphate dehydrogenase (GPDH) assay.....	52
2.9.1.1	Theoretical Background.....	52
2.9.1.2	Reagents.....	52
2.9.1.3	Method.....	53
2.9.2	Oil Red O/Haematoxylin staining.....	53
2.9.2.1	Theoretical Background.....	53
2.9.2.2	Reagents.....	53
2.9.2.3	Method.....	54
2.9.3	Nile Red.....	54
2.9.3.1	Theoretical Background.....	54
2.9.3.2	Reagents.....	54
2.9.3.3	Method.....	54
2.10	Peptidomics.....	55
2.10.1	Theoretical Background and Method.....	55
2.11	Statistical analysis.....	56
3	RESULTS.....	59
3.1	Culture conditions of SGBS cells and HMEC-1 cells.....	59
3.1.1	Introduction.....	59
3.1.2	HMEC-1 cell proliferation using different basal media.....	61
3.1.3	SGBS proliferation using different basal media.....	61
3.1.4	Differentiation capacity of SGBS cells using different basal media.....	61
3.1.5	Differentiation time course of SGBS cells.....	65
3.1.6	Coculture between SGBS and HMEC-1 cells.....	65
3.2	Gene expression and cytokine secretion of SGBS preadipocytes and adipocytes.....	69
3.2.1	Introduction.....	69
3.2.2	Cytokine expression and secretion of SGBS preadipocytes and adipocytes.....	69
3.2.3	Adipokine secretion of SGBS cells cultured in the presence and in the absence of hormones and antibiotics.....	70
3.2.4	Comparison of the morphology, GPDH activity and adipokine secretion in SGBS preadipocytes at confluence and after 16 days culture period.....	71

3.3	Impact of preadipocyte- and adipocyte-CM on HMEC-1 cell activation and signalling pathways	76
3.3.1	Introduction.....	76
3.3.2	Establishment of a monocyte-endothelial cell-cell adhesion assay and ICAM-1 and VCAM-1 cell surface ELISA	76
3.3.3	Impact of SGBS preadipocyte- and adipocyte-CM on endothelial ICAM-1 cell surface expression and monocyte-endothelial cell-cell adhesion	79
3.3.4	Impact of concentrated SGBS-CM on monocyte-endothelial cell-cell adhesion	81
3.3.5	Impact of TNF- α treated SGBS cells on monocyte endothelial cell-cell adhesion	83
3.3.6	Impact of hypoxia on adipokine gene expression and secretion of SGBS cells and analysis of their CM on endothelial cell activation	87
3.3.7	Impact of SGBS preadipocyte- and adipocyte-CM on endothelial cell signalling pathways	94
3.3.8	The role of endothelial signalling pathways on monocyte endothelial cell-cell adhesion and ICAM-1 protein expression	98
3.4	Functional analysis of factors in CM mediating endothelial cell activation.....	101
3.4.1	Introduction.....	101
3.4.2	Gene and protein expression of the obese receptor (Ob-R) b, VEGFR-2, gp130 and IL-6 receptor (IL-6R) α in HMEC-1 cells	101
3.4.2.1	Ob-Rb gene expression.....	101
3.4.2.2	VEGFR-2 gene expression	102
3.4.2.3	gp130 and IL-6 R α gene and protein expression	102
3.4.3	Functional analysis of factors in CM mediating endothelial ICAM-1 expression and monocyte endothelial cell-cell adhesion.....	105
3.4.4	Impact of IL-6 in SGBS-CM on phosphorylations of STAT1/3 in HMEC-1 cells	110
3.5	Impact of CM derived from different-sized human primary mature adipocytes on HMEC-1 cell activation.....	114
3.6	Peptidomics analysis of SGBS cell supernatants.....	116
3.6.1	Introduction.....	116
3.6.2	Analysis of markers for cell lyses in CM of preadipocytes and adipocytes...	116
3.6.3	Putative peptides with different expressions in SGBS preadipocytes and adipocytes	117
3.6.4	Validation of putative peptide candidates.....	121
3.6.4.1	Progranulin.....	121
3.6.4.2	Secretogranin II	121
3.6.4.3	Secretogranin V	122
4	DISCUSSION.....	125
4.1	Introduction	125
4.2	Coculture between SGBS cells and HMEC-1 cells.....	127

4.3	Adipokine expression of SGBS preadipocytes and adipocytes under normoxia and hypoxia	128
4.4	Endothelial cell activation by CM of normoxic, hypoxic and TNF- α treated SGBS cells and different-sized primary mature adipocytes	135
4.5	Molecular mechanisms of endothelial cells activated by CM of SGBS cells	140
4.6	Functional analysis of mediators in the CM of SGBS cells responsible for endothelial cell activation	142
4.7	Peptidomics analysis of SGBS cell supernatants	143
4.8	Concluding comments and perspectives	146
5	SUMMARY	148
6	REFERENCES	150
7	APPENDIX	I
7.1	List of abbreviations	I
7.2	List of figures	VI
7.3	List of tables	VII
7.4	Chemicals, consumables and equipment	VIII
7.4.1	Chemicals	VIII
7.4.2	Consumables	XIV
7.4.3	Equipment	XV
7.5	Monocyte-endothelial cell-cell adhesion assay	XVI
7.5.1	Quantitation of <i>Calcein green AM</i> labelled U937 cells	XVI
7.5.2	Example for the analysis of the monocytes-endothelial cell-cell adhesion assay data	XVII
7.6	Acknowledgements	XIX
7.7	Curriculum Vitae	XXI

1 Introduction

1.1 Obesity

Obesity is becoming a key and rapidly growing public health problem in adults and children (Hotamisligil, 2006). Its prevalence is increasing worldwide with epidemic levels having been reached in Western industrialized societies (Van Gaal *et al.*, 2006). Obesity is defined as an excess gain in white adipose tissue (WAT) which increases the risk of developing a number of medical problems, ranging from features of the metabolic syndrome to sleep apnoea, structural problems with joints and malignancies (Molavi *et al.*, 2006). Several methods are available for measuring the degree of obesity but the commonest and simplest way for classification is the worldwide accepted body mass index (BMI) which is defined as the weight in kilograms divided by the square of the height in metres (kg/m^2). According to the World Health Organisation (WHO), the normal weight range falls between a BMI of 18.5 and 24.9. An individual is regarded as being underweight if the BMI is $< 18.5 \text{ kg}/\text{m}^2$, overweight if the BMI is $\geq 25 \text{ kg}/\text{m}^2$, obese if it is $\geq 30 \text{ kg}/\text{m}^2$ and morbidly obese if the BMI is $\geq 40 \text{ kg}/\text{m}^2$ (<http://www.who.int/nut/#obs>). A BMI between 22.5 and $25 \text{ kg}/\text{m}^2$ is associated with the highest life expectancy in both sexes, while mortality of individuals with a BMI between 20 to $22.4 \text{ kg}/\text{m}^2$ is even higher than in individuals with a BMI between 25 and $27.4 \text{ kg}/\text{m}^2$, whereas a BMI $\geq 30 \text{ kg}/\text{m}^2$ not only increases the risk of several diseases dramatically, but also the risk of death (Whitlock *et al.*, 2009). Since the BMI alone is not a good indicator for the health risk assessment in overweight and obese individuals, the estimation of the adipose tissue distribution is extremely important (Eisele and Hauner, 2006; Hauner, 2009; Manolopoulos *et al.*, 2010). In practice, the waist circumference is measured because the abdominal type of obesity (“apple-shaped”) is especially linked to a high cardiovascular and metabolic risk. The risk is heightened for waistline circumferences over 92 cm for men and over 80 cm for women and significantly heightened for waistline circumferences over 102 cm for men and over 92 cm for women (Hauner, 2007). In contrast, a gluteofemoral body fat distribution (“pear-shaped”), may be associated with a protective lipid and glucose profile, as well as a decrease in cardiovascular and metabolic risk (Manolopoulos *et al.*, 2010). However, independent of the type of body fat the risk for concomitant diseases is increased when a BMI of $30 \text{ kg}/\text{m}^2$ or more is reached (Skurk and Hauner, 2002). The rise in obesity can be explained by the growing trend of physical inactivity, coupled with a high calorie intake of easily available and highly palatable energy-rich foods. Susceptibility to obesity is thought to be genetically

dependent throughout the population by a factor differing between 30 % and 70 % in individuals (Berthoud, 2002; Lyon and Hirschhorn, 2005). Such a wide range makes it difficult to generalise susceptibility due to factors such as diet and lifestyle unless the genetic susceptibility can be more accurately determined for an individual or group (Baskin *et al.*, 2005; Weyer *et al.*, 1999). Nevertheless, only a few obesity cases are attributed to a rare single genetic cause (Berthoud, 2002; O'Rahilly, 2009). Therefore, the development of obesity involves the interplay of a large number of susceptible genes with obesigenic environmental factors.

1.1.1 Prevalence of obesity

The most recent figures available for Germany indicate that 66 % of men and 51 % of women are either overweight or obese. One individual in five has a BMI equal or above 30 kg/m² (Nationale Verzehrsstudie II, 2008; <http://www.was-esse-ich.de/>). According to the National Health and Nutrition Examination Survey 33 % of the adult Americans are overweight, 34 % are obese and almost 6 % are morbidly obese (<http://www.cdc.gov/obesity/data/index.html>). Additionally, the prevalence of childhood obesity is increasing at alarming rates. Referring to the International Obesity TaskForce report around 15 % of the children aged 5-17 years in Europe are overweight and 5 % are obese. For America the figures are worse, with about 25 % of the children being overweight and about 8 % being obese (<http://www.who.int/childhoodobesity>). Bearing in mind, that weight, BMI and waist circumference which are used to define obesity continually rise with increasing age in both sexes (Nationale Verzehrsstudie II, 2008; <http://www.was-esse-ich.de/>), health care costs for obesity associated diseases will foreseeable increase further. As yet, the annual expenditure of the German health care system for the treatment of obesity's comorbidities, primarily type 2 diabetes, is estimated to be about 13 billion euros (Hauner, 2006) clearly a serious economic strain.

1.1.2 Obesity-associated diseases

The metabolic syndrome is a cluster of medical disorders which increase the risk of developing cardiovascular disease (CVD). Depending on the definition, obesity or central obesity may be one component out of three of the following criteria: glucose intolerance (impaired glucose tolerance, impaired fasting glycaemia or diabetes), dyslipidaemia

(depressed high-density lipoprotein [HDL] cholesterol and/or elevated blood triacylglycerols [TAG]), hypertension, insulin resistance and microalbuminuria (Alberti *et al.*, 2006; Zimmet *et al.*, 2005). According to the US National Health Statistic Report, the prevalence of the metabolic syndrome among adults 20 years of age and above is 34 % on average when the National Cholesterol Education Program/Adult Treatment Panel III (NCEP/ATP III) criteria are applied and increases with the age but even more strikingly with rising BMI (Ervin, 2009). For Germany no appropriate studies are available but the prevalence is assumed to be around 25 % or 18 % when estimated by the WHO or NCEP/ATP III criteria, respectively (Wirth, 2007).

Type 2 Diabetes is generally a combined disturbance of insulin secretion by the pancreas and the inability of the tissues in the body, mainly muscle, adipose tissue and liver, to respond appropriately to insulin, the latter being the prominent feature if the individual is obese (Hauner, 2007). Obesity and increased abdominal fat distribution are the greatest risk factors for developing type 2 diabetes, other factors include genetic predisposition, age, hypertension, dyslipidaemia, glucose intolerance during pregnancy and physical inactivity. The main complications of type 2 diabetes are micro- and macroangiopathies and neuropathies. It is estimated that around 5 million individuals in Germany, equivalent to 5-6 % of the population, have a diagnosed type 2 diabetes (Hauner, 2007) causing the health care system enormous costs as addressed in chapter 1.1.1

Endothelial dysfunction of the micro- and macrovasculature (see chapter 1.2.4.1) is central to the development of CVD (Krentz *et al.*, 2009; Singhal, 2005) which is strongly associated with obesity (Whitlock *et al.*, 2009). According to a recently published meta-analysis which included 57 prospective studies, ischemic heart diseases, stroke and other vascular diseases are the most common cause of premature death in obese people (Whitlock *et al.*, 2009).

Obesity also appears to be associated with an increased mortality from cancer, with a higher incidence of certain cancers, including the colorectum, (post menopausal) breast, endometrium, kidney, pancreas and oesophagus (Anderson and Caswell, 2009). Obesity is also linked to orthopaedic problems, respiratory diseases (Molavi *et al.*, 2006) and renal disorders (Nguyen and Hsu, 2007; Wahba and Mak, 2007).

1.1.3 Obesity as an inflammatory state

Obesity is associated with a state of chronic low-grade inflammation which possibly provides a connection between obesity, insulin resistance and the other aspects of the metabolic syndrome (Trayhurn and Wood, 2004). More precisely, this state of low-grade inflammation also contributes to the micro- and macrovascular endothelial dysfunction and vascular remodelling (Hotamisligil, 2006; Singer and Granger, 2007; Van Gaal *et al.*, 2006); leading to hypertension, atherosclerosis and microvascular complications (Nguyen and Hsu, 2007; Van Gaal *et al.*, 2006). Changes in the microcirculation might even be a cause of the development of insulin resistance and the metabolic syndrome (Wiernsperger *et al.*, 2007). The systemic inflammation, involves the elevated circulation of inflammatory cytokines and acute phase proteins such as C-reactive protein (CRP), interleukin (IL) 6, plasminogen activator inhibitor-1 (PAI-1), P-selectin, vascular cell adhesion molecule-1 (VCAM-1) and fibrinogen (Van Gaal *et al.*, 2006). Their source has been suggested to be the liver and also WAT (Van Gaal *et al.*, 2006), since WAT expansion is linked to increased levels of several adipokines e.g. IL-6 and PAI-1 within the tissue (Wellen and Hotamisligil, 2005). Many adipokines may act locally in WAT, but others, typically leptin and adiponectin also reach the circulation and thus, it is suggested that some adipokines contribute to the state of the systemic chronic low-grade inflammation (Molavi *et al.*, 2006; Trayhurn, 2005).

The question of the origin of inflammation in obesity is not clear but four main mechanisms are discussed which are likely to increase the production of proinflammatory molecules in WAT; hypoxia, endoplasmatic reticulum (ER) stress, oxidative stress and immune cell accumulation (Bourlier and Bouloumie, 2009; Hotamisligil, 2006; Trayhurn and Wood, 2004; Wellen and Hotamisligil, 2005).

Hypoxia is likely to occur in expanding WAT, which appears to lead to an inflammatory response in adipocytes to increase blood flow and stimulate angiogenesis (Trayhurn and Wood, 2004; Ye, 2009) as addressed in chapter 1.2.6. Obesity also generates conditions that increase the demand on the ER, especially in WAT due to tissue remodelling and metabolic turnover. As result ER stress may occur leading to the activation of inflammatory pathways including the stress-activated phospho-kinases/c-Jun N-terminale Kinase (SAPK/JNK) and Nuclear factor kappa B (NfKB) pathways (Wellen and Hotamisligil, 2005). Relevant for the initiation of inflammation in obesity may be also oxidative stress. ROS (radical oxygen species) produced by adipose tissue endothelial cell mitochondria due to hyperglycaemic

conditions could result in oxidative damage and the activation of inflammatory signalling pathways. Activated and/or damaged endothelial cells then may enforce immune cell attraction in WAT. Additionally, hyperglycaemia may also increase ROS production in adipocytes leading to a further enhanced production of proinflammatory adipokines (Wellen and Hotamisligil, 2005). Finally, once immune cell accumulation has occurred in WAT this further may amplify cytokine production, secreted by immune cells and other cells present in WAT (Bourlier and Bouloumie, 2009; Wellen and Hotamisligil, 2005).

1.2 Adipose Tissue

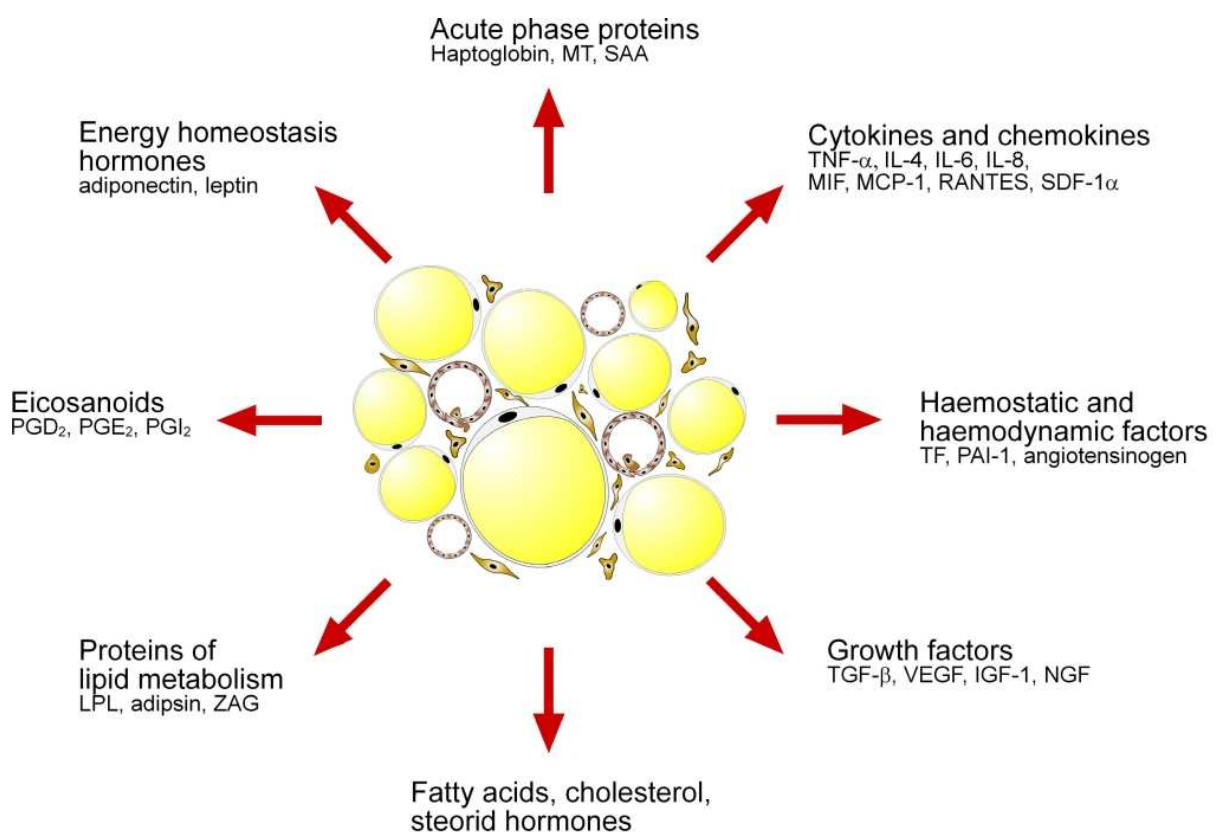
1.2.1 Adipose tissue function

Adipose tissue in the bodies of women and men of normal weight generally consists of 20 to 30 % and 12 to 20 % respectively, of their total body weight (Klaus, 2001). Whole adipose is categorized in three different types according to their location and function: 1) WAT, 2) brown adipose tissue (BAT) which plays an essential role in thermogenesis, especially in rodents, and 3) bone marrow fat which serves among other things as energy reservoir (Klaus, 2001). In the following the focus lies on WAT, since in humans, it quantitatively plays the most important role (Tanzi and Fare, 2009). WAT is in the first place an energy reservoir and essential for energy homeostasis. During periods of fuel surplus, glucose and fatty acids (FA) are taken up by adipocytes and converted into triglycerides for storage. *De novo* FA synthesis appears to play only a minor role in humans due to their habitual high fat intake (Löffler, 1998). The term lipogenesis encompasses the processes of fatty acid synthesis and triglyceride synthesis. During periods of fuel deprivation, the TAG are broken down by the adipocytes into FA and glycerol and released into the circulation; this process is termed lipolysis (Boschmann, 2001). WAT is also an important endocrine and secretory organ as discussed in chapter 1.2.2 and necessary for mechanical and thermal insulation (Klaus, 2001). For desert and marine mammals WAT may be, in addition to its property as energy reservoir important as source of metabolic water (Klaus, 2001).

1.2.2 WAT secretory function

WAT has been recognized as a critical secretory organ, releasing a wide range of molecules. The main groups of these molecules with examples are presented in figure 1, some of them will be addressed in detail in the following. Notably, FA are quantitatively the primary released substance from WAT, which are produced during the lipolysis of TAG.

Figure 1 Secretory products of white adipose tissue



White adipose tissue secretes a wide range of factors with the majority being synthesized *de novo* and only some molecules being converted from precursor molecules. This figure represents a number of selected molecules secreted by WAT. MT, metallothionein; SAA, serum amyloid A; TNF- α , tumour necrosis factor- α ; IL, interleukin; MIF, macrophage migratory inhibitory factor; MCP-1, monocyte chemoattractant protein-1; RANTES, regulated upon activation, normally T-expressed, and presumably secreted; SDF-1 α , stromal cell-derived factor 1 alpha; TF, tissue factor; PAI-1, plasminogen activator inhibitor-1; TGF- β , transforming growth factor β ; VEGF, vascular endothelial growth factor; IGF-1, insulin-like growth factor-1; NGF, nerve growth factor; LPL, lipoprotein lipase; ZAG, zinc- α 2-glycoprotein; PG, prostaglandin (Bing and Trayhurn, 2009; Fischer-Posovszky *et al.*, 2007; Kintscher *et al.*, 2008; Peeraully *et al.*, 2004; Skurk *et al.*, 2009; Trayhurn, 2005).

1.2.2.1 Leptin

The gene of leptin was discovered by positional cloning in mice (Zhang *et al.*, 1994). Leptin is a 16 kDa, cytokine-like hormone and is primarily secreted by WAT but its expression is also found in other organs (Trayhurn and Beattie, 2001). In obesity leptin expression is elevated and strongly correlates with body fat mass (Trayhurn *et al.*, 2001). Leptin is a key regulatory protein in energy balance, being also involved in haematopoiesis, reproduction, the immune system and angiogenesis (Beltowski, 2006; Trayhurn and Beattie, 2001). In obesity, when circulating leptin levels are high, it may also contribute to endothelial dysfunction and atherosclerosis (Beltowski, 2006). Leptin promotes endothelial cell proliferation, migration and the formation of fenestrated capillaries and upregulates vascular endothelial growth factor (VEGF) expression (Beltowski, 2006; Christiaens and Lijnen, 2009). Its role in endothelial cell activation in the context of leukocyte infiltration is discussed controversially in the literature (Curat *et al.*, 2004; Skilton *et al.*, 2005). Leptin has several receptors belonging to the obese receptor (Ob-R) family. In endothelial cells leptin signals via the Ob-Rb receptor leading in the activation of the janus kinase signal transducer and activator of transcription (JAK/STAT) pathway (Sierra-Honigmann *et al.*, 1998; Suganami *et al.*, 2004). Leptin expression is upregulated by insulin, glucocorticoids, tumor necrosis factor alpha (TNF- α) and oestrogens and is suppressed by noradrenaline and adrenaline. The sympathetic nervous system which innervates WAT plays an important role in leptin regulation (Bartness and Bamshad, 1998; Trayhurn *et al.*, 2001; Wabitsch *et al.*, 1996).

1.2.2.2 Adiponectin

Adiponectin is an abundant circulating protein, is mainly secreted by mature adipocytes and exists in several distinct forms (Whitehead *et al.*, 2006). Its expression is decreased in obesity and even further reduced in insulin resistance and type 2 diabetes (Christiaens and Lijnen, 2009). There also exists a sexual dimorphism in humans, with women having higher adiponectin plasma levels than men (Nishizawa *et al.*, 2002). Besides its important role in metabolism (Yamauchi *et al.*, 2002) it has anti-inflammatory properties and mediates beneficial effects in the vasculature *in vivo* and *in vitro* (Goldstein and Scalia, 2004). Adiponectin may function pro- and anti-angiogenic (Christiaens and Lijnen, 2009). It is downregulated by glucocorticoids, TNF- α , IL-6 and β -adrenoceptor agonists and upregulated by peroxisome proliferators-activated receptor gamma (PPAR γ) agonists, e.g.

thiazolidindiones (Fasshauer and Paschke, 2003). Adiponectin signals via the adiponectin receptors 1 and 2 (AdipoR1 and AdipoR2) (Whitehead *et al.*, 2006).

1.2.2.3 IL-6

IL-6 is a cytokine which is produced by many cell types and also by those of WAT. It is important in the regulation of inflammatory processes (Jones, 2005) but it also plays a role in carbohydrate and lipid metabolism (Glund and Krook, 2008). In obesity and insulin resistance, IL-6 plasma levels and WAT IL-6 expression are increased (Kim *et al.*, 2009) and thus, it can contribute to the state of chronic low-grade inflammation. IL-6 is downregulated by glucocorticoids and upregulated by insulin, TNF- α and β -adrenoreceptor agonists (Fasshauer and Paschke, 2003). Its signalling is mediated via a tyrosine kinase associated receptor involving the JAK/STAT pathway (Kim *et al.*, 2009).

1.2.2.4 Vascular endothelial growth factor (VEGF)

VEGF is necessary for vasculogenesis and angiogenesis during development and postnatal e.g. during pregnancy, wound healing and pathophysiologic conditions, including cancer, rheumatoid arthritis and cardiovascular disease. The complexity of the VEGF family and its receptors allows a broad range of biological actions not only in endothelial cells but also many other cell types (Ferrara and Davis-Smyth, 1997). The VEGF family consists of VEGF-A, VEGF-B, VEGF-C, VEGF-D and VEGF-F and placenta growth factor (PlGF) and its receptors VEGFR-1 (Flt-1), VEGFR-2 (KDR/Flk-1) and VEGFR-3 (Flt-4) and belong to the family of receptor tyrosine kinases (Ferrara *et al.*, 2003; Zachary and Glick, 2001). VEGF-A is the most abundant form and VEGFR-2 appears to play a major role in endothelial VEGF signalling. VEGF is produced by many cell types, including endothelial cells, vascular smooth muscle cells, epithelial cells, preadipocytes and adipocytes (Fain *et al.*, 2004; Ferrara and Davis-Smyth, 1997; Ferrara *et al.*, 2003). VEGF is extremely important for endothelial cell survival or anti-apoptotic signalling, proliferation, migration, nitric oxide (NO) and prostacyclin (PGI₂) induction and vascular permeability (Zachary and Glick, 2001). VEGF expression is regulated by hypoxia, several cytokines, including IL-1 and IL-6 and cell differentiation and transformation (Ferrara and Davis-Smyth, 1997).

1.2.2.5 Chemokines

Obesity is connected with an increased level of infiltrating immune cells in WAT (Kintscher *et al.*, 2008; Weisberg *et al.*, 2003), the latter being also source of a range of chemokines such as monocyte chemoattractant protein-1 (MCP-1) (Fain and Madan, 2005), CCL5, also called RANTES (regulated upon activation, normally T-expressed and presumably secreted; Skurk *et al.*, 2009), Il-8 (Fain and Madan, 2005) and stromal cell-derived factor 1 alpha (SDF-1 α) (Kintscher *et al.*, 2008). The production of inflammatory chemokines occurs in response to inflammatory cytokines, including Il-1, TNF and interferons and bacterial toxins in most tissues and immigrating leukocytes with the aim to recruit leukocytes to inflamed and infected tissues (Baggiolini, 2001).

1.2.3 WAT morphology

WAT depots are distributed throughout the body and can be roughly categorized as visceral and subcutaneous. Small quantities can also be found within and around organs and blood vessels (Cinti, 2005). WAT is not homogeneous, rather it displays depot and sex-specific metabolic properties and is subject to differential neural and endocrine regulation. Body fat distribution generally differs between men and women even at comparable body fat content. Women tend to depot subcutaneous adipose tissue in the gluteo-femoral area whereas men in the abdominal region and normally also have larger amounts of visceral fat mass than women (Boschmann, 2001).

Mature adipocytes represent about 50% of the total cell content of WAT (Hausman, 1985) and store the TAG which in turn constitute up to 85 % of tissue weight (Trayhurn *et al.*, 2006). The remaining stromal vascular fraction consists of many cell types, including preadipocytes, fibroblasts, endothelial cells, pericytes, blood and endothelial cells, diverse precursor cells and immune cells, such as macrophages and T-lymphocytes. Increased immune cell infiltration occurs in obesity (Cinti, 2001; Rausch *et al.*, 2007; Weisberg *et al.*, 2003) as discussed in chapter 1.2.7. All cells of WAT are involved in autocrine, paracrine and endocrine processes and cross-talks (Hauner, 2005) but their differential contribution to the total pool of adipokines is not clear (Antuna-Puente *et al.*, 2008; Fain *et al.*, 2008; Fain *et al.*, 2004; Weisberg *et al.*, 2003). Adipose tissue is highly vascularized (see chapter 1.2.5) and innervated by the sympathetic (Cinti, 2001) and the parasympathetic (Kreier and Buijs, 2007) nervous system.

White adipocytes have a diameter ranging from 10 to 150 μm which is due to the ability of the cells to accumulate different amounts of TAG in a single vacuole. The nucleus is located peripherally in white adipocytes which also have less well-developed mitochondria compared with brown adipocytes (Cinti, 2001; Cinti, 2009).

1.2.4 WAT growth and vasculature

1.2.4.1 Blood vessels, endothelial cells and endothelial dysfunction

Blood vessels are very heterogeneous in architecture and function but can be roughly categorized as macrovascular and microvascular (Aird, 2003; Aird, 2007; Aird, 2007; Steinbeck, 2002). The inner lining of the circulatory system consists of a single layer of endothelial cells adhering to the basal lamina which are the gatekeeper between the blood and tissues. In the large blood vessels of the macrovasculature, the endothelial cells are surrounded by vascular smooth muscle cells followed by a third layer, the adventitia which consists of connective tissue and elastic elements. In contrast, microvascular endothelial cells, the cells of the capillaries, in general reside on a basal lamina and are only supported by sparsely distributed pericytes. Microvascular endothelial cells are either of the continuous, the fenestrated or sinusoidal type, exert organ-specific activities and are necessary for gas and nutrient exchange (Randall *et al.*, 1997). Overall, resting endothelial cells have four main functions: they maintain blood fluidity, regulate blood flow, control vessel wall permeability and quiesce circulating leukocytes. Endothelial dysfunction describes the situation when endothelial cells fail to appropriately perform any of these basal functions, although this term is often used to describe only the failure of arterial endothelial cells to produce sufficient of the vasorelaxant NO (Pober and Sessa, 2007). Importantly, endothelial cells can be activated by stimuli from the environment such as inflammatory mediators leading to a series of changes in the cells which enables them to offer a new repertoire of activities and receptors which are further adapted during transition from acute to chronic inflammation. Upon activation, the blood flow and the vascular leakage of plasma proteins may be elevated and the endothelial cells control the recruitment of leukocytes into the underlying tissue (see chapter 1.2.7.1). This process generally occurs in the microvascular beds in tissues, an exception is found in atherosclerosis where monocytes transmigrate over the macrovascular aortic wall following initial lipoprotein entrapment in the subendothelial matrix. Additionally,

upon activation, the microvascular endothelial cells are subject to angiogenesis in wounding or inflammatory processes (Kuldo *et al.*, 2005; Pober and Sessa, 2007; van Hinsbergh, 2001; Zimmerman *et al.*, 1999).

1.2.4.2 WAT growth

WAT growth requires continuous remodelling of the vascular network, mainly the microvasculature, which is then subject to neovascularization and/or remodelling of existing capillaries (Christiaens and Lijnen, 2009). WAT can increase either due to hypertrophy of existing adipocytes or hyperplasia where the number of adipocytes is increased (Schling and Loffler, 2002). The determining factors of fat mass in adults are not completely understood but increased lipid storage due to hypertrophy appears to be most important (Bjorntorp, 1974; Hirsch and Batchelor, 1976). In contrast, hyperplasia and the determination of adipocyte number appear to occur during childhood (Knittle *et al.*, 1979; Spalding *et al.*, 2008), since in adults the adipocyte number remains unchanged in lean and obese individuals even after marked weight loss which had been stable for two years at the time of the measurements (Spalding *et al.*, 2008). Nevertheless, if it comes to massive increases in body weight and adipocytes have reached a critical size, hyperplasia also appears to occur (Hirsch and Batchelor, 1976) which is achieved by inducing adipogenesis. In this process undifferentiated fibroblast-like preadipocytes which are found in adipose tissue along with pluripotent precursor cells that can be induced to follow the path of adipose cell lineage, differentiate to mature adipocytes (Gregoire, 2001). Adipogenesis also takes place in normal weight individuals since adipose tissue is a plastic organ with an annual turnover of adipocytes of approximately 10 % (Spalding *et al.*, 2008).

1.2.4.3 Adipogenesis

Some of the key features of adipogenic differentiation can be summarized as follows. Adipogenesis is a complex and tightly controlled process which is accompanied by dramatic changes in the extracellular matrix (ECM). For conversion of preadipocytes into adipocytes clonal expansion is necessary which is the re-entry of growth-arrested preadipocytes into the cell cycle and the progression through at least two cell-cycle divisions. At early differentiation CCAAT-enhancer binding proteins (C/EBP) β and δ are expressed and important to stop clonal expansion and increase the expression of PPAR γ 2. PPAR γ 2 heterodimerizes with

retinoic X receptors (RXR) and activates C/EBP α which exerts positive feedback on PPAR γ 2 until both transcription factors reach maximum levels as differentiation proceeds. This is paralleled by declining levels of C/EBP β and δ . PPAR γ 2 and C/EBP α coordinate the activation of many late and terminally expressed genes in the adipocyte differentiation process e.g. aP2, GLUT-4 and phosphoenolpyruvate carboxykinase (PEPCK). Additionally, the insulin receptor number and sensitivity increases and adipokines such as adiponectin are expressed. Sterol responsive element binding protein 1c, also called adipocyte determination and differentiation factor 1 (ADD1/SREBP1) can increase the transcriptional activity of PPAR γ while Forkhead box C2 (FOXC2) can enhance the activity of C/EBP α , PPAR γ , and ADD1/SREBP1 (Farmer, 2006; Gregoire, 2001; Gregoire *et al.*, 1998; Reed *et al.*, 1977; Reed *et al.*, 1981; Rosen and Spiegelman, 2000; Valet *et al.*, 2002).

1.2.4.4 WAT vasculature

Organ function is critically dependent on tissue perfusion. In organ growth this is generally associated with a compensatory increase in vascular supply (angiogenesis), otherwise this may lead to organ dysfunction as e.g. in cardiac hypertrophy with arterial hypertension (Tomanek *et al.*, 1986). Angiogenesis is tightly regulated reducing the likelihood of different pathologies including rheumatoid arthritis and diabetic retinopathy (Koch, 2003).

WAT is generally well vascularized but depot differences (Bjorntorp, 1996; Crandall *et al.*, 1997) and differences within the tissue have been observed (Gersh and Still, 1945; Rutkowski *et al.*, 2009). This may be due to specific depot-dependent cell replication rate as shown for rat endothelial cells (Hausman and Richardson, 2004). Overall, subcutaneous WAT is less vascularized than visceral WAT (Bjorntorp, 1996). Additionally, variation from individual to individual and age dependency in angiogenic potential is likely, e.g. aging and diabetes in obese mice impaired the neovascular potential of adipose-derived stromal cells (El-Ftesi *et al.*, 2009).

1.2.5 WAT blood flow

Adipose tissue blood flow varies between species, depots and during different metabolic conditions and is regulated via the nervous system, hormones, exercise and diet (Crandall *et al.*, 1997). For example, subcutaneous WAT resting blood flow expressed as ml per 100 g tissue per minute varies extremely in dogs (3 to 19 ml), rats (5 to 40 ml), rabbits (1.37 to 22 ml) and humans (0.5 to 8.63 ml) (Di Girolamo *et al.*, 1971; Larsen *et al.*, 1966). Additionally, in humans total adipose tissue blood flow is elevated in the obese, reflecting the increased total adipose mass (Lesser and Deutsch, 1967). On the other hand, the blood flow per unit weight of adipose tissue in humans (Adams *et al.*, 2005; Lesser and Deutsch, 1967) and in dogs (Di Girolamo *et al.*, 1971) is reduced with increasing fat mass. An explanation for these observations is given in the following. In humans, moderate gain weight is mainly achieved by hypertrophy of adipocytes (Bjorntorp, 1974; Hirsch and Batchelor, 1976)(see chapter 1.2.4.2) and thus, it appears as if depots containing larger fat cells contain fewer fat cells per unit of wet weight. *In vivo* experiments in dogs (Di Girolamo *et al.*, 1971), humans (Jansson *et al.*, 1992) and other species (Crandall *et al.*, 1997) show that when the blood flow is related to the number of adipocytes, the blood flow per cell is relatively constant, irrespectively of fat cell size. In humans the blood flow is 20-30 pl/cell/min (Blaak *et al.*, 1995). These results are supported by the observation that each adipocyte appears to be in contact with at least one capillary in rats (Gersh and Still, 1945). Altogether, this explains the great variety of WAT resting blood flow between species and why, in obese individuals, the blood flow per unit weight of adipose tissue is decreased.

1.2.6 WAT hypoxia

A lack of oxygen availability, a state which is called hypoxia, leads to several adaptation processes in an organism. At cellular level, the affected cells counteract with adapting their energy metabolism by switching to anaerobic glycolysis and induce mechanisms in order to prevent cell death and to induce vascular supply (e.g. angiogenesis) (Brahimi-Horn *et al.*, 2007; Semenza, 2002). The key transcription factor involved in the transmission of the hypoxic response is the hypoxia-inducible transcription factor 1 (HIF-1) (Brahimi-Horn and Pouyssegur, 2009) which is composed of one of the HIF- α -subunits (HIF-1 α , HIF-2 α and HIF-3 α) and HIF-1 β . HIF-1 β is constitutively expressed but not regulated by oxygen. In contrast, HIF-1 α , being the most prominent member of the α -subunits is constitutively expressed and degraded at the same time. Upon hypoxia the protein is stabilized and the gene expression is increased. HIF-1 α has an oxygen-dependent degradation domain which contains two regulatory proline residues which are under normoxia hydroxylated by prolyl hydroxylase domain-containing enzymes (PHD) 1 to 4. This allows binding of von Hippel-Lindau tumor suppressor protein (pVHL) which forms an E3-ubiquitin ligase complex with co-factors which allows for subsequent poly-ubiquitination and degradation of HIF-1 α in the proteasome. When oxygen and/or Fe²⁺ are missing, the PHDs become inactive and HIF-1 α protein accumulates (Brahimi-Horn *et al.*, 2007; Brahimi-Horn and Pouyssegur, 2009). HIF-1 activates a series of genes, ranging from molecules being involved in cell proliferation, cell survival, angiogenesis, vascular tone, cell adhesion, cytoskeletal structure and extracellular matrix metabolism to energy metabolism (Semenza, 2003). Notably, HIF-1 is also alternatively regulated by heat shock proteins, cytokines, growth factors and oncogenes. For example, TNF- α has been found to accumulate and activate HIF-1 (Brahimi-Horn and Pouyssegur, 2009; Hellwig-Burgel *et al.*, 2005). Therefore, HIF-1 may be upregulated in many biological situations in tissues but not due to hypoxia and so conclusions should be drawn carefully.

Hypoxia occurs in normal physiology (e.g. development of tissues and exercise) but also in pathophysiology (e.g. tumours and wound healing). It also occurs in the interstitial stromal areas of WAT, especially in obese mice as measured with *in vivo* oxygen sensor techniques and pimonidazole stainings (Rausch *et al.*, 2007; Ye *et al.*, 2007; Yin *et al.*, 2009). An explanation may be that the increasing diameter of fat cells during adipose tissue growth, despite constant vascularization per adipocyte (Crandall *et al.*, 1997), may exceed the oxygen

diffusion limit of 100 μm (Carmeliet and Jain, 2000; Rausch *et al.*, 2007). Additionally, it is conceivable that the decreased WAT vascularization per weight may especially decrease the oxygen availability of the other homing cells in WAT located more than 100 μm away from the next capillary, since their vascular supply appears not to be cell number dependent. It is not known whether the observed hypoxia is intermittent or chronic. Supporting evidence for hypoxia in human WAT is an increased HIF-1 α expression in adipose tissue of obese individuals which decreases after surgery-induced weight loss (Cancello *et al.*, 2005) bearing in mind that this could be also due to other mechanisms than hypoxia. HIF-1 α protein expression was also found to be enhanced in hypoxic human adipocytes (Wang *et al.*, 2007) and the specific role of hypoxia in the induction of HIF-1 α in adipose tissue was shown in mice (Ye *et al.*, 2007). The glucose uptake is increased in hypoxic human adipocytes *in vitro* by increased GLUT-1 expression. This is due to increased demand of glucose because the occurring glycolysis during hypoxia produces less adenosine triphosphate (ATP) per glucose molecule (Wood *et al.*, 2007). Adipogenesis appears to be regulated by oxygen sensitive mechanisms and preadipocyte differentiation is inhibited under hypoxia (Carriere *et al.*, 2004; Lin *et al.*, 2006; Macfarlane, 1997; Swiersz *et al.*, 2004; Yun *et al.*, 2002). Additionally, children possessing cyanotic heart disease had correlated less body fat (Baum and Stern, 1977). Rats exposed to hypoxia significantly lost weight (Tanaka *et al.*, 1997). Importantly, human microvascular endothelial cells sustain human preadipocyte viability under hypoxia (Frye *et al.*, 2005). It has been proposed, that hypoxia may lead to an inflammatory response in adipocytes to increase the blood flow and stimulate angiogenesis (Trayhurn and Wood, 2004). Severe hypoxia leads to a proinflammatory response in human and murine adipocytes *in vitro* (Trayhurn *et al.*, 2008; Wang *et al.*, 2007; Ye, 2009). Examples of the upregulated target genes and proteins include VEGF, leptin, PAI-1, migration inhibitory factor (MIF). Concurrently, adiponectin expression appears to be downregulated. A first direct relationship between hypoxia and insulin resistance has been shown *in vitro* for murine and human adipocytes where the autophosphorylation of the insulin receptor was impaired upon hypoxia exposure which was quickly reversed, after only 45 min reoxygenation (Regazzetti *et al.*, 2009). Additionally, hypoxia may play a role in adipocyte death which preferentially occurs in WAT of obese mice and humans and is positively correlated with adipocyte hypertrophy in contrast to lean mice and humans where adipocyte death is seldom. In WAT the dead adipocytes are surrounded by macrophages which together form so-called crown-like structures (Cinti *et al.*, 2005; Surmi and Hasty, 2008).

1.2.7 WAT immune cell infiltration

Many cell types reside in WAT, including immune cells such as T-lymphocytes and macrophages with their number being increased in obese mice (Weisberg *et al.*, 2003; Xu *et al.*, 2003) and humans (Cancello *et al.*, 2006; Curat *et al.*, 2006). It has been suggested that especially the macrophages in WAT induce insulin resistance by promoting a proinflammatory environment (Surmi and Hasty, 2008). As yet, it is neither clear what initiates the increased immune cell infiltration nor the sequence in which the different immune cell types appear in WAT. Severe hypertrophy of adipocytes, being mostly connected with fatty acid flux, hypoxia (see chapter 1.2.6), adipocyte cell death, increased leptin secretion (see chapter 1.2.2.1) and endothelial dysfunction (1.2.4.1) may be all contributing factors (Surmi and Hasty, 2008).

There is evidence, that ahead of monocyte infiltration into WAT, recruitment of neutrophils (Elgazar-Carmon *et al.*, 2008) and T-lymphocytes (Kintscher *et al.*, 2008) occurs. One study in mouse WAT showed that neutrophil recruitment transiently precedes monocyte infiltration as it is also known from several other inflammatory diseases. An important chemoattractant for neutrophils is IL-18 which is also expressed by WAT (Elgazar-Carmon *et al.*, 2008; Skurk *et al.*, 2005). The expression of RANTES and its receptor CCR5 is increased in WAT of obese mice and has been attributed for the paralleled elevated number of CD3⁺ T-lymphocytes (Rausch *et al.*, 2007; Wu *et al.*, 2007). Similar observations were made in WAT of obese individuals, where RANTES and CCR5 gene expression correlated with gene expression of macrophage markers (Wu *et al.*, 2007). Other chemoattractants for the recruitment of T-lymphocytes besides RANTES, are MCP-1, interferon-inducible protein 10 (IP-10) and SDF-1 α , known to be secreted by several cell types, including preadipocytes and adipocytes (Kintscher *et al.*, 2008).

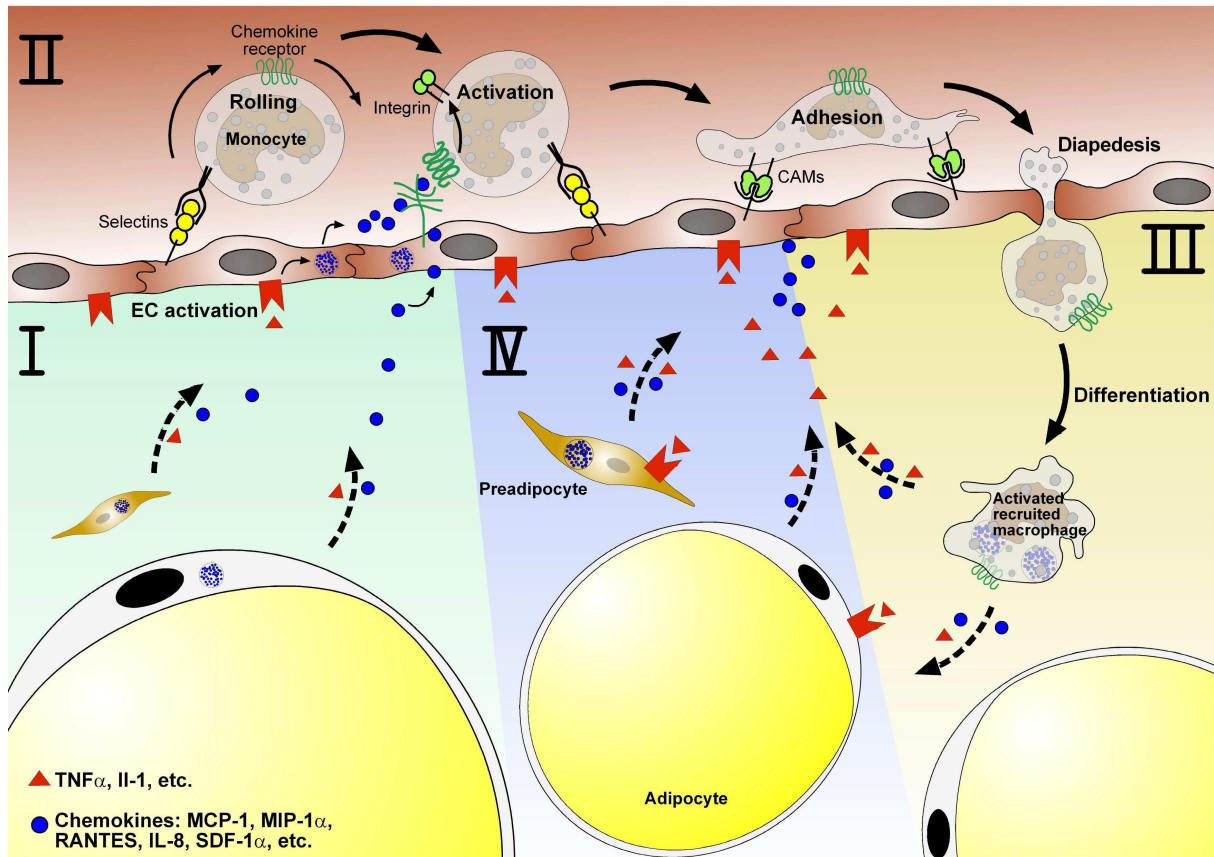
The number of T-lymphocytes in WAT correlates with the waist circumference of type 2 diabetes patients. Additionally, it was shown in a mouse model of high fat diet induced obesity, that T-lymphocyte infiltration precedes the accumulation of macrophages in WAT during the development of insulin resistance (Kintscher *et al.*, 2008). At one stage during WAT growth monocytes infiltrate the tissue and differentiate to macrophages producing further cytokines such as TNF- α and IL-1 (Mosser, 2003), which are very potent proinflammatory activators of endothelial cells (Petzelbauer *et al.*, 1993), adipocytes (Wang and Trayhurn, 2006) and other cell types. Additionally, an *in vitro* co-culture study between

macrophages and adipocytes showed that the macrophage TNF- α release interferes with adipocyte insulin signalling and induces fatty acid lipolysis (Suganami *et al.*, 2005). These mechanisms altogether may result in a positive feedback loop and are visualized in figure 2.

Monocyte recruitment may be initiated by an activated endothelium and adipocytes, preadipocytes and other cells residing in WAT, producing chemoattractants such as MCP-1 and IL-8 (Fain and Madan, 2005; Fain *et al.*, 2004; Gerszten *et al.*, 1999). Additionally, T-lymphocytes secrete IFN- γ which in turn may stimulate other cell types, such as preadipocytes to increase their MCP-1 secretion and activate other cells, including endothelial cells and macrophages. Staining of human WAT showed that the majority of the T-lymphocytes were CD4⁺, the subset of lymphocytes producing IFN- γ (Kintscher *et al.*, 2008).

Macrophages can be distinguished in M1- classically activated - and M2- alternatively activated - subpopulations, as well as intermediate types having M1 and M2 characteristics and are found in WAT (Bourlier *et al.*, 2008; Lumeng *et al.*, 2007; Zeyda *et al.*, 2007). M1 macrophages are induced by inflammatory agents, have phagocytotic activity, predominantly secrete pro-inflammatory cytokines and are important in the initiation of inflammation. M2 macrophages were induced by IL-4 and IL-13 and secrete predominantly anti-inflammatory cytokines having a reparative and remodelling function by promoting the formation of new blood vessels and are important in terminating inflammatory process (Bourlier *et al.*, 2008; Mosser, 2003). In WAT of lean mice the M2 polarized macrophages appear to play a dominant role while in WAT of obese mice the M1 polarized macrophages take over (Lumeng *et al.*, 2007). In human WAT the macrophage population appears to be of the intermediate type, having both M1 and M2 characteristics. The M1 characteristics may be important in order to phagocytose dead adipocytes and explain the crown-like structures found in WAT (Cinti *et al.*, 2005), while the M2 characteristics may contribute to repair and remodelling of WAT during expansion. Interestingly, phagocytosis of a dead cell can induce an M2 phenotype in macrophages (Kintscher *et al.*, 2008).

Figure 2 Monocyte infiltration into white adipose tissue



I: Some adipokines (e.g. TNF- α) are able to activate the endothelium. This is characterized by the expression of selectins and adhesion molecules such as ICAM-1 and VCAM-1 and the release of chemokines e.g. from the Weibel-Pallade Bodies. II: Activated monocytes and other immune cells adhere to the adhesion proteins on the endothelium via integrins which is followed by transmigration. III: After the diapedesis the monocytes differentiate into macrophages. Activated macrophages release large amounts of TNF- α and IL-1 and several chemokines. IV: The released cytokines from macrophages activate the endothelium itself and trigger the adipocytes and preadipocytes to change their secretion to a more inflammatory pattern. CAMs, cellular adhesion molecules; IL, interleukin; MCP-1, monocyte chemoattractant protein-1; MIP-1 α , macrophage inflammatory protein 1-alpha; RANTES, regulated upon activation, normally T-expressed, and presumably secreted; SDF-1 α , stromal cell-derived factor 1 alpha; TNF α , tumour necrosis factor- α .

1.2.7.1 Mechanisms of leukocyte infiltration in tissues – Extravasation

The endothelium as the interface between circulating blood and immune cells and adipose tissue plays an interactive role in these infiltration and inflammatory processes (Pober and Sessa, 2007). In this context, the MAPK and JAK pathways mediating extracellular signals and the intracellular signal-regulated transcription factors STAT, NFκB and AP-1 play important roles (Hoefen and Berk, 2002; Kuldo *et al.*, 2005; Pober and Sessa, 2007).

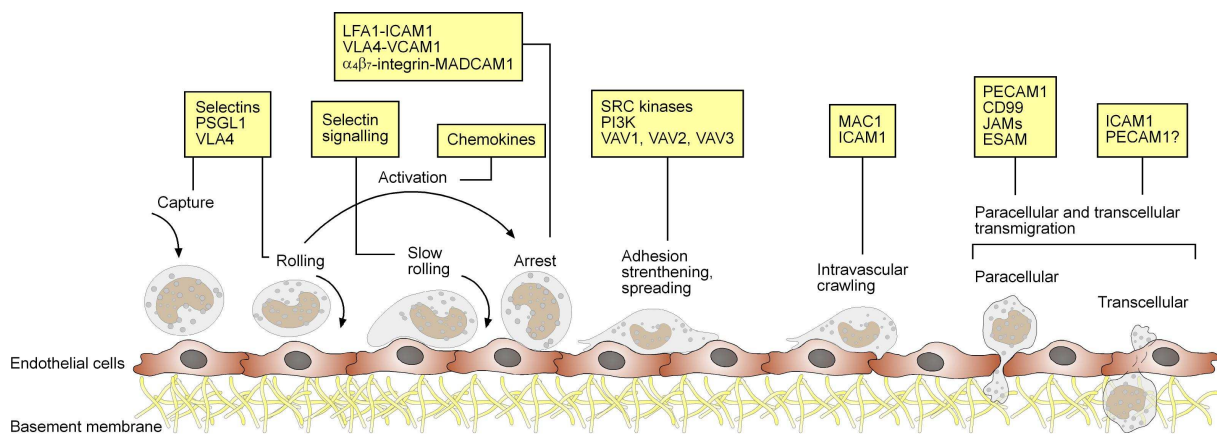
Interaction between leukocytes and the endothelial cell lining occurs in great complexity in physiologic and pathophysiologic conditions. During inflammation the microvascular endothelial cells tightly control the recruitment of leukocytes, including lymphocytes, monocytes and neutrophils into the underlying tissue, a process being termed extravasation (Randall *et al.*, 1997) which consists of leukocyte rolling, activation, slow rolling, arrest/adhesion, adhesion strengthening, intraluminal crawling, paracellular and transcellular migration, and migration through the basement membrane (Ley *et al.*, 2007). The series of complex molecular and cellular interactions involved in this process is given schematically together with the known key molecules involved in each step in figure 3.

Activation of microvascular endothelial cells via potent inducers such as TNF-α, IL-1 and interferon gamma (IFN-γ) results in the presentation of a range of adhesion proteins and chemokines at their luminal surface. The rolling of leukocytes is mediated via selectins, with P-selectin (CD62P) and E-selectin (CD62E) being most important and expressed at the cell surface of endothelial cells which interact with glycoprotein ligands e.g. P-selectin glycoprotein ligand 1 (PSGL1) being expressed on almost all leukocytes and Sialyl-Lewis^x being constitutively expressed on granulocytes and monocytes and activated b-lymphocytes and T-helper 1 (Th1) lymphocytes.

The rolling allows close contact between leukocytes and endothelium, the latter presenting chemokines e.g. MCP-1, IL-8, IL-6 and RANTES or other chemotactic compounds at the luminal surface; either released by the endothelial cells themselves, transported by them from their abluminal site or generated by proteolytic cleavage in activated mast cells and platelets, and delivered to endothelial cells through circulating microparticles or exocytosis of intracellular granules. These chemokines activate the leukocytes which involves the conformational change of integrins also called “activatable receptors” which are then

presented at the cells surface with high-affinity. Integrins also participate in rolling but especially mediate leukocyte arrest and firm adhesion together in the presence of chemokines. Depending on the leukocyte subset and the type of endothelial cells, different combinations of adhesion molecules, cytokines and chemokines are necessary for rolling, adhesion and transendothelial migration.

Figure 3 The leukocyte adhesion cascade



Adopted from Ley *et al.*, 2007

The leukocyte adhesion cascade consists of the following steps: capture, rolling, slow rolling, adhesion strengthening and spreading, intravascular crawling, and paracellular and transcellular transmigration. Key molecules involved in each step are indicated in boxes. CD99, cluster of differentiation 99; ESAM, endothelial cell-selective adhesion molecule; ICAM1, intercellular adhesion molecule 1; JAM, junctional adhesion molecule; LFA1, lymphocyte function-associated antigen 1 (also known as $\alpha_L\beta_2$ -integrin); MAC1, macrophage antigen 1; MADCAM1, mucosal vascular addressin cell-adhesion molecule 1; PSGL1, P-selectin glycoprotein ligand 1; PECAM1, platelet/endothelial-cell adhesion molecule 1; PI3K, phosphoinositide 3-kinase; SRC kinases, sarcoma kinase; VAV, vav guanine nucleotide exchange factor; VCAM1, vascular cell-adhesion molecule 1; VLA4, very late antigen 4 (also known as $\alpha_4\beta_1$ -integrin).

Well studied integrins are $\alpha_L\beta_2$ integrin also called lymphocyte function-associated antigen 1 (LFA-1) and CD11a-CD18, $\alpha_4\beta_1$ integrin, also known as very late antigen 4 (VLA-4) and CD49d-CD29 and $\alpha_M\beta_2$ integrin, also known as macrophage antigen 1 (MAC-1) and CD11b/CD18. The leukocyte integrins then bind to immunoglobulin superfamily members, typically intercellular adhesion molecule 1 (ICAM-1; CD54) and vascular cell adhesion molecule 1 (VCAM-1; CD106) which are expressed by activated endothelial cells finally leading to leukocyte arrest.

LFA-1, expressed by monocytes, macrophages, T-lymphocytes and granulocytes and dendritic cells and MAC-1 expressed by monocytes, macrophages and granulocytes bind to ICAM-1 while VLA-4 is expressed on most leukocytes and binds to VCAM-1. Adhesion strengthening occurs by so-called outside-in signalling through integrins where the integrins mediate intracellular signals which regulate several cellular functions such as cell motility, proliferation and apoptosis. This is followed by leukocyte crawling mediated via MAC-1/ICAM-1 interactions, where in postcapillary venules monocytes and neutrophils crawl inside blood vessels in order to find preferred sites of transmigration/diapedesis. Although, leukocytes have to pass the endothelial cells, endothelial cell basement membrane and pericytes, transmigration is connected with minor disruption of the complex morphology of vessel walls. Transmigration preferentially occurs via the paracellular but also the transcellular route as shown *in vivo* and *in vitro*, the latter especially if crawling is impaired. The series of molecules involved in transmigration are presented in figure 2. In the tissue the leukocytes migrate along a chemokine gradient until the site of inflammation is reached and monocytes differentiate to macrophages (Imhof and Aurrand-Lions, 2004; Ley *et al.*, 2007; Lim *et al.*, 2003; Middleton *et al.*, 2002; Vestweber, 2000).

ICAM-1 is the most extensively studied molecule of the ICAM family which consists of five members. ICAM-1 spans the cell membrane and contains a short cytoplasmic tail. It has five Ig-like domains, the first domain being responsible for LFA-1 and the third domain for MAC-1 binding. Besides its important role in leukocyte trafficking it also participates in signal transduction across cell membranes. Ligand binding may result in the activation of transcription factors, increased production of cytokines, cell membrane protein expression, ROS and cell proliferation (Hubbard and Rothlein, 2000). ICAM-1 is expressed constitutively at low levels on endothelial and other cells. Stimulation of endothelial cells with TNF- α , IL-1, IFN- γ , hydrogen peroxide (H₂O₂) and lipopolysaccharide (LPS) either alone or in combination leads to a strong upregulation of ICAM-1. Its expression is regulated mainly via protein kinase C (PKC), the mitogen-activated protein kinases (MAPK) extracellular-regulated kinases (ERK), SAPK/JNK and p38, the JAK/STAT and the NF κ B intracellular signal transduction pathways. The major nuclear transcription factors for the activation of ICAM-1 expression are activator protein 1 (AP-1), NF κ B, C/EBP, E-twenty six (Ets), STAT and Sp1. IFN- γ is the traditionally classic molecule which induces ICAM-1 gene expression via the JAK/STAT pathway (Roebuck and Finnegan, 1999).

1.2.8 Study of adipose tissue and adipocytes

The study of WAT physiology *in vivo* is generally conducted in animal models (Garofalo *et al.*, 1996; Rayner, 2001) but also in humans by using the microdialysis technique, adipose tissue vein cannulation, and measurement of blood flow by $^{133}\text{Xenon}$ washout and stable isotope tracers (Summers, 2006). *In vivo* experiments allow observing the full integrated physiological response to a stimulus. Consequently, certain investigations, such as the response to fasting, can only be performed using live animals.

Much of our knowledge of complex *in vivo* phenomena are based on studies performed in simplified *in vitro* model systems under controlled conditions (Kiely *et al.*, 1999). In order to study the effects of different ascendancies on isolated cells under defined conditions and to get insights how distinct cell types under different biological circumstances such as WAT expansion interact and how they contribute to the pool of pro-inflammatory and anti-inflammatory molecules, *in vitro* studies are indispensable (Farmer, 2006).

The study of WAT and adipocytes *in vitro* is performed by culturing tissue extracts (Fain and Madan, 2005) and primary mature adipocytes (Rodbell, 1964), primary preadipocytes (Hauner *et al.*, 2001) or immortalized preadipocyte cell lines (Chen *et al.*, 1989; Green and Meuth, 1974; Rodriguez *et al.*, 2004), respectively.

Primary mature adipocyte culture is considered to be the most true-to-life *in vitro* system, since the adipocytes are derived directly from a donor. However, the separation process of mature adipocytes from the freshly dissected WAT by collagenase digestion (Rodbell, 1964) is also stressful, e.g. leading to an increase of inflammatory adipokine expression (Eisele *et al.*, 2005; Ruan *et al.*, 2003). In addition, the life span of these cells is limited from hours to several days.

The conversion of preadipocytes into adipocytes *in vitro* is achieved by exposing the cultured preadipocytes to a mixture of molecules which include insulin, glucocorticoids, isobutylmethylxanthine (IBMX) (Gregoire *et al.*, 1998) and thiazolidinediones (Hausman *et al.*, 2008). IGF-1, rather than insulin is the physiological inducer of adipocyte differentiation (Gregoire *et al.*, 1998; Smith *et al.*, 1988). However, in cell culture experiments generally unphysiologically high concentrations of insulin are used to activate the IGF-1 receptor, due to

insulins low binding affinity for this receptor which is expressed in high numbers on preadipocytes in contrast to a small number of insulin receptors which begin to increase only after induction of differentiation (Gregoire *et al.*, 1998; Reed *et al.*, 1977; Reed *et al.*, 1981; Smith *et al.*, 1988). IBMX functions via intracellular cAMP level accumulation and increases together with glucocorticoids C/EBP- β expression which is required for subsequent PPAR γ expression (Gregoire *et al.*, 1998; Wiper-Bergeron *et al.*, 2007) whereas thiazolidinediones function as direct high-affinity ligands and activators of PPAR- γ (Hausman *et al.*, 2008).

Primary preadipocytes are obtained from the stromal vascular fraction of collagenase-digested WAT (Hauner *et al.*, 2001). They are then taken into culture conditions and differentiated into adipocytes. These cells can be passaged several times without losing their capacity of adipocyte differentiation (Skurk *et al.*, 2007) before they stop proliferating. In contrast, the human Simpson-Golabi-Behmel syndrome (SGBS) cell strain, which consists of unmanipulated stromal vascular cells derived from WAT of an infant with the SGBS, can be passaged over several months and by the same time remain their capacity for adipocyte differentiation (Wabitsch *et al.*, 2001).

Clonal cell lines are widely used in the study of adipocytes (Chen *et al.*, 1989; Green and Meuth, 1974; Rodriguez *et al.*, 2004). They provide a homogeneous cell population and can be ideally passaged indefinitely. In practice they are easier to use than primary cells. However, in contrast to primary cells, the distance from their original source is greater and they have changed at least some properties due to the genetic changes which allow for immortality (Masters, 2002). Murine clonal preadipocyte lines which derive from embryonic mouse fibroblasts are 3T3-L1 (Green and Meuth, 1974) and 3T3-F422A cells (Chen *et al.*, 1989). A new human clonal cell culture system has been described using multipotent adipose-derived stem cells (hMADS) (Rodriguez *et al.*, 2004).

1.2.9 Study of endothelial cells *in vitro*

Important findings on endothelial cell function come from *in vitro* experiments by culturing either microvascular or macrovascular endothelial cells derived from a variety of organs (Bouis *et al.*, 2001; Hillyer and Male, 2005) including WAT (Curat *et al.*, 2004). As primary endothelial cells often human umbilical vein endothelial cells (HUVECS) (Gimbrone, 1976) and human aortic endothelial cells (HAEC) are used (Krishnaswamy *et al.*, 1999). The best characterized vascular endothelial cell lines are ECV304 (Takahashi *et al.*, 1990), EA.hy926 (Edgell *et al.*, 1983) and human microvascular endothelial cells 1 (HMEC-1) (Ades *et al.*, 1992). The behaviour of endothelial cells strongly depends on their vascular origin. HUVECS, ECV304 and EA.hy926 are used for the study of macrovascular endothelial cells and HMEC-1, simian-virus-human cerebromicrovascular endothelial cells (SV-HCEC) and human telomerase reverse transcriptase – human dermal microvascular endothelial cells (hTERT-HDMEC) for the study of microvascular endothelial cells (Bouis *et al.*, 2001). HMEC-1 cells have been derived from human foreskins by transfection with large T antigens of simian-virus 40 (SV40) (Ades *et al.*, 1992). They have morphological, phenotypical and functional characteristics of microvascular endothelial cells (Bouis *et al.*, 2001). A comparison between HMEC-1, ECV304 and EA.hy926 with regard to induced expression and surface antigens in the context with leukocytes and transmigration found HMEC-1 to be most similar to the primary endothelium (Lidington *et al.*, 1999). It was found that for investigating microvascular endothelial cells HMEC-1 and hTERT-HDMEC are the most appropriate models (Bouis *et al.*, 2001).

1.2.10 Study of cross-talk between cell types

Coculture experiments are commonly conducted to study the molecular and cellular cross-talk between distinct cell types *in vitro*. There are three types of coculture techniques described and named as ‘coculture’ in the literature: firstly, coculture using transwell plates, here cells in two different compartments separated from each other via a membrane share the same medium. Secondly, coculture where cell types are cultured on the same surface or in a three-dimensional matrix which allows direct cell-cell interactions besides sharing the same medium. Thirdly, indirect coculture where the cell culture medium of cells of a distinct cell type, called conditioned medium (CM), is used to stimulate other cells, e.g. cells of another cell type (Armbrust and Rohl, 2008; Laterra *et al.*, 1990; Lumeng *et al.*, 2007). Since in coculture experiments both cell types either have to share the same medium or the CM of one cell type is used to stimulate the other, it is experimentally of importance to use or develop a cell culture medium which is suitable for both cell types.

To increase the knowledge in WAT biology it is important to understand how distinct cell types under different biological conditions such as WAT expansion interact and how they contribute to the pool of pro-inflammatory and anti-inflammatory molecules. The role of distinct cell types in orchestrating WAT immune cell infiltration is not clear (Surmi and Hasty, 2008) but the contribution of other cell types beside adipocytes is likely, representing 50 % of the total cell content (Hausman, 1985). In the context of immunological mechanisms, preadipocytes are of special interest due to their ability of displaying a macrophagic or endothelial potential according to their environment (Casteilla *et al.*, 2005). Transcriptome profiling demonstrated a closer relationship between preadipocytes and macrophages than between preadipocytes and adipocytes and the conversion of preadipocytes into macrophages has been shown to be efficient and rapid (Charriere *et al.*, 2003). Proliferating preadipocytes also develop phagocytotic activity towards microorganisms (Cousin *et al.*, 1999; Villena *et al.*, 2001).

An informative *in vitro* technique for studying the interactions between endothelial cells and immune cells in infiltration processes are adhesion assays (Kiely *et al.*, 1999). In these assays the firm binding of leukocytes to the endothelium is observed. The degree of adhesion varies with the magnitude of the activation of either the endothelial cells, the leukocytes or both cell types (Ley *et al.*, 2007). Human monocyte-endothelial cell-cell adhesion is studied commonly

by using human primary monocytes (Curat *et al.*, 2004), peripheral blood mononuclear cells (PBMC) (Mills *et al.*, 2006), the human histiocytic lymphoma cell line (U937 cells) (Sundstrom and Nilsson, 1976) or the human acute monocytic leukaemia cell line (THP-1 cells) (Tsuchiya *et al.*, 1980) as sources of monocytes.

PBMC consist of a mixture of blood cells having a round nucleus, including lymphocytes and monocytes. PBMC are generally isolated from whole blood by the hydrophilic polysaccharide *ficoll* which separates blood to its cellular components. The buffy coat, consisting of monocytes and lymphocytes, is generated under a layer of plasma (Roitt *et al.*, 2006).

U937 cells are derived from the histiocytic lymphoma of a 37 year old male patient (Sundstrom and Nilsson, 1976). These cells have been extensively characterized and are used to study monocytic behaviour, including the differentiation to macrophages (Harris and Ralph, 1985).

As yet, two papers have been published analyzing the effect of conditioned medium (CM) from mature adipocytes isolated from adipose tissue on monocyte-endothelial cell-cell adhesion. The study by Curat *et al.*, 2004 investigated the increased macrophage accumulation in WAT of obese people. In the study by Kralisch *et al.*, 2007 the influence of CM from mature adipocytes on macrovascular endothelial cell function was analysed in the context of obesity and atherosclerosis. In contrast, the impact of adipocytes differentiated from preadipocytes *in vitro* on endothelial cell activation has not been studied so far. The studies mentioned above neglected the role of preadipocytes in the context of the molecular and cellular cross-talk with endothelial cells and underlying molecular signalling pathways have only been sparsely investigated.

Overall, the nature of the preadipocyte and adipocyte-derived factors and the cellular and molecular cross-talk which mediate endothelial activation and promote the infiltration processes of immune cells into adipose tissue are rather poorly understood. Therefore, it will be important to apply different *in vitro* coculture systems between preadipocytes, adipocytes and endothelial cells and cell biological, molecular and biochemical methods in order to dissect the differential gene expression and secretion pattern of preadipocytes and adipocytes and their impact on endothelial cell function. This should also give new insights into the mechanisms of endothelial cell activation and dysfunction which occurs in WAT or other organs in the course of obesity and its related disorders.

1.3 Aim of the study

Obesity is associated with a state of chronic low-grade inflammation which is thought to contribute strongly to the development of features of the metabolic syndrome. A hallmark of inflammation is the infiltration of immune cells such as macrophages and T-lymphocytes into inflamed tissue. Obesity is connected with an increased number of immune cells, especially macrophages, in white adipose tissue (WAT) in humans and mice. The microvascular endothelium as the interface between adipose tissue and circulating immune cells in the blood plays an interactive role in these infiltration processes. Endothelial cell activation, which is a change in phenotype and/or function in endothelial cells in response to stimuli from the environment, is a prerequisite for controlling the recruitment of leukocytes into the underlying tissue. It is a regulated event in physiologic vascular responses which can lead if dysregulated under pathophysiologic conditions, to endothelial cell dysfunction. The mature and hypertrophic adipocytes are generally considered to be the major adipogenic cell type secreting proinflammatory cytokines in WAT. In contrast, the proinflammatory capacity of preadipocytes and their impact under different biological conditions on endothelial cell activation has been widely neglected in the research field so far. Therefore, the overall aim of this study was to gain new insights into the cellular interactions and molecular mechanisms and to identify factors involved in this cross-talk of preadipocytes, adipocytes and endothelial cells.

The primary experimental aim of this study was to establish a human coculture system and sensitive assays in order to mimic the processes mentioned above *in vitro*. This was achieved by establishing a co-culture system between the conditioned medium (CM) of human primary SGBS preadipocytes/adipocytes and human microvascular endothelial cells, HMEC-1 cells and measuring endothelial cell activation by monocyte endothelial cell-cell adhesion. The interactions were studied using the following methods: cell culture of HMEC-1 cells, SGBS cells, U937 cells and primary mature adipocytes, monocyte endothelial cell-cell adhesion assay, cell surface ELISAs, proliferation assay, ELISAs and multiplex bead-based Luminex® assays, reverse transcriptase-polymerase chain reactions (RT-PCR) and quantitative real time PCR (qRT-PCR), Western blotting, inhibitor experiments, functional analysis, and peptidomic analysis.

Use of these techniques should allow the analysis of the following:

1. adipokine expression and secretion of SGBS preadipocytes and adipocytes under different biological conditions e.g. normoxia and hypoxia
2. the impact of CM from non-stimulated and stimulated SGBS preadipocytes and adipocytes, mimicking different biological conditions, on endothelial cell function by investigating monocyte-endothelial cell-cell adhesion, endothelial cell proliferation and signalling pathways
3. functional analysis of mediators in the CM of preadipocytes and adipocytes responsible for changes in monocyte-endothelial cell-cell adhesion
4. the effect of CM from different-sized primary mature adipocytes on monocyte-endothelial cell-cell adhesion
5. detection of candidate peptides in the CM of SGBS cells, possibly involved in the molecular cross-talk between preadipocytes, adipocytes and microvascular endothelial cells, by a peptidomics approach.

2 Materials and Methods

2.1 Cell Culture

2.1.1 Primary cell culture and size fractionation of human mature adipocytes

2.1.1.1 Reagents

Dulbecco's Modified Eagle Medium: nutrient mixture F-12 (DMEM/F12; Invitrogen)

MCDB 131 (Invitrogen)

Bovine serum albumin (BSA; Sigma-Aldrich)

Collagenase 250U/mg (Biochrom)

Krebs-Ringer phosphate (KRP) buffer

- 154 mM NaCl (Sigma-Aldrich)
- 154 mM KCl (Sigma-Aldrich)
- 11 mM CaCl₂ (Merck KgaA)
- 154 mM MgSO₄ (Sigma-Aldrich)
- 100 mM NaH₂PO₄ (Sigma-Aldrich)
- adjustment to pH 7.4, sterile filtration

2.1.1.2 Theoretical Background and Method

For theoretical background information refer to chapter 1.2.8. Adipose tissue was obtained from healthy patients undergoing elective plastic surgery or abdominal surgery after having obtained informed consent. There was no selection for BMI, age or gender. The tissue was collected under sterile conditions and stored in DMEM/F12 medium and was immediately transported to the laboratory. Mature adipocytes were isolated according to the protocol by Rodbell (Rodbell, 1964) with the following modifications on the day of surgery: connective tissue and blood vessels were excised. The remaining WAT was minced into small pieces. Collagenase digestion of WAT was performed in KRP buffer containing 4 % BSA and 100 U/ml collagenase at 37 °C for not more than 1 hr in a shaking water bath (80 rpm). Floating cells were aspirated and filtered twice, first through a 2 mm and next through a 250 µm mesh. The cells in the flow-through were washed three times with KRP buffer containing 0.1 % BSA and were finally collected by aspiration of the wash solution.

Separation of adipocytes by size was achieved by flotation as described recently (Skurk *et al.*, 2007). Briefly, 10 ml of isolated adipocytes were transferred to a 100 ml separating funnel filled with 50 ml KRP buffer containing 0.1 % BSA. The cell-buffer suspension was gently mixed by inversion and cells were allowed to float for 60 sec before 35 ml of the suspension, containing the small cells, was collected. Next, 35 ml KRP buffer containing 0.1 % BSA was added to the remaining suspension in the separating funnel followed by mixing as described above. The adipocytes of medium size were removed by allowing them to float for 45 sec and 30 sec, respectively, and 35 ml of suspension was discarded and then refilled with buffer after each step. The remaining large adipocytes in the KRP buffer containing 0.1 % BSA in the separating funnel were collected. The protocols were approved by the ethical committee of the Technische Universität München.

The cell diameters of 100 cells from the original sample and both fractions were determined by light microscopy in order to calculate the fat cell count, volume and cell surface area. The conditioned medium (CM) was generated by culturing 1 ml of cells in 5 ml MCDB 131 medium at 37 °C for 16 hrs in an incubator with a humidified atmosphere of 5 % CO₂ and 95 % air. The cell volume (V) and the cell surface area (A) were calculated from the cell diameter (d) using the formulas $V = 1/6\pi d^3$ and $A = \pi d^2$, respectively.

2.1.2 SGBS cell culture

2.1.2.1 Reagents

Proliferation medium

- DMEM/F12 (Invitrogen) supplemented with:
- 100 U/ml penicillin 100 µg/ml streptomycin (Invitrogen)
- 33 µM biotin (Roth)
- 17 µM D-pantothenat (Sigma-Aldrich)
- 10 % fetal calf serum (FCS; Invitrogen)

Adipose medium

- 1/3:2/3 mixture of DMEM/F12 and MCDB 131 (Invitrogen) supplemented with:
- 100 U/ml penicillin 100 µg/ml streptomycin
- 11 µM biotin
- 6 µM D-pantothenat
- 66 nM insulin (Sigma-Aldrich)
- 1 nM triiodothyronine (T₃; Sigma-Aldrich)
- 100 nM hydrocortisone (Sigma-Aldrich)
- 10 µg/ml transferrin (Sigma-Aldrich)

Induction medium

- Adipose medium supplemented with:
- 2 μ M rosiglitazone (Cayman)
- 25 nM dexamethasone (Sigma-Aldrich)
- 0.5 mM Isobutylmethylxanthine (IBMX; Serva)

MCDB 131 (Invitrogen)

Phosphate buffered saline (PBS) w/o Ca^{2+} and Mg^{2+} (Sigma-Aldrich)

- 1 tablet PBS per 200 ml dH_2O yields
- 10 mM phosphate buffer
- 2.7 mM KCL
- 0.137 M NaCl
- adjustment to pH 7.4, sterile filtration

Trypsin/EDTA solution (PAA)

- PBS w/o Ca^{2+} and Mg^{2+}
- 0.5 mg/ml trypsin
- 0.75 mM ethylenediaminetetraacetic acid (EDTA)

2.1.2.2 Theoretical Background and Method

For theoretical background information refer to chapter 1.2.8. Preadipocytes from the SGBS cell strain (Wabitsch *et al.*, 2001), kindly obtained from Prof. Wabitsch (Department of Pediatrics and Adolescent Medicine, University of Ulm, Ulm, Germany) were cultured as described recently (Mack *et al.*, 2009). In detail: SGBS cells were cultured at 37 °C in an incubator with a humidified atmosphere of 5 % CO_2 and 95 % air. In experiments with hypoxia the cells were cultured at 37 °C in an incubator with a humidified atmosphere of 1 % O_2 , 5 % CO_2 and 94 % N_2 or 4 % O_2 , 5 % CO_2 and 91 % N_2 , respectively (Hypoxia workstation, InVivo O2 400, IUL Instruments).

SGBS preadipocytes were proliferated in proliferation medium. Subconfluent cells were split by washing once with PBS and treatment with trypsin/EDTA solution at 37 °C for 5 min. The reaction was stopped by adding proliferation medium. The cells were plated at the following densities: 10.000 cells per well of a 6-well cell culture plate and 600 cells per well of a 96-well cell culture plate. The scheme of the cell culture strategy is shown in figure 10.

To obtain differentiated adipocytes, confluent preadipocytes were washed 3 times with PBS and induced with induction medium (d0). Preadipocytes serving as uninduced controls were cultured in adipose medium. After 4 days of induction of differentiation (d4), the media of all cells were replaced with adipose medium and the cells were fed twice per week for additional 10 days (d14). Adipocyte differentiation was detectable only in cell cultures that were initially supplemented with adipogenic differentiation inducers (induction medium). This was observed in 80 % or more of all cells. To obtain CM from SGBS cells without any additional

supplements the cell culture conditions were shifted from adipose medium to MCDB 131 medium after 14 days of differentiation. Depending on the experimental conditions, MCDB 131 medium was changed to fresh medium at day 15 (d15), and the cells were kept under normoxic or hypoxic conditions for 24 hrs (d16) or were stimulated with TNF- α (d16). The corresponding supernatants representing the CM (d16) were centrifuged at 1000 g for 5 min and passed through a 0.25 μ m nylon filter. CM derived from hypoxic cells were reoxygenated for at least 15 minutes and not more than 1 hr in 50 ml tubes under the cell culture hood. Then, CM were either used directly or concentrated for coculture experiments, or were immediately frozen in liquid nitrogen and stored at -80 °C.

For concentrating the CM, ultrafiltration centrifugal filter devices (Amicon Ultra centrifugal filter device) were applied. The procedure was carried out according to the manual instructions. Molecules larger than 5 kDa accumulated in the concentrate and the medium was exchanged by fresh MCDB 131 medium in order to remove any remaining molecules of less than 5 kDa. The permeate contained the non-concentrated molecules of less than 5 kDa.

2.1.3 HMEC-1 cell culture

2.1.3.1 Reagents

HMEC-1 medium

- MCDB 131 (Invitrogen) supplemented with:
- 100 U/ml penicillin, 100 μ g/ml streptomycin (Invitrogen)
- 10 % FCS (Invitrogen)
- 2 mM L-glutamine (Invitrogen)
- 10 ng/ml epidermal growth factor (EGF; Immunotools)
- 2.8 μ M hydrocortisone (Sigma-Aldrich)

MCDB 131 (Invitrogen)

PBS w/o Ca²⁺ and Mg²⁺ (Sigma-Aldrich)

- 1 tablet PBS per 200 ml dH₂O yields
- 10 mM phosphate buffer
- 2.7 mM KCL
- 0.137 M NaCl
- adjustment to pH 7.4, sterile filtration

Trypsin/ EDTA solution (PAA)

- PBS w/o Ca²⁺ and Mg²⁺
- 0.5 mg/ml trypsin
- 0.75 mM EDTA

2.1.3.2 Theoretical Background and Method

For theoretical background information refer to chapter 1.2.9. HMEC-1 cells (Ades *et al.*, 1992; Bouis *et al.*, 2001), obtained from the Centers for Disease Control and Prevention, Atlanta, USA, were cultured as has been reported elsewhere (BelAiba *et al.*, 2007; Mack *et al.*, 2009). In detail: HMEC-1 cells were proliferated in HMEC-1 medium and only used up to passage 30 in order to maintain their phenotypic endothelial characteristics. Cell splitting was performed at subconfluency by one PBS washing step and trypsinisation at 37 °C for 5 min. The reaction was stopped with HMEC-1 medium. The cells were either plated on 6 cm dishes, 6-well cell culture plates or 96-well cell culture plates at cell densities ranging between 1×10^5 cells per ml and 1×10^4 cells per ml. Generally, the experiments were performed with confluent HMEC-1 cells. Ahead of experiments, HMEC-1 cells were starved in MCDB 131 medium overnight (14-16 hrs). In all experiments the cells were cultured at 37 °C in an incubator with a humidified atmosphere of 5 % CO₂ and 95 % air.

2.1.4 U937 cell culture

2.1.4.1 Reagents

U937 medium

- Roswell Park Memorial Institute 1640 medium (RPMI 1640; Invitrogen) supplemented with:
- 100 U/ml penicillin, 100 µg/ml streptomycin (Invitrogen)
- 10 % FCS (Invitrogen)

2.1.4.2 Theoretical Background and Method

The U937 cell line was derived from malignant cells obtained from the pleural effusion of a patient with histiocytic lymphoma (Sundstrom and Nilsson, 1976). U937 cells display many monocytic characteristics and can differentiate to macrophages by a series of stimuli (Harris and Ralph, 1985). Monocytic U937 cells, supplied by Helmut Laumen (Department of Nutritional Medicine, Technische Universität München, Freising, Germany) were cultured as has been published elsewhere (Mack *et al.*, 2009). In detail: U937 suspension cells were cultured in U937 medium. Cell passaging was performed by centrifugation at 200 g for 5 min. The supernatant was discarded and the cells were resuspended in U937 medium at densities between 5×10^4 per ml and 5×10^5 cells per ml and subcultured. For experiments, the cell

number was adjusted to 5×10^5 cells per ml one day before the experiments. In all experiments the cells were cultured at 37 °C in an incubator with a humidified atmosphere of 5 % CO₂ and 95 % air.

2.1.5 Coculture between CM of SGBS cells and HMEC-1 cells

For detailed information of the coculture strategy refer to chapter 3.1.6. Starved HMEC-1 cells were treated under serum-free conditions with MCDB 131 medium (control), MCDB 131 medium supplemented with TNF- α , IL-6, VEGF, leptin or cocultured with fresh and concentrated CM of SGBS cells or CM of human primary mature adipocytes for different time periods. In inhibitor experiments, HMEC-1 cells were pretreated with JNK inhibitor II, SB-203580, PD-98059, or JAK inhibitor 1 for 45 min before the coculture with CM supplemented with the corresponding inhibitor at the appropriate concentration. When IL-6 inhibitor experiments were performed, the CM were preincubated with 5 mg/ml monoclonal anti-human IL-6 antibody or the corresponding immunoglobulin G1 (IgG₁) isotype control for 15 min. For blockade of TNF- α activity, the CM were preincubated for 10 min with Enbrel® (Tracey *et al.*, 2008), a soluble TNF- α receptor antagonist.

2.1.6 Coculture and monocyte-endothelial cell-cell adhesion assay

2.1.6.1 Theoretical Background

In various inflammatory processes, leukocytes adhere to and subsequently migrate across locally activated endothelial lining to form exudates. In order to study these monocyte endothelial cell interactions, a monolayer adhesion assay *in vitro* under static conditions is useful to characterize the adhesion-stimulatory or inhibitory properties of substances acting on either the leukocyte or endothelial cell. Moreover, ligand-receptor interactions involved in leukocyte adhesion can be analysed (Kiely *et al.*, 1999). In this assay the monocytes were labelled with the fluorogenic dye *Calcein green AM* (De Clerck *et al.*, 1994). *Calcein green AM* passes as nonfluorescent molecule through the cell membrane of viable cells. Inside the cell, it is hydrolysed by intracellular esterases producing a negatively charged green fluorescent calcein that is retained in the cytoplasm. Thus, the degree of *Calcein green AM* labelled monocytes adhering to treated and control endothelial cells can be determined by

comparing the fluorescence data. The fluorescence increases linearly after cell lysis with cell numbers ranging between 30 and 3000 U937 cells per well of a 96-well cell culture plate (see chapter 7.5.1) and without lysis with cell numbers ranging between 200 and 16 200 HeLa cells per well of a 96-well cell culture plate (Manual: Calcein AM cell viability assay kit, catalog number: 30026, Biotium, Inc. [Hayward, USA]).

2.1.6.2 Reagents

PBS w/o Ca^{2+} and Mg^{2+} (Sigma-Aldrich)

- 1 tablet PBS per 200 ml dH_2O yields
10 mM phosphate buffer
2.7 mM KCL
0.137 M NaCl
- adjustment to pH 7.4, sterile filtration

Calcein green AM stock solution

- 1mM *Calcein green AM* (Invitrogen) in dimethyl sulfoxide (DMSO; Sigma-Aldrich)

Lysis buffer

- 50 mM Tris-HCL (Sigma-Aldrich)
- 0.1 % sodium dodecylsulfate (SDS; Sigma-Aldrich) in dH_2O
- adjustment to pH 8.2 to 8.4

2.1.6.3 Method

Monocyte-endothelial cell-cell adhesion between HMEC-1 and U937 cells was carried out as described elsewhere (Kong *et al.*, 2004) with the following modifications (Mack *et al.*, 2009; Seebach, 2006): the assays were performed in 96-well cell culture plates. Confluent HMEC-1 cells were treated with 100 μl MCDB 131 medium (control), MCDB 131 supplemented with TNF- α , IL-6, VEGF or leptin, fresh/concentrated CM of SGBS cells or CM of human primary mature adipocytes for 6 hrs. For the adhesion assay U937 cells were washed twice with PBS, then loaded with *Calcein green AM* (5 μM per 5×10^6 cells) at 37 °C for 30 min and again washed twice with MCDB 131 to remove extracellular *Calcein green AM*. Next, after 6 hrs treatment HMEC-1 cells were washed twice with MCDB 131 medium, and 2.5×10^5 *Calcein green AM* labeled U937 cells per well were added to HMEC-1 cells and incubated at 37 °C for 1 hr. Non-adherent U937 monocytes were removed by washing four times with PBS. The remaining cells in the well were incubated in lysis buffer at 37 °C in the dark for 5 min. Lysed cells were centrifuged at 3500 g for 5 min, and the fluorescence of the supernatants was measured at 494 and 517 nm using a spectrometer (Varioskan multiwell

photo- and fluorometer, Thermo Scientific). HMEC-1 cells and unlabeled U937 cells were used as blanks. Samples were analysed at least in four replicates. An example for the analysis of the monocyte-endothelial cell-cell adhesion data is given in chapter 7.5.2.

2.2 Cell surface expression analysis by cell-ELISA

2.2.1 Theoretical Background

Leukocyte adhesion to endothelial cells lining the vasculature is mediated by a series of adhesion molecules such as ICAM-1 and VCAM-1 (Ley *et al.*, 2007). The cell-ELISA is a technique to study cell surface antigens under different stimulations (Morandini *et al.*, 2001). Therefore, an antigen is detected on live or fixed cells using the ELISA principals (chapter 2.6.1.1). Comparative studies showed that the cell-ELISA technique can be as sensitive and specific as flow cytometry (Grunow *et al.*, 1994; Ogino *et al.*, 2003).

2.2.2 Reagents

PBS with Ca²⁺ and Mg²⁺

- 1 tablet PBS per 200 ml dH₂O (Sigma-Aldrich)
- 0.84 mM MgCl₂ (Merck KGaA)
- 0.72 mM CaCl₂ (Merck KGaA)
- adjustment to pH 7.4, sterile filtration

4 % paraformaldehyde (PFA; Sigma-Aldrich) in PBS with Ca²⁺ and Mg²⁺, adjustment to pH 7.4

Washing buffer

- PBS with Ca²⁺ and Mg²⁺
- 0.5 % Tween 20 (v/v; Sigma-Aldrich)

Blocking buffer

- PBS with Ca²⁺ and Mg²⁺
- 1 % BSA (Sigma-Aldrich)
- 30 % donkey serum (Chemicon International)

Goat anti-human ICAM-1 antibody (R&D Systems)

Goat anti human VCAM-1 antibody (R&D Systems)

horeseradish peroxidase (HRP)-conjugated donkey anti-goat antibody (Dianova)

tetramethylbenzidine (TMB; Sigma Aldrich)

1 M H₂SO₄ (Serva)

2.2.3 Method

The cell-ELISA assay was carried out as described elsewhere (Amin *et al.*, 2006; Shiojima and Walsh, 2002; Zhu *et al.*, 2003) with the following modifications (Mack *et al.*, 2009): the experiments were conducted in 96-well cell culture plates. Confluent HMEC-1 cells were stimulated with MCDB 131 medium (control), TNF- α , IL-6, VEGF, leptin, fresh CM of SGBS cells or CM of human primary mature adipocytes for 6 hrs. The cells were washed with cold PBS supplemented with Mg²⁺ and Ca²⁺ (PBS + Mg/Ca) and then fixed with 4% PFA at 4 °C for 10 min. After two PBS + Mg/Ca washing steps, the cells were incubated with blocking buffer at RT for 1h and then exposed to goat anti-human ICAM-1 or VCAM-1 antibody (1:200 dilution in blocking buffer) at RT for 1 hr. Next, the cells were rinsed twice and then washed three times with washing buffer for 5 min followed by incubation with HRP-conjugated donkey anti-goat antibody (1:5000 dilution in blocking buffer) at RT for 30 min. After the cells were rinsed twice and washed three times with washing buffer for 5 min, 200 μ l TMB per well was added as substrate. The reaction was stopped after 15 min with 50 μ l 1M H₂SO₄. The absorbance was measured at 450 nm and 690 nm using a spectrometer (Varioskan multiwell photo- and fluorometer, Thermo Scientific). The data were normalized to the blank controls, where at least two wells with TNF- α treated HMEC-1 cells were incubated without the first antibody (ICAM-1 or VCAM-1 antibody). Initial experiments with isotype-matched control antibodies did not detect non-specific binding from the secondary antibody. Samples were analysed at least in duplicate. The analysis of the cell-ELISA data was similar to the approach used for the monocyte-endothelial cell-cell adhesion data (see chapter 7.5.2).

2.3 Proliferation assay

2.3.1 Theoretical Background

5-bromo-2-deoxyuridine (BrdU) is used for the detection of cell proliferation by assessing DNA synthesis. BrdU is a synthetic nucleotide, an analogue of thymidine and can be incorporated into newly synthesized DNA of replicating cells during the S-phase. Using a specific antibody against BrdU, allows detection of replicating cells (Schutte *et al.*, 1987; Schutte *et al.*, 1987) with the ELISA technique (chapter 2.6.1.1)

2.3.2 Reagents

Cell Proliferation ELISA; BrdU (colorimetric; Roche)

1 M H₂SO₄ (Serva)

2.3.3 Method

DNA synthesis was assessed by BrdU-labelling according to the manufacturer's instructions. In brief, HMEC-1 cells were seeded in 96-well cell culture plates at a density of 1500 cells per well and exposed to different media or factors, such as MCDB 131 (control), MCDB 131 containing IL-6, leptin or VEGF and CM, all supplemented with 1% FCS. After 48 hrs, BrdU was added at a final concentration of 10 µM for 16 hrs. Incorporated BrdU was detected with HRP-conjugated anti-BrdU antibody using TMB as a substrate. The reaction was stopped with 1M H₂SO₄ and the absorbance was measured at 450 nm and 690 nm using a spectrometer (Varioskan multiwell photo- and fluorometer, Thermo Scientific). At least three wells were incubated without the first antibody (BrdU) and served as blank controls.

2.4 RNA extraction, DNase I treatment and RNA integrity check

2.4.1 Reagents

Trizol® (Invitrogen)

Chloroform (Roth)

Isopropanol (Roth)

75 % Ethanol (Roth)

Nuclease-free water (Sigma-Aldrich)

DNA-free™ kit (kit containing DNase I; Ambion)

Reagents for agarose gel electrophoresis

- sample buffer [40 % glycerol (Merck KGaA), 60 % ddH₂O, 0.01 % bromphenol blue (Merck KGaA)]

- agarose (Sigma-Aldrich)

- 0.5x TBE [45 mM Tris (Roche), 4 mM boric acid (Merck KGaA), 1 mM EDTA (Merck KGaA), adjustment to pH 8]

- 0.5 µg/ml EtBr (Sigma-Aldrich)

2.4.2 Theoretical Background and Method

RNA isolation using Trizol® is based on the guanidinium thiocyanate-phenol-chloroform extraction method (Chomczynski and Sacchi, 1987; Chomczynski and Sacchi, 2006). It is a liquid-liquid extraction technique and allows isolating RNA, protein and DNA from the same sample. Total RNA was isolated from the cells using the Trizol® protocol according to the manufacturer's instructions with the following modifications: for RNA extraction from cells, the media of 2 wells from a 6-well cell culture plate were aspirated and 1 ml of Trizol® added. In order to maximize the cell homogenisation, the Trizol®-cell mixture was triturated 12 times using a 1 ml syringe with a 23 gauge needle. This was followed by incubation with 200 µl chloroform and centrifugation at 12000 g at 4°C for 15 min, leading to the formation of three layers: aqueous, interphase and phenol. The aqueous layer containing the RNA was transferred to a new tube and incubated with 50 µl of isopropanol. After centrifugation at 12000 g at 4°C for 10 min the RNA in the supernatant is likely to contain less contaminating DNA. Next, 450 µl isopropanol was added to the supernatant in order to precipitate the RNA. After centrifugation at 12000 g at 4 °C for 10 min the RNA pellet was washed with 1 ml 75 % ethanol in order to remove salts. The RNA pellet was then dissolved in nuclease-free water

and subjected to DNase I treatment (Vanecko and Laskowski, 1961) according to the manufacturer's instructions in order to minimize contaminating DNA in the sample.

RNA samples were quantitated by spectrophotometry at 260 nm using the Beer-Lambert law (Beer, 1852). The 260 to 280 nm absorbance ratio was between 1.7 and 1.9. RNA integrity was analysed by agarose gel electrophoresis of total RNA and visualization of the 18S and 28S ribosomal RNA (rRNA) bands. Briefly, 0.8 µg of total RNA was loaded onto a 1 % agarose gel containing 0.5 µg/ml ethidium bromide (EtBr) and 0.5x tris-borate-EDTA (TBE) buffer. For RNA detection a UV transilluminator was used and the results recorded using a digital camera (INTAS UV Systeme, Intas Science Imaging Instruments) Distinct bands for 28S and 18S rRNA forming about a 2:1 ratio of staining intensities were observed.

Additionally, the RNA integrity of some samples was confirmed by analysis with the Bioanalyser from Agilent Technologies. The RNA Integrity Number (RIN) was then between 9 and 10. The highest RIN which can be achieved is 10 (Schroeder *et al.*, 2006).

2.5 Reverse transcription (RT), polymerase chain reaction (PCR) and quantitative real-time PCR (qRT-PCR)

2.5.1 Theoretical background

RT-PCR and qRT-PCR are powerful and sensitive techniques to detect gene expression. In the reverse transcription step the enzyme reverse transcriptase (Baltimore, 1995) extends an oligonucleotide primer hybridized to a single-stranded (ss) RNA or DNA template in the presence of deoxynucleotide triphosphates (dNTPs) producing a complementary DNA strand. These DNA strands are referred to as cDNA which is further used as template for the PCR. During this process, one complementary DNA (cDNA) of interest is amplified using gene-specific primers, dNTPs and the DNA Taq polymerase. RT-PCR is used for qualitative and qRT-PCR for both qualitative and quantitative detection of gene expression.

In general, the PCR process (Kleppe *et al.*, 1971; Mullis, 1990) begins with a denaturation phase at 94 °C followed by 15 to 40 amplification cycles and in the qRT-PCR process (Giulietti *et al.*, 2001; VanGuilder *et al.*, 2008) by 40 amplification cycles. Each cycle consists of three steps: denaturation, annealing and extension. Denaturation at 94 °C results in the dissociation of double-stranded (ds) DNA into ssDNA. The annealing temperature (T_A) is

primer specific depending on primer length and GC content. The duration of the extension step increases with amplicon size, but is usually 20 to 60 s.

The PCR process is characterized by three phases: exponential, linear and plateau. In the exponential phase the amplicon ideally doubles every cycle, the reaction is very specific and precise. In the linear phase, the reaction components have been consumed and products start to degrade until finally, the plateau phase is reached where the reaction has stopped.

PCR products are analysed at the endpoint of the reaction by subjecting them to an agarose gel electrophoresis. For visualisation, EtBr intercalates into the DNA and fluorescence under UV light. In contrast, in qRT-PCR experiments the accumulation of the amplicon is detected during the reaction. The data for the quantitative analyses are acquired from the exponential phase of the reaction. Four different chemistries are available for qRT-PCR – TaqMan®, Molecular Beacons, Scorpions® and SYBR® Green. The TaqMan® and SYBR® Green chemistries were used in this work.

2.5.1.1 SYBR® Green

SYBR® Green intercalates into dsDNA and upon excitation emits light. Thus, the fluorescence increases with PCR product accumulation. In contrast to the TaqMan® chemistry, SYBR® Green also binds to primer dimers and other dsDNA unspecific PCR products, leading to enhanced fluorescent signals. This problem can be minimized with well designed primers and the performance of a melting curve analysis at the end of the reaction where the dissociation-characteristics of double-stranded DNA during heating are investigated. The DNA is slowly heated from 60 °C to 95 °C. dsDNA products are dissociated at a specific temperature, depending on their strand length, GC content and complementarity. Intercalated dye is released in parallel, leading to a decrease in fluorescence. The specific PCR products can be distinguished from the unwanted by-products by their higher melting temperature (Giulietti *et al.*, 2001; VanGuilder *et al.*, 2008).

2.5.1.2 TaqMan®

TaqMan® probes are oligonucleotides which have a fluorescent reporter dye attached to the 5' end and a quencher coupled to the 3' end. The proximity of both molecules prevents the detection of a fluorescent signal from the probe. TaqMan® probes are designed to hybridize to the internal region of the PCR product. The Taq polymerase has also a 5'-3'-exonuklease-activity. During PCR, the 5'-nuclease activity of the polymerase cleaves the probe. This leads to the decoupling of the fluorescent and quenching molecules and consequently, to increasing fluorescence with each cycle, proportional to the amount of probe cleavage (Giulietti *et al.*, 2001; VanGuilder *et al.*, 2008).

2.5.1.3 Primer design

Two different primer design strategies were followed. Firstly, the DNA-sequence of one primer of the primer pair spanned an intron/exon boundary of the specific gene of interest. Thus, the primers will anneal only to the cDNA synthesized from the spliced mRNAs, but not to cDNA from unspliced RNA or genomic DNA. Secondly, the primers flanked at least one intron. If the intron(s) are large enough only amplicons of the cDNA should be formed. Otherwise, the products amplified from the cDNA will be smaller than those amplified from genomic DNA. Thus, they can be distinguished by size.

2.5.2 RT

2.5.2.1 Reagents

High capacity cDNA reverse transcriptase kit (Applied Biosystems)

2.5.2.2 Method

For cDNA synthesis, 1 µg of total RNA was reverse transcribed using random primers, according to the manufacturer's instructions. Controls without reverse transcriptase were carried out to exclude the possibility of DNA contamination. Subsequently, a PCR reaction

using primers specific for human β -actin was performed in order to control the success of the RT.

2.5.3 PCR

2.5.3.1 Reagents

HotStarTaq DNA Polymerase kit (Qiagen)

Reagents for agarose gel electrophoresis

- sample buffer [40 % glycerol (Merck KGaA), 60 % ddH₂O, 0.01 % bromphenol blue (Merck KGaA)]
- agarose (Sigma-Aldrich)
- 0.5x TBE [45 mM Tris (Roche), 4 mM boric acid (Merck KGaA), 1 mM EDTA (Merck KGaA), adjustment to pH 8]
- 0.5 μ g/ml EtBr (Sigma-Aldrich)

Primer (Eurofins MWG, see appendix)

2.5.3.2 Method

PCR analysis was carried out in 20 μ l reactions using cDNA equivalents of 20 ng of RNA. The reactions were carried out according to the manufacturer's instructions. Detection of mRNA for the human β -actin served as endogenous reference gene expression for HMEC-1 cells and PBMCs. The PCR amplification parameters were one initial 15-min denaturation step followed by 26 (β -actin) or 35 cycles (gp130, IL-6R α , Ob-Rb and VEGFR-2) of denaturation, annealing, and elongation (95 °C for 15 s, specific T_A for 30 s, and 72 °C for 30 s, respectively) and a final step at 72 °C for 10 min.

Finally, sample buffer was added to each sample prior to loading onto a 1 % agarose gel containing 0.5 μ g/ml EtBr and 0.5x TBE as buffer. For detection of PCR products a UV transilluminator was used and the results recorded using a digital camera (INTAS UV Systeme, Intas Science Imaging Instruments).

2.5.4 qRT-PCR

2.5.4.1 Reagents

TaqMan® Universal PCR Master Mix, No Amp Erase UNG (Applied Biosystems)

SYBR® Green PCR Master Mix (Applied Biosystems)

TaqMan® Primer and Probes (Applied Biosystems; see appendix)

Primer for qRT-PCRs with SYBR® Green (Eurofins MWG; see appendix)

2.5.4.2 Method

Quantitative real-time PCRs were carried out in 20 µl reactions using cDNA equivalents of 20 ng of RNA. Reagents for qRT-PCR and the ABI 7700 sequence detection system were used according to the manufacturer's instructions. 18S rRNA and the mRNA of the gene for glyceraldehydes-3-phosphate dehydrogenase (GAPDH) served as endogenous reference for SGBS cells and HMEC-1 cells. Samples were analysed at least in duplicate using one initial activation-step at 95 °C for 10 min, and, subsequently, 40 cycles of denaturation, annealing and elongation (95 °C for 30 s, 60 °C for 30 s, 72 °C for 45 s, respectively). This was followed by melting curve analysis when SYBR® Green was used (95 °C for 15 s, 60 °C for 15 s, gradual heating to 95 °C within 20 min, 95 °C for 15 s)

For quantitation of qRT-PCR data, the $\Delta\Delta C_t$ method (Livak and Schmittgen, 2001) was employed where the expression of the target gene is normalized to the expression of the endogenous reference gene and compared with the expression of the untreated controls.

2.6 Measurement of adipokines in CM

2.6.1 Theoretical Background

Adipokine concentrations were measured in the CM by sandwich ELISAs (Engvall and Perlmann, 1971; Lequin, 2005; Van Weemen and Schuurs, 1971) and multiplex bead-based Luminex® assays (Elshal and McCoy, 2006; Horan and Wheelless, 1977; Morgan *et al.*, 2004). Both methods are highly sensitive, specific and rapid immunochemical tests used to detect molecules that have antigenic properties in a given sample.

2.6.1.1 ELISA

The sandwich ELISA measures the amount of antigen between two layers of antibodies therefore two different antibodies (capture antibody and detection/primary antibody) are used. They are specific for the same antigen, but bind to different antigenic sites. First, the capture antibody is bound to an ELISA microplate surface; this is followed by a blocking step in order to prevent non-specific binding. Next, the antigen-containing sample is added to the plate. The antigen binds to the capture antibody and is immobilized. Extensive washing steps remove the unbound constituent parts of the sample. Next, the detection or primary antibody binds to the captured antigen and a “sandwich” is formed. Washing removes the excess of unbound primary antibody. An enzyme-linked secondary antibody (e.g. HRP-linked secondary antibody) is added which binds specifically only to the Fc-region of the detection antibody. A final washing step removes excess unbound secondary antibody. A suitable substrate (e.g. TMB) is applied which is converted by the enzyme into a colour or fluorescent signal. Next, the absorbance or fluorescence is measured.

2.6.1.2 Multiplex bead-based Luminex® assays

This technology is used to simultaneously detect secreted proteins or signal transduction molecules within a single sample and applies the principle of a sandwich ELISA. In contrast to the ELISA, the capture antibody is attached to polystyrene beads and not to a microplate well. The beads are internally dyed with different ratios of two spectrally distinct fluorophores (red and near-infrared). Such, they can be distinguished from each other (Probst *et al.*, 2003). The detection of cytokine-bound beads is achieved with phycoerythrin (PE)-labelled streptavidin which binds to the biotinylated detection antibodies.

2.6.2 Reagents

ELISA kits for adiponectin (R&D Systems), leptin (R&D Systems), MCP-1 (eBioscience), PAI-1 (Technoclone), and IL-6 (eBioscience)

Bio-plex cytokine reagents (Bio-Rad)

Bio-plex cytokine assays for IL-8, VEGF 121 and 165, TNF α , IL-1 α , IL-1 β , IFN γ , RANTES, IL-4, IP-10 and SDF-1 α (Bio-Rad)

2.6.3 Method

Adiponectin, leptin, MCP-1, PAI-1, and IL-6 were measured in the CM by ELISA, with the detection limits of 3,9 ng/ml, 15,6 pg/ml, 62,5 pg/ml, 3,8 ng/ml and 12,5 pg/ml, respectively. The assays were performed according to the manufacture's instructions. The protein concentrations for IL-8, VEGF 121 and 165, TNF α , IL-1 α , IL-1 β , IFN γ , RANTES, IL-4, IP-10 and SDF-1 α in the CM were measured by a multiplex bead-based Luminex® assay. The detection limits were depending on the analyte and varied between 1 and 10 pg /ml. The assay was performed according to the manufacture's instructions. The data of the CM were normalized to the total protein content of the corresponding cells.

2.7 Protein determination

2.7.1 Bicinchoninic acid (BCA) method

2.7.1.1 Reagents

BCA Protein Assay Kit including BSA protein standard (Pierce)

2.7.1.2 Theoretical Background and Method

The BCA method (Smith *et al.*, 1985) is based on the Biuret method where a Cu^{2+} ion forms a complex with a peptide bond in alkaline solution and is then reduced to a Cu^+ ion. The extinction of this violet complex can be measured and the protein concentration calculated according to the Beer-Lambert law (Beer, 1852). The sensitivity of the Biuret reaction can be increased in the presence of BCA. Two molecules of BCA chelate a single Cu^{1+} ion, forming a purple water-soluble complex which strongly absorbs light at 562 nm. Protein detection ranges between 0.5 $\mu\text{g/ml}$ and 2 mg/ml . The assay was carried out in 96-well microplates and protein detection was performed according to the manufacturer's instructions. BSA was used for the protein standard curve.

2.7.2 Modified Bradford method

2.7.2.1 Theoretical Background

This method is based on the Bradford procedure (Bradford, 1976), but is carried out in 96-well microplates. It relies on the ability of Coomassie® Brilliant Blue G-250 to shift its absorbance maximum in an acidic solution from 465 nm to 595 nm when protein binding occurs. More precisely, Coomassie® Brilliant Blue G-250 primarily binds to arginine and to less extent to other aromatic and basic amino acid residues.

2.7.2.2 Reagents

Modified Bradford buffer stock

- 11.5 % H₃PO₄ (Serva)
- 4.75 % ethanol (Roth)
- 0.005 % Coomassie® Brilliant Blue G-250 (Merck KGaA)

Modified Bradford buffer

- Modified Bradford buffer stock
- 7 µl 10 M NaOH (Sigma-Aldrich)/ml Biorad buffer stock

BSA protein standard solutions ranging from 0.5 to 3 µg/µl (Pierce)

2.7.2.3 Method

The assay was carried out in 96-well microplates. 1 µl BSA standard or sample was pipetted at least in duplicate into the appropriate wells. Next, 250 µl of fresh Modified Bradford buffer was added. The plate was placed for at RT 20 min on a shaking platform. Finally, the absorbance was measured at 595 nm using a spectrometer (Varioskan multiwell photo- and fluorometer, Thermo Scientific)

2.7.3 Amido Black method

2.7.3.1 Reagents

Amido Black staining solution

- 0.1 % Amido Black 10B (Merck KGaA)
- 40 % methanol (Roth)
- 40 % acetic acid (Roth)
- 20 % H₂O

Amido Black decolourizer

- 50 % methanol
- 50 % H₂O

BSA protein standard ranging from 0.5 µg to 4 µg (Sigma-Aldrich)

2.7.3.2 Theoretical Background and Method

Amido Black 10B is a diazo dye which is traditionally used to stain precipitated total protein on a membrane (Schaffner and Weissmann, 1973). Here, Amido Black 10B was used to

control and estimate the protein content of samples which were dissolved in sample-buffer prior loading onto a SDS-polyacrylamid-gel. Therefore, a polyvinylidene difluoride (PVDF) membrane was equilibrated in methanol. Next, 1 µl of BSA standard or sample were dotted on the membrane. When the membrane had dried, it was subjected to Amido Black staining solution for 2 min. Unspecific staining of the membrane was removed by Amido Black decolourizer. The comparison of the staining intensities between the samples and the standards by eye allowed estimating the protein content of the samples.

2.8 SDS-Polyacrylamidgelectrophoresis (SDS-PAGE) and Western blot analysis

2.8.1 Theoretical Background

The Western blot technique (Burnette, 1981; Eckert and Kartenbeck, 1997; Towbin *et al.*, 1979) is used for specific protein detection in a given sample of tissue, homogenate or extract. The proteins are separated by SDS-PAGE, transferred to a membrane and finally detected using antibodies. In the loading buffer, the proteins are initially denatured using heat, SDS and mercaptoethanol. SDS destroys hydrogen bonds and hydrophobic and ionic interactions and mercaptoethanol reduces disulfide bonds; thus, a straightened primary structure of the proteins results. After the breakdown of secondary structures, SDS binds to the proteins leading to an attachment of 1.4 g of SDS per 1 g of protein; thus, there is an equal proportion of mass to charge. The samples are then subjected to SDS-PAGE. By using this process the proteins separate according to their sizes.

The negatively charged proteins are transferred from the gel to a nitrocellulose or PVDF membrane by electroblotting (Burnette, 1981; Eckert and Kartenbeck, 1997). A specific primary antibody is then used which recognizes its antigen on the proteins on the blot. Next a secondary antibody binds to the constant region (Fc) of the bound primary antibody. The Fc of the secondary antibody is labelled with HRP. In the presence of H₂O₂ and alkaline conditions HRP oxidizes cyclic diacylhydrazides, such as luminol which is then in an excited state. This chemiluminescent reaction emits light at a maximum emission of 428 nm for up to one hour and can be detected by exposure of the membrane to a blue-light sensitive autoradiography film.

2.8.2 Reagents

Radioimmunoprecipitation assay buffer (RIPA-buffer)

- 50 mM tris-HCl pH 7.4 (Sigma-Aldrich)
- 1 % nonyl enoxyl-polyethoxylethanol (NP-40; Sigma-Aldrich)
- 0.25 % SDS (Sigma-Aldrich)
- 150 mM NaCl (Sigma-Aldrich)
- 1 mM EDTA (Merck KGaA)
- 1 mM phenylmethanesulfonyl-fluoride (PMSF; Sigma-Aldrich)
- 1 mM dithiothreitol (DTT; Omni Life Science)
- 10 mM NaF (Sigma-Aldrich)
- 1 tablet/10 ml Complete Mini (Roche)
- 1 tablet/10 ml PhosStop (Roche)

5 x Loading buffer

- 300 mM Tris-HCL pH 6.8
- 5 % SDS
- 40 % glycerol (Merck KGaA)
- 0.05 M DTT
- 2.5 mM EDTA
- 0.01 % bromphenol blue (Merck KGaA)

SDS-PAGE:

Running gel

- 7.5-10 % acrylamide (Roth)
- 375 mM Tris-HCl pH 8.8
- 1 % SDS
- 1 % Ammonium persulfate (APS; Sigma-Aldrich)
- 0.04 % (v/v) tetramethyl-ethylenediamine (TEMED; Roth)

Stacking gel

- 5 % acrylamide
- 125 mM Tris-HCl pH 6.8
- 1 % SDS
- 0.75 % APS
- 0.1 % (v/v) TEMED
- 0.005 % bromphenol blue

10x Running buffer (pH 8.3)

- 250 mM Tris (Roche)
- 2 M glycine (Merck KGaA)
- 1 % SDS

Transfer:

Transfer buffer anode 1 (pH 10.4)

- 0.3 M tris
- 20 % (v/v) methanol (Roth)

Transfer buffer anode 2 (pH 10.4)

- 25 mM tris
- 20 % (v/v) methanol

Transfer buffer cathode 1 (pH 9.4)

- 25 mM tris
- 40 mM aminocaproic acid (Merck KGaA)
- 20 % (v/v) methanol

Hybond P PVDF transfer membrane (GE Healthcare)

1 x TBST washing buffer

- 20 mM tris-HCl pH 7.2
- 140 mM NaCl (Sigma-Aldrich)
- 0.1 % Tween 20 (Sigma-Aldrich)

Ponceau S solution

- 0.5 % Ponceau S (Sigma-Aldrich) in 1 % acetic acid (Roth)

ECL advance blocking reagent (GE Healthcare)

ECL advance solution A and B (GE Healthcare)

Antibodies (see appendix)

2.8.3 Method

Whole cell lysates were prepared from HMEC-1 cells, SGBS cells and human PBMC. PBMC were obtained from whole blood of healthy individuals, collected in BD Vacutainer cell preparation tubes containing sodium heparin as an anticoagulant, and were processed according to the instruction from BD Biosciences. For whole cell lysates, cells were lysed in ice-cold RIPA-buffer containing protease and phosphatase inhibitors for protein extraction. After centrifugation at 12,000 g at 4 °C for 5 min the supernatants containing the total soluble proteins were dissolved in loading buffer and heated at 95 °C for 5 min according to Laemmli (Laemmli, 1970). Next, the protein samples were separated by SDS-PAGE. SDS-PAGE was performed by using generally 20 µg protein sample, 5 % acrylamide stacking gels, 7.5-10 % acrylamide running gels and 1x running buffer. Next, the proteins were semi-dry electroblotted onto a PVDF-membrane, using the anode 1-, anode 2-, and cathode 1- transfer buffers. Next, the membranes were stained with Ponceau S solution in order to assure protein transfer to the membrane and to visualize equal protein load of the samples. The next steps were carried out according to the manual instructions of the ECL-Advanced System. Briefly, after a blocking step at RT for 1h, the membranes were incubated with the primary antibody at 4 °C overnight. After extensive washing with TBST, the membrane was incubated with HRP-conjugated secondary antibody at RT for 1h and then again washed with TBST. Immunoreactive bands were visualised with the ECL Advanced solutions A and B. Densitometric scanning was performed to quantify the intensities of the bands (ImageQuantTL, Amersham Biosciences).

2.9 Methods to monitor adipocyte differentiation

2.9.1 Glycerinphosphate dehydrogenase (GPDH) assay

2.9.1.1 Theoretical Background

GPDH is an enzyme which catalyzes the reversible reaction between dihydroxyacetone phosphate and glycerol 3-phosphate with nicotinamide adenine dinucleotide (NADH+H⁺/NAD⁺) as coenzyme. GPDH activity rapidly increases upon differentiation of preadipocytes into adipocytes. Consequently, GPDH activity is used as major indicator for this process (Skurk *et al.*, 2006; Van Harmelen *et al.*, 2004). NADH+H⁺ has its maxima of adsorption at 260 nm and 340 nm and NAD⁺ only at 260 nm. A decrease in NADH+H⁺ is accompanied by a decrease in adsorption at 340 nm. Since the amount of dihydroxyacetone phosphate is proportional to the amount of converted NADH+H⁺ the turnover of dihydroxyacetone phosphate can be indirectly measured using the Beer-Lambert law.

2.9.1.2 Reagents

GPDH harvest buffer

- 0.05 M tris-HCl pH 7.4 (Roche)
- 1 mM EDTA (Sigma-Aldrich)
- 1 mM mercaptoethanol (Sigma-Aldrich)

GPDH reaction buffer

- 0.12 M triethanolamin-HCl pH 7.5 (Sigma-Aldrich)
- 3 mM EDTA
- 1.4 mM nicotinamidadeninucleotide (NADH; Sigma-Aldrich)
- 0.6 mM mercaptoethanol

2.4 mM dihydroxyacetone phosphate (DHAP; Sigma-Aldrich)

2.9.1.3 Method

GPDH activity was determined as described elsewhere (Wise and Green, 1979) with the following modifications: SGBS preadipocytes at day 0 and day 16 and adipocytes at day 16 after induction of differentiation were detached in GPDH harvest buffer on ice with a cell scraper and sonicated. After centrifugation at 10 000 g at 4 °C for 10 min, GPDH activity was determined in the supernatants by measuring the NADH+H⁺ consumption. Therefore, the cell lysate (150 µl for preadipocytes and 10 µl for adipocytes) was mixed with water (280 µl for preadipocytes and 420 µl for adipocytes) and 65 µl GPDH reaction buffer. The reaction was initiated by adding 5 µl DHAP. The absorption at 340 nm was determined at 25 °C for 5 min using a spectral photometer. GPDH mU/ml was calculated from the linear NADH+H⁺ consumption related to the protein content (mg/ml) of the cell extracts which was determined by the Modified Bradford Assay.

2.9.2 Oil Red O/Haematoxylin staining

2.9.2.1 Theoretical Background

Oil Red O is a diazo lipophilic dye and stains neutral triglycerides and lipids deep red. This dye has been successfully used to monitor the differentiation process of adipocytes (Fukumoto and Fujimoto, 2002; Jaiswal *et al.*, 2000). Metal-haematein complexes, haematein being oxidized haematoxylin, stain cell nuclei by binding to basophilic structures such as nucleic acids (Romeis and Böck, 1989).

2.9.2.2 Reagents

PBS with Ca²⁺ and Mg²⁺

- 1 tablet PBS per 200 ml dH₂O, sterile filtration (Sigma-Aldrich)
- 0.84 mM MgCl₂ (Merck KGaA)
- 0.72 mM CaCl₂ (Merck KGaA)

4 % PFA (Sigma-Aldrich) in PBS with Ca²⁺ and Mg²⁺

0.3 % Oil Red O (Sigma-Aldrich) in isopropanol (Roth), filtered

Mayer`s Hematoxylin solution (ready to use; Merck KGaA)

2.9.2.3 Method

The Oil Red O stain method was performed as described elsewhere (Lillie and Ashburn, 1943) and with the following modifications: SGBS cells were washed twice with PBS, fixed with 4 % PFA for 10 min and washed again twice with PBS. Next, the cells were incubated with Oil Red O for 1h on a shaking platform. Then, the cells were washed twice with water. Haematoxylin was added and the cells incubated for 5 min on a shaking platform. The stained cells were then repeatedly washed with hot water and examined under a microscope.

2.9.3 Nile Red

2.9.3.1 Theoretical Background

Nile Red is a hydrophobic, fluorogenic stain which may be used with live or fixed cells for the detection of intracellular lipid droplets (Greenspan *et al.*, 1985). The dye also interacts with other hydrophobic structures and its fluorescence is strongly influenced by the polarity of its environment (Sackett and Wolff, 1987).

2.9.3.2 Reagents

PBS with Ca²⁺ and Mg²⁺

- 1 tablet PBS per 200 ml dH₂O, sterile filtration (Sigma Aldrich)
- 0.84 mM MgCl₂ (Merck KGaA)
- 0.72 mM CaCl₂ (Merck KGaA)

4 % PFA (Sigma Aldrich) in PBS with Ca²⁺ and Mg²⁺

Nile Red stock solution

- 1 mg/ml Nile Red (Invitrogen) in DMSO (Roth)

Nile Red working solution

- 1 µg/ml Nile Red in PBS

2.9.3.3 Method

This method was carried out as described elsewhere (Tiller *et al.*, 2009) and with the following modifications. SGBS cells were washed twice with PBS, fixed with 4 % PFA for 10 min, washed again twice with PBS and incubated with 60 % isopropanol for 3-5 min. This was followed by incubation with the Nile Red working solution for 60 min. Next, the cells were washed twice with PBS. The cells were examined under the microscope (fluorescence

microscope DMIL and camera DC300, Leica Microsystems). Alternatively, the Nile Red stained SGBS cells were exposed to 100 % isopropanol for 15 min in order to dissolve the bound dye for quantification of the degree of adipocyte differentiation. The fluorescence was measured at 550 nm and 638 nm using a spectrometer (Varioskan multiwell photo- and fluorometer, Thermo Scientific). In these experiments, undifferentiated control cells were measured in parallel in order to determine the degree of unspecific binding of Nile Red to other hydrophobic cell structures. The data were corrected for this background fluorescence.

2.10 Peptidomics

2.10.1 Theoretical Background and Method

Peptidomics is defined as the systematic, comprehensive, qualitative and quantitative multiplex analysis of endogenous peptides in a biological sample at a defined time point and location. These peptides are either intact small molecules (hormones, cytokines, growth factors) or represent degradation products of proteins due to proteolytic cleavage (Schulte *et al.*, 2005; Zucht *et al.*, 2005). With the method as described elsewhere (Budde *et al.*, 2005; Zucht *et al.*, 2005), molecules with sizes between 1 kDa to 15 kDa can be detected. The peptidomic analysis of CM derived from SGBS preadipocytes and adipocytes was performed by the company Digilab BioVisioN (Hannover, Germany). For sample collection, SGBS adipocytes and control preadipocytes were washed once with 4 ml MCDB 131 w/o phenol red medium (PAN Biotech) and fed with 1 ml MCDB 131 w/o phenol red medium per well of a 6-well cell culture plate at day 15 after induction of differentiation. 24 hrs later, the medium was harvested and centrifuged at 1000 g at 4 °C for 10 min and filtered through a 0.2 µm filter. Next, 100 µl of the medium were removed for protein concentration analysis. To the remaining medium 5 µl/ml 30% HCL was added. The samples were snap frozen in liquid nitrogen and stored at -80 °C until shipment. The samples were “blinded” before being sent to the company with the following coding (#): #1: adipocyte-CM derived of cells under normoxia, #3: adipocyte-CM derived of cells under 1 % hypoxia, #4: preadipocyte-CM derived of cells under normoxia, #6: preadipocyte-CM derived of cells under 1 % hypoxia. For the peptidomic-analysis, the complexity of the samples was reduced by the extraction of peptides and separation by liquid chromatography by hydrophilicity into 96 fractions using an 4-40 % (v/v) acetonitrile gradient on a conventional reverse phase column. Each fraction was then subjected to mass spectrometry using the ABI 4700 MALDI TOF-TOF mass

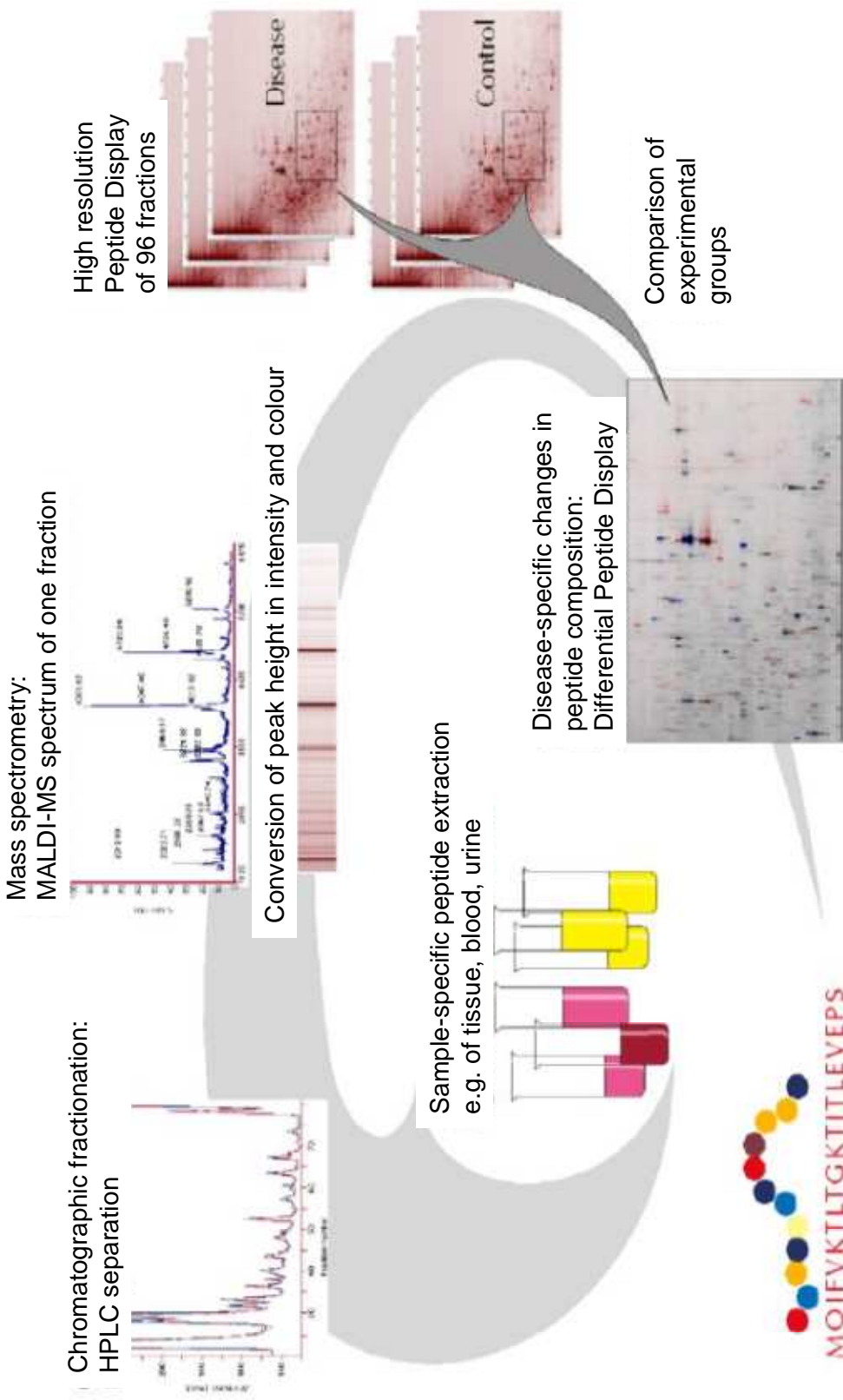
spectrometer. After mass spectrometry data processing the data of each sample was transferred into an “in house”-database which also contained information on the peptide display of WAT supernatants. The liquid chromatography and mass spectrometry data were visualized as 2D peptide displays containing the information of the mass to charge ratio of the peptides on the horizontal axis, the elution profile (96 fractions, separated by hydrophilicity) on the vertical axis and the signal intensity shown as colour. An overview of the process is given in figure 4. As quality control each sample was spiked with a mixture of standard peptides to monitor the sample processing. In order to obtain the 2D peptide display, the data were pre-processed which involved a baseline correction procedure and a mass to charge ratio of the peptide-recalibration of the mass spectrometric data.

Unfortunately the company went bankrupt and the sample analysis, including peptide sequencing, was delayed and finally stopped. However, it was possible to receive data of a few “in silico annotated” peptides. This means that the profile (defined mass and defined fraction number) of candidate peptides is matched to the profile of already identified peptides using the database. This database also contained information on peptides found in CM of human WAT. Since the identity of these annotated peptides is only a prediction, their biochemical identification must be confirmed in the respective material such as CM by a preparative approach and peptide sequencing of the isolated peptide spot. Further techniques to detect the candidate peptides in the CM or in case of proteolytic cleavage products of proteins are Western blot and other immuno techniques such as sensitive ELISAs or radioimmunoassays (RIA). The expression of the genes encoding the peptides or proteins can be analysed in the RNA of the corresponding SGBS cells by qRT-PCR.

2.11 Statistical analysis

Results were obtained by at least three independent experiments if not stated otherwise. All data are presented as means \pm SE. Statistical comparisons between two groups were analysed by Student's *t*-test and between several groups by one-way analysis of variance (ANOVA) followed by Student-Newman-Keuls *t*-test. Probability values of $P < 0.05$ were considered statistically significant. For data analysis the computer programs different versions of Microsoft Excel, SPSS 11 and GraphPad Prism 4 were used.

Figure 4 Overview of the peptide profiling process.



The picture was taken from the Digilab BioVision report from 30 May 2008

3 Results

3.1 Culture conditions of SGBS cells and HMEC-1 cells

3.1.1 Introduction

In order to study the cross-talk between human preadipocytes/adipocytes and microvascular endothelial cells an appropriate coculture system had to be established. SGBS cells were found to be suitable to study human preadipocytes and adipocytes (Wabitsch *et al.*, 2001) and HMEC-1 cells to study human microvascular endothelial cells (Ades *et al.*, 1992; Bouis *et al.*, 2001). The indirect coculture strategy was chosen where the CM of SGBS cells was used to stimulate HMEC-1 cells. The initial experiments were performed to establish a cell culturing strategy which is suitable for both, endothelial cells and preadipocytes/adipocytes. In this respect, the following situation for SGBS and HMEC-1 cells had to be considered. The basal medium of HMEC-1 cells is MCDB- 131 which contains 5 mM glucose. In contrast, the basal medium of SGBS cells, which is DMEM/F12 contains 25 mM glucose. Moreover, the media have different compositions of amino acids, vitamins and salts (Table 1). It is important to note that high glucose levels lead to endothelial dysfunction *in vitro* and *in vivo* causing there micro- and macrovascular complications (Bakker *et al.*, 2009; Salameh *et al.*, 1997; Stenina, 2005; Varma *et al.*, 2005). Moreover, high glucose concentrations cause impairment of insulin stimulated glucose uptake, disturbance of the insulin signalling pathway and cytokine secretion pattern of adipocytes at least *in vitro* (Lin *et al.*, 2005; Renstrom *et al.*, 2007).

Table 1 Comparison of the components of DMEM/F12 and MCDB 131 medium

	DMEM/F12	MCDB 131
Components		
Amino acids		
Glycine	250 µM	30.67 µM
L-Alanine	50 µM	30.34 µM
L-Arginine hydrochloride	699.05 µM	299.53 µM
L-Asparagine-H2O	50 µM	100 µM
L-Aspartic acid	50 µM	100 µM
L-Cysteine hydrochloride-H2O	99.77 µM	/
L-Cystine 2HCl	99.97 µM	198.86 µM
L-Glutamic acid	50 µM	29.93 µM
L-Histidine hydrochloride-H2O	149.91 µM	200 µM
L-Isoleucine	415.8 µM	503.82 µM
L-Leucine	450.76 µM	1000 µM
L-Lysine hydrochloride	498.63 µM	994.54 µM
L-Methionine	115.71 µM	100.67 µM
L-Phenylalanine	215.03 µM	200 µM
L-Proline	150 µM	100 µM
L-Serine	250 µM	304.76 µM
L-Threonine	449.16 µM	100.84 µM
L-Tryptophan	44.22 µM	20.1 µM
L-Tyrosine	/	100 µM
L-Tyrosine disodium salt dihydrate	213.76 µM	/
L-Valine	451.71 µM	1000 µM
Vitamins		
Ascorbic acid phosphate	8.63 µM	/
Biotin	14 nM	29.9 nM
Choline chloride	64.14 µM	100 µM
D-Calcium pantothenate	4.7 µM	25.16 µM
Folic acid	6.01 µM	/
Folinic acid calcium salt	/	1.17 µM
Niacinamide	16.56 µM	50 µM
Pyridoxine hydrochloride	9.71 µM	10.2 µM
Riboflavin	582 nM	10.1 nM
Thiamine hydrochloride	6.44 µM	10.09 µM
Vitamin B12	502 nM	10 nM
i-Inositol	70 µM	40 µM

	DMEM/F12	MCDB 131
Components		
Inorganic salts		
Ammonium metavanadate NaVO3	3 nM	4.9 nM
Ammonium molybdate ((NH4)6Mo7O24-4H2O)	/	3 nM
Calcium chloride (CaCl2) (anhyd.)	1.05 mM	1.6 mM
Cupric sulfate (CuSO4-5H2O)	5 nM	4.8 nM
Ferric nitrate (Fe(NO3)3·9H2O)	124 nM	/
Ferric sulfate (FeSO4-7H2O)	1.5 µM	1.02 µM
Magnesium chloride (anhyd.)	301.47 µM	/
Magnesium sulfate (MgSO4) (anhyd.)	0.41 mM	10.02 mM
Manganese sulfate (MnSO4-H2O)	/	1.2 nM
Nickelous chloride NiCl2 6H2O	/	0.3 nM
Potassium chloride (KCl)	4.16 mM	3.97 mM
Selenious acid H2SeO3	/	29.5 nM
Sodium bicarbonate (NaHCO3)	29.02 mM	14 mM
Sodium chloride (NaCl)	120.61 mM	110.86 mM
Sodium phosphate dibasic (Na2HPO4) (anhyd.)	0.5 mM	0.5 mM
Sodium phosphate monobasic (NaH2PO4-H2O)	452.9 µM	/
Sodium meta silicate Na2SiO3 9H2O	/	9.86 µM
Zinc sulfate (ZnSO4-7H2O)	3000 nM	1 nM
Sodium selenite	29 nM	/
Other Components		
Adenine	/	1 µM
D-Glucose (Dextrose)	25 mM	5 mM
Ethanolamine	19.48 µM	/
Hypoxanthine Na	15 µM	/
Linoleic acid	150 nM	/
Lipoic acid	510 nM	10.2 nM
Phenol red	21.52 µM	32.94 µM
Putrescine 2HCl	503 nM	1.2 nM
Sodium pyruvate	1 mM	1 mM
Thymidine	1508 nM	99.2 nM

3.1.2 HMEC-1 cell proliferation using different basal media

Firstly, HMEC-1 cell proliferation was examined using different mixtures of MCDB 131 and DMEM/F12 as basal media. Using light microscopy (Figure 5A) and BrdU analysis (Figure 5B) a cell growth decrease of HMEC-1 cells, morphology changes and cell death were observed with increasing amounts of DMEM/F12 as basal medium. Thus, it was necessary to proliferate the HMEC-1 cells according to the standard protocol using MCDB 131 as basal medium.

3.1.3 SGBS proliferation using different basal media

As for HMEC-1 cells, SGBS cells were proliferated in different mixtures of MCDB 131 and DMEM/F12 as basal media. Microscopy (Figure 6A) and BrdU (Figure 6B) analysis showed a decrease of SGBS cell growth with increasing concentrations of MCDB 131 as basal medium. Moreover, the differentiation rate of SGBS cells was impaired when the cells were proliferated in medium containing MCDB 131 as basal medium (observed data) and so SGBS cells were proliferated in the traditional medium containing DMEM/F12 as basal medium.

3.1.4 Differentiation capacity of SGBS cells using different basal media

In contrast, differentiation of SGBS cells in a mixture of 2/3 MCDB 131 and 1/3 DMEM/F12 did not affect the differentiation capacity of SGBS cells when those were proliferated ahead in the traditional proliferation medium containing DMEM/F12 as basal medium. This was examined by microscopy (Figures 7A and B) and measuring Nile Red fluorescence (Figure 7C) and GPDH activity (Figure 7D). Consequently, the SGBS cells were differentiated in later experiments in the above mentioned ratio of basal media mixture with a final glucose concentration of 11.6 mM. For 3T3-L1 cells it has been shown before that the differentiation capacity of preadipocytes to adipocytes does not decrease when lower glucose concentrations than 25 mM are used (Gagnon and Sorisky, 1998). However, the morphology of the adipocytes appeared to change. A greater number of small lipid droplets could be observed by microscopy using 5 mM glucose versus big lipid droplets using 25 mM glucose (data not shown). This trend was also found in this experimental setup (Figures 7A and B).

Figure 5 HMEC-1 cell proliferation

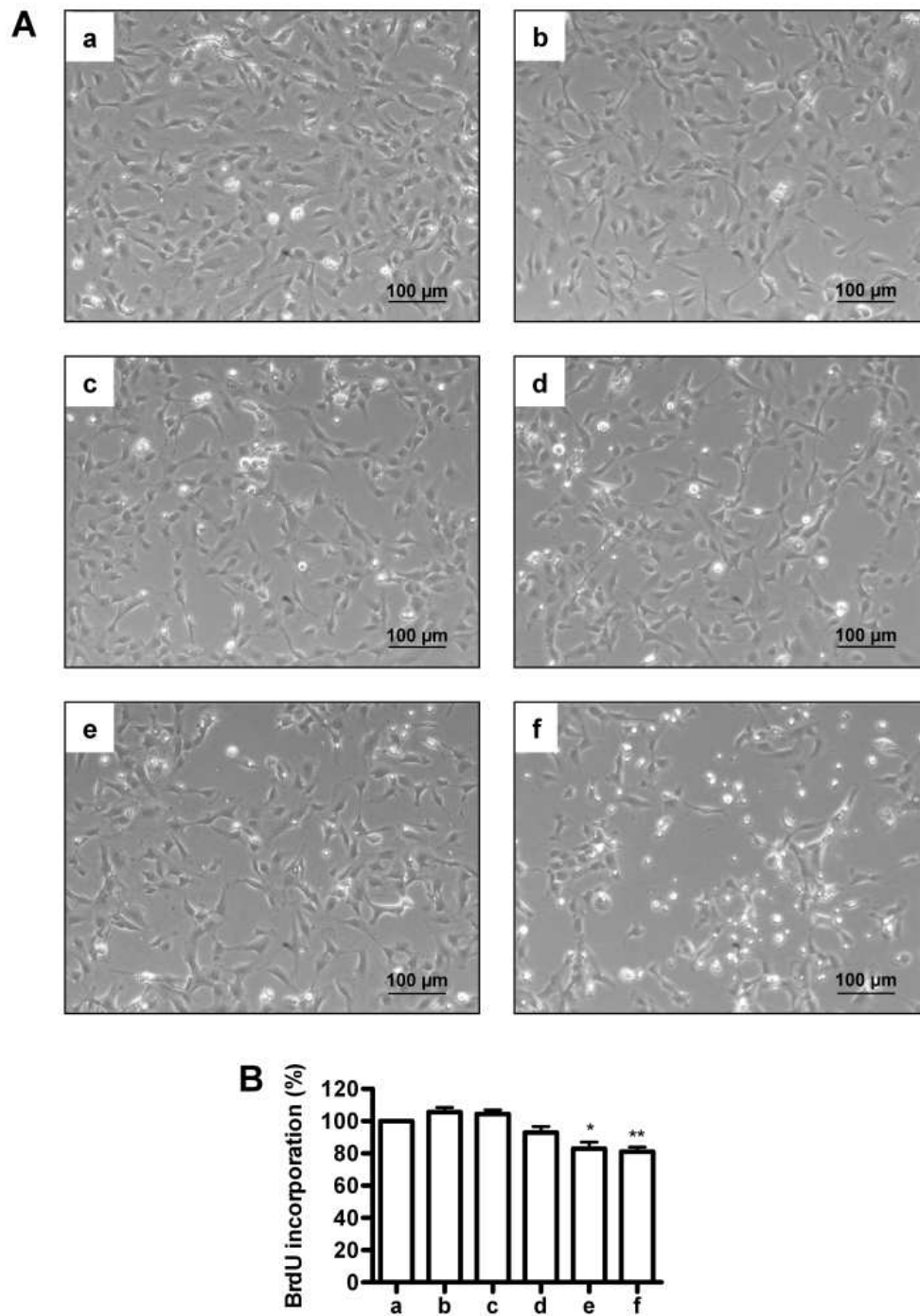


Figure 5

HMEC-1 cells were proliferated in HMEC-1 medium as positive control (*a*) or in different cell culture media mixtures containing 10 % FCS (*b-f*). The media mixtures were as follows: *b*: MCDB 131 medium, *c*: MCDB 131/ DMEM/F12 medium, ratio 3:1, *d*: MCDB 131/ DMEM/F12 medium, ratio 1:2, *e*: MCDB 131/ DMEM/F12 medium, ratio 1:3 and *f*: DMEM/F12 medium. Phase contrast microscopy (*A*) and BrdU incorporation as proliferation assay (*B*) were used for examination. For the analysis of the experiments in *B* the obtained fluorescence data from the positive control (*a*) were considered as 100 %. Results are means \pm SE ($n=3$). * $P<0.05$, ** $P<0.01$.

Figure 6 SGBS cell proliferation

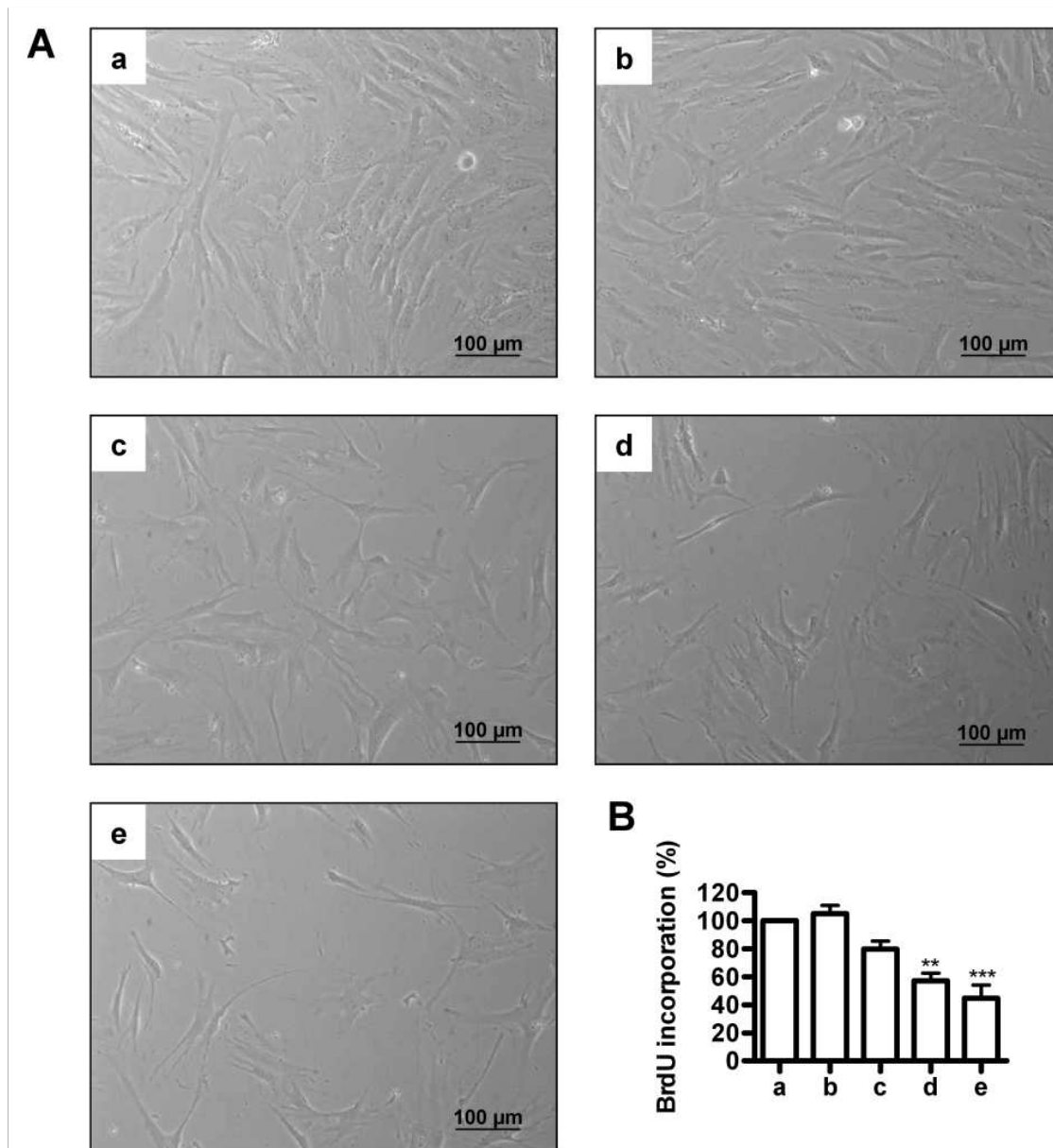


Figure 6

SGBS cells were proliferated in different cell culture media mixtures containing 10 % FCS (*a-e*). The media mixtures were as follows: *a*: DMEM/F12 medium (positive control), *b*: DMEM/F12/MCDB 131 medium, ratio 3:1, *c*: DMEM/F12:MCDB 131 medium, ratio 1:2, *d*: DMEM/F12:MCDB 131 medium, ratio 1:3, *e*: MCDB 131 medium. Phase contrast microscopy (*A*) and BrdU incorporation as proliferation assay (*B*) were used for examination. For the analysis of the experiments in *B* the obtained fluorescence data from the positive control (*a*) were considered as 100 %. Results are means \pm SE ($n=3$). ** $P<0.01$, *** $P<0.001$.

Figure 7 SGBS cell differentiation capacity using different basal media

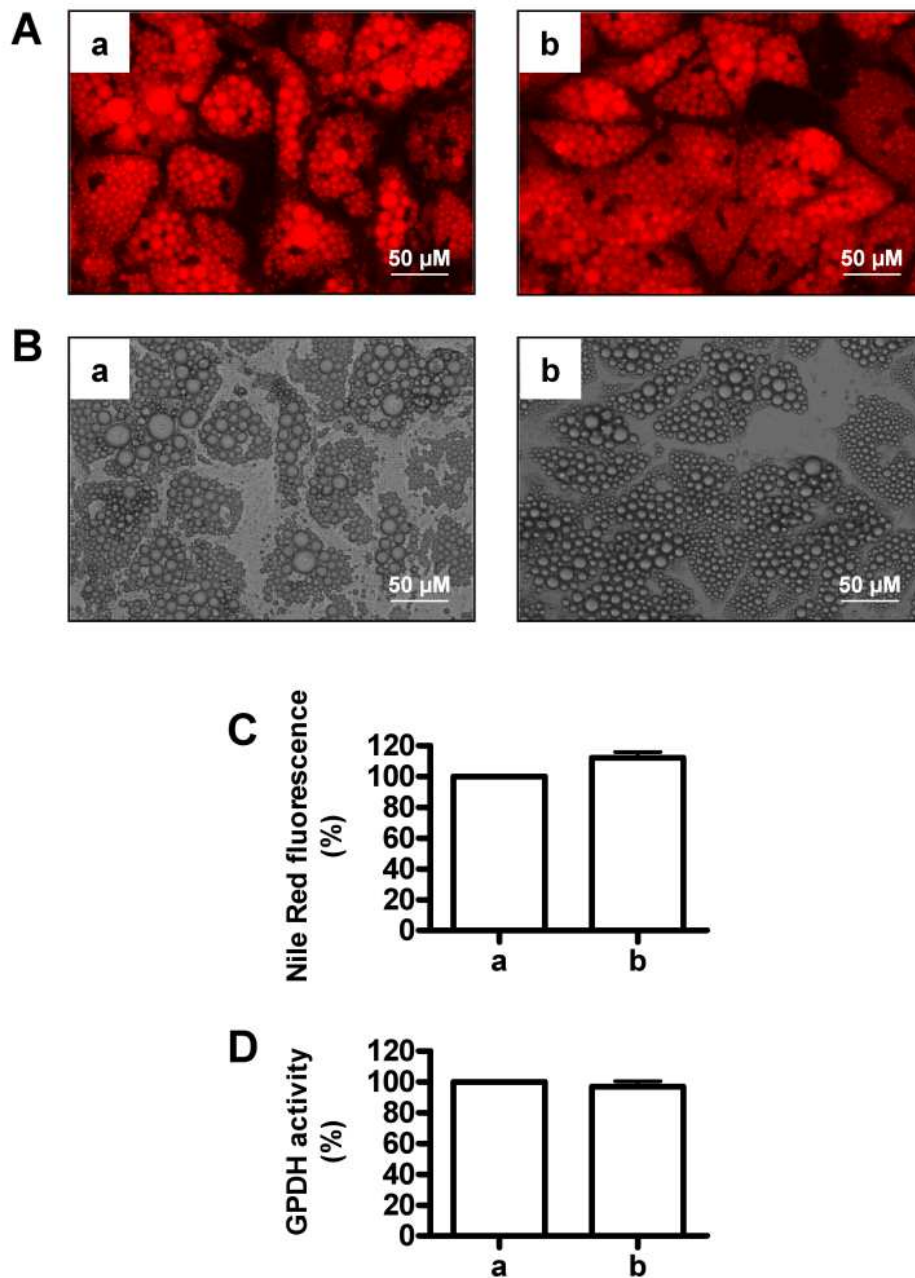


Figure 7

SGBS cells were examined after 16 days post-induction of differentiation. Cells fed post-induction using as basal medium either DMEM/F12 (*a*) or MCDB 131/DMEM/F12, ratio 3:1 (*b*). Fluorescence (*A*) and phase contrast (*B*) microscopy visualized the Nile Red stained cells. The degree of differentiation was assessed quantitatively by Nile Red fluorescence (*C*) and GPDH activity (*D*). For the analysis of the experiments in *C* and *D*, the obtained fluorescence data or GPDH activity respectively, from the condition *a* were considered as 100 %. Results are means \pm SE (n=3).

3.1.5 Differentiation time course of SGBS cells

The efficient differentiation of SGBS cells cultured in a basal medium mixture of 2/3 MCDB 131 and 1/3 DMEM/F12 is shown in a differentiation time course (Figure 8). The confluent preadipocytes at day 0 (Figure 8A) were induced to differentiate from preadipocytes into adipocytes by the addition of induction medium. By day 4 (Figure 8B) the preadipocytes had started to develop into adipocytes, showing first signs of lipid accumulation. To visualize the lipid cells were specifically stained with Oil Red O. Lipid droplets appeared as red coloured dots in the cells under the microscope. By day 8 (Figure 8C) the accumulation of small lipid droplets within the cells was universal. The adipocytes continued to increase lipid accumulation and the size of lipid droplets (Figures 8D and E) reaching a maximum around day 14 to 16 (Figure 8F) at which point the lipid droplets were most pronounced. At that time, adipocyte differentiation was observed in $\geq 80\%$ of the cells.

3.1.6 Coculture between SGBS and HMEC-1 cells

In this study the indirect coculture approach was chosen by using CM from SGBS cells to stimulate starved HMEC-1 cells (Figure 9). “Starving” cells means to deprive them of FCS and other additives to force the cells to enter the same cell cycle phase, namely, the G₀ phase. Moreover, pre-activated cells may decrease their level of activation. Thus, the cells may be more sensible and react more homogeneously on stimuli. HMEC-1 cells are generally starved ahead of experiments (BelAiba *et al.*, 2007; Sapet *et al.*, 2006; Wang *et al.*, 2004). Since HMEC-1 cells need MCDB 131 as basal medium it was necessary that the SGBS-CM used in the coculture experiments with HMEC-1 cells was based on MCDB 131. SGBS cell differentiation was performed in serum-free 2/3 MCDB 131 and 1/3 DMEM/F12 as basal medium mixture. Therefore, a last adaptation step for SGBS cells before CM were taken, was necessary. In order to exclude stress effects on SGBS cells when changing the basal medium, they were cultured for several hours in MCDB 131 medium before the medium was changed again and left for generally 24 hours on the SGBS cells to generate the CM. Changing the media did not effect negatively the cell culture. A scheme of the cell culture strategy is shown in figure 10. Since differentiating SGBS cells are cultured over a period of 14 days in medium containing insulin, hydrocortisol, T3 and transferrin, control preadipocytes were cultured in

parallel but were not induced to differentiate. The characterisation of these cells is shown in chapter 3.2.4 and 3.2.3.

Figure 8 SGBS cell differentiation time course

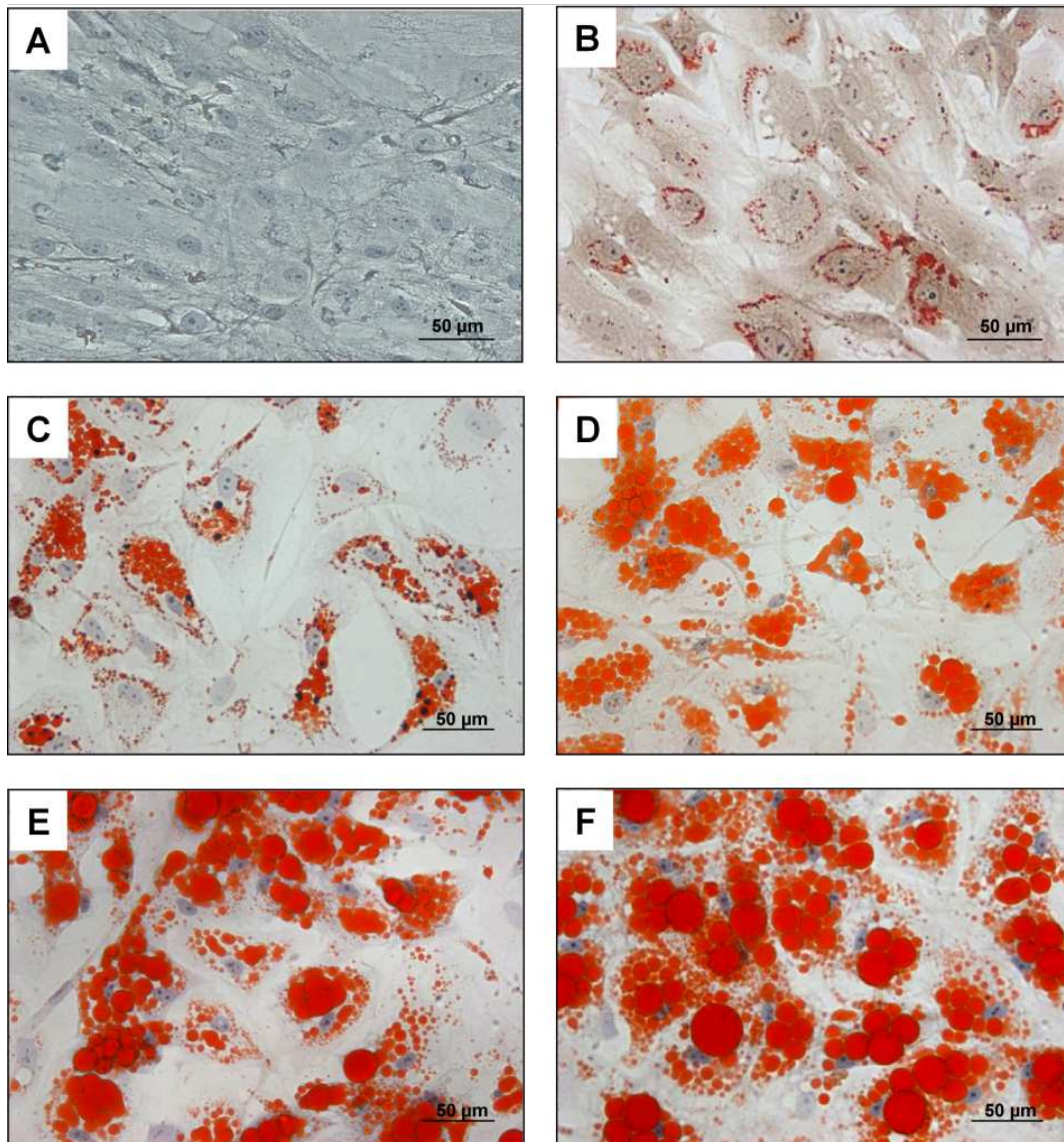


Figure 8
Phase contrast microscopy of SGBS cells prior to induction of differentiation (day 0; *A*), and post-induction on day 4 (*B*), day 8 (*C*), day 10 (*D*), day 12 (*E*) and day 16 (*F*) stained with Oil Red O (red) and haematoxylin (blue).

Figure 9 HMEC-1 cell culture

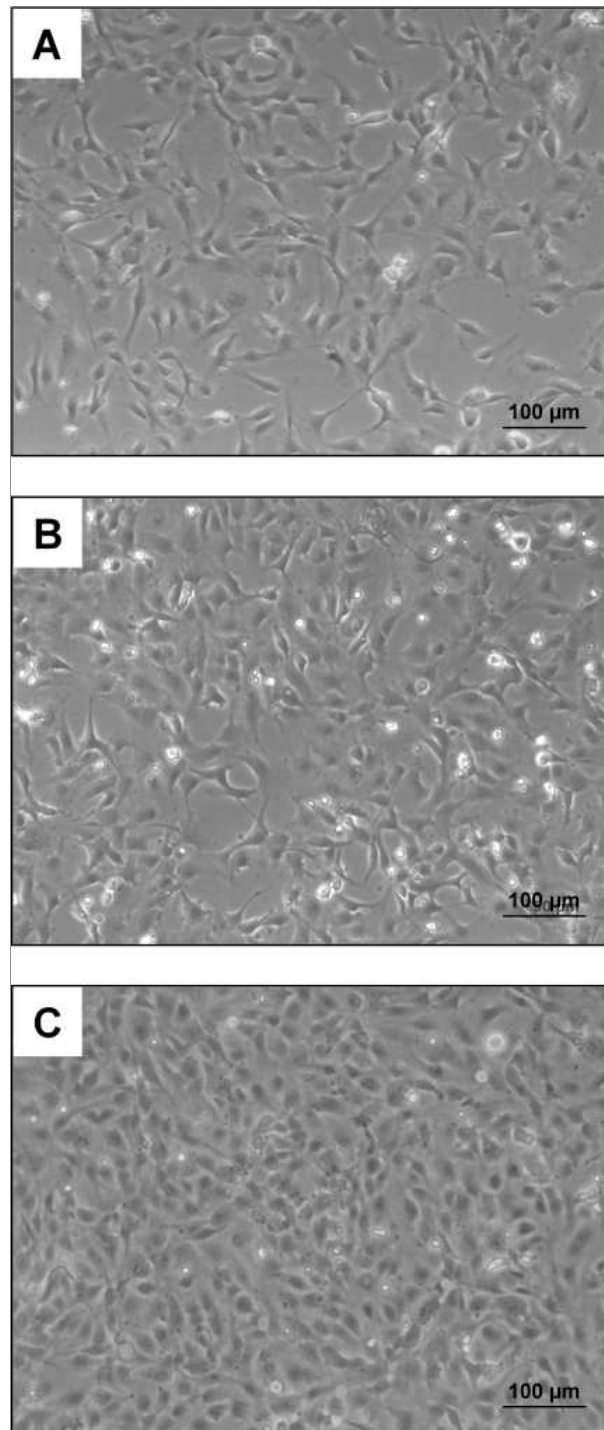


Figure 9
HMEC-1 cells were proliferated in HMEC-1 medium. Pre-confluent cells at approximately 40 % confluence (A), 70 % confluence (B) and confluence (C) were visualized by phase contrast microscopy. The confluent HMEC-1 cells display the typical endothelial phenotype with clear and defined cell borders (cobblestone appearance).

Figure 10 Scheme of the cell culture strategy

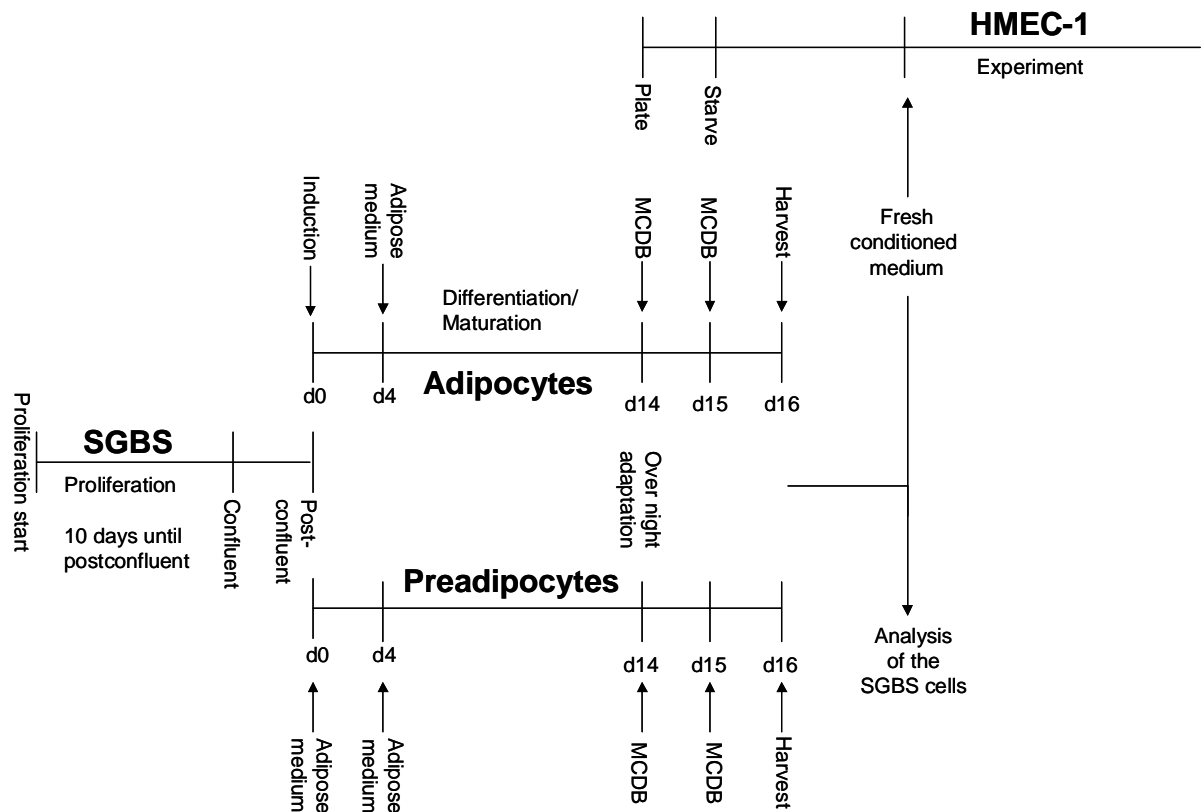


Figure 10

SGBS cells were seeded at low densities until post-confluence occurred 10 days later. Next, the cells were exposed to induction medium and the control preadipocytes were exposed to adipose medium (d0). After four days (d4) the medium was changed to adipose medium until day 14 post-induction (d14). For adaptation, the cells were exposed from day 14 to day 15 to MCDB 131 medium. In order to generate conditioned media (CM), the cells were cultured from day 15 to day 16 for 24 hrs in MCDB 131 medium. The CM were either used for analysis or for treatment of starved HMEC-1 cells.

3.2 Gene expression and cytokine secretion of SGBS preadipocytes and adipocytes

3.2.1 Introduction

For further characterization and in order to get more insights into the secretory capacity of SGBS cells, adipokine-mRNAs and -proteins at different times and under different conditions were measured. Therefore, the analysis was focused on the following adipokines: leptin, adiponectin, PAI-1, IL-6, VEGF, MCP-1, IL-8, RANTES, SDF1- α , IL-4, IL-1 α , IL-1 β , TNF- α and IFN- γ . Leptin and adiponectin (see chapters 1.2.2.1 and 1.2.2.2) are typically secreted by WAT and reach the blood stream. PAI-1 (Alessi and Juhan-Vague, 2006) is involved in vascular haemostasis and IL-6 (see chapter 1.2.2.3) in inflammatory processes. VEGF is important in vascular remodelling (see chapter 1.2.2.4). MCP-1, IL-8, RANTES, SDF-1 α are chemoattractants (see chapter 1.2.2.5). IL-4 has anti-inflammatory features but can act in concert with TNF- α and IL-1 as endothelial cell activator (Petzelbauer *et al.*, 1993). IL-1 and TNF- α are potent pro-inflammatory proteins and activator of endothelial cells (see chapter 1.2.7.1). Detailed information about the conducted experiments and fold-changes are presented in the corresponding figure legends.

3.2.2 Cytokine expression and secretion of SGBS preadipocytes and adipocytes

The measurements of selected adipokines using qRT-PCR, ELISAs and multiplex bead-based Luminex® assays, revealed that the mRNA expressions and/or protein secretions of PAI-1, IL-6, VEGF and the chemoattractants MCP-1, IL-8 (Figure 11A) and SDF-1 α (Figure 11B) were significantly higher in preadipocytes than in adipocytes. The mRNA for RANTES (Figure 11A) was slightly stronger expressed at mRNA level in adipocytes compared with preadipocytes whereas at protein level it was the opposite. However, both observations were not statistically significant. In order to elucidate whether classical endothelial cell activators besides VEGF were expressed or secreted by preadipocytes and adipocytes a selected panel of molecules including TNF- α , IL-1, IFN- γ (Figure 12) and IL-4 (Figure 11) was analysed. IL-4 (Figure 11) protein secretion was higher in preadipocytes as compared with adipocytes. IL-1 α gene expression in preadipocytes was robust after 30 amplification cycles by qRT-PCR

compared with weak signals for adipocytes. However, at protein level IL-1 α was at the detection limit. In contrast, IL-1 β gene expression was measured after 25 amplification cycles in adipocytes versus 31 cycles in preadipocytes. As for IL-1 α , IL-1 β protein was also at the detection limit. TNF- α gene expression was weak in preadipocytes (after 36 cycles) and not observed in adipocytes. Moreover, in the supernatants of preadipocytes and adipocytes TNF- α and also IFN- γ protein were at the detection limit. As expected, adiponectin, an adipocyte marker, was measured at high levels at mRNA (after 20 cycles, data not shown) and at protein level in adipocytes (220 ng/ml), but not in preadipocytes (Figure 11B). Interestingly, leptin expression was detected, not only in adipocytes, but also in subconfluent preadipocytes. An increase in leptin expression was observed in confluent preadipocytes (data not shown), as reported previously for primary preadipocytes (Simons *et al.*, 2005).

3.2.3 Adipokine secretion of SGBS cells cultured in the presence and in the absence of hormones and antibiotics

Analyses using specific ELISAs for PAI-1, IL-6 and MCP-1 were performed in order to get insights into the cytokine secretion of SGBS cells cultured from day 14 to day 16 either according to the standard protocol in adipose medium or according to the protocol used to generate the CM for coculture experiments. Adipose medium contains hydrocortisone, insulin, T₃ and Pen/Strep. Insulin and other hormones are known to change the cytokine secretion pattern of several cell types, including adipocytes (Fain and Madan, 2005; Wabitsch *et al.*, 1996). For coculture experiments, CM of SGBS cells deprived of hydrocortisone-, insulin-, T₃- and Pen/Strep were used (see chapter 3.1.6). The protein concentrations of the three obesity relevant cytokines PAI-1, IL-6 and MCP-1 were measured in these CM and compared with the CM of SGBS cells cultured in adipose medium in the presence of the above mentioned hormones and antibiotics (Figure 13). PAI-1 secretion did not change in preadipocytes and adipocytes. Interestingly, IL-6 secretion increased in preadipocytes and adipocytes when the cells were deprived of the indicated hormones and antibiotics, although this effect was not statistically significant for the adipocytes. Moreover, MCP-1 secretion was significantly elevated in adipocytes when cultured in medium lacking hormones and antibiotics. The opposite trend was observed for the preadipocytes but was not statistically significant. It is important to note, that the applied cell culture protocols affected the cells in their behaviour of cytokine secretion. As a consequence and in order to allow a comparison between preadipocytes and adipocytes in gene expression, cytokine secretion and the effect of

their CM on endothelial cell activation, the preadipocytes were always cultured in parallel in the same media as the adipocytes, except for the induction to differentiate.

3.2.4 Comparison of the morphology, GPDH activity and adipokine secretion in SGBS preadipocytes at confluence and after 16 days culture period

Since confluent preadipocytes (Pd0) were cultured for another 16 days (Pd16) in the same media as differentiating adipocytes except that they were not induced to differentiate (see chapter 3.1.6 and 3.2.3), it was investigated whether differences in morphology, GPDH activity and cytokine secretion between Pd0 and Pd16 occurred. Therefore, phase contrast microscopy was performed (Figures 14A and B) and GPDH activity (Figure 14C) and the adipokines PAI-1, IL-6 and MCP-1 (Figure 14D) measured by specific ELISAs. Small morphology changes between day 0 and day 16 preadipocytes were observed. Nevertheless, the preadipocytes kept the image of fibroblastic-like cells over the culture period (Figure 14A and B). Generally, no lipid accumulation was found which is in agreement with the GPDH results (Figure 14C). PAI-1 and Il-6 protein release (Figure 14D.) was higher in the confluent preadipocytes (Pd0) in comparison with 16 days postconfluent preadipocytes (Pd16). For MCP-1 release (Figure 14D.), no changes were observed.

Figure 11 Comparison of the preadipocyte and adipocyte gene expression and protein secretion of selected adipokines

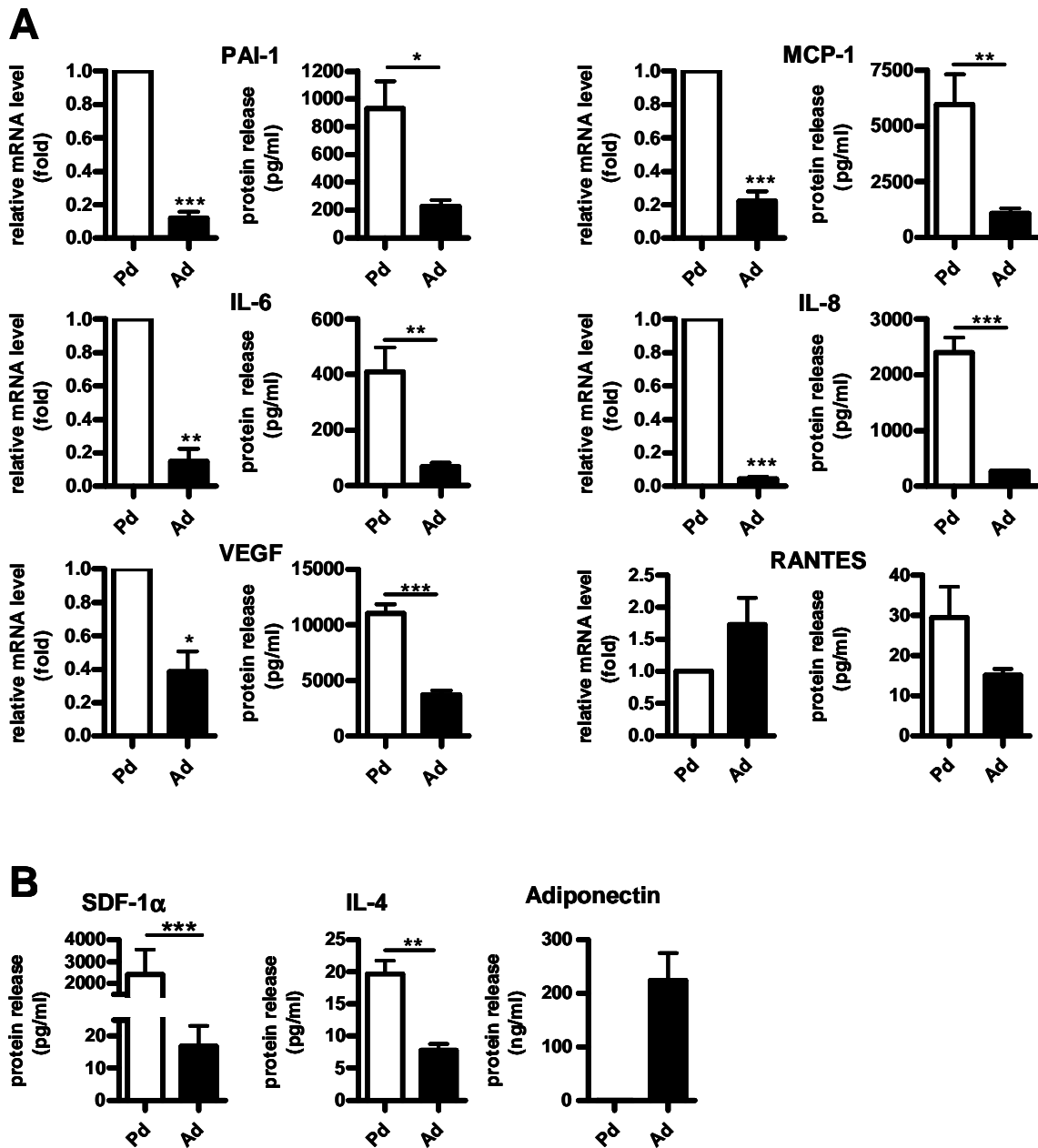


Figure 11

A: adipokine mRNA levels were quantified by qRT-PCR and adipocyte (Ad) values are presented as relative expression compared with values of the corresponding preadipocytes (Pd). Adipokine concentrations in conditioned media (CM) were quantified by specific ELISAs or bead-based Luminex assays. The relative differences between the values for mRNA and protein of Pd and Ad are 8- and 4.1-fold for PAI-1, 6-fold and 6-fold for IL-6, 2.5- and 3-fold for VEGF, 4.5- and 5.5-fold for MCP-1, 20- and 8.9-fold for IL-8. No differences for RANTES were observed. B: a 140-fold difference was measured for SDF-1 α protein and for IL-4 a 2.6-fold difference. Adiponectin concentration of 220 ng/ml was measured for Ad-CM whereas adiponectin was not detectable in Pd. Results are means \pm SE (n=4). *P<0.05, **P<0.01, ***P<0.001.

Figure 12 Overview of the preadipocyte and adipocyte gene expression and protein secretion of IL-1 α , IL-1 β , TNF- α and IFN- γ

Preadipocyte versus Adipocyte		
	RNA	Protein
IL-1 α	<p>relative mRNA level (fold)</p> <p>***</p>	values at detection limit (below 10 pg/ml)
IL-1 β	<p>relative mRNA level (fold)</p> <p>*</p>	values at detection limit (below 10 pg/ml)
TNF- α	weak detectable in preadipocytes, not detectable in adipocytes	values at detection limit (below 10 pg/ml)
IFN- γ	not measured	not detectable (detection limit: 10 pg/ml)

Figure 12 Adipokine mRNA levels were quantified by qRT-PCR and are presented as relative expression compared with values of the corresponding preadipocytes (Pd). The relative increase of IL-1 α in Pd vs. adipocytes (Ad) was 18-fold. In contrast, IL-1 β was increased in Ad compared with Pd by 53-fold. Adipokine concentrations in conditioned media were quantified by bead-based Luminex assays with detection limits below 10 pg/ml. Results are means \pm SE (n=4). *P<0.05, ***P<0.001.

Figure 13 Adipokine release of SGBS cells cultured in the presence and absence of hormones and antibiotics

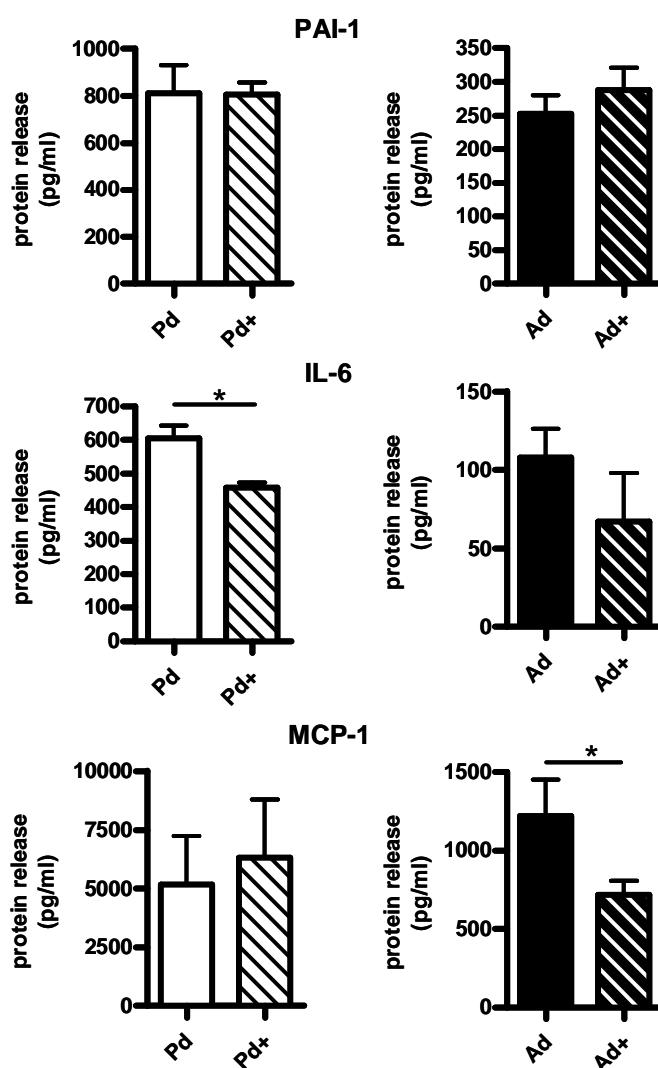


Figure 13 SGBS preadipocytes (Pd) and adipocytes (Ad) were cultured from day 15 to day 16 for 24 hrs in MCDB 131 medium lacking (Pd, Ad) or containing (Pd+, Ad+) 66 nM insulin, 100 mM hydrocortisone, 10 µg/ml T3, 100 U/ml penicillin and 100 µg/ml streptomycin. PAI-1, Il-6 and MCP-1 were measured in the CM by specific ELISAs. Relative differences for IL-6 are 1.3-fold for Pd vs. Pd+ and for MCP-1 1.7-fold for Ad vs. Ad+. Results are means ± SE (n=4). n.s. means statistically not significant. *P<0.05.

Figure 14 Comparison of the GPDH activity and adipokine secretion in SGBS preadipocytes at day 0 and 16 days culture period

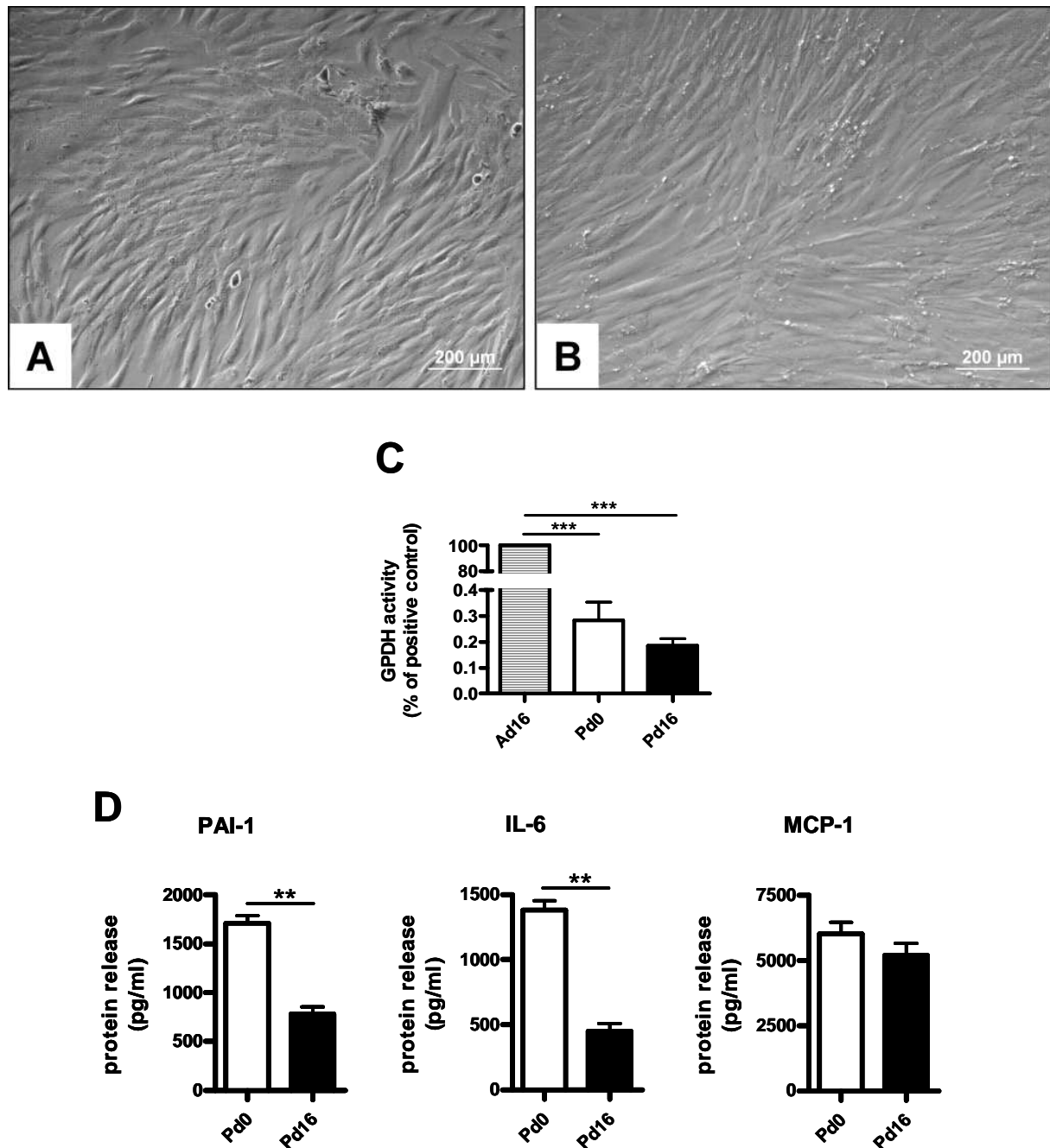


Figure 14 SGBS cells were cultured until confluence (Pd0) and then kept for 16 days in adipose medium (Pd16). Phase contrast microscopy was used to visualize Pd0 (A) and Pd16 (B) cells. The GPDH values of Pd0 and Pd16 cells (C) are illustrated in comparison to differentiated cells (Ad16). Protein secretion by Pd0 and Pd16 cells was measured using specific ELISAs for PAI-1, IL-6 and MCP-1 (D). Relative differences for the secretion by Pd0 compared with Pd16 are 2.2-fold for PAI-1 and 3-fold for IL-6. Results are means \pm SE (n=4). n.s. means statistically not significant. **P<0.01, ***P<0.001.

3.3 Impact of preadipocyte- and adipocyte-CM on HMEC-1 cell activation and signalling pathways

3.3.1 Introduction

In order to investigate the impact of SGBS preadipocyte- and adipocyte-CM on endothelial cell function, RNA and protein expression analysis, functional assays and signalling pathway experiments were conducted. The endothelium serves as the interface between circulating blood immune cells and adipose tissue and plays an interactive role in infiltration and inflammatory processes of immune cells. Therefore, a monocyte-endothelial cell-cell adhesion assay was used as main cell biological read-out system for endothelial activation, which is a change in phenotype or function in endothelial cells in response to stimuli from the environment (Zimmerman *et al.*, 1999). In addition to the monocyte-endothelial cell-cell adhesion assay, an ICAM-1 cell surface ELISA was chosen to characterize this process at the molecular level. The SGBS preadipocytes and adipocytes were subjected to different biologically relevant physiologic/pathophysiologic conditions, including normoxia, hypoxia and TNF- α treatment and their CM were tested as mentioned above. Finally, the impact of CM of mature adipocytes with different sizes isolated from human WAT was analysed on endothelial cell activation. Note, corresponding information about the experiments and fold-changes are presented in the figure legends.

3.3.2 Establishment of a monocyte-endothelial cell-cell adhesion assay and ICAM-1 and VCAM-1 cell surface ELISA

In order to analyse the impact of SGBS-CM on endothelial cell activation, a monocyte endothelial cell-cell adhesion assay and an ICAM-1 and VCAM-1 cell surface ELISA were developed as described in chapter 2.1.6 and 2.2. Microscopic analysis of *Calcein green AM* stained U937 monocytes and of U937 monocytes adhering to HMEC-1 cells is shown in figures 15A and B, respectively. ICAM-1 and VCAM-1 are known to mediate the leukocyte-endothelial cell-cell adhesion. Stimulation of endothelial cells with TNF- α is known to induce ICAM-1 and VCAM-1 cell surface expression and to promote leukocyte adhesion (Johnston and Butcher, 2002; Weber *et al.*, 1995). Therefore, to test TNF- α stimulation as positive control, HMEC-1 cells were treated with different TNF- α concentrations before applied to the assays. The levels of monocytic U937 endothelial cell-cell adhesion (Figure

16A) and ICAM-1 (Figure 16B) and VCAM-1 (Figure 16C) protein expressions increased with increasing TNF- α concentrations. Since stimulation of HMEC-1 cells with 25 ng/ml of TNF- α led to a robust maximum in monocyte adhesion, this concentration was used in further experiments as positive control.

Figure 15 U937 monocyte-HMEC-1 cell adhesion

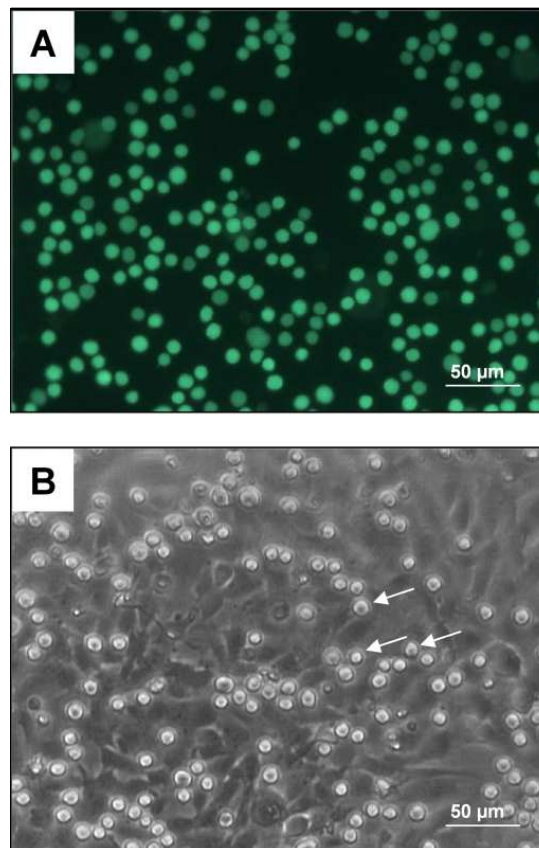


Figure 15
Monocytes were stained with *Calcein green AM* and visualized using fluorescence microscopy (A). Endothelial cells were treated with 25 ng/ml TNF- α for 6 hrs before the monocyte-endothelial cell-cell adhesion assay was performed and phase contrast microscopy used for visualization (B). U937 monocytes (see arrows) adhere to the confluent endothelial cells (B).

Figure 16 Effect of TNF- α on microvascular endothelial cells

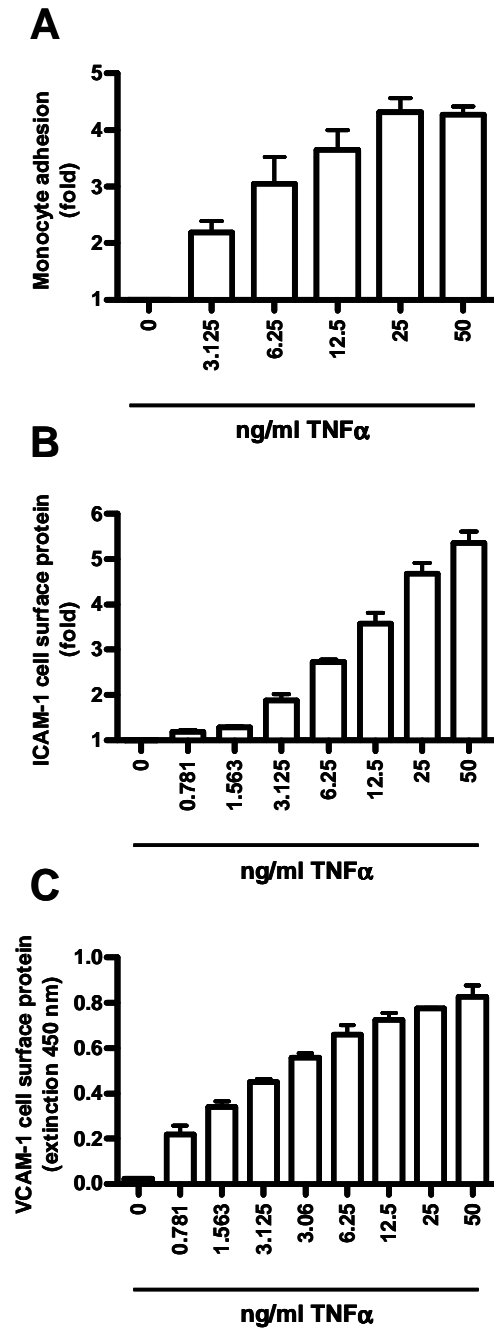


Figure 16
HMEC-1 cells were treated with different concentrations of TNF- α . Subsequently U937 monocyte-endothelial cell-cell adhesion (A) and ICAM-1 (B) and VCAM-1 (C) cell surface expression were analysed. Results are means \pm SE (n=2).

3.3.3 Impact of SGBS preadipocyte- and adipocyte-CM on endothelial ICAM-1 cell surface expression and monocyte-endothelial cell-cell adhesion

To determine the functional impact of CM from SGBS cells on endothelial cell activation, the adhesion of U937 cells to HMEC-1 cells stimulated either with CM or control medium was measured. In addition, ICAM-1 and VCAM-1 endothelial cell surface expression was analysed. The adhesion of U937 cells was substantially increased after preadipocyte-CM treatment compared with control medium whereas after adipocyte-CM treatment, only a modest increase in adhesion was observed, which was statistically not significant. In contrast, TNF- α -stimulated HMEC-1 cells showed a high level of adhesion (Figure 17A). In order to rule out the possibility, that adipocyte-CM did not activate endothelial cells because of the long differentiation period (16 days of culture), the same experiments were performed with CM of adipocytes cultured for only 7 days in adipose medium (less mature adipocytes). No significant differences in endothelial cell activation between these two types of Ad-CM were observed (data not shown). Concordantly with the U937 adhesion experiments, endothelial ICAM-1 expression was significantly upregulated after stimulation with preadipocyte-CM and TNF- α but not with adipocyte-CM (Figure 17B). However, VCAM-1 cell surface expression was neither increased on HMEC-1 cells after stimulation with preadipocyte- nor adipocyte-CM (data not shown) in contrast to incubation with TNF α (Figure 16C). Since the CM mediated monocyte adhesion was independent of VCAM-1 cell surface expression this protein was not further investigated. Next, the endothelial expression of MCP-1 and IL-8 operating as strong activators of monocytes and important for adhesion was assessed (Gerszten *et al.*, 1999). For preadipocyte-CM and adipocyte-CM a marked increase of gene expression for both target genes was measured (Figures 17C and D).

Figure 17 Effects of preadipocyte- and adipocyte-CM on microvascular endothelial cells

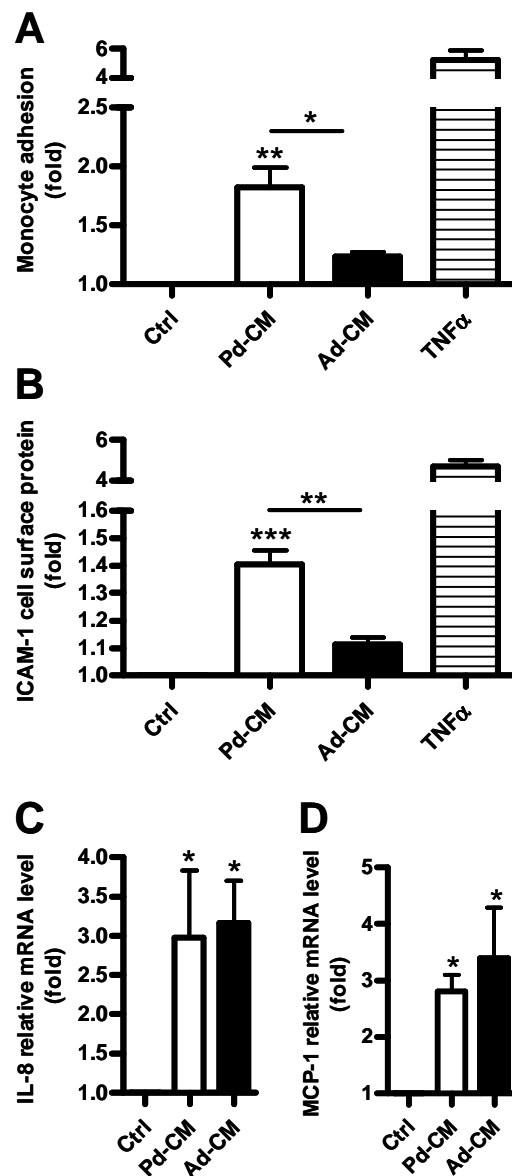


Figure 17

HMEC-1 cells were treated with control medium (Ctrl), preadipocyte-conditioned medium (Pd-CM) and adipocyte-CM (Ad-CM) and subsequently analysed for the adhesion of U937 cells to HMEC-1(A), ICAM-1 cell surface expression (B), and the gene expression of the monocytic activators IL-8 (C) and MCP-1 (D). 25 ng/ml TNF- α was used as a positive control (TNF α). Monocyte adhesion (A) and ICAM-1 (B) increased 1.8- and 1.4-fold after treatment with Pd-CM and 1.2- and 1.1-fold (n.s.) with Ad-CM, respectively, compared with the Ctrl-treatment. Monocyte adhesion and ICAM-1 differences between the treatments with CM were 1.5- and 1.3-fold, respectively. C and D: Gene expression levels of IL-8 (C) and MCP-1(D) increased in HMEC-1 after treatment with Pd-CM and Ad-CM 3- and 2.8-fold vs. 3.2- and 3.4-fold, respectively, compared with the Ctrl. Results are means \pm SE (n \geq 3). n.s. means statistically not significant. *P<0.05, **P<0.01, ***P<0.001.

3.3.4 Impact of concentrated SGBS-CM on monocyte-endothelial cell-cell adhesion

To determine whether the concentration of CM by ultrafiltration lead to an increase in monocyte adhesion and whether the exerted effects could be attributed to low or high molecular substances further analysis was performed (Figure 18). 13x concentrated CM of both preadipocytes and adipocytes, containing only molecules of more than 5 kDa led to an increase in monocyte adhesion. During the concentration process protein or protein activity was lost as can be seen for the TNF- α positive control. 2.5 ng/ml TNF- α was concentrated 10x to achieve presumably a final concentration of 25 ng/ml. When compared with fresh 25 ng/ml TNF- α , the monocyte adhesion is decreased. The unconcentrated CM, only containing molecules of less than 5 kDa, had negligible effects on monocyte adhesion (Figure 18). Consequently, the exerted effects by the CM are likely to be attributed to molecules secreted by SGBS cells of more than 5 kDa which justifies focusing on the analysis of cytokines in the CM of SGBS cells. However, effects of molecules of less than 5 KDa on monocytes adhesion can not be ruled out, since they may act in concert with molecules of more than 5 kDa.

Figure 18 Impact of concentrated SGBS-CM on monocyte-endothelial cell-cell adhesion

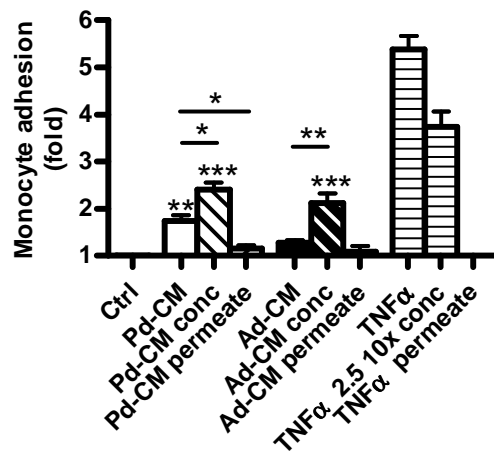


Figure 18

HMEC-1 cells were treated with medium (Ctrl), preadipocyte-conditioned medium (Pd-CM) and adipocyte-CM (Ad-CM) and 10x concentrated (conc) CM, only containing molecules >5kDa (Pd-CM conc, Ad-CM conc) and CM containing only molecules <5kDa (permeate; Pd-CM permeate, Ad-CM permeate). 25 ng/ml TNF- α (TNF- α) was used as positive control. 2.5 ng/ml TNF- α was used in the CM-concentrating procedure to test the efficiency of this technique (TNF- α 2.5 10x conc and TNF- α permeate). Subsequently, the monocyte adhesion assay was performed. The relative increase in monocyte adhesion after stimulation with Pd-CM were 1.7-fold, with Pd-CM conc 2.4-fold, with Ad-CM 1.2-fold (n.s.) and with Ad-CM conc 2.1-fold, compared with the Ctrl-treatment. TNF- α exposure led to a 5.4-fold and with TNF- α 2.5 10x conc 3.7-fold elevation. The permeate treatments showed only baseline levels in monocyte adhesion. Monocyte adhesion differences between Pd-CM and Pd-CM conc were 40 % and between Ad-CM and Ad-CM conc 75 %, respectively. Differences between TNF- α and TNF- α 2.5 10x conc were 45 %. Results are means \pm SE (n \geq 3). n.s. means statistically not significant. *P<0.05, **P<0.01, ***P<0.001.

3.3.5 Impact of TNF- α treated SGBS cells on monocyte endothelial cell-cell adhesion

TNF- α is expressed primarily by macrophages in WAT, can operate as negative regulator of fat storage and induces its own TNF- α gene expression in adipocytes (Haurer *et al.*, 1995; Neels *et al.*, 2006). To examine the direct influence of TNF- α on the endothelial activation capacity of SGBS cells in the absence of macrophages and other paracrine or juxtacrine disturbances, adipokine expression of TNF- α -treated SGBS cells and the impact of their CM on monocyte-endothelial cell-cell adhesion were assessed. TNF- α -stimulation induced a robust TNF- α mRNA expression in preadipocytes and adipocytes (Figure 19A). Fresh CM of TNF- α -stimulated SGBS cells substantially induced the U937 cell adhesion to HMEC-1 (Figure 19B). To rule out that exogenous TNF- α remaining in the CM after TNF- α -stimulation was functional, MCDB 131 medium in the absence of cells without and with TNF- α was kept in the incubator in parallel with SGBS cells as control media and then used in the adhesion assay. For these control media, only baseline levels of adhesion were detected. To test whether CM of TNF- α -induced SGBS cells contained functional TNF- α -activity, CM were pre-incubated with the potent TNF- α -antagonist Enbrel® (Tracey *et al.*, 2008) or mock-pre-incubated before stimulating HMEC-1. The used Enbrel® concentration of 200 ng/ml was sufficient to achieve a maximum of blocking efficiency in the monocyte adhesion assay (Figure 19C). Enbrel®-pre-treatment significantly decreased the monocyte-endothelial cell-cell adhesion to 50% and 28% of the levels achieved with CM of TNF- α -stimulated preadipocytes and adipocytes, respectively (Figure 19D). In order to support these data, total and phosphorylated I κ B α were analysed in HMEC-1 cells (Figure 19E) since TNF- α exerted effects in endothelial cells have been shown to be mediated via the Nf κ B-signalling pathway (Weber *et al.*, 1995). I κ B α phosphorylation was increased in HMEC-1 cells after treatment with CM of TNF- α exposed SGBS cells and abrogated when these CM were preincubated with Enbrel®, although not to baseline levels. For total I κ B α the opposite was observed.

Figure 19 Effects of TNF- α -stimulated preadipocytes and adipocytes on microvascular endothelial cell activation

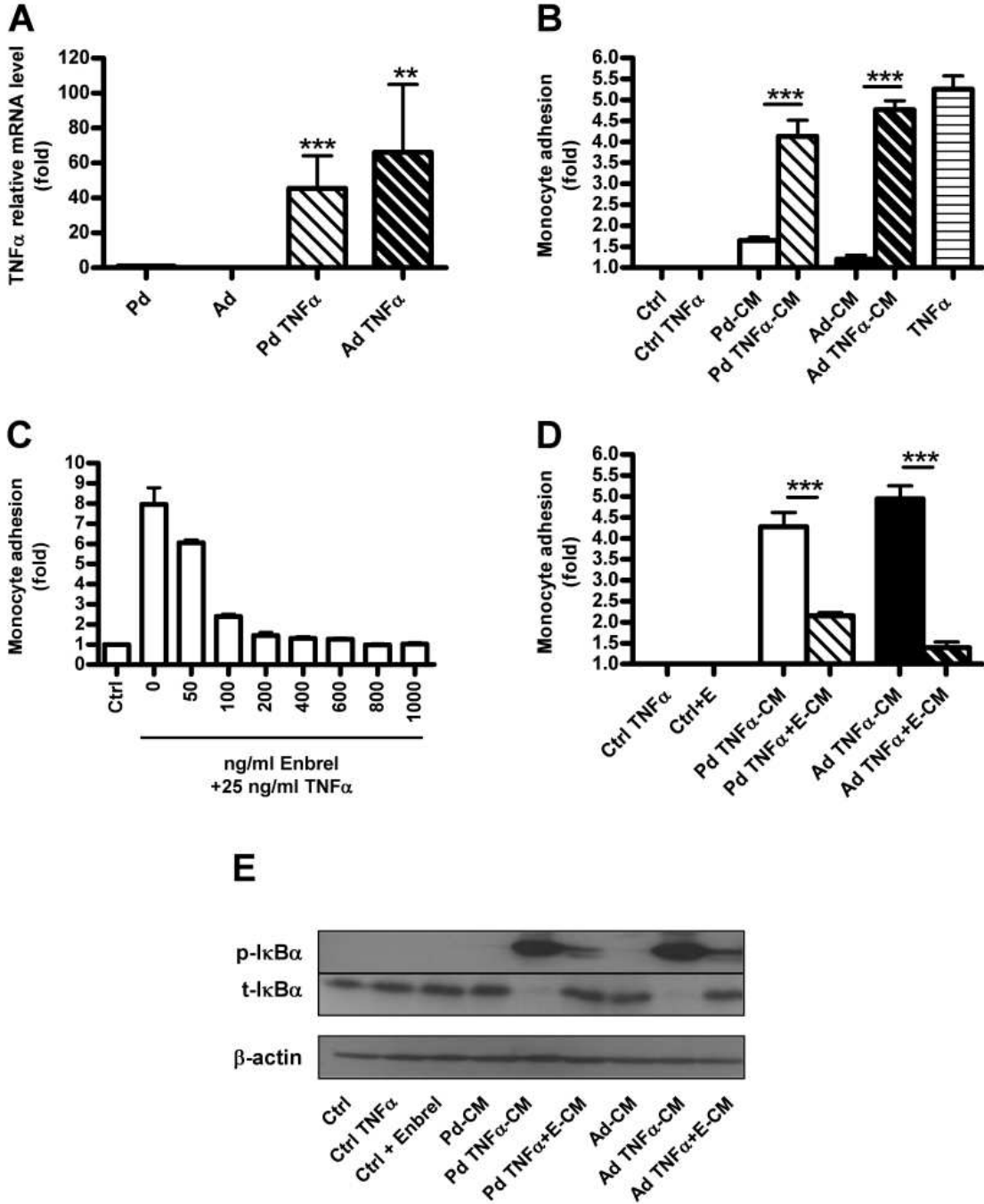


Figure 19

A: TNF- α gene expression of preadipocytes (Pd) and adipocytes (Ad) was assessed after treatment with either medium (Pd, Ad) or 25 ng/ml TNF- α (Pd TNF- α , Ad TNF- α) for 24 hrs. TNF- α gene expression was 46 ± 19 - and 66 ± 38 -fold in TNF- α -treated Pd and Ad, respectively, compared with untreated Pd. No TNF- α was detectable in untreated Ad. The conditioned media (CM) were used for stimulating HMEC-1 cells. Subsequently, the adhesion of U937 cells to HMEC-1 cells (B-D) and total (t-) and (p-) phosphorylated I κ B α in HMEC-1 cells (E) using Western blotting, was assessed. To rule out that the exogenous TNF- α remaining in the CM after TNF- α -stimulation was functional, MCDB-131 medium without (Ctrl) and with 25 ng/ml TNF- α (Ctrl TNF- α) were kept in the incubator at 37 °C for 24 hrs as control medium and then used in the adhesion assay (B and D) or for Western blot analysis (E). For these control media only baseline levels of adhesion and t- and p-I κ B α were detected. B: In contrast, monocyte adhesion to HMEC-1 increased 1.7-fold with Pd-CM, 1.2-fold (n.s.) with Ad-CM, 4.1-fold with CM of TNF- α -treated Pd (Pd TNF α -CM) and 4.7-fold with CM of TNF- α -treated Ad (Ad-TNF α -CM). Fresh TNF- α added to MCBD-131 medium at 25 ng/ml was used as a positive control (TNF α ; 5.3-fold increase). The enhancement in monocyte adhesion with CM derived from TNF- α -treated Pd and Ad were 2.5- and 3.9-fold, respectively. C: TNF- α (25 ng/ml) exerted monocyte-endothelial cell-cell adhesion was blocked using several concentrations of the TNF- α receptor blocker Enbrel®. D: For blockade of TNF- α -activity, CM from TNF- α -induced SGBS cells and control media were preincubated with 200 ng/ml Enbrel® (Pd TNF α +E-CM, Ad TNF α +E-CM, Ctrl+E), a soluble TNF- α receptor antagonist, at 37 °C for 10 min before stimulating HMEC-1. Monocyte adhesion was induced 4.3- and 2.2-fold after treatment with Pd TNF α -CM and Pd TNF α +E-CM, respectively, when compared with the Ctrl. Monocyte adhesion was induced 4.9- and 1.4-fold after treatment with Ad TNF α -CM and Ad TNF α +E-CM, respectively, compared with the Ctrl. The Enbrel®-treatment of CM from Pd and Ad decreased the monocyte adhesion 2.0- and 3.6-fold, respectively. E: signals for p-I κ B α were strong in HMEC-1 cells after treatment with Pd TNF α -CM and Ad TNF α -CM and decreased after treatment with Pd TNF α +E-CM and Ad TNF α +E-CM, respectively. The opposite is shown for t-I κ B α . β -actin served as loading control. Results for A, B and D are means \pm SE (n=3) and for C and E (n=2). n.s. means statistically not significant. *P<0.05, **P<0.01, ***P<0.001.

3.3.6 Impact of hypoxia on adipokine gene expression and secretion of SGBS cells and analysis of their CM on endothelial cell activation

Since WAT mass expansion can generate a hypoxic environment (see chapter 1.2.6) it is of interest to find out how the different cell types in WAT react to hypoxia and how this influences their cross-talk. *In vitro* experiments are important to get valuable insights into these complex interactions. Thus, CM of SGBS cells exposed to normoxia, moderate (4% O₂) and/or severe hypoxia (1% O₂) were used for comparative studies applying endothelial cell proliferation and monocyte-endothelial cell-cell adhesion assays and adipokines measurements. CM of hypoxia-treated preadipocytes and adipocytes increased the cell proliferation of HMEC-1 at similar rates (Figure 20A). Monocyte-endothelial cell-cell adhesion was enhanced with preadipocyte-CM and significantly induced with adipocyte-CM compared with CM of normoxic SGBS cells (Figure 20B). Importantly, CM of hypoxic adipocytes significantly induced the endothelial ICAM-1 cell surface expression, whereas CM of hypoxic preadipocytes did not further reinforce the already high endothelial ICAM-1 expression induced by CM of normoxic preadipocytes (Figure 20C). A gradual and pronounced upregulation of the hypoxia-sensitive transcription factor HIF-1 α (see chapter 1.2.6) was measured to similar amount for preadipocytes and adipocytes under hypoxia demonstrating the impact of hypoxia on SGBS cells (Figure 20D). Adipokine gene expression and secretion of preadipocytes and adipocytes under 4% and 1% hypoxia were analysed using qRT-PCR and specific ELISAs or bead-based Luminex® assays. An overview of the results shown in Figure 21 is given in Table 2. For adipokine secretion of preadipocytes and adipocytes under 4% hypoxia, an increase of VEGF, leptin, PAI-1 and IL-6 in CM was measured which was strongly enhanced under 1% hypoxia (Figure 21A). The corresponding gene expression data for VEGF and leptin are in agreement with the protein secretion data. In contrast, gene expression for PAI-1 and IL-6 increased in SGBS cells under hypoxia but did not change with the degree of hypoxia (Figure 21A). Adiponectin secretion in adipocytes was not altered by hypoxia, although at mRNA level a decrease was observed (Figure 21A). For MCP-1, an upregulation of secretion was observed in preadipocytes whereas at mRNA level no significant changes were found (Figure 21B). In adipocytes a decrease of MCP-1 secretion was measured under 1% hypoxia (Figure 21B) which is in agreement with the gene expression data. A similar secretion pattern was observed for IL-8, although the IL-8 increase in preadipocytes and the decrease in adipocytes under 1% hypoxia was not statistically significant (Figure 21B). Moreover, RANTES secretion of preadipocytes and adipocytes

increased under 4 % hypoxia and was strongly enhanced in preadipocytes under 1 % hypoxia whereas in adipocytes only baseline levels were observed (Figure 21B). At gene expression level no significant differences were observed (Figure 21B). IL-4 known as endothelial cell co-activator together with IL-1 and TNF- α (Petzelbauer *et al.*, 1993) was significantly increased in preadipocyte-CM and adipocyte-CM under 1 % hypoxia (Figure 21B). Interestingly, SDF1- α showed a trend towards enhancement in CM of preadipocytes exposed to hypoxia (Figure 21B) however, these results were not statistically significant. The proteins of the cytokines IL-1, TNF- α and IFN- γ were measured at detection limit (Figure 21C). In contrast, at mRNA level IL-1 α increased in adipocytes exposed to 1 % hypoxia. TNF- α gene expression was elevated in preadipocytes under 4 % hypoxia whereas under 1 % hypoxia no change was observed.

Figure 20 Effects of hypoxia on HIF-1 α protein in preadipocytes and adipocytes and their CM on microvascular endothelial cell activation

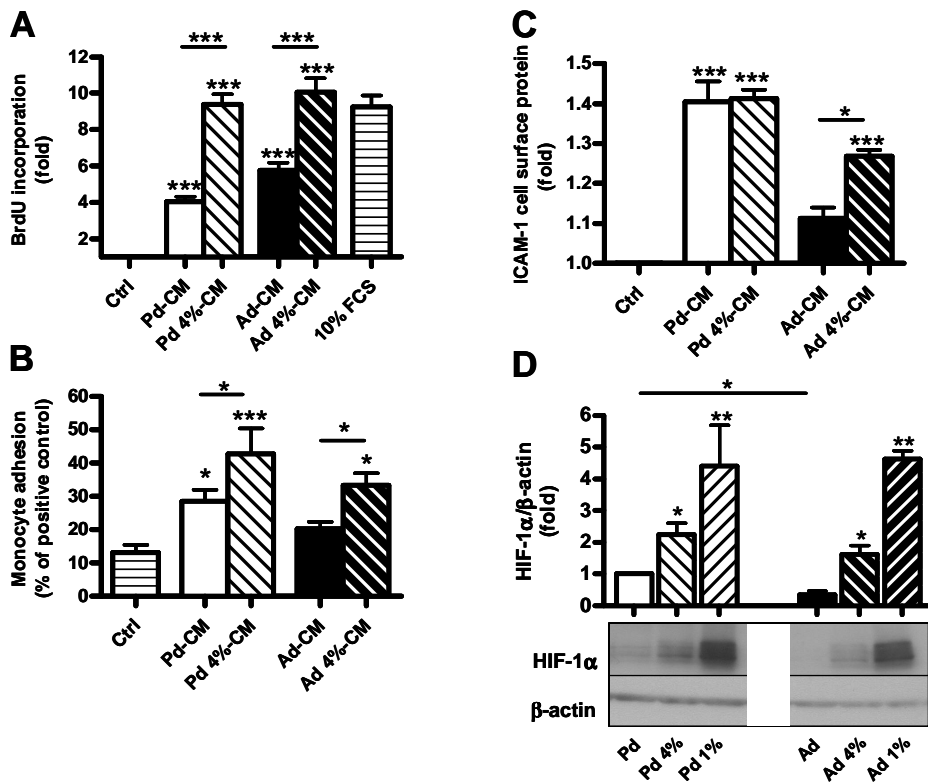


Figure 20 Preadipocytes (Pd) and adipocytes (Ad) were exposed to normoxia and hypoxia. Subsequently, HMEC-1 cells were treated with control medium (Ctrl), conditioned media (CM) of normoxic cells (Pd-CM, Ad-CM), and reoxygenated CM derived from SGBS cells under 4 % hypoxia (Pd 4%-CM, Ad 4%-CM). Endothelial cell proliferation (A), adhesion of U937 monocytes to HMEC-1 (B) and ICAM-1 cell surface expression (C) on HMEC-1 and HIF-1 α protein in SGBS cells (D) was assessed. A: proliferation was increased after treatment with Pd-CM of normoxic vs. hypoxic cells 4- and 9.3-fold and after treatment with Ad-CM of normoxic vs. hypoxic cells 5.5- and 10-fold, respectively, when compared with the Ctrl. The proliferation difference between the treatments with CM of normoxic and hypoxic Pd and Ad was 2.3- and 1.8-fold, respectively. As positive control HMEC-1 were treated with MCDB 131 medium containing 10 % FCS. B: measured monocyte adhesion of TNF- α -treatment (25 ng/ml) of HMEC-1 was considered as 100 % monocyte adhesion (positive control). Correspondingly, monocyte adhesion for Pd-CM of normoxic and hypoxic cells was 28 % and 43 % and for Ad-CM of normoxic and hypoxic cells 20 % and 33 %, respectively. Monocyte adhesion of the control medium was 13 %. Monocyte adhesion differences between the treatment with CM of normoxic and hypoxic Pd and Ad were 1.5- vs. 1.7-fold. C: the increase of ICAM-1 expression after treatment with Pd-CM of normoxic and hypoxic cells was 1.4-fold. Ad-CM of normoxic and hypoxic cells increased ICAM-1 1.1- (n.s.) and 1.3-fold, respectively. ICAM-1 levels differed between the treatments with Ad-CM of normoxic and hypoxic cells by 15 %. (D): the response of Pd and Ad to hypoxia was confirmed by measuring HIF-1 α protein. SGBS cells were kept under normoxia and 4 % (Pd 4%, Ad 4%) and 1 % hypoxia (Pd 1%, Ad 1%) for 4 hrs. Western blot analysis was performed using antibodies against HIF-1 α and β -actin. For the analysis of the experiments, the protein HIF-1 α / β -actin ratio of Pd was considered as 1. HIF-1 α / β -actin ratio was 2.8-fold higher in Pd compared with Ad under normoxia. Under 4 % and 1 % hypoxia, the ratio was 2.2- and 4.4-fold increased in Pd and 1.8- and 4.8-fold in Ad, respectively, when compared with baseline levels of Pd. Results are means \pm SE (n=4). n.s. means statistically not significant. *P<0.05, **P<0.01, ***P<0.001. Representative blots are shown.

Table 2 Impact of hypoxia on adipokine gene expression and protein secretion of preadipocytes and adipocytes

	Preadipocyte				Adipocyte			
	RNA		Protein		RNA		Protein	
	4%	1%	4%	1%	4%	1%	4%	1%
VEGF	1.7x ↑	2.8x ↑	1.5x ↑	5.3x ↑	1.7x ↑	3.9x ↑	1.7x ↑	2.7x ↑
Leptin	1.8 ↑	7.4x ↑	2.3x ↑	9.8x ↑	3.5x ↑	24x ↑	3.5x ↑	24x ↑
PAI-1	1.2x ↑ (n.s.)	1.5x ↑ (n.s.)	1.5x ↑	5.3x ↑	2.1x ↑	1.5x ↑ (n.s.)	1.5x ↑	2.7x ↑
IL-6	2x ↑	1.6x ↑	1.5x ↑	3.6x ↑	2.3x ↑	2.4x ↑	1.6x ↑	2.3x ↑
Adiponectin	-	-	-	-	0.4x ↓	0.4x ↓	no change	no change
MCP-1	0.35x ↓ (n.s.)	0.23x ↓ (n.s.)	1.16x ↑ (n.s.)	1.45x ↑	0.4x ↓	0.6x ↓	0.2x ↓ (n.s.)	0.35 ↓
IL-8	0.48x ↓ (n.s.)	0.34x ↓ (n.s.)	no change	2x ↑ (n.s.)	1.3x ↑ (n.s.)	1.3x ↑ (n.s.)	no change	0.5x ↓ (n.s.)
RANTES	no change	no change	1.36x↑	3x ↑	no change	0.55x↓ (n.s.)	1.48x↑	1.15x ↑ (n.s.)
IL-4	not measured	not measured	1.7x ↑ (n.s.)	4.4x ↑	not measured	not measured	1.4x ↑ (n.s.)	1.8x ↑
SDF1-α	not measured	not measured	1.3x ↑ (n.s.)	2.3x ↑ (n.s.)	not measured	not measured	-	-
IL-1α	no change	1.4x ↑ (n.s.)	-	-	0.4x ↓ (n.s.)	2x ↑	-	-
IL-1β	1.4x ↑ (n.s.)	1.8x ↑ (n.s.)	-	-	no change	no change	-	-
TNF-α	2.3x ↑	no change	-	-	-	-	-	-
IFN-γ	not measured	not measured	-	-	not measured	not measured	-	-

Preadipocytes (Pd) and adipocytes (Ad) were kept under normoxia, 4 % hypoxia (4%) and 1 % hypoxia (1%) for 24 hrs. Their adipokine mRNA expressions and protein concentrations in the corresponding conditioned media were quantified by qRT-PCR and specific ELISAs or bead-based Luminex assays, respectively. The analysed molecules were: VEGF, leptin, PAI-1, IL-6, adiponectin, MCP-1, IL-8, RANTES, IL-4, SDF1-α, IL-1α, IL-1β, TNF-α and IFN-γ. The values for SGBS cells under 4 % and 1 % hypoxia are presented as relative RNA and protein release in x-fold (x) compared with values of corresponding Pd and Ad under normoxia which were set to the value of 1. Results are means ± SE (n=4). n.s. means statistically not significant. **P<0.01, ***P<0.001.

Figure 21 A Impact of hypoxia on adipokine mRNA expression and protein secretion of preadipocytes and adipocytes

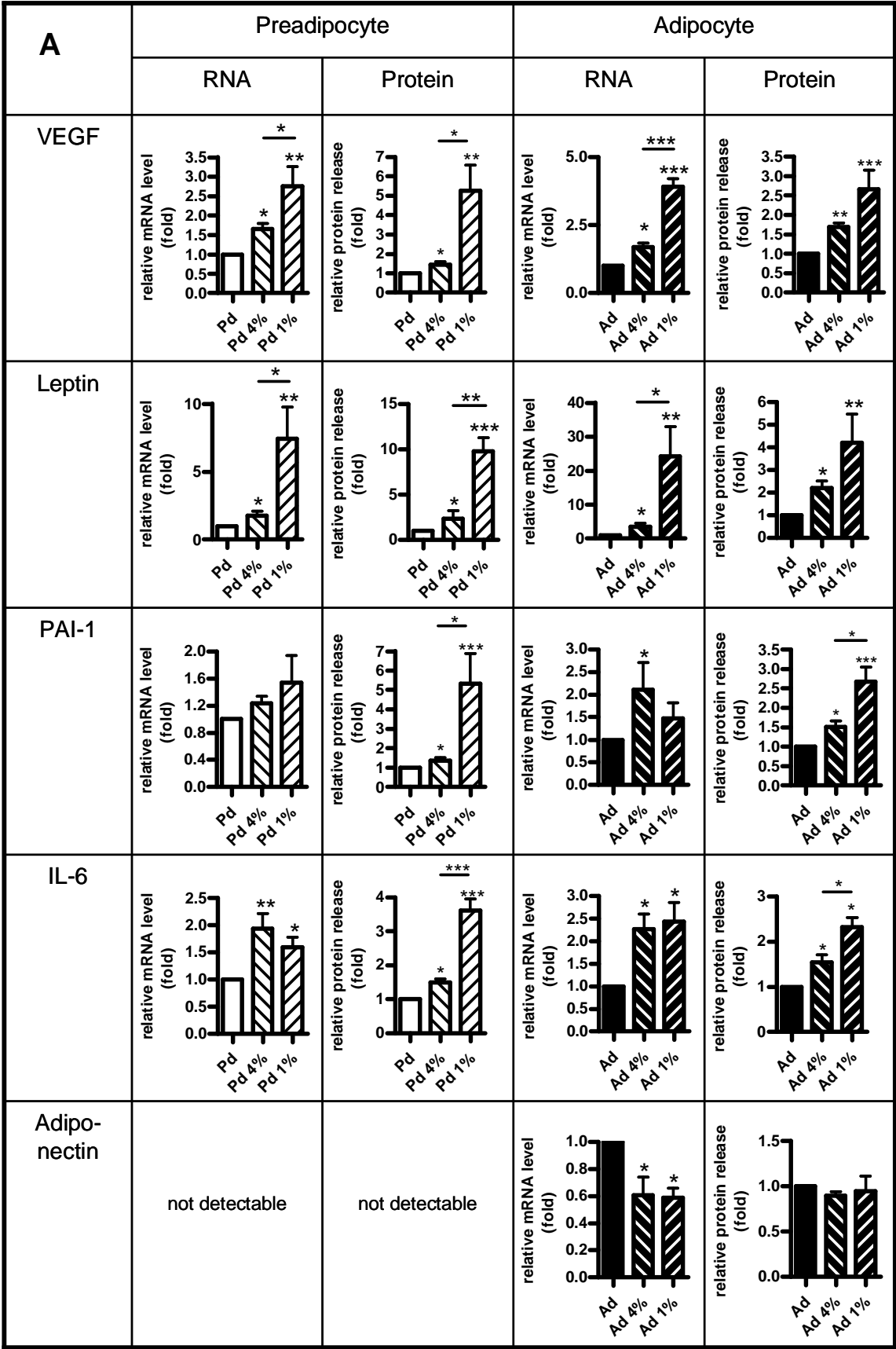


Figure 21 B Impact of hypoxia on adipokine mRNA expression and protein secretion of preadipocytes and adipocytes

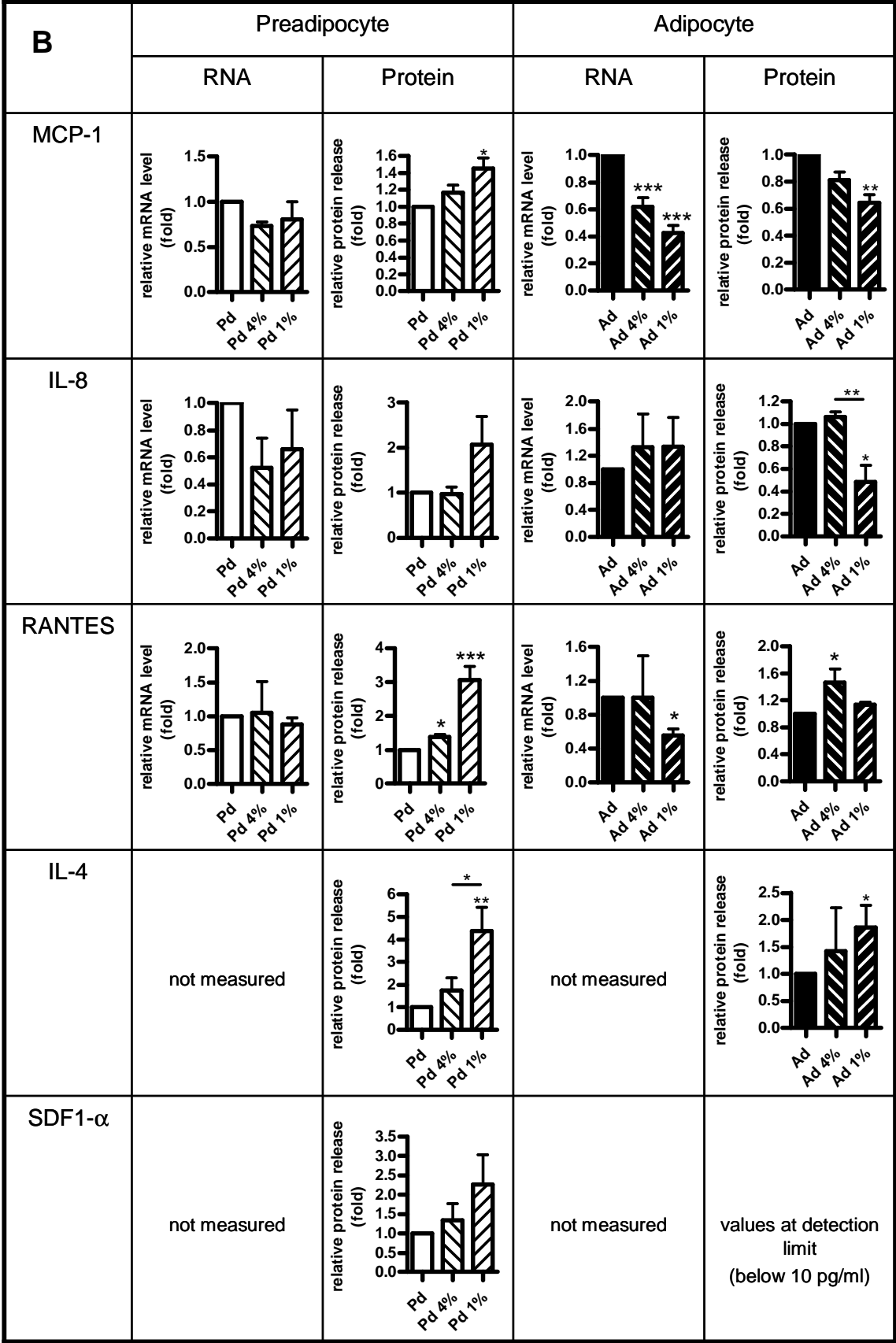


Figure 21 C Impact of hypoxia on adipokine mRNA expression and protein secretion of preadipocytes and adipocytes

C	Preadipocyte		Adipocyte	
	RNA	Protein	RNA	Protein
IL-1 α	<p>IL-1α relative mRNA level (fold)</p> <p>Pd Pd 4% Pd 1%</p>	values at detection limit (below 10 pg/ml)	<p>IL-1α relative mRNA level (fold)</p> <p>Ad Ad 4% Ad 1%</p>	values at detection limit (below 10 pg/ml)
IL-1 β	<p>IL-1β relative mRNA level (fold)</p> <p>Pd Pd 4% Pd 1%</p>	values at detection limit (below 10 pg/ml)	<p>IL-1β relative mRNA level (fold)</p> <p>Ad Ad 4% Ad 1%</p>	values at detection limit (below 10 pg/ml)
TNF- α	<p>TNF-α relative mRNA level (fold)</p> <p>Pd Pd 4% Pd 1%</p>	values at detection limit (below 10 pg/ml)	not detectable	values at detection limit (below 10 pg/ml)
IFN- γ	not measured	not detectable (detection limit: 10 pg/ml)	not measured	not detectable (detection limit: 10 pg/ml)

Figure 21

Preadipocytes (Pd) and adipocytes (Ad) were kept under normoxia, 4 % hypoxia (4%) and 1 % hypoxia (1%) for 24 hrs. Their adipokine mRNA expressions and protein concentrations in the corresponding conditioned media were quantified by qRT-PCR and specific ELISAs or bead-based Luminex assays, respectively. The analysed molecules were: VEGF, leptin, PAI-1, IL-6, adiponectin, MCP-1, IL-8, RANTES, IL-4, SDF1- α , IL-1 α , IL-1 β , TNF- α and IFN- γ . The values for SGBS cells under 4 % and 1 % hypoxia are presented as relative RNA and protein release in x-fold (x) compared with values of corresponding Pd and Ad under normoxia which were set to the value of 1. Results are means \pm SE (n=4). n.s. means statistically not significant. *P<0.05, **P<0.01, ***P<0.001.

3.3.7 Impact of SGBS preadipocyte- and adipocyte-CM on endothelial cell signalling pathways

To further evaluate the signalling pathways activated upon CM-treatment of HMEC-1 cells and involved in CM-induced expression of MCP-1, IL-8 and ICAM-1, different signalling molecules were evaluated. On the basis of their promoters, the regulation of these genes can occur through the stimulation of multiple pathways such as the NF- κ B, AP-1 or the JAK/STAT pathway (Roebuck *et al.*, 1999; Roebuck and Finnegan, 1999). Therefore, total and specifically phosphorylated forms of I κ B α , RelA, p38MAPK, ERK 1/2, SAPK/JNK, c-Jun, STAT-3 and STAT-1 were analysed at appropriate time intervals by Western blot analysis (Figs. 22 to 24). These time intervals were determined with control and stimulated HMEC-1 ahead of the shown experiments (Figures 22A-D; Figures 23A, C, E and G; Figures 24A and C). Interestingly, the phosphorylation status of I κ B α (Figure 22E), RelA (Figure 22F) and the level of total I κ B α (Figure 22E) did not change after CM-stimulation in HMEC-1 cells. In contrast, the phosphorylations of RelA and I κ B α increased and total I κ B α decreased in HMEC-1 cells treated with TNF- α , serving as positive control (Figure 22G). The ratios of phosphorylated forms to total specific protein of endothelial SAP/JNK (Figure 23B), p38 MAPK (Figure 23D), ERK1/2 (Figure 23F), c-Jun (Figure 23H), STAT-1 (Figure 24B) and STAT-3 (Figure 24D) were substantially elevated after stimulation with preadipocyte-CM and adipocyte-CM. Note, the measured increase of SAP/JNK, ERK1/2 and c-Jun after stimulation with adipocyte-CM was not statistically significant. For SAPK/JNK, STAT-1 and STAT-3, the differences in phosphorylation between preadipocyte and adipocyte-CM treated HMEC-1 cells was statistically significant.

Figure 22 Impact of CM from SGBS cells on microvascular endothelial cell NFκB signalling pathway

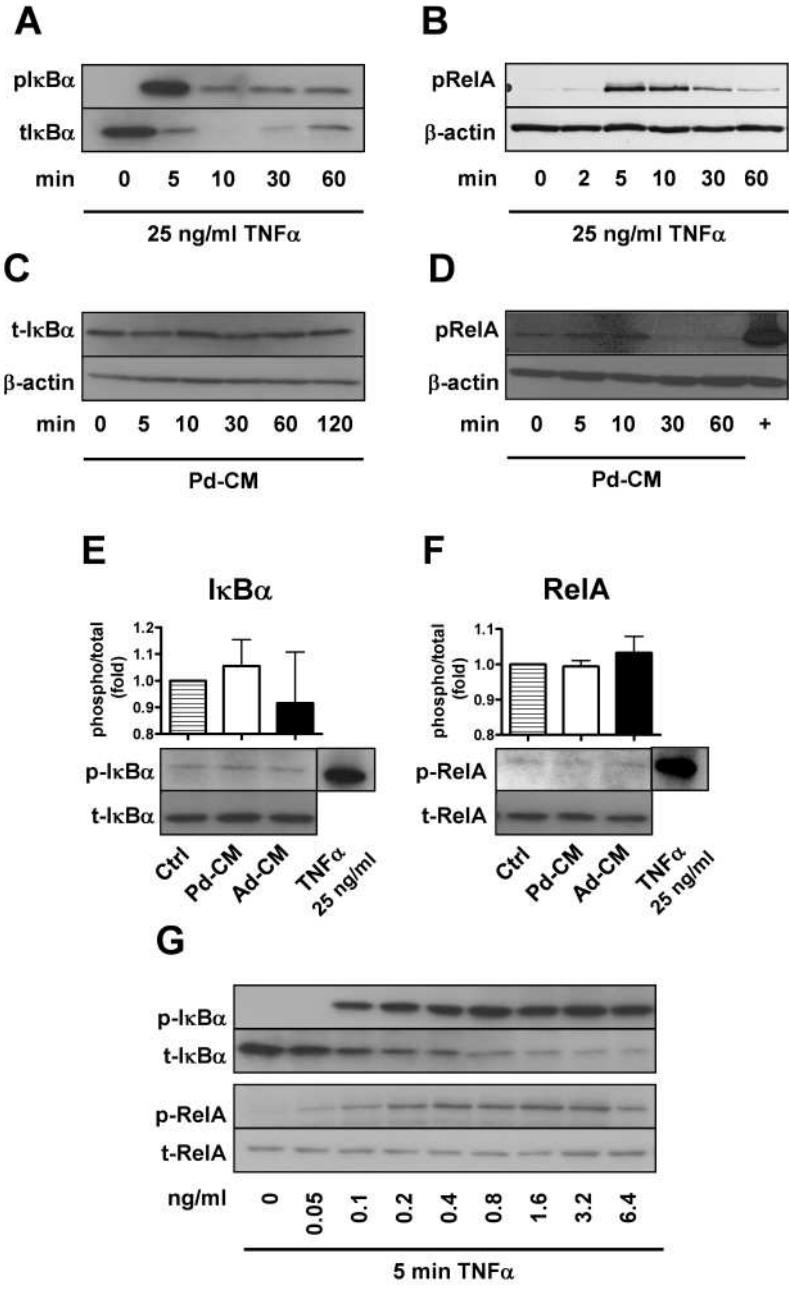


Figure 22
HMEC-1 cells were treated with control medium (Ctrl), TNF-α at indicated concentrations, preadipocyte-conditioned medium (Pd-CM) and adipocyte-CM (Ad-CM) for different time-points. Western blot analysis was performed using antibodies against the total (t-) and/or phosphorylated (p-) forms of IκBα (A, C, E, G) and RelA (B, D, F and G) and β-actin (B, C and D). A and B: a time course was conducted for HMEC-1 cells after treatment with 25 ng/ml TNF-α was performed. C and D: a time course was conducted for HMEC-1 cells after treatment with Pd-CM was conducted. E and F: HMEC-1 cells were treated for 5 min with Pd-CM and Ad-CM. G: HMEC-1 cells were treated for 5 min with different concentrations of TNF-α. For the analysis of these experiments, protein levels under Ctrl-conditions were considered as 1. Results are means ± SE (n=3).

Figure 23 Impact of CM from SGBS cells on microvascular endothelial cell MAPK and c-Jun signalling

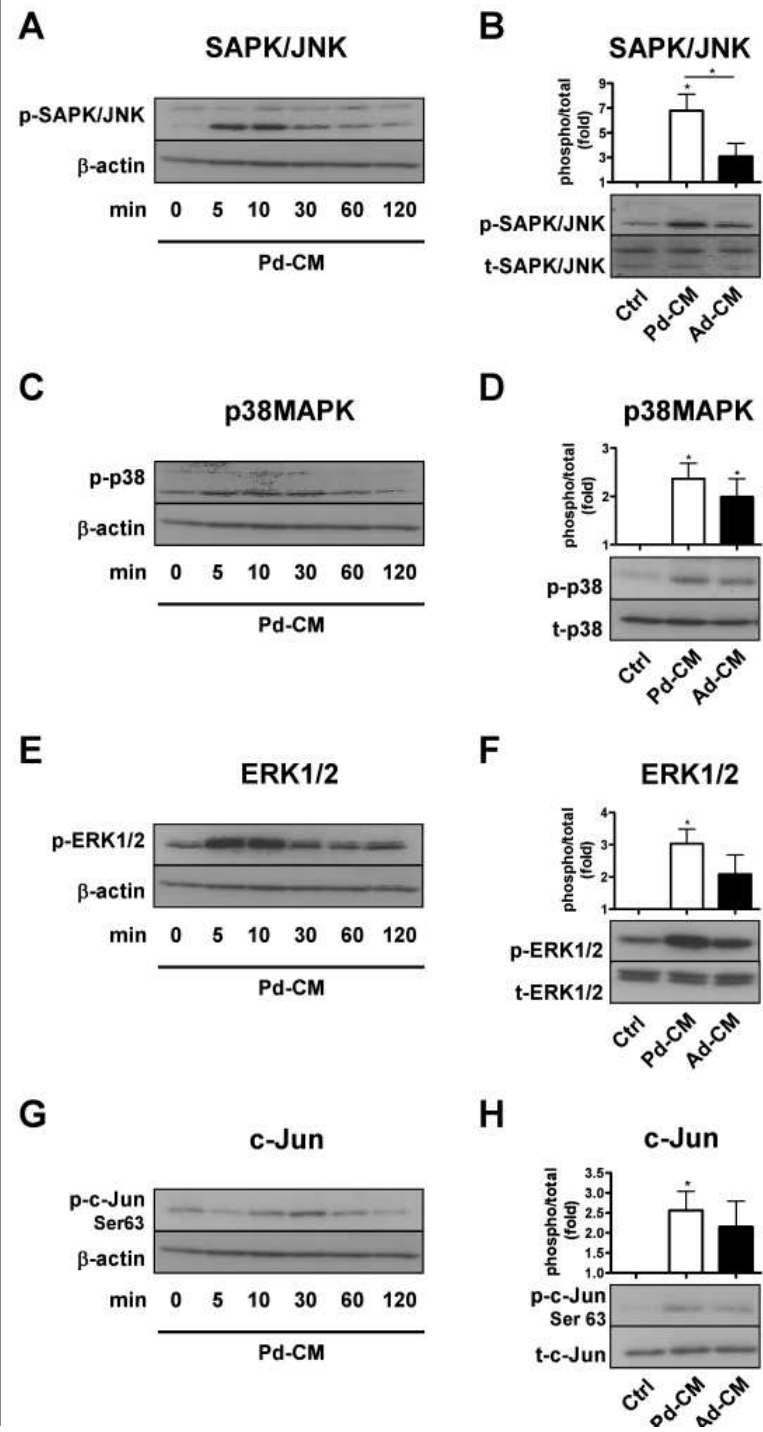


Figure 23

HMEC-1 cells were treated with control medium (Ctrl), preadipocyte-conditioned medium (Pd-CM) and adipocyte-CM (Ad-CM) for different intervals. Western blot analysis was performed using antibodies against β -actin (A, C, E and G) serving as loading control, the phosphorylated (p-) and total (t-) forms of SAPK/JNK (A and B), p38MAPK (C and D), ERK1/2 (E and F) and c-Jun (G and H). For all p-molecules a time course in HMEC-1 cells after treatment with Pd-CM was performed (A, C, E and G). For the quantitative detection of SAPK/JNK (B) p38MAPK (D) and ERK1/2 (F) HMEC-1 were treated with CM for 10 min and for detection of c-Jun (H) for 30 min. B, D, F and H: protein levels under Ctrl-conditions were considered as 1. Phospho/total protein increased 6.8- and 3-fold for SAPK/JNK (B), 2.4- and 2-fold for p38MAPK (D), 3- and 2-fold (n.s.) for ERK1/2 (F) and 2.6- and 2.1-fold (n.s.) for c-Jun (H) after treatment with Pd-CM and Ad-CM when compared with the Ctrl. The differences for the phospho/total protein ratio between the treatments with CM were 2.3-fold for SAP/JNK, 1.2-fold for p38MAPK (n.s.), 1.5-fold for ERK1/2 (n.s.) and 1.2-fold for c-Jun (n.s.). Results are means \pm SE (n=3). n.s. means statistically not significant. *P<0.05 Representative blots are shown.

Figure 24 Impact of CM from SGBS cells on microvascular endothelial cell STAT signalling

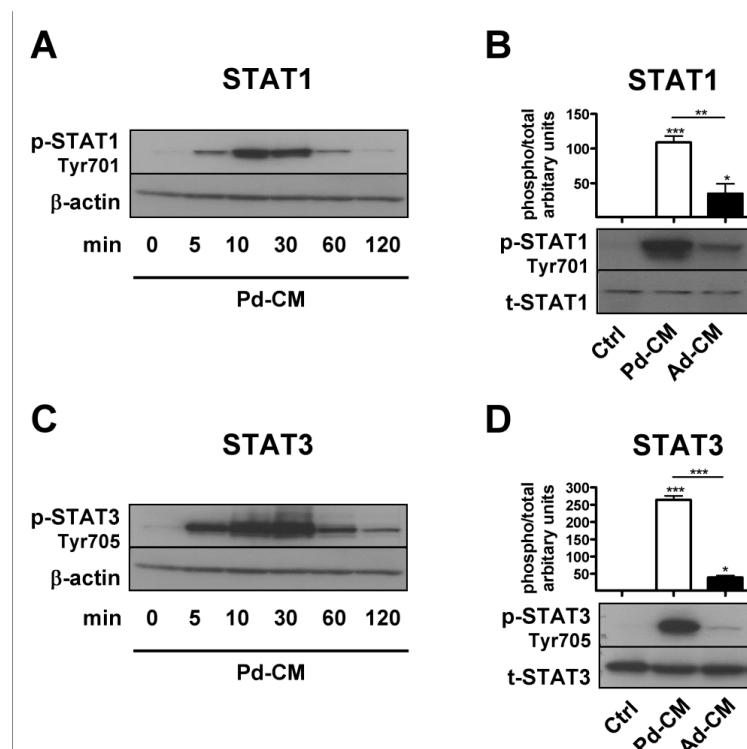


Figure 24

HMEC-1 cells were treated with control medium (Ctrl), preadipocyte-conditioned medium (Pd-CM) and adipocyte-CM (Ad-CM) for different time-points. Western blot analysis was performed using antibodies against β -actin (A and C) serving as loading control, the phosphorylated (p-) and total (t-) forms of STAT-1 (A and B) and STAT-3 (C and D). For both p-molecules a time course in HMEC-1 cells after treatment with Pd-CM was performed (A and C). For the quantitative detection of STAT-1 (B) and STAT-3 (D) HMEC-1 were treated with CM for 30 min (arbitrary units shown). The differences for the phospho/total protein ratio between the treatments with CM were 6.7-fold for STAT-3 and 3.1-fold for STAT-1. Results are means \pm SE (n=3). *P<0.05, **P<0.01, ***P<0.001. Representative blots are shown.

3.3.8 The role of endothelial signalling pathways on monocyte endothelial cell-cell adhesion and ICAM-1 protein expression

To determine the role of the above mentioned signalling pathways in the monocyte endothelial cell-cell adhesion and ICAM-1 protein expression, HMEC-1 cells pre-treated with JNK inhibitor II, SB203580 (p38 MAPK inhibitor), PD98059 (MEK1 inhibitor) or JAK inhibitor I and stimulated with preadipocyte-CM in the presence of the corresponding inhibitors were examined. A low and a high dose of each inhibitor was applied. Preadipocyte-CM significantly increased monocyte adhesion and ICAM-1 cell surface protein expression of HMEC-1 cells whereas in the presence of JNK inhibitor II these effects were suppressed to baseline levels (Figures 25A and B). Concordantly, the CM mediated SAPK/JNK phosphorylation decreased dose dependently, supporting the efficacy of the inhibitor (Figure 25C). In contrast, application of PD98059 (Figures 25D and E) and SB203580 (Figures 25G and H) had no significant effect on the increase of monocyte adhesion or ICAM-1 cell surface protein of preadipocyte-CM treated HMEC-1 cells. The efficacy of the inhibitor PD98059 was confirmed by its ability to decrease preadipocyte-CM mediated ERK1/2 phosphorylation (Figure 25F). SB203580 hinders the activity but not the activation of p38 MAPK and therefore, no phosphorylation experiments are shown (Kumar *et al.*, 1999). The JAK inhibitor I (Figures 25I and J) significantly inhibited the increase of monocyte adhesion and ICAM-1 cell surface expression by preadipocyte-CM to the same extent as the JNK inhibitor II (Figures 25A and B). Since STAT-1 and STAT-3 are mediators of JAK-signalling (Murray, 2007) and activated upon stimulation of HMEC-1 cells with preadipocyte-CM, the effect of JAK inhibitor I on STAT-1 and STAT-3 activation by Western blot analysis was assessed. Stimulation of HMEC-1 cells with CM resulted in a robust phosphorylation of STAT-1 and STAT-3, whereas the blockade with JAK inhibitor I effectively abrogated the phosphorylation of STAT-1 and STAT-3 (Figure 25K).

Figure 25 Blockade of signalling pathways in HMEC-1 cells by specific inhibitors

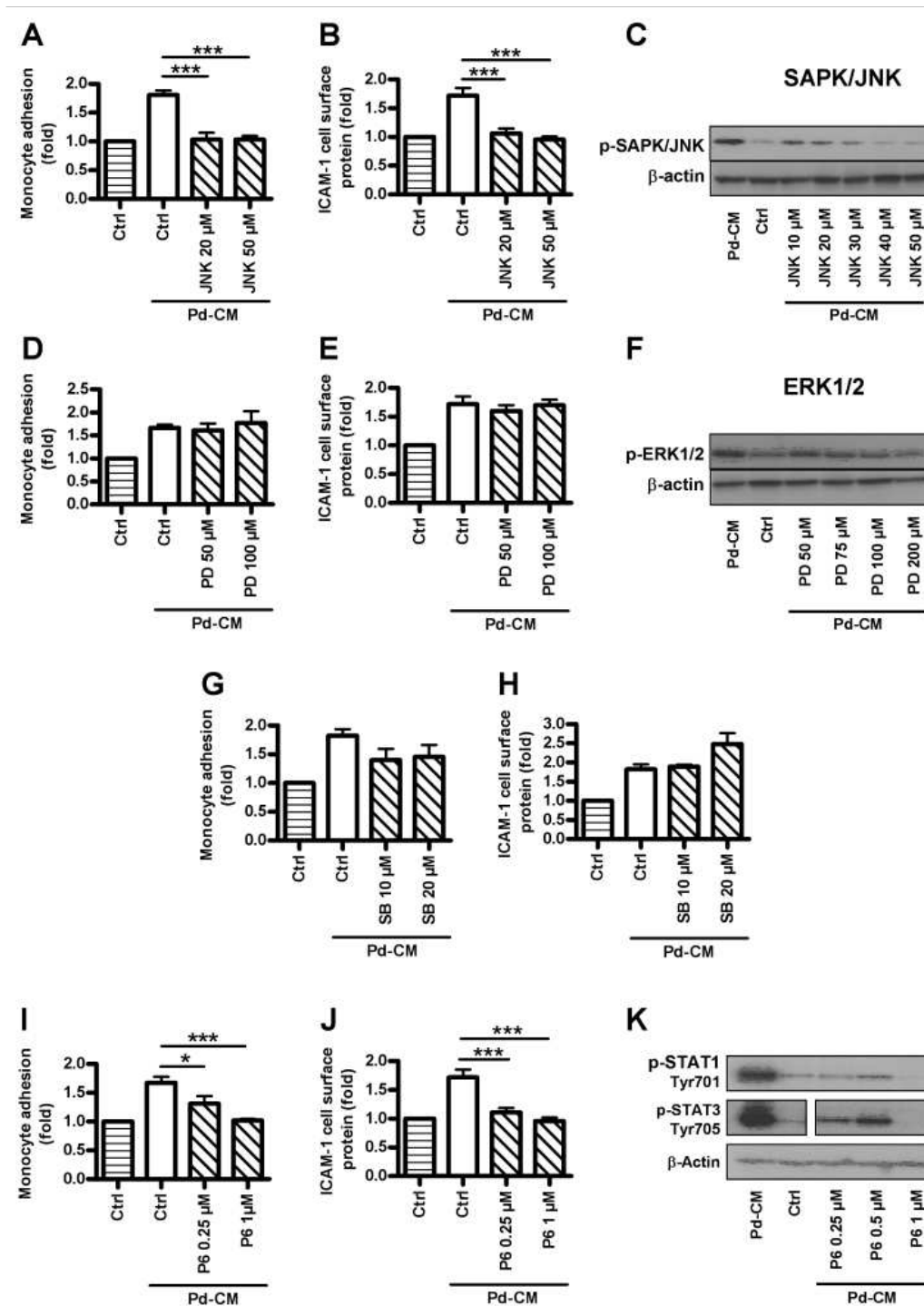


Figure 25

HMEC-1 cells were preincubated with indicated concentrations of JNK inhibitor II (JNK), SB203580 a p38MAPK inhibitor (SB), PD98059 a MEK1 inhibitor (PD) and JAK inhibitor I (P6) for 45 min. After stimulation with control medium (Ctrl), preadipocyte-conditioned medium (Pd-CM) and Pd-CM supplemented with the corresponding inhibitors at indicated concentrations, monocyte adhesion assay (A, D, G and I), ICAM-1 cell surface ELISA (B, E, H and J) and Western blot analysis for β-actin (C, F and K) and the phosphorylated forms (p-) of SAPK/JNK (C), ERK1/2 (F), STAT1 and STAT3 (G) were performed. Results are means ± SE (n≥3) *P<0.05, ***P<0.001. Representative blots are shown.

3.4 Functional analysis of factors in CM mediating endothelial cell activation

3.4.1 Introduction

To get initial insights into the mediators in preadipocyte-CM and adipocyte-CM which induce the STAT-1/3 dependent endothelial ICAM-1 expression and monocyte-endothelial cell-cell adhesion, the functional analysis was focussed on the adipokines IL-6, leptin and VEGF known to signal via the STAT-pathways (Bartoli *et al.*, 2000; Jin *et al.*, 2003; Korpelainen *et al.*, 1999; Ni *et al.*, 2004; Pan *et al.*, 2007; Wincewicz *et al.*, 2007; Yahata *et al.*, 2003). First, the gene expression of the receptors which mainly signal for these cytokines in HMEC-1 cells were analysed and the expression of the IL-6 receptor at protein level was investigated. Next, function-neutralizing antibodies specific for the above mentioned adipokines and corresponding isotype-matched control antibodies were used in proliferation, ICAM-1 cell surface ELISA, monocyte-endothelial cell-cell adhesion and STAT-1/3 phosphorylations assays. Note, corresponding information about the experiments and fold-changes are presented in the figure legends.

3.4.2 Gene and protein expression of the obese receptor (Ob-R) b, VEGFR-2, gp130 and IL-6 receptor (IL-6R) α in HMEC-1 cells

3.4.2.1 Ob-Rb gene expression

The leptin receptor gene encodes five alternatively spliced variants. They are named Ob-Ra, Ob-Rb, Ob-Rc, Ob-Rd and Ob-Re. Only the Ob-Rb has a long cytoplasmic region which contains several motifs which are required for signal transduction. Upon leptin binding, the Ob-Rb signals e.g. via the JAK/STAT pathway (Friedman and Halaas, 1998; Schwartz *et al.*, 2000). The Ob-Rb is found on many cell types including endothelial cells (Quehenberger *et al.*, 2002). By RT-PCR experiments with total RNA, a PCR product specific for Ob-Rb in HMEC-1 cells was observed after 35 and less amplification cycles (185-bp; Figure 26A).

3.4.2.2 VEGFR-2 gene expression

The VEGF ligand and VEGF receptor biology is complex (see chapter 1.2.2.4). However, VEGF₁₆₅ belonging to the VEGF-A family is the most abundant isoform and according to *in vitro* studies the most biologically active form. Additionally, VEGF₁₂₁ and VEGF₁₄₅ also belonging to the VEGF-A family are biologically active in endothelial cells. The VEGF proteins measured in the SGBS-CM were VEGF₁₂₁ and VEGF₁₆₅. The members of the VEGF-A family bind to VEGFR-1 and VEGFR-2 which both belong to the family of tyrosine kinase receptors. VEGFR-2 (Oh *et al.*, 2002) is described to be the most functional mediator of endothelial VEGF signalling (Zachary and Glicki, 2001). In contrast, it is uncertain if VEGFR-1 has a biological important function in endothelial cells. VEGFR-2 gene expression was detected in HMEC-1 cells by RT-PCR experiments using total RNA, specific primers for VEGFR-2 and 35 and less amplification cycles (793-bp; Figure 26B).

3.4.2.3 gp130 and IL-6 R α gene and protein expression

The cellular IL-6R complex basically consists of the 80 kDa ligand (IL-6) binding glycoprotein IL-6R α and the 130 kDa glycoprotein (gp130) involved in signal transduction. The gp130 protein is ubiquitously expressed on most cell-types including endothelial cells, whereas the IL-6R α subunit is cell type-specifically expressed. A membrane-bound form of IL-6R α of approx. 80 kDa and soluble isoforms of IL-6R α (sIL-6R α) of approximately 55 kDa can be generated due to differential mRNA-splicing and/or limited proteolysis (Rose-John *et al.*, 2006). Since there is a discrepancy in the literature about the presence of the IL-6R α on endothelial cells, especially on HUVECs (Modur *et al.*, 1997; Romano *et al.*, 1997; Watson *et al.*, 1996; Waxman *et al.*, 2003), the expression of the IL-6 receptor subunits in the microvascular endothelial cells, HMEC-1, used in this study was assessed. PBMC, known to express IL-6R α (Jablonska *et al.*, 1999) were used as positive control. By RT-PCR experiments with total RNA, robust amounts of PCR-products specific for the gp130-mRNA (253-bp; Figure 26A) and the 80 kDa IL-6R α -mRNA (350 bp; Figure 26B) in both PBMC and HMEC-1 cells were observed. In contrast, rather small amounts of PCR-product specific for the soluble IL-6R α mRNA-splice variant in PBMC and HMEC-1 cells (256-bp; Figure 26B) were detected. β -actin served as housekeeper gene (281 bp, Fig 26C).

For immunoblot experiments, total protein lysates from HMEC-1 cells and PBMC and human IL-6R α -specific antibody recognizing the membrane-bound (80 kDa) and soluble isoforms of IL-6R α (50 to 60 kDa) were used. For the 80 kDa IL-6R α protein, the signal in PBMC was stronger compared with the signals for the 80 kDa IL-6R α in HMEC-1 cells and the 55 kDa soluble IL-6R α protein in PBMC and HMEC-1 cells (Figure 26D). It is known that the soluble IL-6R α after binding IL-6 is able to bind to the gp130 subunit on the cell surface forming a functional IL-6 receptor complex (Rose-John *et al.*, 2006). Therefore, our gene expression data for the gp130 and IL-6 α subunits (Figures 26A and B) and the membrane-bound and soluble isoforms of the IL-6R α protein (Figure 26D) indicate the presence of functional IL-6 receptor complexes on HMEC-1 cells and the generation of IL-6 α isoforms by alternative splicing and/or shedding of the membrane-bound IL-6R α .

Figure 26 Expression analysis of leptin receptor b (Ob-Rb), VEGF receptor 2 (VEGFR-2), IL-6 receptor- α (IL-6R α) and gp130 in HMEC-1 cells and/or peripheral blood mononuclear cells (PBMC)

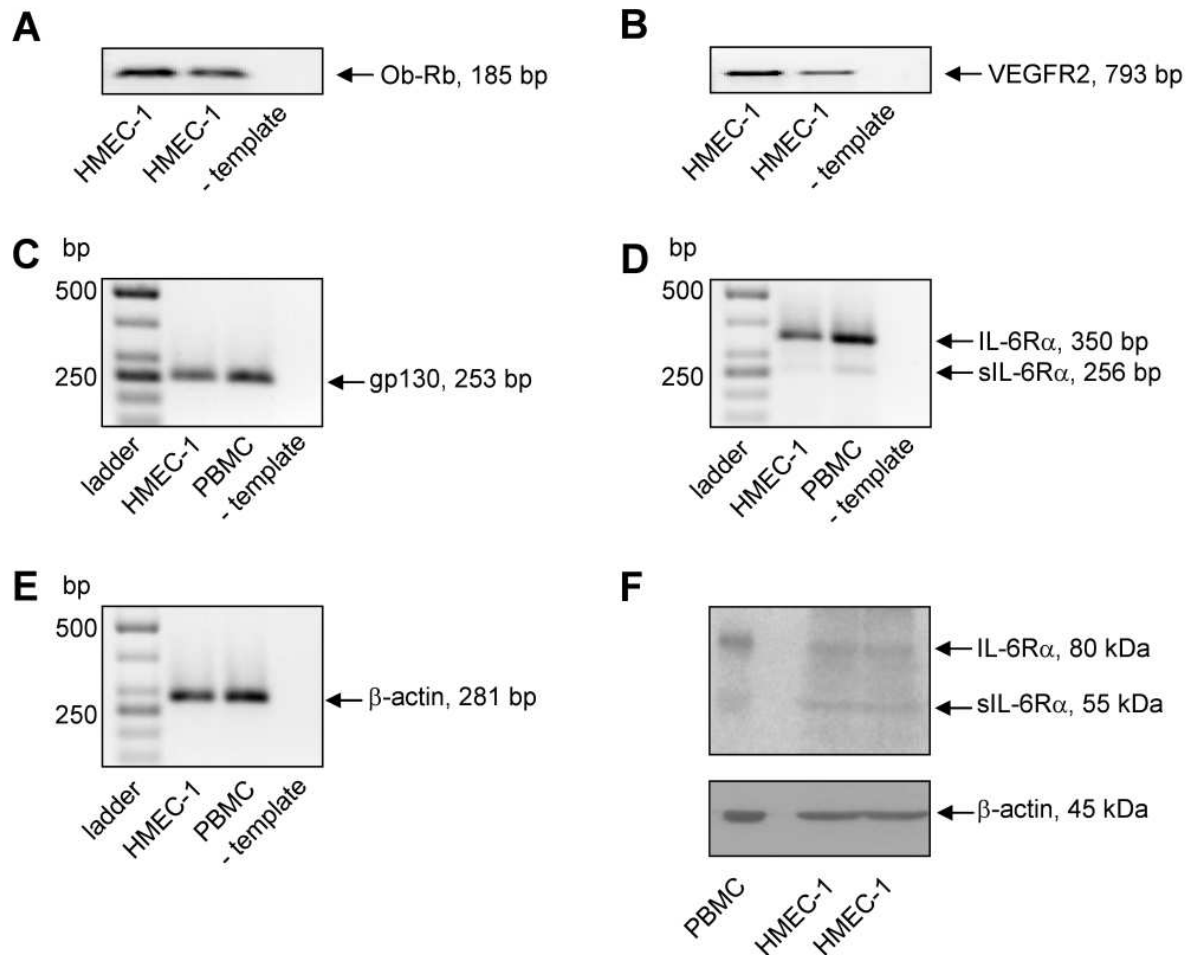


Figure 26
A, B, C and D: robust PCR-products are shown for mRNAs encoding for Ob-Rb (arrow 185 bp; *A*), VEGFR-2 (arrow 793 bp; *B*), gp130 (arrow 253 bp; *C*) and membrane bound IL-6R α (arrow 350 bp; *D*). The PCR-product for the IL-6R α splice-variant coding for the soluble IL-6R α (arrow 256 bp; *D*) in HMEC-1 cells and PBMC (positive control) is weak. *E:* as reference gene for *C* and *D* β -actin (arrow 281 bp) is shown. 50 bp-DNA ladder (ladder) was used to determine the size of the PCR products. *F:* immunoblot analysis of IL-6R α (80 kDa) and soluble IL-6R (sIL-6R α , 55kDa) in protein lysates of HMEC-1 cells and PBMCs (positive control). The applied IL-6R α detecting antibody specific for both forms of IL-6R α generates signals with the expected sizes for the 80 kDa IL-6R α and 55 kDa sIL-6R α protein. The signals for the 80 kDa IL-6R α are stronger compared with the faint signals for the 55 kDa sIL-6R α . β -actin served as loading control. Representative immunoblots are shown (n=4).

3.4.3 Functional analysis of factors in CM mediating endothelial ICAM-1 expression and monocyte endothelial cell-cell adhesion

First, the effects of recombinant proteins for IL-6, leptin and VEGF₁₆₅ added separately to serum-free HMEC-1 cell cultures were assessed. For IL-6, a robust and significant increase in monocyte endothelial cell-cell adhesion and ICAM-1 protein cell surface expression was observed at a IL-6 concentration of 1 ng/ml. In further experiments 10 ng/ml of IL-6 was used as positive control since this concentration was sufficient to induce stable and rather high levels of monocyte adhesion (Figure 27A) to HMEC-1 cells and ICAM-1 cell surface protein (Figure 27B) on HMEC-1 cells. In the presence of a function-neutralizing anti-human IL-6 antibody, the IL-6 effect on monocyte adhesion and ICAM-1 expression was significantly blocked (Figures 29A, B, E and F). For VEGF₁₆₅ and leptin, no consistent significant effects on ICAM-1 protein expression and monocyte endothelial cell-cell adhesion were detectable (data not shown). However, in endothelial cell proliferation assays performed in parallel, both adipokines VEGF₁₆₅ and leptin and also IL-6 increased HMEC-1 cell proliferation as expected already at concentrations of 1 ng/ml of the respective cytokine (Figures 28A-C) demonstrating their biofunctionality. Since leptin and VEGF₁₆₅ did not appear to play an important role in triggering HMEC-1 cells for endothelial cell-monocyte adhesion and ICAM-1 expression, further analysis was focussed on the function of IL-6 in CM. As illustrated in Figures 29A and B, the increase of monocyte adhesion and ICAM-1 protein of HMEC-1 cells stimulated with CM of normoxic preadipocytes in the presence or absence of isotype-matched control antibody was significantly suppressed in the presence of the IL-6 antagonist. Treatment of HMEC-1 cells with CM of normoxic adipocytes in the presence of IL-6 antagonist had no effect on ICAM-1 protein but slightly increased monocyte adhesion, although this effect is not statistically significant within the adipocyte-CM group. To exclude the possibility that basal IL-6 secretion of HMEC-1 cells already exerted effects on monocyte adhesion (Figure 29C) and ICAM-1 cells surface expression (Figure 29D), untreated HMEC-1 cells were stimulated with the IL-6 antagonist or the corresponding isotype control alone. No significant changes were observed. Treatment of HMEC-1 cells with CM from hypoxic preadipocytes or adipocytes containing the IL-6 antagonist, further decreased monocyte adhesion (Figure 29E) and ICAM-1 expression (Figure 29F) significantly, with the exception that the inhibitory effect of preadipocyte-CM on ICAM-1 expression was slightly less compared with the normoxic situation.

Figure 27 Impact of IL-6 on monocyte adhesion to and ICAM-1 cell surface protein expression of HMEC-1 cells

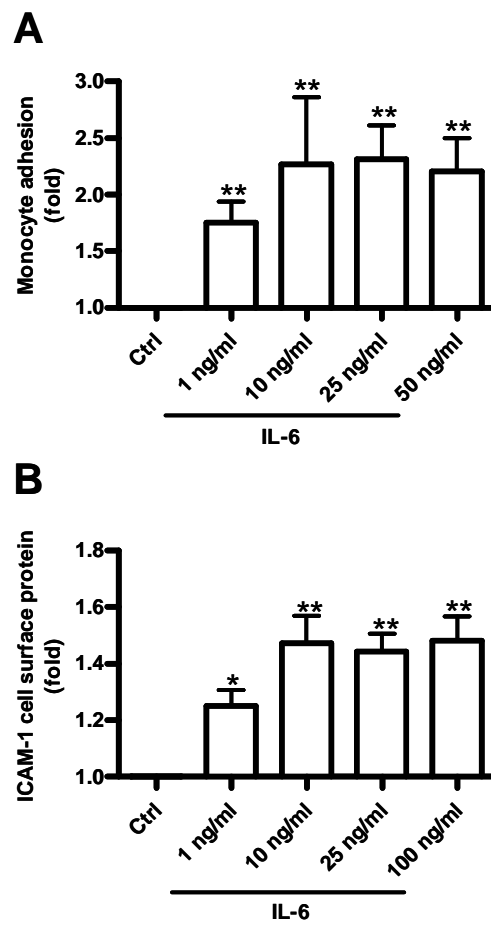


Figure 27
HMEC-1 cells were treated with control medium (Ctrl) and different concentrations of recombinant IL-6. Subsequently, monocyte adhesion (A) and cell surface expression of ICAM-1 (B) was assessed. A: The increase in monocyte adhesion upon IL-6 treatment was 1.8-fold for 1 ng/ml, 2.3-fold for 10 and 25 ng/ml and 2.2-fold for 50 ng/ml, when compared with the Ctrl-treatment. B: ICAM-1 expression was elevated upon IL-6 exposure by 1.25-fold for 1 ng/ml, 1.5-fold for 10 ng/, 1.4-fold for 25 ng/ml and 1.5 fold for 50 ng/ml when compared with the Ctrl-treatment. Results are means \pm SE (n=4). *P<0.05, **P<0.01.

Figure 28 Proliferation analysis of HMEC-1 cells after treatment with recombinant proteins for VEGF₁₆₅, leptin and IL-6

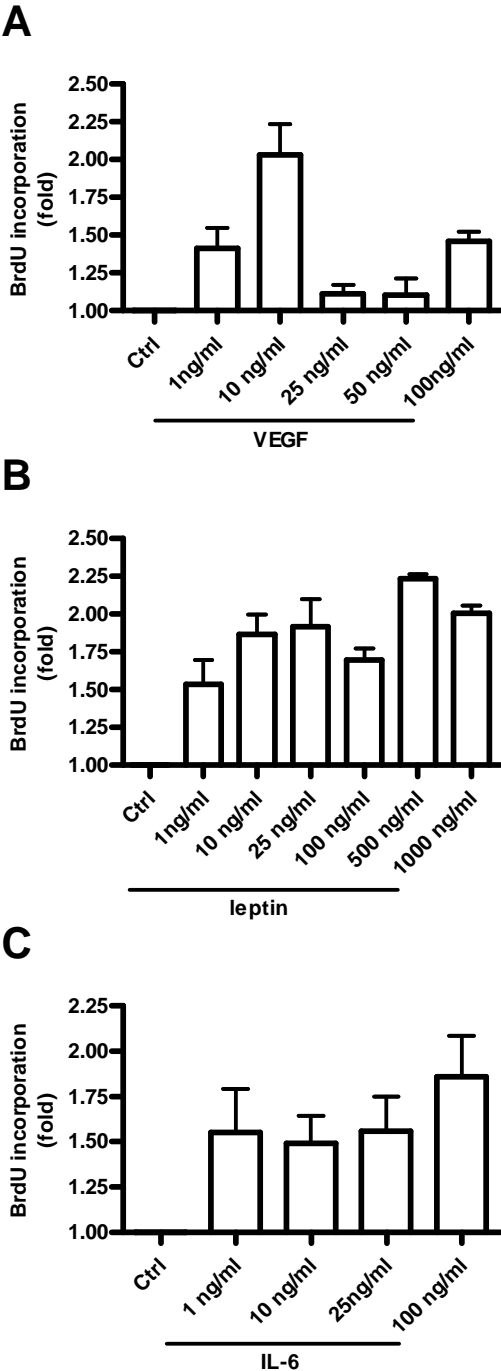


Figure 28
HMEC-1 cells were incubated in the presence of control medium (Ctrl) and different concentrations of VEGF₁₆₅ (A), leptin (B) and IL-6 (C) for 48 hrs. Additionally, BrdU was added for the next 16 hrs. Representative data for 2 independent experiments are shown.

Figure 29 Functional analysis of IL-6 in CM from normoxic and hypoxic SGBS cells on monocyte adhesion to and ICAM-1 cell surface expression of HMEC-1 cells

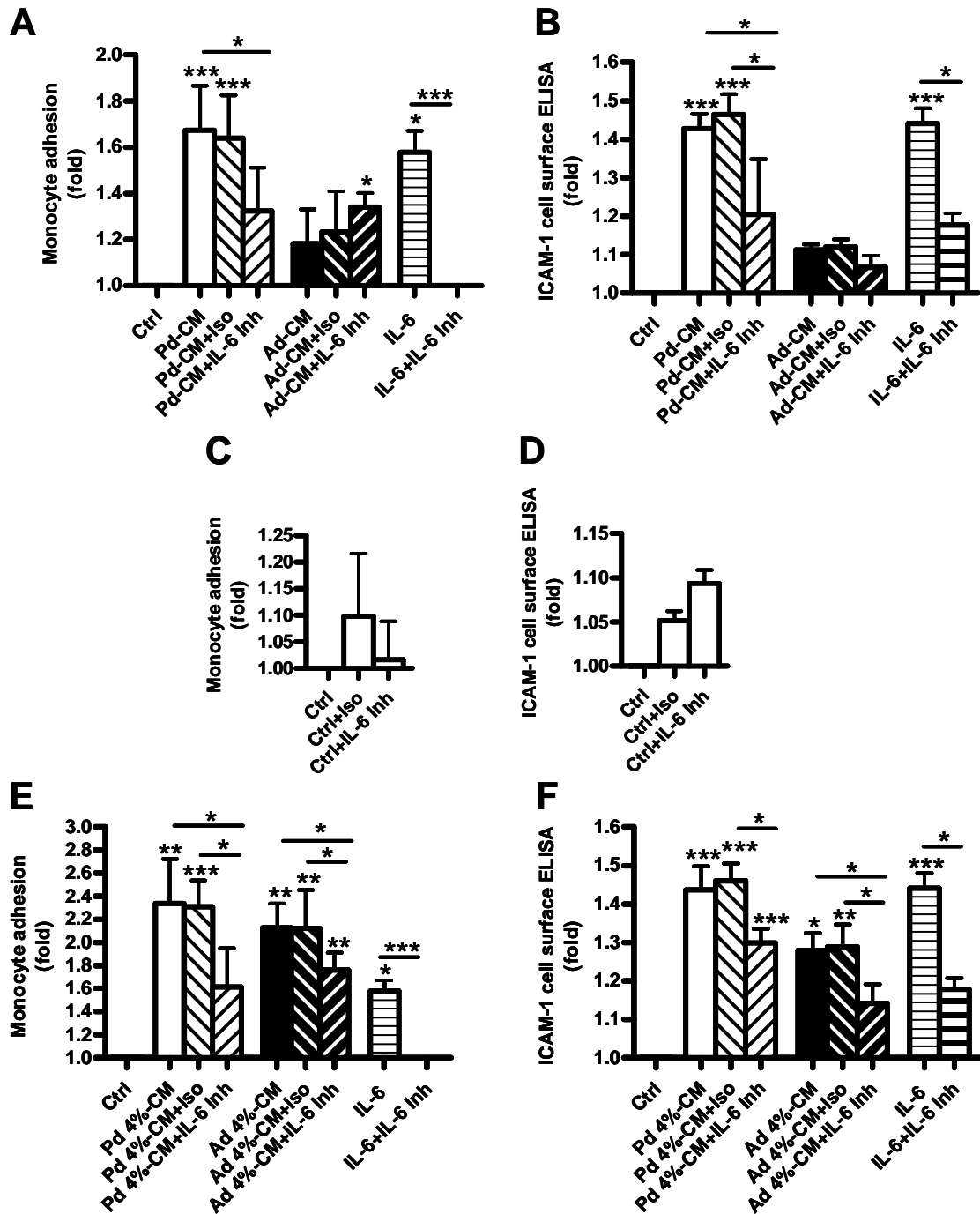


Figure 29

Control media (Ctrl) and conditioned media (CM) from preadipocytes (Pd) and adipocytes (Ad) exposed to normoxia were preincubated either with 5 µg/ml function-neutralizing anti-IL-6 antibody as IL-6 inhibitor (IL-6 Inh) or with 5 µg/ml of the corresponding IgG1 isotype-matched control antibody (Iso) for 15 min and subsequently used to stimulate HMEC-1 cells. HMEC-1 cells were treated with Ctrl, CM of Pd (Pd-CM) and Ad (Ad-CM), Ctrl and CM of cells pre-incubated with IL-6 inhibitor (Ctrl+IL-6 Inh, Pd-CM+IL-6 Inh, Ad-CM+IL-6 Inh) and Ctrl and CM of cells pre-incubated with the isotype-matched control antibody (Ctrl+Iso, Pd-CM+Iso, Ad-CM+Iso). Likewise, HMEC-1 cells were treated with reoxygenated CM derived from 4 % hypoxic Pd (Pd 4%-CM) and Ad (Ad 4%-CM), CM of hypoxic cells pre-incubated with IL-6 inhibitor (Pd 4% CM+IL-6 Inh, Ad 4%-CM+IL-6 Inh) and CM of hypoxic cells pre-incubated with the isotype-matched control antibody (Pd 4%-CM+Iso, Ad 4%-CM+Iso). HMEC-1 cells treated with 10 ng/ml IL-6 added to Ctrl medium (IL-6) or in combination with 5 µg/ml IL-6 inhibitor (IL-6+IL-6 Inh) were used to control the IL-6 blocking efficiency of the IL-6 inhibitor. Monocyte-endothelial cell-cell adhesion (*A*, *C* and *E*) and ICAM-1 cells surface expression of HMEC-1 cells (*B*, *D* and *F*) were determined. The data are presented as x-fold of the Ctrl-treatments. *A*: Treatment of HMEC-1 cells with Pd-CM+IL-6 Inh decreased monocyte adhesion by 26 % and 24 % compared with the Pd-CM and Pd-CM+Iso. For Ad-CM+IL6 Inh, a slight increase in monocyte adhesion was observed, although, this effect was not significant between the Ad-CM group members. *B*: Treatment of HMEC-1 cells with Pd-CM+IL-6 Inh decreased ICAM-1 protein expression by 19 % and 22 % compared with the Pd-CM and Pd-CM+Iso. No differences were observed for the Ad-CM group. *C* and *D*: Exposure of IL-6 Inh or Iso alone had no significant effects on monocyte adhesion or ICAM-1 cells surface protein expression. *E*: Treatment of HMEC-1 cells with Pd 4%-CM+IL-6 Inh further decreased monocyte adhesion by 45 % and 43 % compared with HMEC-1 cells stimulated with Pd 4%-CM and Pd 4%-CM+Iso. For HMEC-1 cells treated with Ad 4%-CM a decrease of monocyte adhesion by 21 % was determined. *F*: As for normoxic CM, ICAM-1 protein expression on HMEC-1 cells decreased by 11 % and 12 % after treatment with Pd 4%-CM+IL-6 Inh compared with the treatment with Pd 4%-CM (n.s.) and Pd 4%-CM+Iso, respectively. In contrast to normoxic Ad-CM, treatment of HMEC-1 with Ad 4%-CM+IL-6 Inh decreased endothelial ICAM-1 protein expression by 14 % compared with the stimulation of HMEC-1 cells with Ad 4%-CM and Ad 4%-CM+Iso. Results are means ± SE (n=6). n.s. means statistically not significant. *P<0.05, **P<0.01, ***P<0.001.

3.4.4 Impact of IL-6 in SGBS-CM on phosphorylations of STAT1/3 in HMEC-1 cells

The IL-6 blockade strategy was applied in order to determine the functional role of IL-6 on the phosphorylations of STAT-1/3 in HMEC-1 cells. First, a time-course for STAT-1/3 phosphorylations using 10 ng/ml IL-6 was performed in order to choose the right time interval for the experiments (Figure 30A). At 30 minutes post-treatment of HMEC-1 cells with IL-6 the signals for STAT-1/3 phosphorylations were strongest as it was also for the treatment with CM, therefore, in further experiments this time was used for stimulations with IL-6. The phosphorylation intensity of STAT-1 and STAT-3 was found to be IL-6 concentration dependent. For STAT-1 and STAT-3 a phosphorylation increase was detectable at least up to IL-6 concentrations of 310 pg/ml and 39 pg/ml IL-6, respectively (Figure 30B). In comparison, SGBS preadipocytes secrete IL-6 on average 400 pg/ml and adipocytes 40 pg/ml (Figure 11A). Therefore, these IL-6 concentrations in the SGBS-CM are high enough to exert effects on STAT-1/3 phosphorylations. Stimulation of HMEC-1 cells with 10 ng IL-6 for 30 min increased phosphorylations of STAT-1 4.6-fold (Figures 31A and C) and STAT-3 5 to 6-fold (Figures 31B and D) compared to the stimulation of HMEC-1 cells with control medium. In the presence of 5 µg/ml IL-6 inhibitor, STAT-1 and STAT-3 phosphorylations were abolished to almost baseline levels (Figures 31A-D). Next, we treated HMEC-1 cells with preadipocyte-CM containing IL-6 inhibitor and noticed a decrease of STAT-1 phosphorylation by 2.4- and 2.3-fold (Figure 31A) and STAT-3 phosphorylation by 2.6-fold (Figure 31B) when compared to HMEC-1 stimulated with preadipocyte-CM in the presence or absence of isotype-matched control antibody, respectively. Treatment of HMEC-1 cells with adipocyte-CM containing IL-6 inhibitor also decreased STAT-1 phosphorylation 1.5- and 1.4-fold (Figure 31A) and STAT-3 phosphorylation 1.6-fold (Figure 31B) compared to HMEC-1 cells stimulated with adipocyte-CM in the presence and absence, respectively, of isotype-matched control antibody.

Similar phosphorylations levels of STAT-1 (Figure 31C) and STAT-3 (Figure 31D) were observed for analogue experiments with CM of hypoxic SGBS cells. For the monocyte adhesion and ICAM-1 cell surface experiments, IL-6 antagonist treatment alone of HMEC-1 cells exerted no effects (Figures 31C and D) and neither did the corresponding isotype control (data not shown).

Figure 30 Impact of IL-6 dependent on incubation time and concentration on the phosphorylations of STAT-1 and STAT-3 in HMEC-1 cells

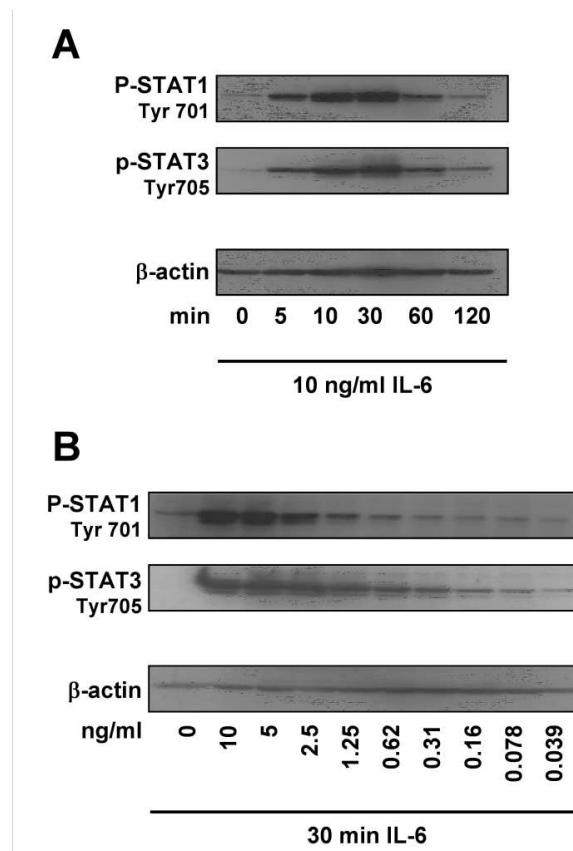


Figure 30 HMEC-1 cells were treated for indicated time intervals with 10 ng/ml of recombinant IL-6. Subsequently, the proteins were analysed for the phosphorylations of STAT-1, STAT-3 and β-actin, serving as loading reference (A). Next, HMEC-1 cells were treated with indicated concentrations of recombinant IL-6 for 30 min. The protein was analysed as described for A (B). Representative blots are shown (n=2).

Figure 31 Functional analysis of IL-6 in CM from normoxic and hypoxic SGBS cells on STAT-1 and STAT-3 phosphorylations in HMEC-1 cells

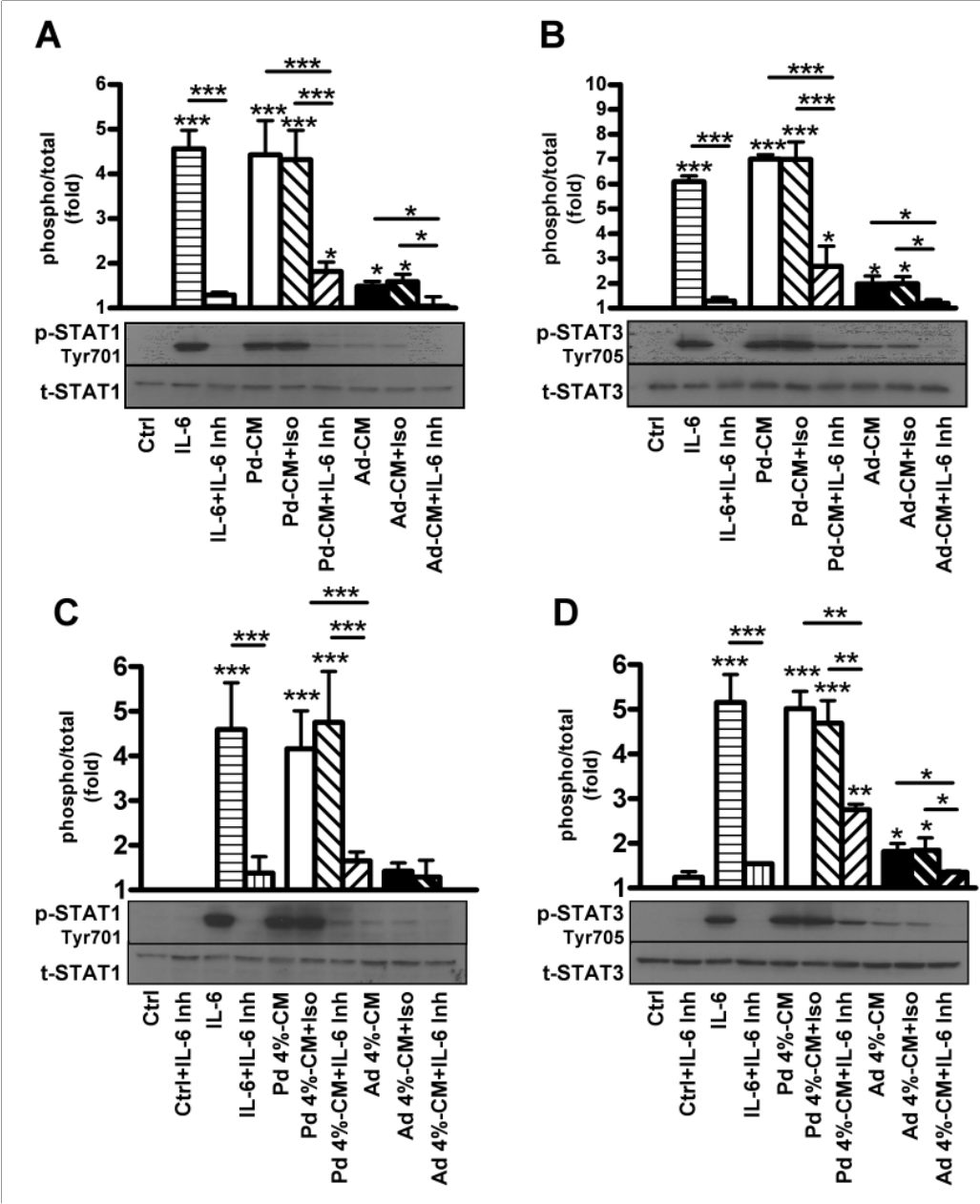


Figure 31

Control media (Ctrl) and conditioned media (CM) from preadipocytes (Pd) and adipocytes (Ad) exposed to normoxia were preincubated either with 5 $\mu\text{g/ml}$ function-neutralizing anti-IL-6 antibody as IL-6 inhibitor (IL-6 Inh) or with 5 $\mu\text{g/ml}$ of the corresponding IgG1 isotype-matched control antibody (Iso) for 15 min and subsequently used to stimulate HMEC-1 cells. HMEC-1 cells were treated with Ctrl, CM of Pd (Pd-CM) and Ad (Ad-CM), Ctrl and CM of cells pre-incubated with IL-6 inhibitor (Ctrl+IL-6 Inh, Pd-CM+IL-6 Inh, Ad-CM+IL-6 Inh) and Ctrl and CM of cells pre-incubated with the isotype-matched control antibody (Ctrl+Iso, Pd-CM+Iso, Ad-CM+Iso). Likewise, HMEC-1 cells were treated with reoxygenated CM derived from 4 % hypoxic Pd (Pd 4%-CM) and Ad (Ad 4%-CM), CM of hypoxic cells pre-incubated with IL-6 inhibitor (Pd 4% CM+IL-6 Inh, Ad 4%-CM+IL-6 Inh) and CM of hypoxic cells pre-incubated with the isotype-matched control antibody (Pd 4%-CM+Iso, Ad 4%-CM+Iso). HMEC-1 cells treated with 10 ng/ml IL-6 added to Ctrl medium (IL-6) or in combination with 5 $\mu\text{g/ml}$ IL-6 inhibitor (IL-6+IL-6 Inh) were used to control the IL-6 blocking efficiency of the IL-6 inhibitor. Total (t-) and phosphorylated (p-) STAT-1 and STAT-3 in HMEC-1 cells were determined by Western blot analysis. The data are presented as x-fold of the Ctrl-treatments. *A* and *B*: Stimulation of HMEC-1 cells with 10 ng IL-6 for 30 min (IL-6) increased phosphorylations of STAT-1 4.6-fold and STAT-3 6.1-fold compared with the stimulation of HMEC-1 cells with control medium (Ctrl). In the presence of 5 $\mu\text{g/ml}$ IL-6 inhibitor (IL-6+IL-6 Inh) STAT-1 and STAT-3 phosphorylations were abolished to almost baseline levels. Treatment of HMEC-1 cells with Pd-CM+IL-6 Inh decreased STAT-1 phosphorylation by 2.4- and 2.3-fold and STAT-3 phosphorylation by 2.6-fold when compared with the stimulation of HMEC-1 cells with Pd-CM and Pd-CM+Iso, respectively. Treatment of HMEC-1 cells with Ad CM+IL-6 Inh also decreased STAT-1 phosphorylation 1.5- and 1.4-fold and STAT-3 phosphorylation 1.6-fold compared with HMEC-1 cells stimulated with Ad-CM and Ad-CM+Iso, respectively. *C* and *D*: Stimulation of HMEC-1 cells with 10 ng IL-6 for 30 min (IL-6) increased phosphorylations of STAT-1 4.6-fold and STAT-3 5.2-fold compared with the stimulation of HMEC-1 cells with control medium (Ctrl). In the presence of 5 $\mu\text{g/ml}$ IL-6 inhibitor (IL-6+IL-6 Inh) STAT-1 and STAT-3 phosphorylations were abolished to almost baseline levels. Treatment of HMEC-1 cells with Pd 4%-CM+IL-6 Inh decreased STAT-1 phosphorylation by 2.5- and 2.9-fold and STAT-3 phosphorylation by 1.8-fold when compared with the stimulation of HMEC-1 cells with Pd-CM and Pd-CM+Iso, respectively. Treatment of HMEC-1 cells with Ad CM+IL-6 Inh also decreased STAT-1 phosphorylation 1.5- and 1.4-fold (both n.s.) and STAT-3 phosphorylation 1.3-fold compared with HMEC-1 cells stimulated with Ad-CM and Ad-CM+Iso, respectively. Results are means \pm SE (n=3). n.s. means statistically not significant. *P<0.05, **P<0.01, ***P<0.001.

3.5 Impact of CM derived from different-sized human primary mature adipocytes on HMEC-1 cell activation

In WAT adipocytes of various cell sizes exist. In obesity the size and/or number of adipocytes increases (see chapter 1.2.4.2). A positive correlation of secretion has been shown for several cytokines, including leptin, IL-6, IL-8 and MCP-1 with increasing fat cell size (Skurk *et al.*, 2007). In contrast, another study found that the fraction of small adipocytes was consistently associated with inflammatory gene expression, independently of BMI and insulin resistance (McLaughlin *et al.*, 2009). Therefore, the role of adipocyte size on endothelial cell activation in the context of adipocyte/endothelial cross-talk in WAT was analysed. Mature adipocytes, consisting of various cell sizes (entirety of adipocytes), were isolated from human WAT by collagenase digestion. These adipocytes were then separated by flotation in order to obtain a fraction with small and a fraction with large adipocytes. The fraction containing adipocytes with medium size was discarded due to technical reasons. HMEC-1 cells were treated with CM derived from the entirety of adipocytes (average diameter: 113 μm), small adipocytes (average diameter: 95 μm) and large adipocytes (average diameter: 130 μm), respectively. Subsequently, monocyte-endothelial cell-cell adhesion (Figures 32A, C and E) and ICAM-1 cell surface expression (Figures 32B, D and F) assays were performed. The corresponding data were normalized to adipocyte cell volume (Figures 32A and B), adipocyte cell surface area (Figures 32C and D) and adipocyte cell count (Figures 32E and F). The absolute cell count for the entirety of adipocytes was $1.2 \times 10^6 \pm 2.8 \times 10^5$ per ml, for small adipocytes $1.9 \times 10^6 \pm 4.1 \times 10^5$ per ml and for large adipocytes $8.5 \times 10^5 \pm 1.7 \times 10^5$ per ml. The data normalized to adipocyte cell volume are equal to the non-normalized data since for CM generation 1 ml of the entirety of adipocytes or of the respective adipocyte fraction was cultured in 5 ml medium, respectively. The data normalized to adipocyte cell volume reveal that monocyte adhesion and ICAM-1 cell surface expression increased after treatment with CM of the entirety of adipocytes, small and large adipocytes (Figures 32A and B). However, there was a tendency towards a greater increase in the assays when HMEC-1 cells were treated with the CM of the entirety of adipocytes. Normalization of the data to adipocyte cell surface area yielded similar results, although the effect exerted on monocyte-endothelial cell-cell adhesion by CM of small adipocytes was not statistically significant anymore (Figures 32C and D). When the data were normalized to adipocyte cell count, neither monocyte adhesion (Figure 32E) nor ICAM-1 expression (Figure 32F) of HMEC-1 cells was significant after treatment with CM of small adipocytes, in contrast to treatment with the

entirety of adipocytes and large adipocytes. Moreover, the differences between the treatments with CM of all and small adipocytes were for both assays statistically significant. Additionally, monocyte-endothelial cell-cell adhesion differences between treatments with CM of small and large adipocytes were significant.

Figure 32 Impact of human primary mature adipocytes of different size on endothelial cell activation

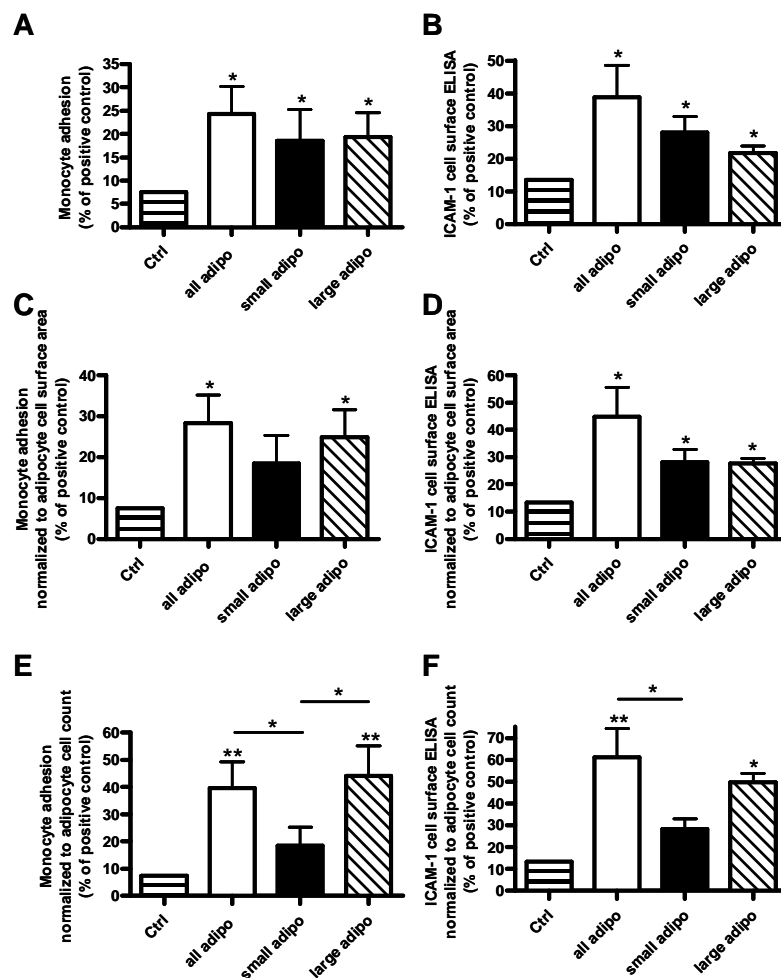


Figure 32

The conditioned media (CM) of the entirety of human primary mature adipocytes (all adipo), small mature adipocytes (small adipo) and large mature adipocytes (large adipo) were used to stimulate HMEC-1 cells. The CM was generated by culturing 1 ml of cells in 5 ml MCDB 131 medium for 16h. Subsequently, monocyte adhesion (A, C and E) to and ICAM-1 cell surface expression (B, D and F) of HMEC-1 cells was assessed. Data are presented as % of the positive control TNF- α . A and B: Monocyte adhesion was 24 %, 18 % and 19 % for all, small and large adipo, respectively. ICAM-1 expression was 38 %, 28 % and 22 % for all, small and large adipo, respectively. C and D: The values for monocyte adhesion and ICAM-1 shown in A and B, were normalized to the cell surface area. Monocyte adhesion was 28 %, 18 % (n.s.) and 24 % and for ICAM-1 45 %, 28 % and 28 % for all, small and large adipo, respectively. E and F: The values shown in A and B were normalized to the adipocyte cell count. Monocyte adhesion was 40 %, 19 % (n.s.) and 44 % and for ICAM-1 61 %, 28 % (n.s.) and 50 % for all, small and large adipo, respectively. Results are means \pm SE (n=4). n.s. means statistically not significant. *P<0.05, **P<0.01.

3.6 Peptidomics analysis of SGBS cell supernatants

3.6.1 Introduction

In order to generate and analyse the peptide secretion profile of SGBS cells and possibly find new secretion products which might be involved in the molecular and cellular cross-talk between preadipocytes, adipocytes and endothelial cells, the peptidomic technology was applied. The CM of normoxic and 1 % hypoxic SGBS preadipocytes and adipocytes were collected for analysis. The peptides were extracted and separated by liquid chromatography into 96 fractions by hydrophility which were then subjected to mass spectrometry. The data were visualized as a 2D peptide display. For detailed information refer to chapter 2.10.

3.6.2 Analysis of markers for cell lyses in CM of preadipocytes and adipocytes

As one of the quality controls of the peptidomic-technology used, the supernatants were tested for peptides from intracellular structures. Their amounts reflect the degree of cell lysis before or during supernatant sampling. If the amounts are high, the data evaluated may not be representative and may generate false-positive and false-negative results. In this setting shotgun sequenced peptides from the supernatant of human adipose tissue as cell lysis marker were used. These contain peptide fragments from the cytoplasm, nucleus, lipid droplets, caveolae and membrane proteins. Table 3 gives an overview of the used cell lyses marker and the number of peptide fractions analysed. In figure 33 the data for these markers in SGBS preadipocyte- and adipocyte-CM were visualized. Mean signal intensities between 10 and 20 are considered near the baseline noise according to the company Digilab BioVisioN (Hannover, Germany). It indicates that the amount of the measured markers for cell lyses is extremely low and mitigates in favour of the cell culture procedure. There were no significant differences in cell leakage observed for any of the marker-groups between SGBS preadipocyte- and adipocyte-CM.

In contrast, the values of the peptide markers for cell lyses in supernatants from primary cells, especially from mature adipocytes cultured in DMEM/F12 medium, had signal intensities above 20 and were significantly higher when compared with SGBS-CM (data not shown).

3.6.3 Putative peptides with different expressions in SGBS preadipocytes and adipocytes

The data shown in this section are limited, since the data were generated by the company Digilab BioVisioN (Hannover, Germany) which went insolvent. However, at least it was possible to obtain the data for eight in silico annotated peptides which are visualized in figure 34. An overview of these peptides is shown in table 4.

The samples were blinded before sending to the company with the following coding (#): #1: adipocyte-CM derived of cells under normoxia, #3: adipocyte-CM derived of cells under 1 % hypoxia, #4: preadipocyte-CM derived of cells under normoxia, #6: preadipocyte-CM derived of cells under 1 % hypoxia. It appeared that in the 2D peptide display strong signal differences occurred between the #1/3 (n=4) and #4/6 (n=6) for perilipin (PLIN), chemokine, CC motif, ligand 14 (CCL14), GRO protein, alpha (GROA), IL-8, Secretogranin II (SCG2), Secretogranin V (7B2) and Progranulin (GRN). Since perilipin is an important protein in fat cell biology it was not unexpected that the signals for two perilipin fragments were stronger in the CM of adipocytes (#1/3) compared with preadipocytes (#4/6). However, the signal intensities for perilipin in adipocyte-CM were below critical values which would have indicated increased cell lysis. Signals for a fragment of IL-8 were more pronounced in the CM of preadipocytes (#4/6) versus adipocytes (#1/3). This is in concordance with the data which had been generated before using qRT-PCR and ELISA techniques (see chapter 3.2.2). The band intensities for the fragments of GROA, CCL14, SCG2 and 7B2 were also stronger in preadipocyte-CM (#4/6) compared with adipocyte-CM (#1/3). In contrast, signals for fragments of GRN were more pronounced in adipocyte-CM (#1/3) versus preadipocyte-CM (#4/6). Due to a limited number of analysed samples, the #1 (n=2) and #3 (n=2) and the #4 (n=3) and #6 (n=3) were combined for data analysis. Differences within the groups (#1 versus #3 and #4 versus #6) were not investigated.

Table 3 Overview of markers used for assessing the extent of cell lyses in CM of SGBS cells

Protein name	Localization	Number of estimated peptide fragments
Polymerase I transcript release factor	Caveolae	4
Actin, cytoplasmic 1	Cytoplasm	2
Vimentin	Lipid droplet	11
Perilipin	Lipid droplet	6
Transmembrane BAX inhibitor motif-containing protein 1	Membrane protein	1
Cytochrom b5	Mitochondrion	1
La-related protein 1	Nucleus	6

The list gives an overview of the markers used, their general location within the cell and the corresponding number of estimated peptides.

Figure 33 Evaluation of the extent of cell lysis before and during supernatant sampling

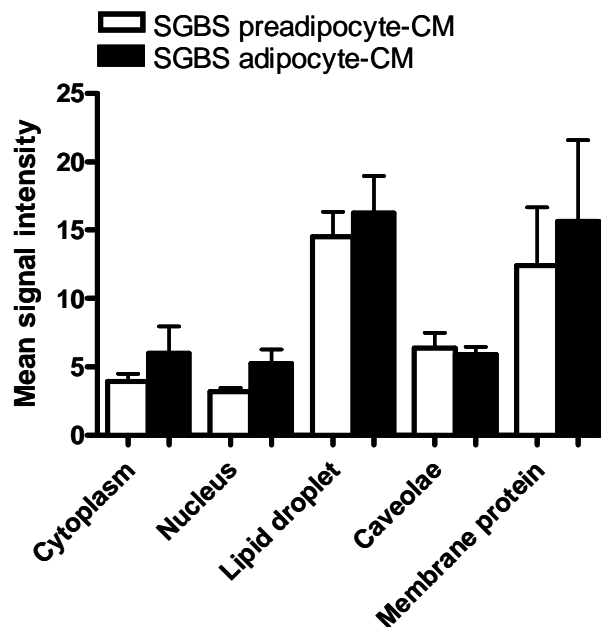


Figure 33

Markers for cell leakage were analysed in the conditioned media (CM) of SGBS preadipocytes and adipocytes. Therefore, sequenced peptides which were evaluated before from the supernatant of human adipose tissue were used. A mean signal intensity between 10 and 20 is near the baseline noise. Values around this level infer that the content of intracellular peptides in the CM is very low. Results are means \pm SE (n=6 for preadipocytes and n=4 for adipocytes).

Figure 34 Visualization of putative peptides identified by the peptidomic-technology

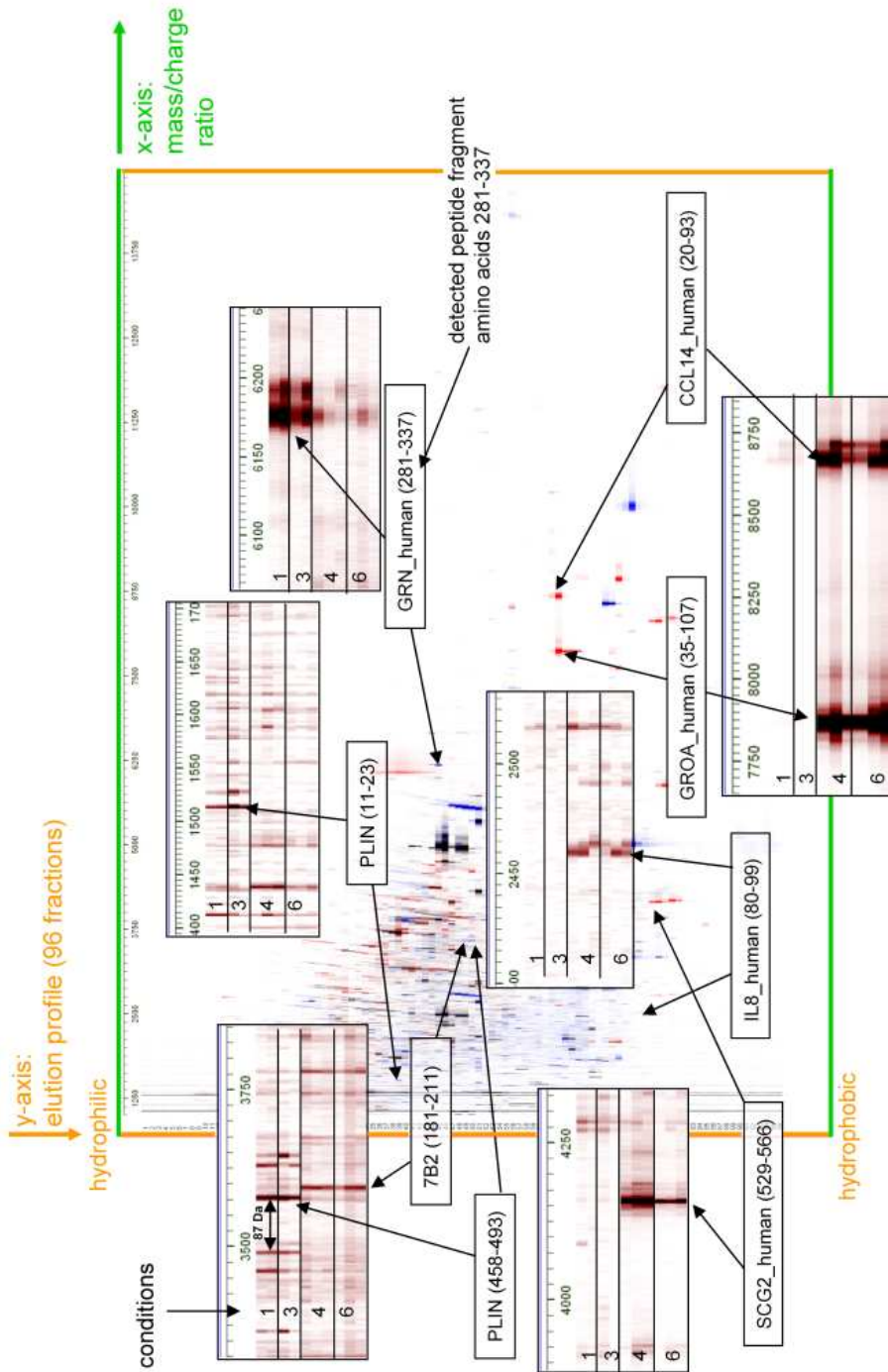


Figure 34
 In the background a 2D peptide display is shown. The x-axis is highlighted in green and represents the mass to charge ratio of peptides. The y-axis is highlighted in orange and represents the 96 chromatographic fractions where the hydrophobicity increases from the top to the bottom. The regions for the presented “in silico” annotated peptides from the 2D peptide display are shown separately enlarged in boxes. The name and the detected amino acid region of the peptide candidates are presented in boxes with arrows pointing to the respective regions on the 2D peptide display. The conditions 1 and 3 (adipocyte-conditioned media) were compared with the conditions 4 and 6 (preadipocyte-conditioned media). The picture was taken from the Digilab BioVisioN report from 18 Nov 2008 and slightly modified.

Table 4 Overview of putative peptide candidates identified by the peptidomic-technology

Names	Fragment/fraction	Upregulated under condition
Perilipin; PLIN	PLIN (11-23)/ F039.1512.5 PLIN (458-493) F050.3577.5	1 and 3 (adipocyte-CM)
Chemokine, CC motif, ligand 14; CCL14 <i>Alternative titles; symbols</i> Small inducible cytokine A, subfamily A, member 14; SCYA14 New CC chemokine 2; NCC2 hemofiltrate CC chemokine 1; HCC1	CCL14 (20-93)/ F063.8673.5	4 and 6 (preadipocyte-CM)
GRO protein, alpha; GROA <i>Alternative titles; symbols</i> chemokine, CXC motif, ligand 1; CXCL1, GRO1 oncogene; GRO1 small inducible cytokine subfamily B, member1; SCYB1 Melanoma growth stimulatory activity, alpha; MGSA KC chemokine, mouse, homolog of	GROA (35-107)/ F063.7861.5	4 and 6 (preadipocyte-CM)
Interleukin-8; IL-8 <i>Alternative titles; symbols</i> Small inducible cytokine subfamily B, member 8; SCYB8 Monocyte-derived neutrophil chemotactic factor neutrophil-activating peptide 1; NAP1 Granulocyte chemotactic protein 1; GCP1 chemokine, CXC motif, ligand 8; CXCL8	IL-8 (80-99)/ F076.2457.5	4 and 6 (preadipocyte-CM)
Secretogranin II; SCG2 <i>Alternative titles; symbols</i> Chromogranin C; CHGC Secretoneurin, included; SN, included	SCG2 (529-566)/ F078.155.5	4 and 6 (preadipocyte-CM)
Secretogranin V <i>Alternative titles; symbols</i> Pituitary polypeptide 7B2; P7B2 Secretory granule neuroendocrine protein 1; SGNE1	7B2 (181-211)/ F050.3594.5	4 and 6 (preadipocyte-CM)
Granulin precursor, GRN <i>Alternative titles; symbols</i> Progranulin; PGRN Epithelin precursor proepithelin; PEPI Granulin-epithelin precursor; GEP PC cell-derived growth factor; PCDGF Acrogranin glycoprotein, 88-KD; GP88 Granulins, included Epithelins, included	GRN (281-337)/ F045.6174.5	1 and 3 (adipocyte-CM)

This table gives an overview of the candidate peptides and their symbols, the analysed fragment-regions (amino-acid region of the candidate peptides) and under which condition the candidate peptides were upregulated. The conditions 1 and 3 (adipocyte-conditioned media) were compared with the conditions 4 and 6 (preadipocyte-conditioned media).

3.6.4 Validation of putative peptide candidates

After the identification of putative peptide candidates (“in silico annotated” peptides) using the peptidomic technology, I focussed on the three peptides progranulin, secretogranin II and secretogranin V which up to that time, to my knowledge had not been described in the literature as adipokines.

3.6.4.1 Progranulin

Progranulin is a 68.5 kDa cysteine-rich protein and secreted in a highly glycosylated, 90 kDa form. It is expressed in many tissues, particularly in epithelial and hematopoietic cells and is found in human plasma. Its function is complex and different in various organs and the central nervous system, e.g. it operates in wound healing responses and modulates inflammatory events. (Eriksen and Mackenzie, 2008; He and Bateman, 2003). For further description refer to chapter 4.7.

In SGBS cells, gene expression of progranulin was slightly higher in normoxic SGBS adipocytes versus preadipocytes (Figure 35A). Interestingly, the gene expression signals appeared very early, around 20 cycles which is in its intensity comparable to adiponectin mRNA, considered to be the most abundant adipokine. Moreover, progranulin was also detected in the CM of preadipocytes and adipocytes using the ELISA technique (Figure 35B). However, in contrast to the prediction of the in silico annotated peptide analysis, progranulin protein was found in greater amounts in the normoxic preadipocyte-CM compared with adipocyte-CM. Notably, the amount of progranulin in the CM of both, preadipocytes and adipocytes was in the ng- range which is comparably higher than many other cytokines.

3.6.4.2 Secretogranin II

Secretogranin II is an extremely hydrophilic and acidic protein with a molecular weight of 67.5 kDa. It is distributed throughout the endocrine and nervous system where it is localized in large dense core vesicles (Fischer-Colbrie *et al.*, 1995). Secretogranin II can be cleaved proteolytically and is found in human plasma (Stridsberg *et al.*, 2008).

Processing of this protein yields proteins of intermediate size and small peptides. The best characterized product is secretoneurin which has a molecular weight of 21 kDa. It is a chemoattractant for monocytes, eosinophils and endothelial cells. It promotes proliferation and angiogenesis and inhibits apoptosis in endothelial cells. Its angiogenic potential has been

said to be comparable to that of VEGF (Egger *et al.*, 1994; Fischer-Colbrie *et al.*, 2005; Kahler *et al.*, 2002). For further description refer to chapter 4.7.

Gene expression of secretogranin II was found in normoxic SGBS preadipocytes and adipocytes. The mRNA expression was more pronounced in the preadipocytes compared with adipocytes (Figure 35C). So far, at mRNA level this is in line with the prediction of the in silico annotated peptide analysis.

3.6.4.3 Secretogranin V

Secretogranin V also known as pituitary polypeptide 7B2 is a 21 kDa protein. Its expression is restricted to neurons and endocrine cells. Secretogranin V is found in human plasma (Stridsberg *et al.*, 2008). Analysis of its genetic variations showed no link to obesity and common forms of type 2 diabetes, although, it was concluded, that some genetic variants might worsen glucose intolerance and insulin resistance in the background of severe and early onset obesity (Bouatia-Naji *et al.*, 2007). For further description refer to chapter 4.7.

In SGBS cells, secretogranin V mRNA was found in both, normoxic preadipocytes and adipocytes. Interestingly, gene expression was higher in the preadipocytes versus adipocytes (Figure 35D) which is in concordance with the prediction of the in silico annotated peptide analysis.

Figure 35 Validation of putative candidate peptides identified by the peptidomic-technology

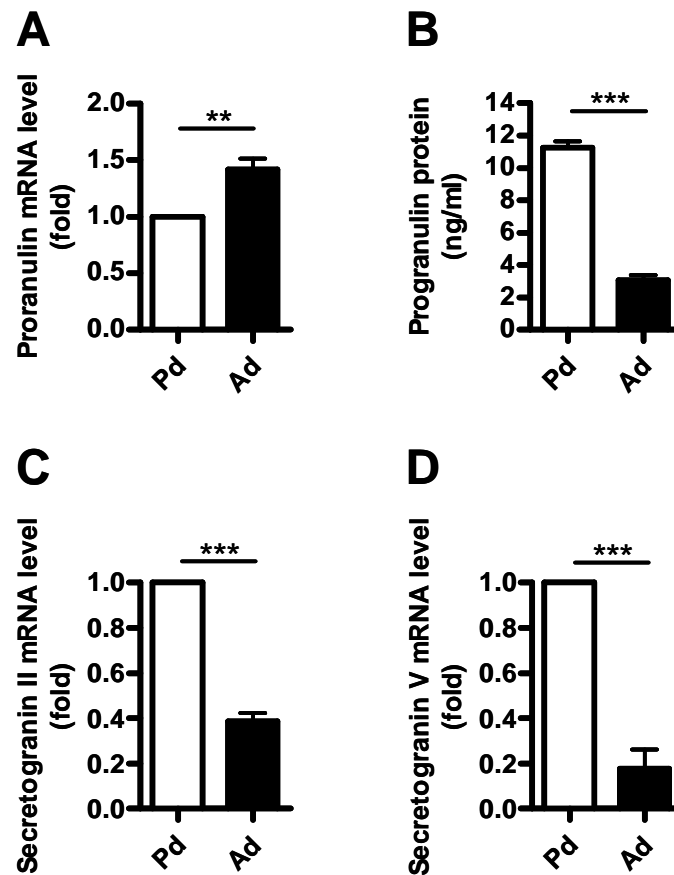


Figure 35
The mRNA quantities of the “in silico” annotated peptides progranulin (A), secretogranin II (C) and secretogranin V (D) was assessed in normoxic SGBS preadipocytes (Pd) and adipocytes (Ad) by qRT-PCR. The Ad values are presented as relative expression compared with values of the corresponding Pd (A, C and D). Progranulin protein was measured in the conditioned media of normoxic Ad and Pd using a specific ELISA (B). A and B: Progranulin mRNA expression was 40 % higher in Ad vs. Pd, whereas the protein was 3.7 fold higher in Pd compared with Ad. C: Secretogranin II mRNA expression was 2.6 fold higher in Pd vs. Ad. D: Secretogranin V gene expression was elevated 5.7 fold in Pd compared with Ad. Results are means \pm SE (n=5). **P<0.01, ***P<0.001.

4 Discussion

4.1 Introduction

Since the discovery of leptin (Zhang *et al.*, 1994) the perspectives on the role of WAT have changed dramatically. Besides its role as important energy reservoir it is a complex secretory and endocrine organ (Hauner, 2005). When WAT mass expands, several inflammatory molecules are found at higher amounts within the tissue (Wellen and Hotamisligil, 2005). It is suggested that some of these adipokines contribute to the state of chronic low-grade inflammation which contributes to insulin resistance and endothelial cell activation, the latter if dysregulated leading to micro- and macrovascular endothelial cell dysfunction (Kuldo *et al.*, 2005; Molavi *et al.*, 2006; Trayhurn, 2005). WAT consists of many cell types including adipocytes, preadipocytes, fibroblasts, endothelial cells and immune cells which differentially contribute to the pool of adipokines and are involved in autocrine, paracrine and endocrine processes and cross-talks (Antuna-Puente *et al.*, 2008; Fain *et al.*, 2008; Fain *et al.*, 2004; Hauner, 2005; Weisberg *et al.*, 2003). Obesity is connected with an increased number of macrophages and other immune cells in WAT (Weisberg *et al.*, 2003; Wu *et al.*, 2007). The endothelium as the interface between circulating blood immune cells and adipose tissue plays an interactive role in these infiltration and inflammatory processes (Pober and Sessa, 2007).

The overall aim of this study was to identify factors and elucidate the cellular interactions and the molecular mechanisms involved in the cross-talk of preadipocytes, adipocytes and endothelial cells. In order to mimic these processes *in vitro* I

1. established a coculture system between SGBS cells and HMEC-1 cells,
2. analysed adipokine expression and secretion of SGBS preadipocytes and adipocytes under normoxia, hypoxia and TNF- α - stimulation by qRT-PCR, ELISA and multiplex bead-based Luminex® assay,
3. analysed the impact of CM from stimulated SGBS cells on microvascular endothelial cell function by investigating monocyte-endothelial cell-cell adhesion, endothelial cell proliferation and signalling pathways,
4. performed functional analysis of mediators in the CM of preadipocytes and adipocytes responsible for the increased monocyte-endothelial cell-cell adhesion,

5. analysed the impact of CM from different-sized primary mature adipocytes on monocyte-endothelial cell-cell adhesion and
6. detected new candidates in SGBS cells which might be involved in the molecular cross-talk between preadipocytes, adipocytes and microvascular endothelial cells by using the peptidomics technology, quantitative qRT-PCR and ELISA.

Major findings mentioned in this study have been presented at congresses (see curriculum vitae) and were published in *American Journal of Physiology – Endocrinology and Metabolism* (Mack *et al.*, 2009) and in *Hormone and Metabolic Research* (Skurk *et al.*, 2009).

The results of this study show that preadipocytes produced higher levels of pro-inflammatory cytokines compared with adipocytes leading to endothelial activation in coculture as demonstrated in the functional assays. Exposure of SGBS preadipocytes and adipocytes to hypoxia and TNF- α enhanced and induced, respectively, endothelial cell activation in coculture. Additionally, endothelial cells were also activated by CM of primary mature adipocytes independently of their size. The characterization of the underlying molecular mechanisms of the observed endothelial cell activation found the MAPK pathway members, c-Jun as important element of the AP-1 complex and STAT-1/-3 to be involved, whereas the NF- κ B pathway was not activated. It was shown that the preadipocyte-CM-induced monocyte-endothelial cell-cell adhesion and ICAM-1 cell surface protein expression on HMEC-1 was JNK and JAK-1/STAT-1/3 pathway dependent. Furthermore, the functional studies of CM-derived factors revealed IL-6 as a mediator in CM from normoxic and hypoxic preadipocytes and hypoxic adipocytes. It was demonstrated that IL-6 operates on microvascular endothelial cells by increasing monocyte-endothelial cell interactions via the STAT-1/3 pathway. Finally, the characterization of the IL-6 receptor signalling complex on HMEC-1 cells supported the finding that IL-6 acts as an important mediator of the molecular cross-talk between preadipocytes, adipocytes and microvascular endothelial cells. Using the peptidomics technology, qRT-PCR and ELISA three new candidates in SGBS cells were revealed, progranulin and secretogranin II and secretogranin V. Progranulin and secretogranin II could be both involved in the cross-talk between preadipocytes, adipocytes and microvascular endothelial cells and are possibly new adipokines.

4.2 Coculture between SGBS cells and HMEC-1 cells

In the first part of the study an *in vitro* coculture system was established using primary SGBS-CM to stimulate HMEC-1 cells. This was a valuable tool for investigating the molecular and cellular cross-talk between human microvascular endothelial cells, preadipocytes and adipocytes. As yet, only two reports are published analyzing the effects of CM from mature adipocytes isolated from adipose tissue on endothelial cells (Curat *et al.*, 2004; Kralisch *et al.*, 2007). Important to note, the impact of adipocytes differentiated from preadipocytes *in vitro* has not been analysed in this context and the studies mentioned (Curat *et al.*, 2004; Kralisch *et al.*, 2007) neglected the role of preadipocytes in the context of cross-talk with endothelial cells. Considering the importance of the specificity of microvascular endothelial cells in the trafficking of monocytes and T-lymphocytes in tissues, the use of HMEC-1 cells as microvascular endothelial cells is more suitable for studying this cross-talk than using macrovascular endothelial cells like HUVECS as applied by Kralisch *et al.*, 2007. Using SGBS and HMEC-1 cells allows high reproducibility of results and makes the scheduling of experiments easier which is very difficult using primary cells due to the following reasons:

1. primary cells are derived from different donors, each having a unique genetic background and individual life style,
2. the ratios between adipocyte cell size in WAT is heterogeneous in each donor,
3. WAT sampling is not uniformly conducted, the collected WAT region is generally not consistent and different techniques are applied and
4. the scheduling of experiments is difficult, especially if coculture experiments are performed since all involved cell types have to be ready for use immediately.

The analysis of the impact of fresh CM from cultured SGBS cells exposed to different treatments such as TNF- α and hypoxia on HMEC-1 cells in the study presented here avoids confounding variables possibly caused by

1. secondary effects if defrosted CM are used and activity changes may have occurred due to freeze-thaw cycles,
2. serum, antibiotics, high glucose levels or other medium components and
3. other cell types as in the tissue or as they may remain with isolated primary cells.

In contrast, in the studies by Curat *et al.*, 2004 and Kralisch *et al.*, 2007 defrosted CM were used in the coculture experiments. In the report by Curat *et al.*, 2004 the CM were derived from mature adipocytes cultured in the presence of 25 units per ml α -thrombin. Thrombin exerts essential effects in the coagulation cascade and can bind to protease-activated receptors on various cells where the corresponding intracellular signalling leads to increased production

of pro-inflammatory cytokines and chemokines (Levi, 2010; Tsopanoglou and Maragoudakis, 2009). In the study by Kralisch *et al.*, 2007 the CM were derived from mature adipocytes cultured in the presence of 10 % FCS and 15 mM glucose.

Importantly, SGBS and HMEC-1 cells are particularly suitable for transfection (BelAiba *et al.*, 2007; Laumen *et al.*, 2008) which for example would be helpful in analysing the importance of signalling pathways. The results obtained by this coculture system with CM give valuable directions for future experiments with primary cells and experiments *in vivo*.

4.3 Adipokine expression of SGBS preadipocytes and adipocytes under normoxia and hypoxia

The reports on the differential contribution of cell types in WAT to the pool of adipokines are heterogeneous (Antuna-Puente *et al.*, 2008; Fain *et al.*, 2008; Fain *et al.*, 2004; Weisberg *et al.*, 2003). In this study, initially the gene expression and secretion of several adipokines in SGBS preadipocytes and adipocytes under normoxic, serum-, hormone- and antibiotic-free conditions with 5 mM glucose in the medium were analysed by qRT-PCRs, ELISAs and bead-based Luminex® assays.

Adiponectin as a late marker for adipocyte differentiation (Scherer *et al.*, 1995) was not expressed by preadipocytes, supporting their preadipocyte status. In contrast, the adipokines IL-4, IL-6, IL-8, MCP-1, VEGF, PAI-1, RANTES and SDF-1 α were significantly stronger expressed by preadipocytes compared with adipocytes. These findings are overall in line with other studies demonstrating a pro-inflammatory expression pattern for preadipocytes mostly derived from stromal-vascular fractions of adipose tissues (Bruun *et al.*, 2004; Chung *et al.*, 2006; Fain and Madan, 2005; Fain *et al.*, 2004; Fain *et al.*, 2009) but also for cell lines like 3T3-L1 cells (Harkins *et al.*, 2004; Poulain-Godefroy and Froguel, 2007) and human primary cells (Crandall *et al.*, 2000; Kintscher *et al.*, 2008; Wang *et al.*, 2005). The results for VEGF differ slightly from observations in the literature where its secretion by human WAT has been accredited mainly to the non-fat cells (Fain *et al.*, 2004) but no significant changes between VEGF secretion of preadipocytes and adipocytes were observed in human (Fain *et al.*, 2004) and rat (Mick *et al.*, 2002) primary cell cultures which could be due to different applied cell culture protocols. The strong pro-inflammatory character of preadipocytes versus adipocytes may reflect the close relationship between preadipocytes and macrophages (Charriere *et al.*, 2003; Cousin *et al.*, 1999). The conversion of preadipocytes into macrophages has been

demonstrated to be efficient and rapid and transcriptome profiling also showed a closer relationship between preadipocytes and macrophages than between preadipocytes and adipocytes (Charriere *et al.*, 2003). Interestingly, proliferating preadipocytes also develop phagocytotic activity towards microorganisms (Cousin *et al.*, 1999; Villena *et al.*, 2001).

With regard to the coculture experiments, the typical pro-inflammatory endothelial cell activators TNF- α , IL-1 and IFN- γ were analysed (Hubbard and Rothlein, 2000; Madge and Pober, 2001; Petzelbauer *et al.*, 1993). TNF- α mRNA expression was detectable in preadipocytes but not in adipocytes whereas, at protein level it was not found in either. The literature on TNF- α expression by adipocytes is controversial (Fain *et al.*, 2004; Poulain-Godefroy and Froguel, 2007; Schlesinger *et al.*, 2006). Interestingly, isolation of primary adipocytes from canine and mouse fat pads was associated with an induction of gene expression (Eisele *et al.*, 2005; Ruan *et al.*, 2003) and protein secretion (Ruan *et al.*, 2003) of inflammatory molecules such as TNF- α due to the collagenase treatment of the cells. This might explain the finding of TNF- α in some primary cell culture systems.

IFN- γ was not secreted by SGBS cells and was also only barely detectable in untreated human primary differentiated adipocytes (Schlesinger *et al.*, 2006). IL-1 α and IL-1 β gene expression but not protein secretion was measured in SGBS cells. In human WAT IL-1 α protein was not found whereas protein of IL-1 β has been found in amounts around 6 pg/mg (Juge-Aubry *et al.*, 2003) with the secretion mainly attributed to the non-fat cells (Fain *et al.*, 2004). In our laboratory IL-1 was hardly detectable in mature adipocytes and differentiated preadipocytes (Thomas Skurk, Department of Nutritional Medicine, Technische Universität München, Freising, Germany; unpublished data).

In order to allow a comparison between preadipocytes and adipocytes regarding gene expression, cytokine secretion and the effect of their CM on endothelial cell activation, the confluent preadipocytes (Pd0) were cultured for another 16 days (Pd16) in parallel to differentiating adipocytes in the same media, except for the induction to differentiate. The preadipocytes kept the image of fibroblastic-like cells over the culture period but PAI-1 and Il-6 protein release was higher in the Pd0 in comparison with the Pd16 whereas the MCP-1 release remained unchanged. Thus, it can be outruled that the 16 days of preadipocyte culture period was the reason for their observed strong pro-inflammatory character since the opposite was shown. Secondly, the cell culture protocol itself with the present hormones might decrease the expression of some inflammatory adipokines possibly also in adipocytes.

However, these hormones are necessary to maintain and promote lipid accumulation in adipocytes after they have been induced to differentiate.

Since increased adipose tissue mass is associated with reduced tissue perfusion (see chapter 1.2.6) in humans (Adams *et al.*, 2005) and in mice (Hosogai *et al.*, 2007; Rausch *et al.*, 2007; Ye *et al.*, 2007) and tissue function is critically dependent on sufficient tissue perfusion it is of interest how expression changes under hypoxia and what the consequences might be in the cross-talk with endothelial cells. The oxygen partial pressure in air is 159 mm Hg which is equivalent to 21 % oxygen. Studies have shown, that normal tissues are perfused with 20 to 70 mm Hg oxygen, equivalent to 2.5 % to 9.2 % oxygen whereas for example solid tumours, joints with rheumatoid arthritis and ischemic peripheral limbs of patients with diabetes are perfused with less than 10 mm Hg oxygen, equivalent to less than 1.3 % oxygen (Lewis *et al.*, 1999). Cell culture experiments are normally performed with 21 % oxygen in the gas mixture which does not reflect the real biological situation and therefore should be ideally conducted under “cell type specific” oxygen conditions. WAT of lean mice is perfused by 4.6-6.5% oxygen and has been shown to be decreased to only 2 % to 3.3 % in WAT of obese mice (Hosogai *et al.*, 2007; Rausch *et al.*, 2007; Ye *et al.*, 2007). Severe hypoxia might occur particularly in the tip regions as has been shown for mouse epididimal WAT (Cho *et al.*, 2007). In that study several tissues, including, WAT, WAT tip, heart, kidney, brain, liver, lung and hypoxic and non-hypoxic areas of lung carcinoma were stained with Hydroxyprobe-1. WAT showed 30% less staining than the hypoxic area of the tumour. In contrast the staining of the tip WAT region was increased 3- fold when compared with the hypoxic area of the tumour. These data allow speculation that in some areas of WAT, the oxygen supply might be even lower than 2 %. Therefore, experiments with SGBS cells under moderate and severe hypoxia, with 4 % and 1 % oxygen in the gas mixture, respectively, were conducted and compared with the standard normoxic situation (21 % oxygen).

HIF-1 (see chapter 1.2.6) is the key transcription factor involved in the transmission of the hypoxic response (Brahimi-Horn and Pouyssegur, 2009). It is composed of one of the HIF- α -subunits and HIF-1 β . Hypoxia stabilizes HIF-1 α protein, which is otherwise degraded by an ubiquitin-dependent proteasome. In this study, HIF-1 α was upregulated upon hypoxia exposure in a dose-dependent manner to comparable levels in preadipocytes and adipocytes, serving as quality control that the hypoxia experiments were carried out appropriately.

Upon 4 % hypoxia mainly modest changes in secretion were examined for both preadipocytes and adipocytes. In contrast, 1 % hypoxia strongly enhanced the release of VEGF, leptin, PAI-1, IL-6 and IL-4 in preadipocytes. In comparison, the secretion from hypoxic adipocytes was less significant achieving approximately one-half of the enhancements. Interestingly, it has been found for 3T3-L1 and human primary cells that preadipocytes have a stronger pro-inflammatory response to LPS treatment than adipocytes (Chung *et al.*, 2006; Poulain-Godefroy and Froguel, 2007). In the literature VEGF gene expression in mouse 3T3-F442A adipocytes was not effected by exposure to 5 % hypoxia (Lolmede *et al.*, 2003) whereas at 1 % hypoxia treatment VEGF gene expression and protein secretion was increased in mouse and human systems in preadipocytes (Wang *et al.*, 2008), stromal vascular cells (Rehman *et al.*, 2004) and differentiated adipocytes (Wang *et al.*, 2007; Ye *et al.*, 2007). These data point towards an important role of VEGF under hypoxia in expanding WAT to promote neovascularization as described for other tissues and tumours (Bishop-Bailey, 2009). Leptin gene expression did not change in 3T3-F442A adipocytes exposed to 5 % hypoxia, (Lolmede *et al.*, 2003) whereas protein release by human PAZ-6 adipocytes increased 3-fold after treatment with 6% hypoxia exposure (Grosfeld *et al.*, 2002) and in primary human differentiated adipocyte elevation of gene expression was 27-fold and of protein expression 4-fold with 1 % hypoxia exposure (Wang *et al.*, 2007). A substantial increase in leptin gene and protein expression by preadipocytes upon hypoxia stimulation was also found by another study using human primary preadipocytes (Wang *et al.*, 2008). Interestingly, one study also reported an increased leptin secretion by preadipocytes upon treatment with TNF α and IL-1 β (Simons *et al.*, 2005). Therefore, it appears that preadipocytes can also contribute considerably to the pool of leptin in WAT, given circumstances like hypoxia and/or TNF- α and IL-1 secreting macrophages in the neighbourhood. This additional leptin secretion by preadipocytes may be necessary in order to stimulate the development of new blood vessels during WAT expansion in concert with VEGF to allow appropriate oxygenation of the tissue.

In this study, IL-4 secretion increased upon hypoxia treatment in preadipocytes and adipocytes. This has been also observed for human peripheral mononuclear cells (Naldini and Carraro, 1999; Naldini *et al.*, 1997). IL-4 acts proangiogenic in the lung under hypoxic conditions (Yamaji-Kegan *et al.*, 2009), has the ability to suppress macrophage cytotoxic activity and exerts inhibitory effects on the expression and/or release of proinflammatory cytokines, including TNF- α , Il-1, Il-6 and IL-8 (Opal and DePalo, 2000). Beneficial effects were found with the administration of human recombinant IL-4 in an experimental model on

hypoxia-induced lung injury (Ozturk *et al.*, 2006) and also hypoxia-induced gastric and intestinal injury (Ozturk *et al.*, 2005). Therefore, IL-4 in the context of WAT hypoxia may protect the cells from hypoxia-inducing adverse effects and contribute to WAT angiogenesis.

In this study, PAI-1 and IL-6 gene expression and cytokine secretion increased in adipocytes after hypoxia treatment. This is in line with other studies, where PAI-1 gene and protein expression was elevated 7-fold and 6-fold, respectively, in mouse 3T3-L1 cells (Chen *et al.*, 2006) and gene expression was elevated in primary human differentiated adipocytes upon 1 % hypoxia treatment (Wang *et al.*, 2007). IL-6 gene expression and protein secretion increased after 1 % hypoxia treatment in mouse (Regazzetti *et al.*, 2009; Ye *et al.*, 2007) and human (Wang *et al.*, 2007) cell culture. PAI-1 and IL-6 elevation upon hypoxia may not primarily be an inflammatory response, but rather of adaptive nature since both molecules are known to be also involved in the development of the vascular system by promoting angiogenesis (Fan *et al.*, 2008; Zagorska and Dulak, 2004). Interestingly, whereas measurements in the study showed a significant hypoxia-sensitive upregulation of IL-6 and PAI-1 in preadipocytes Wang *et al.*, 2008 did not. In most cell types PAI-1 gene regulation is under the control of HIF-1 α and elevated upon hypoxic stimulus (Zagorska and Dulak, 2004). IL-6 is also increased under hypoxia in several cell types but its dependency on HIF-1 α is not clear (Semenza, 2003). The differences in this expression study compared with the study by Wang *et al.*, 2008, could be due to the fact that different sources of human preadipocytes and adipocytes were used and that these may react differently under hypoxia. However, it may be more likely that the obvious clear differences in the cell culture protocols applied are the explanation. In chapter 3.2.3 where adipokine secretion of SGBS cells cultured in the presence and in the absence of hormones and antibiotics had been compared, it was demonstrated that the cell culture protocol itself affected the cells and changed IL-6 secretion in preadipocytes and MCP-1 secretion in adipocytes. In the report by Wang *et al.*, 2008 preadipocytes were cultured in DMEM/F12, containing 10 % FCS, 100 U/ml penicillin, 100 μ g/ml streptomycin and 0.25 μ g/ml amphotericin. In contrast, in this study serum-free medium without antibiotics was used. In addition, MCDB 131 medium served as basal medium, which contains 5 mM glucose compared with DMEM/F12 which contains 25 mM glucose used in the study by Wang *et al.*, 2008. Moreover, observations in this study indicated that the HIF-1 α protein level under normoxia was already elevated in preadipocytes if 10% FCS was present in the medium. After FCS-depletion, the HIF-1 α protein content decreased

(data not shown). It is tempting to speculate, that preadipocytes with low basal HIF-1 α level might be more responsive to hypoxia, leading to differential cytokine secretion.

In this context, it is interesting that in the hypoxia experiments by Wang *et al.*, 2007, normoxic adipocytes showed a lower level of HIF-1 α compared with the preadipocytes cultured in 10% FCS. This might be an explanation why Wang *et al.*, 2007 measured an increase of IL-6 and PAI-1 in adipocytes under hypoxia, but not in preadipocytes. Therefore, using the same cell culture medium would be the first step to resolve this issue in the future.

It is important to note that hypoxia was not always accompanied by a strong upregulation of adipokines, but for example the chemokines MCP-1 and IL-8 decreased in hypoxic adipocytes and only moderately increased in preadipocytes. RANTES secretion was enhanced in preadipocytes after hypoxia exposure, whereas in adipocytes a small increase was only observed with 4 % hypoxia but not with 1% hypoxia treatment. In the literature MCP-1 gene expression was increased 2.8-fold in mouse 3T3-L1 adipocytes (Okada *et al.*, 2008) whereas in human primary differentiated adipocytes no alteration after exposure to 1 % hypoxia (Wang *et al.*, 2007) was observed.

The secretion of chemottractants such as MCP-1 by other hypoxic cell types is also controversial (Bosco *et al.*, 2004; Galindo *et al.*, 2001; Hohensinner *et al.*, 2006). IL-8 expression is generally elevated upon hypoxic stimuli in macrophages and other cell types (Hirani *et al.*, 2001; Karakurum *et al.*, 1994; Rydberg *et al.*, 2003; Scannell, 1996) whereas RANTES expression was either reduced or not regulated in human macrophages exposed to hypoxia (Bosco *et al.*, 2004; Hirani *et al.*, 2001; Turner *et al.*, 1999).

In the following, a possible explanation why adipocytes do not change or even decrease their chemoattractant secretion upon hypoxia exposure *in vitro* is given considering reports that pre-exposure of human epithelial cells and human endothelial cells to hypoxia increased transmigration of human blood polymorphonuclear leukocytes (Colgan *et al.*, 1996) and human monocytes (Kalra *et al.*, 1996), respectively, allowing for recruitment of immune cells. On the other hand, macrophage chemotactic migration during hypoxia within tissues has been reported to be inhibited (Bosco *et al.*, 2008; Grimshaw and Balkwill, 2001; Turner *et al.*, 1999). These observations together may explain how macrophages accumulate in areas of necrosis or inflammation. For human and mouse WAT it has been demonstrated that over 90 % of the WAT macrophages are localized to necrotic adipocytes (Cinti *et al.*, 2005). Macrophages may migrate along a chemotactic gradient until an area of hypoxia is reached where they are rapidly inhibited from progressing further in order to phagocyte cell debris and

also have a role in extracellular matrix remodelling and angiogenesis (Grimshaw and Balkwill, 2001). It has been shown *in vitro*, that chemotaxis via chemoattractants such as MCP-1, RANTES and macrophage inflammatory protein 1 alpha (MIP-1 α) (Turner *et al.*, 1999) is abrogated under hypoxic conditions and therefore may explain why adipocytes even decrease the secretion of MCP-1 and IL-8 under severe hypoxia. Since preadipocytes and adipocytes react completely different in chemoattractant secretion upon hypoxia exposure and intensity this may indicate a highly sensitive and regulated cell type-specific response and cell-cell cross-talk within the tissue in order to orchestrate differential immune cell infiltration and distribution.

Since adiponectin is reduced in plasma of obese individuals and is an antidiabetic protein (Spranger *et al.*, 2003), it was of interest to analyse the influence of hypoxia on adiponectin secretion by adipocytes. Interestingly, the robust adipocyte-specific secretion of adiponectin did not significantly change under hypoxia. This is in contrast to five studies, all performed in mouse 3T3-L1 adipocytes (Chen *et al.*, 2006; Hosogai *et al.*, 2007; Magalang *et al.*, 2009; Nakagawa *et al.*, 2008; Ye *et al.*, 2007) where a decrease of adiponectin in response to hypoxia was observed. In this respect, it appears that adipocytes differentiated from mouse 3T3-L1 preadipocytes, which have been derived from embryonic mesenchymal cells, are more responsive than human SGBS adipocytes as used in this study and primary human adipocytes in the report by Wang *et al.*, 2007 which were both differentiated from preadipocytes of postnatal adipose tissues. In this study, a small but significant decrease of adiponectin mRNA under hypoxia was measured but no changes for adiponectin secretion were observed. The results by Wang *et al.*, 2007 indicate similar results: only a slight decrease of 15 % of adiponectin secretion under 1% hypoxia compared with normoxia was reported. Altogether, the effect of hypoxia on the level of human adiponectin protein in cell culture seems to be rather small in comparison to the data generated in mouse 3T3-L1 cells which show a substantial decrease. It remains to be elucidated whether hypoxia results in a reduction of adiponectin secretion by human adipocytes *in vivo* and if so, whether the reduction would be sufficient to decrease adiponectin plasma levels and thus impact on insulin sensitivity.

Regarding the endothelial cell activators IL-1, TNF- α and IFN- γ no induction of secretion upon hypoxia exposure was measured in this study. At gene expression level, TNF- α increased in preadipocytes under only 4 % hypoxia exposure whereas no TNF- α was

detectable in adipocytes. This is in concordance with the literature in human differentiated adipocytes (Wang *et al.*, 2007) and in contrast to a 1.6-fold increase in mouse primary adipocytes (Ye *et al.*, 2007). In other cell types TNF- α regulation upon hypoxic stimulus is discussed controversially (Gerlach *et al.*, 1993; Hirani *et al.*, 2001; Leeper-Woodford and Detmer, 1999; Scannell, 1996). IL-1 α gene expression was elevated around 2-fold in adipocytes upon 1 % hypoxia but not upon 4 % hypoxia exposure and was unchanged in preadipocytes, whereas IL-1 β gene expression was not changed at all. In mouse primary adipocytes, IL-1 gene expression increased 2-fold after they had been exposed to 1 % hypoxia (Ye *et al.*, 2007) whereas in 3T3-L1 cells IL-1 β secretion was unchanged (Regazzetti *et al.*, 2009). In macrophages IL-1 expression upon hypoxic stimuli is discussed controversially (Gerlach *et al.*, 1993; Koga *et al.*, 1992; Scannell, 1996) as is also IFN- γ expression (Acosta-Iborra *et al.*, 2009; Bosco *et al.*, 2004).

In summary, the strong pro-inflammatory endothelial cell activators IL-1, TNF- α and IFN- γ are not or in negligible amounts produced by preadipocytes and adipocytes under normoxia and hypoxia and their secretion may under these biological situations be limited to immune cells in WAT. This may be important since macrophages can promote neovascularization in a hypoxic environment by producing VEGF, FGF, PDGF and also TNF- α which is both proinflammatory and either pro- or anti-angiogenic and critically depending on the dose applied (Lewis *et al.*, 1999).

4.4 Endothelial cell activation by CM of normoxic, hypoxic and TNF- α treated SGBS cells and different-sized primary mature adipocytes

In this study the overall strongly pro-inflammatory observed character of CM derived from normoxic preadipocytes was confirmed by the increase of the monocyte-endothelial cell-cell adhesion, whereas adipocyte-CM showed baseline levels. Furthermore, the endothelial cell expression analysis clearly showed that preadipocyte-CM and adipocyte-CM significantly induced the mRNA for the chemokines IL-8 and MCP-1, whereas the upregulation of ICAM-1 cell surface expression occurred only with preadipocyte-CM. This suggests that adipocyte-CM can increase the expression of these chemokines, but other functionally important molecules during endothelial cell activation, such as ICAM-1 (see chapter 1.2.7.1) are not upregulated and may explain the weak monocyte-endothelial cell-cell adhesion observed for adipocyte-CM. However, the expression pattern of adipocytes changed upon hypoxic

conditions leading to a significant increase of secreted pro-inflammatory adipokines and monocyte adhesion accompanied by upregulated ICAM-1 expression. Monocyte adhesion also further increased upon treatment with CM of hypoxic preadipocytes but was not followed by ICAM-1 expression, suggesting another molecular mechanism involved, e.g. triggering the presentation of chemoattractants at the endothelial cell surface. For isoprotanes it has been shown that they upregulate monocyte-endothelial cell-cell adhesion independent of the classical adhesion proteins (Kumar *et al.*, 2005). The increase of monocyte-endothelial cell-cell adhesion after treatment with CM of hypoxic SGBS cells matches with findings in the literature where pre-exposure of human epithelial cells and human endothelial cells to hypoxia increased transmigration of human blood polymorphonuclear leukocytes (Colgan *et al.*, 1996) and human monocytes (Kalra *et al.*, 1996), respectively. Thus, the recruitment of immune cells during hypoxia could be increased and together with observations in macrophages where chemotactic migration during hypoxia within tissues was inhibited (Bosco *et al.*, 2008; Grimshaw and Balkwill, 2001; Turner *et al.*, 1999) explain how macrophages accumulate in areas of necrosis or inflammation (see also chapter 4.3).

In addition, the capacity of preadipocyte-CM and adipocyte-CM for endothelial cell activation was characterized additionally by their strong effect on endothelial cell proliferation. Treatment of HMEC-1 cells with CM of SGBS cells exposed to 4 % hypoxia achieved endothelial proliferation values comparable with the positive control and they were not further enhanced or decreased with CM of SGBS cells exposed to 1 % hypoxia (data not shown). This suggests that moderate hypoxia is sufficient for preadipocytes and adipocytes to release a potent mixture of activators for endothelial cell proliferation, possibly VEGF and leptin as shown in chapter 3.4.3 and reported in the literature (Ferrara *et al.*, 2003; Park *et al.*, 2001), in order to achieve a maximum in endothelial cell proliferation as necessary step for neovascularization.

Moreover, it was found that TNF- α -stimulated preadipocytes and adipocytes upregulated the endogenous TNF- α mRNA expression and TNF- α -activity in CM which exerted a marked increase in monocyte adhesion. Since the specific blockade of TNF- α activity by the antagonist Enbrel® (Tracey *et al.*, 2008) reduced the adhesion more than 65%, but not completely, it can be concluded that TNF- α -dependent and TNF- α -independent cell-cell interactions occurred and, besides the TNF- α activity, other adipokines that may act in

concert have been induced. Potential candidates may be among the molecules identified in the gene expression analysis of TNF- α - treated SGBS cells by (Do *et al.*, 2006).

Overall, the strong impact of preadipocyte-CM compared with the adipocyte-CM on HMEC-1 cells can be explained by the generally less pro-inflammatory secretion activity of adipocytes. Further, it is proposed that adiponectin in adipocyte-CM decreases monocyte adhesion and endothelial ICAM-1 as described for TNF- α -stimulated HUVEC (Ouchi *et al.*, 1999) since gene expressions of the adiponectin receptors AdipoR1 and AdipoR2 was also detected in HMEC-1 cells (data not shown).

The interesting and still open questions remain:

1. can the observed strong potency of preadipocytes to secrete proinflammatory cytokines be translated to WAT, and if so
2. how is this proinflammatory potency of preadipocytes in WAT, where preadipocytes and adipocytes exist in the neighbourhood of other cell types, controlled in physiological and pathological situations?

In order to dissect the differential influence of different-sized primary mature adipocytes isolated from human WAT on endothelial cell activation, mature adipocytes were separated by size and their CM were tested in the monocyte-endothelial cell-cell adhesion and ICAM-1 cell surface expression assays. In the literature there is some evidence that a positive correlation exists between proinflammatory adipokines and increasing adipocyte cell size (Skurk *et al.*, 2007) whereas there is also reported the opposite (McLaughlin *et al.*, 2009). This study found that CM of the entirety of primary human mature adipocytes increased monocyte-endothelial cell-cell adhesion and ICAM-1 expression as described in other reports (Curat *et al.*, 2004; Kralisch *et al.*, 2007). Additionally, the CM of large adipocytes enhanced monocyte-endothelial cell-cell adhesion and ICAM-1 expression. These results and those obtained from the CM of the entirety of adipocytes remained from the statistical point of view throughout unchanged when the data of the assays were normalized to adipocyte cell volume, adipocyte cell count and adipocyte cell surface area. In contrast, whereas the CM of small adipocytes normalized to adipocyte cell volume increased monocyte-endothelial cell-cell adhesion, no significant elevation was found when the data of the assays were normalized to adipocyte cell count and adipocyte cell surface area. Additionally, ICAM-1 expression on HMEC-1 cells after treatment with CM of small adipocytes was enhanced when the data were

normalized to adipocyte cell volume and adipocyte cell surface area but not if normalized to adipocyte cell count. The results show, that the CM of mature adipocytes independently of their cell size can activate endothelial cells. Nevertheless, depending on the data normalization the CM derived from small adipocytes may have the least potential to activate endothelial cells which would support the results by Skurk *et al.*, 2007 who showed that the fraction containing the small adipocytes secreted less proinflammatory adipokines than large adipocytes. These conclusions are limited since the normalized data may not be real. This technical problem could be solved in future experiments by generating the CM in three different ways: firstly, incubate equal volumes of adipocytes per defined volumes of medium; secondly, incubate equal cell numbers of adipocytes per defined volumes of medium; and thirdly, incubate adipocytes with equal cell surface area per defined volumes of medium. Overall, it appears as if the CM of the entirety of adipocytes exerted the strongest effects on endothelial cell activation independently of the normalization, although not statistically significant. Possibly, the secretion products of the entirety of different-sized adipocytes together generate the most potent CM for endothelial cell activation by contributing with differential molecule secretion. Since the medium-sized adipocytes were not analysed separately due to technical reasons but were present in the entirety of adipocytes, these cells may also have contributed to these observations.

These results raise the question why CM of untreated mature adipocytes from WAT, depending on data normalization, increase monocyte-endothelial cell-cell adhesion and ICAM-1 cell surface expression whereas untreated differentiated adipocytes derived from SGBS preadipocytes do not. Most likely these are due to technical reasons. Firstly, the CM of mature adipocytes can be easily “concentrated” by using small volumes of cell culture media and rather large volumes of mature adipocytes in contrast to differentiated adipocytes where the concentration procedure is time and biological material consuming (see chapter 2.1.2). Secondly, the mature adipocytes may secrete more pro-inflammatory and other stress molecules than the differentiated adipocytes due to the collagenase treatment as reported elsewhere (Eisele *et al.*, 2005; Ruan *et al.*, 2003). Thirdly, it should be taken in account that the primary adipocytes in WAT are in continuous cellular cross-talk including immune cells, and in expanding WAT, these are exposed to hypoxia. Therefore, primary adipocytes may be preactivated independently of the collagenase procedure.

In this study, a direct comparison between the results generated from coculture experiments with CM of SGBS adipocytes and those obtained from coculture experiments using CM of primary mature adipocytes can not be made. To investigate the differences between coculture experiments using CM of SGBS cells and primary mature adipocytes in more detail, future experiments have to be performed at the same day and cell culture plate in order to get a direct data comparison.

A further question is whether the results obtained from coculture experiments using CM of SGBS preadipocytes and adipocytes would change if their data were normalized to either the protein content or the cell count of preadipocytes and adipocytes, respectively, or the protein content of the CM. Therefore, at least four independent experiments were performed where the CM of SGBS cells were used to test for endothelial cell activation and the corresponding SGBS cells were analysed for their protein content by the Modified Bradford assay and their cell count by staining the cells with Hoechst 33342, trihydrochloride, trihydrate (data not shown). No significant changes were observed after normalizing the results of the monocyte-endothelial cell-cell adhesion assay or ICAM-1 expression ELISA to the protein content or cell count of SGBS preadipocytes and adipocytes, respectively (data not shown). The protein content of preadipocyte-CM and adipocyte-CM was also similar as analysed by the company Digilab BioVisioN (Hannover, Germany; data not shown). Therefore, it can be ruled out that a different cell count or protein content of preadipocytes or adipocytes, respectively, created unequal conditions for the generation of CM or a different protein content of the CM caused the significant differences observed between CM of preadipocytes and adipocytes.

4.5 Molecular mechanisms of endothelial cells activated by CM of SGBS cells

To understand the underlying molecular mechanisms of endothelial cell activation, different signalling pathways in endothelial cells involved in the regulation of ICAM-1, IL-8 and MCP-1 were investigated. The results indicate that preadipocyte-CM and adipocyte-CM activate p38MAPK, SAPK/JNK and ERK1/2 in endothelial cells. Overall, less activity for adipocyte-CM was observed. Additionally, the transcription factor c-Jun was more strongly activated in HMEC-1 cells treated with preadipocyte-CM compared to adipocyte-CM. Moreover, a strong activation of STAT-1 and STAT-3 was detected for preadipocyte-CM which exerted stronger phosphorylations compared to adipocyte-CM.

The performed inhibitor experiments suggest, that JNK, which phosphorylates members of the AP-1 transcription family including c-Jun, JunD and ATF-2 (Hess *et al.*, 2004) is indispensable for monocyte adhesion and ICAM-1 cell surface protein expression induced by preadipocyte-CM. Furthermore, the blockade of JAK-signalling in HMEC-1 with the specific JAK inhibitor I and subsequent inhibition of the STAT1/3 phosphorylation revealed that this pathway and factors are functionally important for the induction of ICAM-1 cell surface protein expression and monocyte-endothelial cell-cell adhesion of HMEC-1 cells treated with preadipocyte-CM.

Surprisingly, the NF- κ B pathway was not involved in the induced endothelial cell activation upon treatment with CM of normoxic and hypoxic (data not shown) SGBS cells. In contrast, stimulation of HMEC-1 cells with TNF- α at low concentration activated the NF- κ B pathway in the positive control suggesting that this pathway is inducible in HMEC-1 cells, but not involved in the induction of ICAM-1 by CM, except when CM of TNF- α stimulated SGBS cells was used. It is likely that the NF κ B pathway was then involved in the endothelial cell activation, since the I κ B α phosphorylation was increased in HMEC-1 cells after treatment with CM of TNF- α exposed SGBS cells and abrogated when these CM were preincubated with Enbrel® whereas, for total I κ B α the opposite was shown. This concept is supported by the literature where TNF- α mediates endothelial cell activation via the Nf κ B pathway (Weber *et al.*, 1995). Further experiments with inhibitors would be necessary for clarification.

STAT-1 which is classically activated in response to IFN- γ (Jaruga *et al.*, 2004) was strongly phosphorylated in HMEC-1 cells stimulated by preadipocyte-CM. However, a substantial functional involvement of IFN- γ in CM as a pro-inflammatory key-activator of endothelium (Ozaki *et al.*, 1999) can be ruled out because IFN- γ was not detectable. Instead of, IL-6, VEGF and leptin which are known to stimulate the JAK/STAT pathways and are present in considerable amounts in CM, are good candidates for transducing signals important for endothelial cell activation (Jin *et al.*, 2003; Ni *et al.*, 2004; Pan *et al.*, 2007; Wincewicz *et al.*, 2007; Yahata *et al.*, 2003). With respect to the apparently uninduced NF- κ B pathway in HMEC-1 cells stimulated by CM of normoxic and hypoxic (data not shown) SGBS cells, it is reasonable to speculate that the upregulation of the genes for ICAM-1, MCP-1 and IL-8 might have occurred through increased c-Jun-mediated AP-1 and STAT-binding activities at functional sites of their promoter regions (Roebuck and Finnegan, 1999). Since the separate blockade of the JNK and JAK pathways with specific inhibitors resulted in the downregulation of ICAM-1 cell surface expression and monocyte-endothelial cell-cell adhesion, it is possible that both pathways are important to coordinate ICAM-1 cell surface expression and functional monocyte-endothelial cell-cell adhesion in this coculture system. Future experiments with electrophoretic mobility shift assays (EMSA) (Fried and Crothers, 1981; Garner and Revzin, 1981) would be useful for confirmation of the transcription factor/DNA interactions.

4.6 Functional analysis of mediators in the CM of SGBS cells responsible for endothelial cell activation

In this study, functional studies with function-neutralizing antibodies were performed in order to get first insights into CM-derived factors which mediate the observed increase in ICAM-1 expression and monocyte-endothelial cell-cell adhesion. For leptin and VEGF, no experimental support could be found that they are important in this process, which is also controversially discussed in the literature (Curat *et al.*, 2004; Kim *et al.*, 2001; Skilton *et al.*, 2005; Zhang and Issekutz, 2002). Interestingly, IL-6 was identified as an important mediator in CM inducing increased endothelial STAT-1/3 phosphorylations, ICAM-1 expression and monocyte adhesion to HMEC-1 cells treated with CM. IL-6 blockade in CM substantially suppressed STAT-1/3 phosphorylations, monocyte endothelial cell-cell adhesion and ICAM-1 expression. STAT-1/3-blockade in HMEC-1 cells also significantly decreased monocyte endothelial cell-cell adhesion and ICAM-1 expression. This study consequently shows that the IL-6 effect is primarily transduced by the endothelial STAT-1/3 signalling pathway as described in other systems (Jin *et al.*, 2003; Ni *et al.*, 2004; Pan *et al.*, 2007; Wincewicz *et al.*, 2007). However, the effect of IL-6 blockade had stronger effects on STAT1/3 phosphorylations compared with the smaller effects on monocyte adhesion and ICAM-1 cell surface expression. The results suggest that the preadipocyte-CM induced increase in monocyte adhesion and ICAM-1 expression in HMEC-1 cells is not only mediated by IL-6 but also by other factors present in the CM. Although the CM-mediated phosphorylations of STAT1/3 are largely IL-6 dependent as shown by IL-6 inhibitor suppression, there are other mediators than IL-6 and STAT1/3 which can increase ICAM-1 expression and monocyte endothelial cell adhesion. Since also the JNK-pathway was also identified to operate in the CM-induced monocyte adhesion and ICAM-1 cell surface expression in these inhibitor experiments (see chapter 3.3.8), the JNK-pathway could be a further functional pathway in this cross-talk.

Finally, the important finding of this study that the IL-6R α /gp130 receptor signalling complex is expressed on HMEC-1 cells, suggests that IL-6 bound to IL-6 receptor complexes on microvascular endothelial cells allows IL-6 signalling and transsignalling in an autocrine and paracrine fashion (Rose-John *et al.*, 2006). This finding integrates IL-6 derived from perivascular preadipocytes and adipocyte as a major mediator in the complex molecular and cellular cross-talk of endothelial cells in adipose tissue especially in the context of IL-6

signalling and transsignalling of soluble IL-6 receptors from lymphocytes and monocytes as described in other biological situations (Marin *et al.*, 2001; Rose-John *et al.*, 2006). In this context, the differential activation of inducible transcription factors by adipokines may provide an important mechanism which can lead to the expression of particular cell-cell adhesion molecules and chemokines in a cell type-specific and stimulus-specific fashion. These regulatory mechanisms could critically influence the site-specific recruitment of distinct leukocyte subsets during the inflammatory response.

4.7 Peptidomics analysis of SGBS cell supernatants

One of the major aims of this study was to establish an experimental basis for the characterisation of the secretion profile of SGBS cells using the described coculture system and the peptidomic technology in order to find interesting and new candidate peptides possibly involved in the molecular and cellular cross-talk between preadipocytes, adipocytes and endothelial cells. The described data are limited since the analyses could be not completed by the company Digilab Biovision due to insolvency. Therefore, the data which were available are restricted to the analysis with “in silico annotation” algorithm, in order to match the peptides in the samples to already identified and sequenced peptides. This means that these putative candidate peptides could not be isolated and sequenced. Furthermore, new hits of the mass spectrometry analysis could not be matched with already identified peptides and thus, their identity remains unknown. Nevertheless, for the putative candidates perilipin, CCL14, GROA, Il-8, secretogranin II and V and progranulin differential signal intensities between preadipocytes and adipocytes were observed. As expected, perilipin fragment signal intensity was found in adipocytes and not in preadipocytes but functions as a quality control, since the samples were “blinded” before sent to the company. Il-8 signal intensity was higher in preadipocytes compared with adipocytes. This was confirmed by the data already generated using the qRT-PCR and ELISA techniques, giving confidence in possibly existing differences for the other “in silico annotated candidates”. Focussing on secretogranin II, V and progranulin, their gene expression was confirmed by qRT-PCR and for progranulin, protein secretion in SGBS preadipocytes and adipocytes were detected using ELISA. At that time, to the best of my knowledge, these molecules had not been described as adipokines. Strikingly, a strong progranulin secretion by SGBS preadipocytes and adipocytes was detected in the ng-range in CM which is higher compared with many other cytokines. In the following time of this study, Youn *et al.*, 2009 reported that progranulin mRNA was found in comparable

amounts in human mature adipocytes and stromal vascular cells, with higher amounts of protein being found in visceral versus subcutaneous WAT using the qRT-PCR and Western blot techniques, respectively. Progranulin serum concentrations were found to correlate with the BMI and macrophage infiltration in omental WAT. The degree of chemotaxis mediated by progranulin was comparable to that of MCP-1 (Youn *et al.*, 2009). Overall, progranulin plays important and complex roles in tumorigenesis (Ong *et al.*, 2006), development (Eriksen and Mackenzie, 2008), neurogenesis (Bateman and Bennett, 2009) and several inflammatory events, especially wound repair (He and Bateman, 2003; He *et al.*, 2003), both suppressing inflammation and also being the source of cleavage products named granulins which exert opposing effects allowing for differential regulation (He *et al.*, 2003; Kojima *et al.*, 2009). Importantly, progranulin promotes neovascularization *in vivo* with similarities to VEGF and induces proliferation, migration and formation of capillary-like tubule structures of human dermal microvascular endothelial cells (He *et al.*, 2003). Therefore, progranulin, like VEGF and leptin (Hausman and Richardson, 2004) may also play an important role in WAT vascularization. Having the capacity to activate endothelial cells with regard to neovascularization it is conceivable that progranulin is also involved in the regulation of endothelial cell adhesion molecules and endothelial cell interactions with immune cells. Experiments with human recombinant progranulin and progranulin inhibition in CM would be useful in gaining new insights into its role in this coculture system and in the context of the molecular and cellular cross-talk between preadipocytes, adipocytes and endothelial cells in WAT.

Another candidate peptide found by the peptidomic technology was secretogranin II and its gene expression was detected in SGBS cells with higher levels having been observed in preadipocytes than adipocytes. This molecule is distributed throughout the endocrine and nervous system. It generates the molecule secretoneurin via proteolytical cleavage (Kahler *et al.*, 1999; Kahler *et al.*, 2002) which can be induced under pathological conditions and hypoxia and has been proposed to play a role in the induction of neo-vascularization in ischemic diseases (Fischer-Colbrie *et al.*, 2005). Secretoneurin is a chemoattractant for monocytes (Kahler *et al.*, 1999; Kahler *et al.*, 2002) and acts as direct angiogenic cytokine *in vitro* and *in vivo* (Kirchmair *et al.*, 2004), its potency being comparable to VEGF (Fischer-Colbrie *et al.*, 2005). Secretoneurin impairs endothelial barrier function via the JNK and ERK1/2 pathways (Yan *et al.*, 2006) and could possibly be involved in endothelial cell interactions with immune cells. It is also highly angiogenic and an activator of the JNK

pathway (Fischer-Colbrie *et al.*, 2005) which is besides the JAK/STAT pathway in this coculture system responsible for increased ICAM-1 expression of and monocyte adhesion to HMEC-1 cells. Thus, secretogranin II may be a very interesting candidate to investigate in the cross-talk between the cell types in WAT, provided that protein expression is also detected in SGBS cells and WAT.

Finally, gene expression of the peptide candidate secretogranin V in SGBS cells was similar to that of secretogranin II. Secretogranin V is expressed by neurons and endocrine cells and is a chaperon for proprotein convertase-2 (PC2). PC2 helps to convert large inactive precursor molecules to generate smaller bioactive molecules. It operates within secretory pathways and is essential in the maturation of several types of membrane-bound and secreted molecules (Mbikay *et al.*, 2001). Secretogranin V-null mice had no demonstrable PC2 activity. They were deficient in processing islet hormones and displayed hypoglycemia, hyperproinsulinemia and hypoglucagonemia. The mice had increased circulating levels of adrenocorticotrophic hormone (ACTH) and corticosterone with adrenocortical expansion. Secretogranin V-null mice died before 9 weeks of severe Cushing syndrome. Thus, Secretogranin V is required for PC2 activation but also functions in the regulation of pituitary hormone secretion (Westphal *et al.*, 1999). If protein expression of secretogranin V in SGBS cells was confirmed using the ELISA or Western blot techniques this molecule may play an important role in the process and regulation of cytokine secretion.

Overall, the peptidomics analysis was and will be very useful for identifying new and known candidates in biological samples and to dissect the contribution of pro-inflammatory and anti-inflammatory molecules by distinct cell types in WAT. Despite the above mentioned limitations, the analysis with “in silico annotation” algorithm delivered valuable results which when confirmed via gene and protein expression analysis are interesting for future experiments in WAT biology.

4.8 Concluding comments and perspectives

Taken together, this *in vitro* study shows that preadipocytes have the potential to contribute considerably to the total pool of adipokines, and with respect to the close vicinity of preadipocytes to endothelial cells, they may operate as potent activators of endothelial cells in WAT and probably also in an endocrine fashion. These effects can be promoted in preadipocytes and induced in adipocytes by TNF- α and hypoxia and mediated by IL-6 in a manner similar to what may occur in the neighbourhood of macrophages in expanding WAT. STAT1/3 and SAPK/JNK were found to be important players in the activation of endothelial cells.

The finding that IL-6 in CM from preadipocytes or adipocytes can operate as activator of microvascular endothelial cells point to a new path to explaining how IL-6 signalling and/or transsignalling via IL-6/soluble IL-6 receptor complexes may act on the microvasculature in adipose tissue. In the case of pathophysiological levels, this may lead to chronic low-grade inflammation and endothelial cell dysfunction. Therefore, it will be of great importance to study the expression profiles of preadipocytes and adipocytes at the cellular level in WAT *in situ*, and to identify the factors and mechanisms which activate or counteract their pro-inflammatory potency.

In future *in vitro* coculture studies using CM of preadipocytes and adipocytes, the specific blockade of adipokines in CM or the corresponding adipokine receptors on endothelial cells may be useful to further dissect the differential functions of adipokines during leukocyte-endothelial cell-cell adhesion and transmigration. For example, knockdown experiments for AdipoR1 and AdipoR2 on endothelial cells will be important to analyse the role of adiponectin in adipocyte-CM. Adiponectin and its signalling in endothelial cells may be possibly responsible for the observed weak endothelial cell activation by neutralizing the actions of other pro-inflammatory adipokines. For example, it has been reported that TNF- α induced monocyte-endothelial cell-cell adhesion can be attenuated by adiponectin (Ouchi *et al.*, 1999).

Transcriptome and peptidome/secretome analyses will promote the expression and secretion profiling of preadipocytes and adipocytes, with this study contributing by the demonstration

of progranulin, secretogranin II and secretogranin V. Secretogranin II may represent a new adipokine with angiogenic properties and regulated by hypoxia.

In order to gain insights into the full integrated molecular and cellular cross-talk between the different cell types in adipose tissue, *in vivo* imaging studies if applied in adipose tissue will be very informative. Use of the stimulated emission depletion (STED) microscopy (Lauterbach *et al.*, 2010) in these experiments may allow the observation of real-time events at molecular level. As yet, *in vivo* imaging showed that leukocyte-endothelial cell interactions were increased in the microcirculation of adipose tissue of obese mice and were normalized by administering an ICAM-1 antibody (Nishimura *et al.*, 2008). It would be interesting to investigate in this experimental setup whether the leukocyte-endothelial cell interactions are reduced in obese endothelial cell-specific gp130 knock out mice (Yao *et al.*, 2005) compared with control wild-type mice. It would be also important to know whether macrophage clustering in adipose tissue was the same in obese IL-6-deficient mice (Di Gregorio *et al.*, 2004; Savale *et al.*, 2009) compared with control wild-type mice. In this context the analysis of endothelial cell-specific knockout mice for relevant signalling pathway members [e.g. STAT1, STAT3 (Kano *et al.*, 2003), SAPK/JNK] would allow gaining insights into underlying signalling pathways *in vivo*. Preceding *in vitro* studies aimed at supporting and complementing the already examined underlying signalling mechanisms in endothelial cells stimulated with CM of preadipocytes and adipocytes exposed for instance to hypoxia would be necessary.

Altogether, this study should contribute to a better understanding of the molecular and cellular cross-talk and underlying mechanisms in WAT regulating the balance between pro-inflammatory and anti-inflammatory factors and insulin sensitivity in the etiology of obesity, the metabolic syndrome and diabetes.

5 Summary

Obesity is associated with a state of chronic low-grade inflammation. Immune cells accumulate in white adipose tissue (WAT) and the vascular endothelium plays an interactive role in these infiltration and inflammatory processes. In humans the underlying molecular and cellular mechanisms are incompletely understood. Mature and hypertrophic adipocytes are considered as the major adipogenic cell type secreting pro-inflammatory cytokines in WAT. In contrast, the investigation of the pro-inflammatory capacity of preadipocytes and their role in endothelial cell activation have been neglected to date.

In this study, the pro-inflammatory expression and secretion of normoxia, hypoxia and TNF- α -treated human preadipocytes and adipocytes (SGBS cells) and their impact and that of different-sized primary mature adipocytes on human microvascular endothelial cell (HMEC-1) activation was examined in order to gain new insights into this molecular and cellular cross-talk. Furthermore, in order to identify new secretion products of SGBS cells possibly involved in this cross-talk, the peptidomic technology was applied.

It was found that HMEC-1 stimulated with conditioned media (CM) from preadipocytes, but not adipocytes, increased endothelial ICAM-1 expression and monocyte adhesion to HMEC-1 cells. After hypoxia and TNF- α -stimulation of SGBS cells, adipocyte-CM induced and preadipocyte-CM enhanced the monocyte adhesion to HMEC-1 cells. Concordantly, the expression of pro-inflammatory adipokines, measured by qRT-PCR, ELISA and multiplex bead-based Luminex® assays, was considerably higher in preadipocytes than in adipocytes. CM up-regulated the phosphorylation of three MAPK pathways, STAT-1/3 and c-Jun in HMEC-1 cells whereas the NF- κ B pathway was not affected. Inhibitor experiments showed that monocyte-endothelial cell-cell adhesion and endothelial ICAM-1 expression was JNK and JAK-1/STAT-1/3 pathway dependent and IL-6 inhibitor experiments revealed IL-6 as a major mediator in CM increasing monocyte-endothelial cell-cell adhesion via the STAT-1/3 pathway. The IL-6R α /gp130 receptor signalling complex was detected on HMEC-1 cells. CM of mature adipocytes, independently of their size, were able to increase monocyte-endothelial cell-cell adhesion and ICAM-1 expression. Peptidomic analysis using “in silico annotation” algorithm and gene expression analysis identified progranulin, secretogranin II and secretogranin V as new factors being expressed by SGBS cells. Progranulin was found to be a new adipokine as demonstrated in CM of SGBS cells by ELISA. These findings were

supported afterwards by data published by another group describing progranulin protein expression in human WAT by Western blot. Further analyses are necessary to confirm secretogranin II and V as new secretory products of preadipocytes and adipocytes in WAT.

Altogether, this study shows that preadipocytes rather than adipocytes can operate as potent activators of endothelial cells. This can be enhanced in preadipocytes and induced in adipocytes by TNF- α and hypoxia in a manner similar to what may occur in WAT in the etiology of obesity. Secretogranin II may be an interesting candidate in the cross-talk of preadipocytes/adipocytes and endothelial cells due to its angiogenic properties and regulation by hypoxia.

6 References

- Acosta-Iborra, B., A. Elorza, I. M. Olazabal, N. B. Martin-Cofreces, S. Martin-Puig, M. Miro, M. J. Calzada, J. Aragoes, F. Sanchez-Madrid and M. O. Landazuri (2009). Macrophage oxygen sensing modulates antigen presentation and phagocytic functions involving IFN-gamma production through the HIF-1 alpha transcription factor. *J Immunol* 182(5): 3155-64.
- Adams, F., J. Jordan, K. Schaller, F. C. Luft and M. Boschmann (2005). Blood flow in subcutaneous adipose tissue depends on skin-fold thickness. *Horm Metab Res* 37(2): 68-73.
- Ades, E. W., F. J. Candal, R. A. Swerlick, V. G. George, S. Summers, D. C. Bosse and T. J. Lawley (1992). HMEC-1: establishment of an immortalized human microvascular endothelial cell line. *J Invest Dermatol* 99(6): 683-90.
- Aird, W. C. (2003). Endothelial cell heterogeneity. *Crit Care Med* 31(4 Suppl): S221-30.
- Aird, W. C. (2007). Phenotypic heterogeneity of the endothelium: I. Structure, function, and mechanisms. *Circ Res* 100(2): 158-73.
- Aird, W. C. (2007). Phenotypic heterogeneity of the endothelium: II. Representative vascular beds. *Circ Res* 100(2): 174-90.
- Alberti, K. G., P. Zimmet and J. Shaw (2006). Metabolic syndrome--a new world-wide definition. A Consensus Statement from the International Diabetes Federation. *Diabet Med* 23(5): 469-80.
- Alessi, M. C. and I. Juhan-Vague (2006). PAI-1 and the metabolic syndrome: links, causes, and consequences. *Arterioscler Thromb Vasc Biol* 26(10): 2200-7.
- Amin, M. A., C. S. Haas, K. Zhu, P. J. Mansfield, M. J. Kim, N. P. Lackowski and A. E. Koch (2006). Migration inhibitory factor up-regulates vascular cell adhesion molecule-1 and intercellular adhesion molecule-1 via Src, PI3 kinase, and NFkappaB. *Blood* 107(6): 2252-61.
- Anderson, A. S. and S. Caswell (2009). Obesity management--an opportunity for cancer prevention. *Surgeon* 7(5): 282-5.
- Antuna-Puente, B., B. Feve, S. Fellahi and J. P. Bastard (2008). Adipokines: the missing link between insulin resistance and obesity. *Diabetes Metab* 34(1): 2-11.
- Armbrust, E. and C. Rohl (2008). Time- and activation-dependency of the protective effect of microglia on astrocytes exposed to peroxide-induced oxidative stress. *Toxicol In Vitro* 22(5): 1399-404.
- Baggiolini, M. (2001). Chemokines in pathology and medicine. *J Intern Med* 250(2): 91-104.
- Bakker, W., E. C. Eringa, P. Sipkema and V. W. van Hinsbergh (2009). Endothelial dysfunction and diabetes: roles of hyperglycemia, impaired insulin signaling and obesity. *Cell Tissue Res* 335(1): 165-89.
- Baltimore, D. (1995). Discovery of the reverse transcriptase. *Faseb J* 9(15): 1660-3.
- Bartness, T. J. and M. Bamshad (1998). Innervation of mammalian white adipose tissue: implications for the regulation of total body fat. *Am J Physiol* 275(5 Pt 2): R1399-411.
- Bartoli, M., X. Gu, N. T. Tsai, R. C. Venema, S. E. Brooks, M. B. Marrero and R. B. Caldwell (2000). Vascular endothelial growth factor activates STAT proteins in aortic endothelial cells. *J Biol Chem* 275(43): 33189-92.
- Baskin, M. L., J. Ard, F. Franklin and D. B. Allison (2005). Prevalence of obesity in the United States. *Obes Rev* 6(1): 5-7.
- Bateman, A. and H. P. Bennett (2009). The granulin gene family: from cancer to dementia. *Bioessays* 31(11): 1245-54.
- Baum, D. and M. P. Stern (1977). Adipose hypocellularity in cyanotic congenital heart disease. *Circulation* 55(6): 916-20.

- Beer, A. (1852). Bestimmung der Absorption des rothen Lichts in farbigen Flüssigkeiten. *Annalen der Physik* 86: 78–87.
- BelAiba, R. S., T. Djordjevic, A. Petry, K. Diemer, S. Bonello, B. Banfi, J. Hess, A. Pogrebniak, C. Bickel and A. Gorlach (2007). NOX5 variants are functionally active in endothelial cells. *Free Radic Biol Med* 42(4): 446-59.
- Beltowski, J. (2006). Leptin and atherosclerosis. *Atherosclerosis* 189(1): 47-60.
- Berthoud, H. R. (2002). Multiple neural systems controlling food intake and body weight. *Neurosci Biobehav Rev* 26(4): 393-428.
- Bing, C. and P. Trayhurn (2009). New insights into adipose tissue atrophy in cancer cachexia. *Proc Nutr Soc* 68(4): 385-92.
- Bishop-Bailey, D. (2009). Tumour vascularisation: a druggable target. *Curr Opin Pharmacol* 9(2): 96-101.
- Bjorntorp, P. (1974). Effects of age, sex, and clinical conditions on adipose tissue cellularity in man. *Metabolism* 23(11): 1091-102.
- Bjorntorp, P. (1996). The regulation of adipose tissue distribution in humans. *Int J Obes Relat Metab Disord* 20(4): 291-302.
- Blaak, E. E., M. A. van Baak, G. J. Kemerink, M. T. Pakbiers, G. A. Heidendal and W. H. Saris (1995). Beta-adrenergic stimulation and abdominal subcutaneous fat blood flow in lean, obese, and reduced-obese subjects. *Metabolism* 44(2): 183-7.
- Boschmann, M. (2001). Heterogeneity of adipose tissue metabolism. *Adipose Tissues. Eurekah.com / Landes Bioscience*: 131-149.
- Boschmann, M. (2001). Heterogeneity of adipose tissue metabolism. *Adipose Tissues. Eurekah.com / Landes Bioscience*: 131-157.
- Bosco, M. C., M. Puppo, F. Blengio, T. Fraone, P. Cappello, M. Giovarelli and L. Varesio (2008). Monocytes and dendritic cells in a hypoxic environment: Spotlights on chemotaxis and migration. *Immunobiology* 213(9-10): 733-49.
- Bosco, M. C., M. Puppo, S. Pastorino, Z. Mi, G. Melillo, S. Massazza, A. Rapisarda and L. Varesio (2004). Hypoxia selectively inhibits monocyte chemoattractant protein-1 production by macrophages. *J Immunol* 172(3): 1681-90.
- Bouatia-Naji, N., V. Vatin, C. Lecoeur, B. Heude, C. Proenca, J. Veslot, B. Jouret, J. Tichet, G. Charpentier, M. Marre, B. Balkau, P. Froguel and D. Meyre (2007). Secretory granule neuroendocrine protein 1 (SGNE1) genetic variation and glucose intolerance in severe childhood and adult obesity. *BMC Med Genet* 8: 44.
- Bouis, D., G. A. Hospers, C. Meijer, G. Molema and N. H. Mulder (2001). Endothelium in vitro: a review of human vascular endothelial cell lines for blood vessel-related research. *Angiogenesis* 4(2): 91-102.
- Bourlier, V. and A. Bouloumie (2009). Role of macrophage tissue infiltration in obesity and insulin resistance. *Diabetes Metab* 35(4): 251-60.
- Bourlier, V., A. Zakaroff-Girard, A. Miranville, S. De Barros, M. Maumus, C. Sengenès, J. Galitzky, M. Lafontan, F. Karpe, K. N. Frayn and A. Bouloumie (2008). Remodeling phenotype of human subcutaneous adipose tissue macrophages. *Circulation* 117(6): 806-15.
- Bradford, M. M. (1976). A rapid and sensitive method for the quantitation of microgram quantities of protein utilizing the principle of protein-dye binding. *Anal Biochem* 72: 248-54.
- Brahimi-Horn, M. C., J. Chiche and J. Pouyssegur (2007). Hypoxia signalling controls metabolic demand. *Curr Opin Cell Biol* 19(2): 223-9.
- Brahimi-Horn, M. C. and J. Pouyssegur (2009). HIF at a glance. *J Cell Sci* 122(Pt 8): 1055-7.
- Bruun, J. M., A. S. Lihn, A. K. Madan, S. B. Pedersen, K. M. Schiott, J. N. Fain and B. Richelsen (2004). Higher production of IL-8 in visceral vs. subcutaneous adipose

- tissue. Implication of nonadipose cells in adipose tissue. *Am J Physiol Endocrinol Metab* 286(1): E8-13.
- Budde, P., I. Schulte, A. Appel, S. Neitz, M. Kellmann, H. Tammen, R. Hess and H. Rose (2005). Peptidomics biomarker discovery in mouse models of obesity and type 2 diabetes. *Comb Chem High Throughput Screen* 8(8): 775-81.
- Burnette, W. N. (1981). "Western blotting": electrophoretic transfer of proteins from sodium dodecyl sulfate--polyacrylamide gels to unmodified nitrocellulose and radiographic detection with antibody and radioiodinated protein A. *Anal Biochem* 112(2): 195-203.
- Canello, R., C. Henegar, N. Viguerie, S. Taleb, C. Poitou, C. Rouault, M. Coupaye, V. Pelloux, D. Hugol, J. L. Bouillot, A. Bouloumie, G. Barbatelli, S. Cinti, P. A. Svensson, G. S. Barsh, J. D. Zucker, A. Basdevant, D. Langin and K. Clement (2005). Reduction of macrophage infiltration and chemoattractant gene expression changes in white adipose tissue of morbidly obese subjects after surgery-induced weight loss. *Diabetes* 54(8): 2277-86.
- Canello, R., J. Tordjman, C. Poitou, G. Guilhem, J. L. Bouillot, D. Hugol, C. Coussieu, A. Basdevant, A. Bar Hen, P. Bedossa, M. Guerre-Millo and K. Clement (2006). Increased infiltration of macrophages in omental adipose tissue is associated with marked hepatic lesions in morbid human obesity. *Diabetes* 55(6): 1554-61.
- Carmeliet, P. and R. K. Jain (2000). Angiogenesis in cancer and other diseases. *Nature* 407(6801): 249-57.
- Carriere, A., M. C. Carmona, Y. Fernandez, M. Rigoulet, R. H. Wenger, L. Penicaud and L. Casteilla (2004). Mitochondrial reactive oxygen species control the transcription factor CHOP-10/GADD153 and adipocyte differentiation: a mechanism for hypoxia-dependent effect. *J Biol Chem* 279(39): 40462-9.
- Casteilla, L., V. Planat-Benard, B. Cousin, J. S. Silvestre, P. Laharrague, G. Charriere, A. Carriere and L. Penicaud (2005). Plasticity of adipose tissue: a promising therapeutic avenue in the treatment of cardiovascular and blood diseases? *Arch Mal Coeur Vaiss* 98(9): 922-6.
- Charriere, G., B. Cousin, E. Arnaud, M. Andre, F. Bacou, L. Penicaud and L. Casteilla (2003). Preadipocyte conversion to macrophage. Evidence of plasticity. *J Biol Chem* 278(11): 9850-5.
- Chen, B., K. S. Lam, Y. Wang, D. Wu, M. C. Lam, J. Shen, L. Wong, R. L. Hoo, J. Zhang and A. Xu (2006). Hypoxia dysregulates the production of adiponectin and plasminogen activator inhibitor-1 independent of reactive oxygen species in adipocytes. *Biochem Biophys Res Commun* 341(2): 549-56.
- Chen, S., L. C. Teicher, D. Kazim, R. E. Pollack and L. S. Wise (1989). Commitment of mouse fibroblasts to adipocyte differentiation by DNA transfection. *Science* 244(4904): 582-5.
- Cho, C. H., Y. J. Koh, J. Han, H. K. Sung, H. Jong Lee, T. Morisada, R. A. Schwendener, R. A. Brekken, G. Kang, Y. Oike, T. S. Choi, T. Suda, O. J. Yoo and G. Y. Koh (2007). Angiogenic role of LYVE-1-positive macrophages in adipose tissue. *Circ Res* 100(4): e47-57.
- Chomczynski, P. and N. Sacchi (1987). Single-step method of RNA isolation by acid guanidinium thiocyanate-phenol-chloroform extraction. *Anal Biochem* 162(1): 156-9.
- Chomczynski, P. and N. Sacchi (2006). The single-step method of RNA isolation by acid guanidinium thiocyanate-phenol-chloroform extraction: twenty-something years on. *Nat Protoc* 1(2): 581-5.
- Christiaens, V. and H. R. Lijnen (2009). Angiogenesis and development of adipose tissue. *Mol Cell Endocrinol*.
- Chung, S., K. Lapoint, K. Martinez, A. Kennedy, M. Boysen Sandberg and M. K. McIntosh (2006). Preadipocytes mediate lipopolysaccharide-induced inflammation and insulin

- resistance in primary cultures of newly differentiated human adipocytes. *Endocrinology* 147(11): 5340-51.
- Cinti, S. (2001). Morphology of the adipose organ. *Adipose Tissues*. Eureka.com / Landes Bioscience: 11-26.
- Cinti, S. (2005). The adipose organ. *Prostaglandins Leukot Essent Fatty Acids* 73(1): 9-15.
- Cinti, S. (2009). Reversible physiological transdifferentiation in the adipose organ. *Proc Nutr Soc* 68(4): 340-9.
- Cinti, S., G. Mitchell, G. Barbatelli, I. Murano, E. Ceresi, E. Faloia, S. Wang, M. Fortier, A. S. Greenberg and M. S. Obin (2005). Adipocyte death defines macrophage localization and function in adipose tissue of obese mice and humans. *J Lipid Res* 46(11): 2347-55.
- Colgan, S. P., A. L. Dzuz and C. A. Parkos (1996). Epithelial exposure to hypoxia modulates neutrophil transepithelial migration. *J Exp Med* 184(3): 1003-15.
- Cousin, B., O. Munoz, M. Andre, A. M. Fontanilles, C. Dani, J. L. Cousin, P. Laharrague, L. Casteilla and L. Penicaud (1999). A role for preadipocytes as macrophage-like cells. *Faseb J* 13(2): 305-12.
- Crandall, D. L., T. M. Groeling, D. E. Busler and T. M. Antrilli (2000). Release of PAI-1 by human preadipocytes and adipocytes independent of insulin and IGF-1. *Biochem Biophys Res Commun* 279(3): 984-8.
- Crandall, D. L., G. J. Hausman and J. G. Kral (1997). A review of the microcirculation of adipose tissue: anatomic, metabolic, and angiogenic perspectives. *Microcirculation* 4(2): 211-32.
- Curat, C. A., A. Miranville, C. Sengenès, M. Diehl, C. Tonus, R. Busse and A. Bouloumie (2004). From blood monocytes to adipose tissue-resident macrophages: induction of diapedesis by human mature adipocytes. *Diabetes* 53(5): 1285-92.
- Curat, C. A., V. Wegner, C. Sengenès, A. Miranville, C. Tonus, R. Busse and A. Bouloumie (2006). Macrophages in human visceral adipose tissue: increased accumulation in obesity and a source of resistin and visfatin. *Diabetologia* 49(4): 744-7.
- De Clerck, L. S., C. H. Bridts, A. M. Mertens, M. M. Moens and W. J. Stevens (1994). Use of fluorescent dyes in the determination of adherence of human leucocytes to endothelial cells and the effect of fluorochromes on cellular function. *J Immunol Methods* 172(1): 115-24.
- Di Girolamo, M., N. S. Skinner, Jr., H. G. Hanley and R. G. Sachs (1971). Relationship of adipose tissue blood flow to fat cell size and number. *Am J Physiol* 220(4): 932-7.
- Di Gregorio, G. B., L. Hensley, T. Lu, G. Ranganathan and P. A. Kern (2004). Lipid and carbohydrate metabolism in mice with a targeted mutation in the IL-6 gene: absence of development of age-related obesity. *Am J Physiol Endocrinol Metab* 287(1): E182-7.
- Do, M. S., H. S. Jeong, B. H. Choi, L. Hunter, S. Langley, L. Pazmany and P. Trayhurn (2006). Inflammatory gene expression patterns revealed by DNA microarray analysis in TNF-alpha-treated SGBS human adipocytes. *Yonsei Med J* 47(5): 729-36.
- Eckert, W. A. and J. Kartenbeck (1997). *Proteine, Standardmethoden der Molekularbiologie und Zellbiologie*. Springer.
- Edgell, C. J., C. C. McDonald and J. B. Graham (1983). Permanent cell line expressing human factor VIII-related antigen established by hybridization. *Proc Natl Acad Sci U S A* 80(12): 3734-7.
- Egger, C., R. Kirchmair, S. Kapelari, R. Fischer-Colbrie, R. Hogue-Angeletti and H. Winkler (1994). Bovine posterior pituitary: presence of p65 (synaptotagmin), PC1, PC2 and secretoneurin in large dense core vesicles. *Neuroendocrinology* 59(2): 169-75.
- Eisele, I. and H. Hauner (2006). Gewichtsabnahme ohne Jojo-Effekt ist keine Utopie. *Ärztezeitung, Forschung und Praxis* 25(426): 8-12.

- Eisele, I., I. S. Wood, A. J. German, L. Hunter and P. Trayhurn (2005). Adipokine gene expression in dog adipose tissues and dog white adipocytes differentiated in primary culture. *Horm Metab Res* 37(8): 474-81.
- El-Ftesi, S., E. I. Chang, M. T. Longaker and G. C. Gurtner (2009). Aging and diabetes impair the neovascular potential of adipose-derived stromal cells. *Plast Reconstr Surg* 123(2): 475-85.
- Elgazar-Carmon, V., A. Rudich, N. Hadad and R. Levy (2008). Neutrophils transiently infiltrate intra-abdominal fat early in the course of high-fat feeding. *J Lipid Res* 49(9): 1894-903.
- Elshal, M. F. and J. P. McCoy (2006). Multiplex bead array assays: performance evaluation and comparison of sensitivity to ELISA. *Methods* 38(4): 317-23.
- Engvall, E. and P. Perlmann (1971). Enzyme-linked immunosorbent assay (ELISA). Quantitative assay of immunoglobulin G. *Immunochemistry* 8(9): 871-4.
- Eriksen, J. L. and I. R. Mackenzie (2008). Progranulin: normal function and role in neurodegeneration. *J Neurochem* 104(2): 287-97.
- Ervin, R. B. (2009). Prevalence of the metabolic syndrome among adults 20 years of age and over, by sex, age, race and ethnicity, and body mass index: 2003–2006. . Centers for Disease Control and Prevention, National Health Statistic Reports 13.
- Fain, J. N., B. Buehrer, S. W. Bahouth, D. S. Tichansky and A. K. Madan (2008). Comparison of messenger RNA distribution for 60 proteins in fat cells vs the nonfat cells of human omental adipose tissue. *Metabolism* 57(7): 1005-15.
- Fain, J. N. and A. K. Madan (2005). Insulin enhances vascular endothelial growth factor, interleukin-8, and plasminogen activator inhibitor 1 but not interleukin-6 release by human adipocytes. *Metabolism* 54(2): 220-6.
- Fain, J. N. and A. K. Madan (2005). Regulation of monocyte chemoattractant protein 1 (MCP-1) release by explants of human visceral adipose tissue. *Int J Obes (Lond)* 29(11): 1299-307.
- Fain, J. N., A. K. Madan, M. L. Hiler, P. Cheema and S. W. Bahouth (2004). Comparison of the release of adipokines by adipose tissue, adipose tissue matrix, and adipocytes from visceral and subcutaneous abdominal adipose tissues of obese humans. *Endocrinology* 145(5): 2273-82.
- Fain, J. N., B. M. Tagele, P. Cheema, A. K. Madan and D. S. Tichansky (2009). Release of 12 Adipokines by Adipose Tissue, Nonfat Cells, and Fat Cells From Obese Women. *Obesity (Silver Spring)*.
- Fan, Y., J. Ye, F. Shen, Y. Zhu, Y. Yeghiazarians, W. Zhu, Y. Chen, M. T. Lawton, W. L. Young and G. Y. Yang (2008). Interleukin-6 stimulates circulating blood-derived endothelial progenitor cell angiogenesis in vitro. *J Cereb Blood Flow Metab* 28(1): 90-8.
- Farmer, S. R. (2006). Transcriptional control of adipocyte formation. *Cell Metab* 4(4): 263-73.
- Fasshauer, M. and R. Paschke (2003). Regulation of adipocytokines and insulin resistance. *Diabetologia* 46(12): 1594-603.
- Ferrara, N. and T. Davis-Smyth (1997). The biology of vascular endothelial growth factor. *Endocr Rev* 18(1): 4-25.
- Ferrara, N., H. P. Gerber and J. LeCouter (2003). The biology of VEGF and its receptors. *Nat Med* 9(6): 669-76.
- Fischer-Colbrie, R., R. Kirchmair, C. M. Kahler, C. J. Wiedermann and A. Saria (2005). Secretoneurin: a new player in angiogenesis and chemotaxis linking nerves, blood vessels and the immune system. *Curr Protein Pept Sci* 6(4): 373-85.

- Fischer-Colbrie, R., A. Laslop and R. Kirchmair (1995). Secretogranin II: molecular properties, regulation of biosynthesis and processing to the neuropeptide secretoneurin. *Prog Neurobiol* 46(1): 49-70.
- Fischer-Posovszky, P., M. Wabitsch and Z. Hochberg (2007). Endocrinology of adipose tissue - an update. *Horm Metab Res* 39(5): 314-21.
- Fried, M. and D. M. Crothers (1981). Equilibria and kinetics of lac repressor-operator interactions by polyacrylamide gel electrophoresis. *Nucleic Acids Res* 9(23): 6505-25.
- Friedman, J. M. and J. L. Halaas (1998). Leptin and the regulation of body weight in mammals. *Nature* 395(6704): 763-70.
- Frye, C. A., X. Wu and C. W. Patrick (2005). Microvascular endothelial cells sustain preadipocyte viability under hypoxic conditions. *In Vitro Cell Dev Biol Anim* 41(5): 160-4.
- Fukumoto, S. and T. Fujimoto (2002). Deformation of lipid droplets in fixed samples. *Histochem Cell Biol* 118(5): 423-8.
- Gagnon, A. and A. Sorisky (1998). The effect of glucose concentration on insulin-induced 3T3-L1 adipose cell differentiation. *Obes Res* 6(2): 157-63.
- Galindo, M., B. Santiago, J. Alcamí, M. Rivero, J. Martín-Serrano and J. L. Pablos (2001). Hypoxia induces expression of the chemokines monocyte chemoattractant protein-1 (MCP-1) and IL-8 in human dermal fibroblasts. *Clin Exp Immunol* 123(1): 36-41.
- Garner, M. M. and A. Revzin (1981). A gel electrophoresis method for quantifying the binding of proteins to specific DNA regions: application to components of the *Escherichia coli* lactose operon regulatory system. *Nucleic Acids Res* 9(13): 3047-60.
- Garofalo, M. A., I. C. Kettelhut, J. E. Roselino and R. H. Migliorini (1996). Effect of acute cold exposure on norepinephrine turnover rates in rat white adipose tissue. *J Auton Nerv Syst* 60(3): 206-8.
- Gerlach, H., M. Gerlach and M. Clauss (1993). Relevance of tumour necrosis factor-alpha and interleukin-1-alpha in the pathogenesis of hypoxia-related organ failure. *Eur J Anaesthesiol* 10(4): 273-85.
- Gersh, I. and M. A. Still (1945). Blood Vessels in Fat Tissue. Relation to Problems of Gas Exchange. *J Exp Med* 81(2): 219-232.
- Gerszten, R. E., E. A. Garcia-Zepeda, Y. C. Lim, M. Yoshida, H. A. Ding, M. A. Gimbrone, Jr., A. D. Luster, F. W. Lusinskas and A. Rosenzweig (1999). MCP-1 and IL-8 trigger firm adhesion of monocytes to vascular endothelium under flow conditions. *Nature* 398(6729): 718-23.
- Gimbrone, M. A., Jr. (1976). Culture of vascular endothelium. *Prog Hemost Thromb* 3: 1-28.
- Giulietti, A., L. Overbergh, D. Valckx, B. Decallonne, R. Bouillon and C. Mathieu (2001). An overview of real-time quantitative PCR: applications to quantify cytokine gene expression. *Methods* 25(4): 386-401.
- Glund, S. and A. Krook (2008). Role of interleukin-6 signalling in glucose and lipid metabolism. *Acta Physiol (Oxf)* 192(1): 37-48.
- Goldstein, B. J. and R. Scalia (2004). Adiponectin: A novel adipokine linking adipocytes and vascular function. *J Clin Endocrinol Metab* 89(6): 2563-8.
- Green, H. and M. Meuth (1974). An established pre-adipose cell line and its differentiation in culture. *Cell* 3(2): 127-33.
- Greenspan, P., E. P. Mayer and S. D. Fowler (1985). Nile red: a selective fluorescent stain for intracellular lipid droplets. *J Cell Biol* 100(3): 965-73.
- Gregoire, F. M. (2001). Adipocyte differentiation: from fibroblast to endocrine cell. *Exp Biol Med (Maywood)* 226(11): 997-1002.
- Gregoire, F. M., C. M. Smas and H. S. Sul (1998). Understanding adipocyte differentiation. *Physiol Rev* 78(3): 783-809.

- Grimshaw, M. J. and F. R. Balkwill (2001). Inhibition of monocyte and macrophage chemotaxis by hypoxia and inflammation--a potential mechanism. *Eur J Immunol* 31(2): 480-9.
- Grosfeld, A., V. Zilberfarb, S. Turban, J. Andre, M. Guerre-Millo and T. Issad (2002). Hypoxia increases leptin expression in human PAZ6 adipose cells. *Diabetologia* 45(4): 527-30.
- Grunow, R., M. D'Apuzzo, T. Wyss-Coray, K. Frutig and W. J. Pichler (1994). A cell surface ELISA for the screening of monoclonal antibodies to antigens on viable cells in suspension. *J Immunol Methods* 171(1): 93-102.
- Harkins, J. M., N. Moustaid-Moussa, Y. J. Chung, K. M. Penner, J. J. Pestka, C. M. North and K. J. Claycombe (2004). Expression of interleukin-6 is greater in preadipocytes than in adipocytes of 3T3-L1 cells and C57BL/6J and ob/ob mice. *J Nutr* 134(10): 2673-7.
- Harris, P. and P. Ralph (1985). Human leukemic models of myelomonocytic development: a review of the HL-60 and U937 cell lines. *J Leukoc Biol* 37(4): 407-22.
- Hauner, H. (2005). Secretory factors from human adipose tissue and their functional role. *Proc Nutr Soc* 64(2): 163-9.
- Hauner, H. (2006). [The costs of diabetes mellitus and its complications in Germany.]. *Dtsch Med Wochenschr* 131 Suppl 8: S240-2.
- Hauner, H. (2007). Adipositas und Metabolisches Syndrom. *Das Metabolische Syndrom*, Urban und Vogel Verlag: 81-104.
- Hauner, H. (2007). Diabetes und Metabolisches Syndrom. *Das Metabolische Syndrom*, Urban und Vogel Verlag: 105-121.
- Hauner, H. (2009). Overweight--not such a big problem? *Dtsch Arztebl Int* 106(40): 639-40.
- Hauner, H., T. Petruschke, M. Russ, K. Rohrig and J. Eckel (1995). Effects of tumour necrosis factor alpha (TNF alpha) on glucose transport and lipid metabolism of newly-differentiated human fat cells in cell culture. *Diabetologia* 38(7): 764-71.
- Hauner, H., T. Skurk and M. Wabitsch (2001). Cultures of human adipose precursor cells. *Methods Mol Biol* 155: 239-47.
- Hausman, G. J. (1985). The comparative anatomy of adipose tissue. New perspectives in adipose tissue: structure, function and development. Cryer A & Van RLR, Butterworths (London): 1-21.
- Hausman, G. J., S. P. Poulos, T. D. Pringle and M. J. Azain (2008). The influence of thiazolidinediones on adipogenesis in vitro and in vivo: potential modifiers of intramuscular adipose tissue deposition in meat animals. *J Anim Sci* 86(14 Suppl): E236-43.
- Hausman, G. J. and R. L. Richardson (2004). Adipose tissue angiogenesis. *J Anim Sci* 82(3): 925-34.
- He, Z. and A. Bateman (2003). Progranulin (granulin-epithelin precursor, PC-cell-derived growth factor, acrogranin) mediates tissue repair and tumorigenesis. *J Mol Med* 81(10): 600-12.
- He, Z., C. H. Ong, J. Halper and A. Bateman (2003). Progranulin is a mediator of the wound response. *Nat Med* 9(2): 225-9.
- Hellwig-Burgel, T., D. P. Stiehl, A. E. Wagner, E. Metzen and W. Jelkmann (2005). Review: hypoxia-inducible factor-1 (HIF-1): a novel transcription factor in immune reactions. *J Interferon Cytokine Res* 25(6): 297-310.
- Hess, J., P. Angel and M. Schorpp-Kistner (2004). AP-1 subunits: quarrel and harmony among siblings. *J Cell Sci* 117(Pt 25): 5965-73.
- Hillyer, P. and D. Male (2005). Expression of chemokines on the surface of different human endothelia. *Immunol Cell Biol* 83(4): 375-82.
- Hirani, N., F. Antonicelli, R. M. Strieter, M. S. Wiesener, P. J. Ratcliffe, C. Haslett and S. C. Donnelly (2001). The regulation of interleukin-8 by hypoxia in human macrophages--

- a potential role in the pathogenesis of the acute respiratory distress syndrome (ARDS). *Mol Med* 7(10): 685-97.
- Hirsch, J. and B. Batchelor (1976). Adipose tissue cellularity in human obesity. *Clin Endocrinol Metab* 5(2): 299-311.
- Hoefen, R. J. and B. C. Berk (2002). The role of MAP kinases in endothelial activation. *Vascul Pharmacol* 38(5): 271-3.
- Hohensinner, P. J., C. Kaun, K. Rychli, E. Ben-Tal Cohen, S. P. Kastl, S. Demyanets, S. Pfaffenberger, W. S. Speidl, G. Rega, R. Ullrich, G. Maurer, K. Huber and J. Wojta (2006). Monocyte chemoattractant protein (MCP-1) is expressed in human cardiac cells and is differentially regulated by inflammatory mediators and hypoxia. *FEBS Lett* 580(14): 3532-8.
- Horan, P. K. and L. L. Wheeless, Jr. (1977). Quantitative single cell analysis and sorting. *Science* 198(4313): 149-57.
- Hosogai, N., A. Fukuhara, K. Oshima, Y. Miyata, S. Tanaka, K. Segawa, S. Furukawa, Y. Tochino, R. Komuro, M. Matsuda and I. Shimomura (2007). Adipose tissue hypoxia in obesity and its impact on adipocytokine dysregulation. *Diabetes* 56(4): 901-11.
- Hotamisligil, G. S. (2006). Inflammation and metabolic disorders. *Nature* 444(7121): 860-7.
- Hubbard, A. K. and R. Rothlein (2000). Intercellular adhesion molecule-1 (ICAM-1) expression and cell signaling cascades. *Free Radic Biol Med* 28(9): 1379-86.
- Imhof, B. A. and M. Aurrand-Lions (2004). Adhesion mechanisms regulating the migration of monocytes. *Nat Rev Immunol* 4(6): 432-44.
- Jablonska, E., J. Jablonski and A. Holownia (1999). Role of neutrophils in release of some cytokines and their soluble receptors. *Immunol Lett* 70(3): 191-7.
- Jaiswal, R. K., N. Jaiswal, S. P. Bruder, G. Mbalaviele, D. R. Marshak and M. F. Pittenger (2000). Adult human mesenchymal stem cell differentiation to the osteogenic or adipogenic lineage is regulated by mitogen-activated protein kinase. *J Biol Chem* 275(13): 9645-52.
- Jansson, P. A., A. Larsson, U. Smith and P. Lonroth (1992). Glycerol production in subcutaneous adipose tissue in lean and obese humans. *J Clin Invest* 89(5): 1610-7.
- Jaruga, B., F. Hong, W. H. Kim and B. Gao (2004). IFN-gamma/STAT1 acts as a proinflammatory signal in T cell-mediated hepatitis via induction of multiple chemokines and adhesion molecules: a critical role of IRF-1. *Am J Physiol Gastrointest Liver Physiol* 287(5): G1044-52.
- Jin, X., N. Fukuda, J. Su, H. Takagi, Y. Lai, Z. Lin, K. Kanmatsuse, Z. W. Wang and R. H. Unger (2003). Effects of leptin on endothelial function with OB-Rb gene transfer in Zucker fatty rats. *Atherosclerosis* 169(2): 225-33.
- Johnston, B. and E. C. Butcher (2002). Chemokines in rapid leukocyte adhesion triggering and migration. *Semin Immunol* 14(2): 83-92.
- Jones, S. A. (2005). Directing transition from innate to acquired immunity: defining a role for IL-6. *J Immunol* 175(6): 3463-8.
- Juge-Aubry, C. E., E. Somm, V. Giusti, A. Pernin, R. Chicheportiche, C. Verdumo, F. Rohner-Jeanraud, D. Burger, J. M. Dayer and C. A. Meier (2003). Adipose tissue is a major source of interleukin-1 receptor antagonist: upregulation in obesity and inflammation. *Diabetes* 52(5): 1104-10.
- Kahler, C. M., G. Kaufmann, R. Hogue-Angeletti, R. Fischer-Colbrie, S. Dunzendorfer, N. Reinisch and C. J. Wiedermann (1999). A soluble gradient of the neuropeptide secretoneurin promotes the transendothelial migration of monocytes in vitro. *Eur J Pharmacol* 365(1): 65-75.
- Kahler, C. M., G. Kaufmann, S. T. Kahler and C. J. Wiedermann (2002). The neuropeptide secretoneurin stimulates adhesion of human monocytes to arterial and venous endothelial cells in vitro. *Regul Pept* 110(1): 65-73.

- Kalra, V. K., Y. Shen, C. Sultana and V. Rattan (1996). Hypoxia induces PECAM-1 phosphorylation and transendothelial migration of monocytes. *Am J Physiol* 271(5 Pt 2): H2025-34.
- Kano, A., M. J. Wolfgang, Q. Gao, J. Jacoby, G. X. Chai, W. Hansen, Y. Iwamoto, J. S. Pober, R. A. Flavell and X. Y. Fu (2003). Endothelial cells require STAT3 for protection against endotoxin-induced inflammation. *J Exp Med* 198(10): 1517-25.
- Karakurum, M., R. Shreeniwas, J. Chen, D. Pinsky, S. D. Yan, M. Anderson, K. Sunouchi, J. Major, T. Hamilton, K. Kuwabara and et al. (1994). Hypoxic induction of interleukin-8 gene expression in human endothelial cells. *J Clin Invest* 93(4): 1564-70.
- Kiely, J. M., F. W. Luscinskas and M. A. Gimbrone, Jr. (1999). Leukocyte-endothelial monolayer adhesion assay (static conditions). *Methods Mol Biol* 96: 131-6.
- Kim, I., S. O. Moon, S. K. Park, S. W. Chae and G. Y. Koh (2001). Angiopoietin-1 reduces VEGF-stimulated leukocyte adhesion to endothelial cells by reducing ICAM-1, VCAM-1, and E-selectin expression. *Circ Res* 89(6): 477-9.
- Kim, J. H., R. A. Bachmann and J. Chen (2009). Interleukin-6 and insulin resistance. *Vitam Horm* 80: 613-33.
- Kintscher, U., M. Hartge, K. Hess, A. Foryst-Ludwig, M. Clemenz, M. Wabitsch, P. Fischer-Posovszky, T. F. Barth, D. Dragan, T. Skurk, H. Hauner, M. Bluher, T. Unger, A. M. Wolf, U. Knippschild, V. Hombach and N. Marx (2008). T-lymphocyte infiltration in visceral adipose tissue: a primary event in adipose tissue inflammation and the development of obesity-mediated insulin resistance. *Arterioscler Thromb Vasc Biol* 28(7): 1304-10.
- Kirchmair, R., R. Gander, M. Egger, A. Hanley, M. Silver, A. Ritsch, T. Murayama, N. Kaneider, W. Sturm, M. Kearny, R. Fischer-Colbrie, B. Kircher, H. Gaenger, C. J. Wiedermann, A. H. Ropper, D. W. Losordo, J. R. Patsch and P. Schratzberger (2004). The neuropeptide secretoneurin acts as a direct angiogenic cytokine in vitro and in vivo. *Circulation* 109(6): 777-83.
- Klaus, S. (2001). Overview: Biological significance of fat and adipose tissue. *Adipose Tissues*. Eureka.com / Landes Bioscience: 1-10.
- Kleppe, K., E. Ohtsuka, R. Kleppe, I. Molineux and H. G. Khorana (1971). Studies on polynucleotides. XCVI. Repair replications of short synthetic DNA's as catalyzed by DNA polymerases. *J Mol Biol* 56(2): 341-61.
- Knittle, J. L., K. Timmers, F. Ginsberg-Fellner, R. E. Brown and D. P. Katz (1979). The growth of adipose tissue in children and adolescents. Cross-sectional and longitudinal studies of adipose cell number and size. *J Clin Invest* 63(2): 239-46.
- Koch, A. E. (2003). Angiogenesis as a target in rheumatoid arthritis. *Ann Rheum Dis* 62 Suppl 2: ii60-7.
- Koga, S., S. Ogawa, K. Kuwabara, J. Brett, J. A. Leavy, J. Ryan, Y. Koga, J. Plocinski, W. Benjamin, D. K. Burns and et al. (1992). Synthesis and release of interleukin 1 by reoxygenated human mononuclear phagocytes. *J Clin Invest* 90(3): 1007-15.
- Kojima, Y., K. Ono, K. Inoue, Y. Takagi, K. Kikuta, M. Nishimura, Y. Yoshida, Y. Nakashima, H. Matsumae, Y. Furukawa, N. Mikuni, M. Nobuyoshi, T. Kimura, T. Kita and M. Tanaka (2009). Progranulin expression in advanced human atherosclerotic plaque. *Atherosclerosis* 206(1): 102-8.
- Kong, T., H. K. Eltzschig, J. Karhausen, S. P. Colgan and C. S. Shelley (2004). Leukocyte adhesion during hypoxia is mediated by HIF-1-dependent induction of beta2 integrin gene expression. *Proc Natl Acad Sci U S A* 101(28): 10440-5.
- Korpelainen, E. I., M. Karkkainen, Y. Gunji, M. Vikkula and K. Alitalo (1999). Endothelial receptor tyrosine kinases activate the STAT signaling pathway: mutant Tie-2 causing venous malformations signals a distinct STAT activation response. *Oncogene* 18(1): 1-8.

- Kralisch, S., G. Sommer, V. Stangl, U. Kohler, J. Kratzsch, H. Stepan, R. Faber, A. Schubert, U. Lossner, A. Vietzke, M. Bluher, M. Stumvoll and M. Fasshauer (2007). Secretory products from human adipocytes impair endothelial function via nuclear factor kappaB. *Atherosclerosis*.
- Kreier, F. and R. M. Buijs (2007). Evidence for parasympathetic innervation of white adipose tissue, clearing up some vagaries. *Am J Physiol Regul Integr Comp Physiol* 293(1): R548-9; author reply R550-2, discussion R553-4.
- Krentz, A. J., G. Clough and C. D. Byrne (2009). Vascular disease in the metabolic syndrome: do we need to target the microcirculation to treat large vessel disease? *J Vasc Res* 46(6): 515-26.
- Krishnaswamy, G., J. Kelley, L. Yerra, J. K. Smith and D. S. Chi (1999). Human endothelium as a source of multifunctional cytokines: molecular regulation and possible role in human disease. *J Interferon Cytokine Res* 19(2): 91-104.
- Kuldo, J. M., K. I. Ogawara, N. Werner, S. A. Ásgeirsdóttir, J. A. A. M. Kamps, R. J. Kok and G. Molema (2005). Molecular Pathways of Endothelial Cell Activation for (Targeted) Pharmacological Intervention of Chronic Inflammatory Diseases. *Current Vascular Pharmacology* 3: 11-39.
- Kumar, A., E. Kingdon and J. Norman (2005). The isoprostane 8-iso-PGF₂α suppresses monocyte adhesion to human microvascular endothelial cells via two independent mechanisms. *Faseb J* 19(3): 443-5.
- Kumar, S., M. S. Jiang, J. L. Adams and J. C. Lee (1999). Pyridinylimidazole compound SB 203580 inhibits the activity but not the activation of p38 mitogen-activated protein kinase. *Biochem Biophys Res Commun* 263(3): 825-31.
- Laemmli, U. K. (1970). Cleavage of structural proteins during the assembly of the head of bacteriophage T4. *Nature* 227(5259): 680-5.
- Larsen, O. A., N. A. Lassen and F. Quaade (1966). Blood flow through human adipose tissue determined with radioactive xenon. *Acta Physiol Scand* 66(3): 337-45.
- Laterra, J., C. Guerin and G. W. Goldstein (1990). Astrocytes induce neural microvascular endothelial cells to form capillary-like structures in vitro. *J Cell Physiol* 144(2): 204-15.
- Laumen, H., T. Skurk and H. Hauner (2008). The HMG-CoA reductase inhibitor rosuvastatin inhibits plasminogen activator inhibitor-1 expression and secretion in human adipocytes. *Atherosclerosis* 196(2): 565-73.
- Lauterbach, M. A., J. Keller, A. Schonle, D. Kamin, V. Westphal, S. O. Rizzoli and S. W. Hell (2010). Comparing video-rate STED nanoscopy and confocal microscopy of living neurons. *J Biophotonics* 3(7): 417-24.
- Leeper-Woodford, S. K. and K. Detmer (1999). Acute hypoxia increases alveolar macrophage tumor necrosis factor activity and alters NF-kappaB expression. *Am J Physiol* 276(6 Pt 1): L909-16.
- Lequin, R. M. (2005). Enzyme immunoassay (EIA)/enzyme-linked immunosorbent assay (ELISA). *Clin Chem* 51(12): 2415-8.
- Lesser, G. T. and S. Deutsch (1967). Measurement of adipose tissue blood flow and perfusion in man by uptake of ⁸⁵Kr. *J Appl Physiol* 23(5): 621-30.
- Levi, M. (2010). The coagulant response in sepsis and inflammation. *Hamostaseologie* 30(1): 10-2, 14-6.
- Lewis, J. S., J. A. Lee, J. C. Underwood, A. L. Harris and C. E. Lewis (1999). Macrophage responses to hypoxia: relevance to disease mechanisms. *J Leukoc Biol* 66(6): 889-900.
- Ley, K., C. Laudanna, M. I. Cybulsky and S. Nourshargh (2007). Getting to the site of inflammation: the leukocyte adhesion cascade updated. *Nat Rev Immunol* 7(9): 678-89.

- Lidington, E. A., D. L. Moyes, A. M. McCormack and M. L. Rose (1999). A comparison of primary endothelial cells and endothelial cell lines for studies of immune interactions. *Transpl Immunol* 7(4): 239-46.
- Lillie, R. D. and L. L. Ashburn (1943). Super-saturated solutions of fat stains in dilute isopropanol for demonstration of acute fatty degenerations not shown by Herxheimer technique. *Arch Pathol* 36: 432-440.
- Lim, Y. C., G. Garcia-Cardena, J. R. Allport, M. Zervoglos, A. J. Connolly, M. A. Gimbrone, Jr. and F. W. Lusinskas (2003). Heterogeneity of endothelial cells from different organ sites in T-cell subset recruitment. *Am J Pathol* 162(5): 1591-601.
- Lin, Q., Y. J. Lee and Z. Yun (2006). Differentiation arrest by hypoxia. *J Biol Chem* 281(41): 30678-83.
- Lin, Y., A. H. Berg, P. Iyengar, T. K. Lam, A. Giacca, T. P. Combs, M. W. Rajala, X. Du, B. Rollman, W. Li, M. Hawkins, N. Barzilai, C. J. Rhodes, I. G. Fantus, M. Brownlee and P. E. Scherer (2005). The hyperglycemia-induced inflammatory response in adipocytes: the role of reactive oxygen species. *J Biol Chem* 280(6): 4617-26.
- Livak, K. J. and T. D. Schmittgen (2001). Analysis of relative gene expression data using real-time quantitative PCR and the 2⁻(Delta Delta C(T)) Method. *Methods* 25(4): 402-8.
- Löffler, G. (1998). Stoffwechsel der Zelle: Energie- und Materieumsatz der Zelle - Stoffwechsel der Lipide. *Biochemie und Pathobiochemie*. Springer Verlag: 425-676.
- Lolmede, K., V. Durand de Saint Front, J. Galitzky, M. Lafontan and A. Bouloumie (2003). Effects of hypoxia on the expression of proangiogenic factors in differentiated 3T3-F442A adipocytes. *Int J Obes Relat Metab Disord* 27(10): 1187-95.
- Lumeng, C. N., J. L. Bodzin and A. R. Saltiel (2007). Obesity induces a phenotypic switch in adipose tissue macrophage polarization. *J Clin Invest* 117(1): 175-84.
- Lumeng, C. N., S. M. Deyoung and A. R. Saltiel (2007). Macrophages block insulin action in adipocytes by altering expression of signaling and glucose transport proteins. *Am J Physiol Endocrinol Metab* 292(1): E166-74.
- Lyon, H. N. and J. N. Hirschhorn (2005). Genetics of common forms of obesity: a brief overview. *Am J Clin Nutr* 82(1 Suppl): 215S-217S.
- Macfarlane, C. M. (1997). In vitro influence of sublethal hypoxia on differentiation of the 3T3-L1 preadipose cell line and its physiological implications. *Life Sci* 60(21): 1923-31.
- Mack, I., R. S. BelAiba, T. Djordjevic, A. Gorchach, H. Hauner and B. L. Bader (2009). Functional analyses reveal the greater potency of preadipocytes compared with adipocytes as endothelial cell activator under normoxia, hypoxia, and TNFalpha exposure. *Am J Physiol Endocrinol Metab* 297(3): E735-48.
- Madge, L. A. and J. S. Pober (2001). TNF signaling in vascular endothelial cells. *Exp Mol Pathol* 70(3): 317-25.
- Magalang, U. J., J. P. Cruick, R. Rajappan, M. G. Hunter, T. Patel, C. B. Marsh, S. V. Raman and N. L. Parinandi (2009). Intermittent hypoxia suppresses adiponectin secretion by adipocytes. *Exp Clin Endocrinol Diabetes* 117(3): 129-34.
- Manolopoulos, K. N., F. Karpe and K. N. Frayn (2010). Gluteofemoral body fat as a determinant of metabolic health. *Int J Obes (Lond)*.
- Marin, V., F. A. Montero-Julian, S. Gres, V. Boulay, P. Bongrand, C. Farnarier and G. Kaplanski (2001). The IL-6-soluble IL-6Ralpha autocrine loop of endothelial activation as an intermediate between acute and chronic inflammation: an experimental model involving thrombin. *J Immunol* 167(6): 3435-42.
- Masters, J. R. (2002). HeLa cells 50 years on: the good, the bad and the ugly. *Nat Rev Cancer* 2(4): 315-9.

- Mbikay, M., N. G. Seidah and M. Chretien (2001). Neuroendocrine secretory protein 7B2: structure, expression and functions. *Biochem J* 357(Pt 2): 329-42.
- McLaughlin, T., A. Deng, G. Yee, C. Lamendola, G. Reaven, P. S. Tsao, S. W. Cushman and A. Sherman (2009). Inflammation in subcutaneous adipose tissue: relationship to adipose cell size. *Diabetologia*.
- Mick, G. J., X. Wang and K. McCormick (2002). White adipocyte vascular endothelial growth factor: regulation by insulin. *Endocrinology* 143(3): 948-53.
- Middleton, J., A. M. Patterson, L. Gardner, C. Schmutz and B. A. Ashton (2002). Leukocyte extravasation: chemokine transport and presentation by the endothelium. *Blood* 100(12): 3853-60.
- Mills, P. J., S. Hong, L. Redwine, S. M. Carter, A. Chiu, M. G. Ziegler, J. E. Dimsdale and A. S. Maisel (2006). Physical fitness attenuates leukocyte-endothelial adhesion in response to acute exercise. *J Appl Physiol* 101(3): 785-8.
- Modur, V., M. J. Feldhaus, A. S. Weyrich, D. L. Jicha, S. M. Prescott, G. A. Zimmerman and T. M. McIntyre (1997). Oncostatin M is a proinflammatory mediator. In vivo effects correlate with endothelial cell expression of inflammatory cytokines and adhesion molecules. *J Clin Invest* 100(1): 158-68.
- Molavi, B., N. Rasouli and P. A. Kern (2006). The prevention and treatment of metabolic syndrome and high-risk obesity. *Curr Opin Cardiol* 21(5): 479-85.
- Morandini, R., J. M. Boeynaems, J. Werenne and G. Ghanem (2001). Tips and step-by-step protocol for the optimization of important factors affecting cellular enzyme-linked immunosorbent assay (CELISA). *J Immunoassay Immunochem* 22(4): 299-321.
- Morgan, E., R. Varro, H. Sepulveda, J. A. Ember, J. Apgar, J. Wilson, L. Lowe, R. Chen, L. Shivraj, A. Agadir, R. Campos, D. Ernst and A. Gaur (2004). Cytometric bead array: a multiplexed assay platform with applications in various areas of biology. *Clin Immunol* 110(3): 252-66.
- Mosser, D. M. (2003). The many faces of macrophage activation. *J Leukoc Biol* 73(2): 209-12.
- Mullis, K. B. (1990). Target amplification for DNA analysis by the polymerase chain reaction. *Ann Biol Clin (Paris)* 48(8): 579-82.
- Murray, P. J. (2007). The JAK-STAT signaling pathway: input and output integration. *J Immunol* 178(5): 2623-9.
- Nakagawa, Y., K. Kishida, S. Kihara, M. Sonoda, A. Hirata, A. Yasui, H. Nishizawa, T. Nakamura, R. Yoshida, I. Shimomura and T. Funahashi (2008). Nocturnal reduction in circulating adiponectin concentrations related to hypoxic stress in severe obstructive sleep apnea-hypopnea syndrome. *Am J Physiol Endocrinol Metab* 294(4): E778-84.
- Naldini, A. and F. Carraro (1999). Hypoxia modulates cyclin and cytokine expression and inhibits peripheral mononuclear cell proliferation. *J Cell Physiol* 181(3): 448-54.
- Naldini, A., F. Carraro, S. Silvestri and V. Bocci (1997). Hypoxia affects cytokine production and proliferative responses by human peripheral mononuclear cells. *J Cell Physiol* 173(3): 335-42.
- Neels, J. G., M. Pandey, G. S. Hotamisligil and F. Samad (2006). Autoamplification of tumor necrosis factor-alpha: a potential mechanism for the maintenance of elevated tumor necrosis factor-alpha in male but not female obese mice. *Am J Pathol* 168(2): 435-44.
- Nguyen, S. and C. Y. Hsu (2007). Excess weight as a risk factor for kidney failure. *Curr Opin Nephrol Hypertens* 16(2): 71-6.
- Ni, C. W., H. J. Hsieh, Y. J. Chao and D. L. Wang (2004). Interleukin-6-induced JAK2/STAT3 signaling pathway in endothelial cells is suppressed by hemodynamic flow. *Am J Physiol Cell Physiol* 287(3): C771-80.
- Nishimura, S., I. Manabe, M. Nagasaki, K. Seo, H. Yamashita, Y. Hosoya, M. Ohsugi, K. Tobe, T. Kadowaki, R. Nagai and S. Sugiura (2008). In vivo imaging in mice reveals

- local cell dynamics and inflammation in obese adipose tissue. *J Clin Invest* 118(2): 710-21.
- Nishizawa, H., I. Shimomura, K. Kishida, N. Maeda, H. Kuriyama, H. Nagaretani, M. Matsuda, H. Kondo, N. Furuyama, S. Kihara, T. Nakamura, Y. Tochino, T. Funahashi and Y. Matsuzawa (2002). Androgens decrease plasma adiponectin, an insulin-sensitizing adipocyte-derived protein. *Diabetes* 51(9): 2734-41.
- O'Rahilly, S. (2009). Human genetics illuminates the paths to metabolic disease. *Nature* 462(7271): 307-14.
- Ogino, T., X. Wang and S. Ferrone (2003). Modified flow cytometry and cell-ELISA methodology to detect HLA class I antigen processing machinery components in cytoplasm and endoplasmic reticulum. *J Immunol Methods* 278(1-2): 33-44.
- Oh, H., H. Takagi, A. Otani, S. Koyama, S. Kemmochi, A. Uemura and Y. Honda (2002). Selective induction of neuropilin-1 by vascular endothelial growth factor (VEGF): a mechanism contributing to VEGF-induced angiogenesis. *Proc Natl Acad Sci U S A* 99(1): 383-8.
- Okada, T., H. Nishizawa, A. Kurata, S. Tamba, M. Sonoda, A. Yasui, Y. Kuroda, T. Hibuse, N. Maeda, S. Kihara, T. Hadama, K. Tobita, S. Akamatsu, K. Maeda, I. Shimomura and T. Funahashi (2008). URB is abundantly expressed in adipose tissue and dysregulated in obesity. *Biochem Biophys Res Commun* 367(2): 370-6.
- Ong, C. H., Z. He, L. Kriazhev, X. Shan, R. G. Palfree and A. Bateman (2006). Regulation of progranulin expression in myeloid cells. *Am J Physiol Regul Integr Comp Physiol* 291(6): R1602-12.
- Opal, S. M. and V. A. DePalo (2000). Anti-inflammatory cytokines. *Chest* 117(4): 1162-72.
- Ouchi, N., S. Kihara, Y. Arita, K. Maeda, H. Kuriyama, Y. Okamoto, K. Hotta, M. Nishida, M. Takahashi, T. Nakamura, S. Yamashita, T. Funahashi and Y. Matsuzawa (1999). Novel modulator for endothelial adhesion molecules: adipocyte-derived plasma protein adiponectin. *Circulation* 100(25): 2473-6.
- Ozaki, H., K. Ishii, H. Horiuchi, H. Arai, T. Kawamoto, K. Okawa, A. Iwamatsu and T. Kita (1999). Cutting edge: combined treatment of TNF-alpha and IFN-gamma causes redistribution of junctional adhesion molecule in human endothelial cells. *J Immunol* 163(2): 553-7.
- Ozturk, H., H. Ozturk and H. Buyukbayram (2005). Protective effects of recombinant human interleukin-4 administration on the hypoxia-reoxygenation-induced gastric and intestinal injury in rat pups. *Fetal Pediatr Pathol* 24(6): 347-58.
- Ozturk, H., H. Ozturk, H. Buyukbayram and M. C. Tuncer (2006). The effects of exogenous interleukin-4 on hypoxia-induced lung injury. *Pediatr Surg Int* 22(2): 197-201.
- Pan, W., H. Tu, H. Hsueh, J. Daniel and A. J. Kastin (2007). Unexpected amplification of leptin-induced Stat3 signaling by urocortin: implications for obesity. *J Mol Neurosci* 33(3): 232-8.
- Park, H. Y., H. M. Kwon, H. J. Lim, B. K. Hong, J. Y. Lee, B. E. Park, Y. Jang, S. Y. Cho and H. S. Kim (2001). Potential role of leptin in angiogenesis: leptin induces endothelial cell proliferation and expression of matrix metalloproteinases in vivo and in vitro. *Exp Mol Med* 33(2): 95-102.
- Peeraully, M. R., J. R. Jenkins and P. Trayhurn (2004). NGF gene expression and secretion in white adipose tissue: regulation in 3T3-L1 adipocytes by hormones and inflammatory cytokines. *Am J Physiol Endocrinol Metab* 287(2): E331-9.
- Petzelbauer, P., J. R. Bender, J. Wilson and J. S. Pober (1993). Heterogeneity of dermal microvascular endothelial cell antigen expression and cytokine responsiveness in situ and in cell culture. *J Immunol* 151(9): 5062-72.
- Pober, J. S. and W. C. Sessa (2007). Evolving functions of endothelial cells in inflammation. *Nat Rev Immunol* 7(10): 803-15.

- Poulain-Godefroy, O. and P. Froguel (2007). Preadipocyte response and impairment of differentiation in an inflammatory environment. *Biochem Biophys Res Commun* 356(3): 662-667.
- Probst, M. C. O., G. Rothe and G. Schmitz (2003). Bead-Based Multiplex Analysis. *Laboratoriums Medizin* 27(5-6): 182-187.
- Quehenberger, P., M. Exner, R. Sunder-Plassmann, K. Ruzicka, C. Bieglmayer, G. Endler, C. Muellner, W. Speiser and O. Wagner (2002). Leptin induces endothelin-1 in endothelial cells in vitro. *Circ Res* 90(6): 711-8.
- Randall, D., W. Burggren and K. French (1997). *Circulation. Eckert Animal Physiology, Mechanisms and Adaptations*, W.H. Freeman and Company: 467-516.
- Rausch, M. E., S. Weisberg, P. Vardhana and D. V. Tortoriello (2007). Obesity in C57BL/6J mice is characterized by adipose tissue hypoxia and cytotoxic T-cell infiltration. *Int J Obes (Lond)* 32(3): 451-463.
- Rayner, D. V. (2001). The sympathetic nervous system in white adipose tissue regulation. *Proc Nutr Soc* 60(3): 357-64.
- Reed, B. C., S. H. Kaufmann, J. C. Mackall, A. K. Student and M. D. Lane (1977). Alterations in insulin binding accompanying differentiation of 3T3-L1 preadipocytes. *Proc Natl Acad Sci U S A* 74(11): 4876-80.
- Reed, B. C., G. V. Ronnett, P. R. Clements and M. D. Lane (1981). Regulation of insulin receptor metabolism. Differentiation-induced alteration of receptor synthesis and degradation. *J Biol Chem* 256(8): 3917-25.
- Regazzetti, C., P. Peraldi, T. Gremeaux, R. Najem-Lendom, I. Ben-Sahra, M. Cormont, F. Bost, Y. Le Marchand-Brustel, J. F. Tanti and S. Giorgetti-Peraldi (2009). Hypoxia decreases insulin signaling pathways in adipocytes. *Diabetes* 58(1): 95-103.
- Rehman, J., D. Traktuev, J. Li, S. Merfeld-Clauss, C. J. Temm-Grove, J. E. Bovenkerk, C. L. Pell, B. H. Johnstone, R. V. Considine and K. L. March (2004). Secretion of angiogenic and antiapoptotic factors by human adipose stromal cells. *Circulation* 109(10): 1292-8.
- Renstrom, F., J. Buren, M. Svensson and J. W. Eriksson (2007). Insulin resistance induced by high glucose and high insulin precedes insulin receptor substrate 1 protein depletion in human adipocytes. *Metabolism* 56(2): 190-8.
- Rodbell, M. (1964). Metabolism of Isolated Fat Cells. I. Effects of Hormones on Glucose Metabolism and Lipolysis. *J Biol Chem* 239: 375-80.
- Rodriguez, A. M., C. Elabd, F. Delteil, J. Astier, C. Vernochet, P. Saint-Marc, J. Guesnet, A. Guezennec, E. Z. Amri, C. Dani and G. Ailhaud (2004). Adipocyte differentiation of multipotent cells established from human adipose tissue. *Biochem Biophys Res Commun* 315(2): 255-63.
- Roebuck, K. A., L. R. Carpenter, V. Lakshminarayanan, S. M. Page, J. N. Moy and L. L. Thomas (1999). Stimulus-specific regulation of chemokine expression involves differential activation of the redox-responsive transcription factors AP-1 and NF-kappaB. *J Leukoc Biol* 65(3): 291-8.
- Roebuck, K. A. and A. Finnegan (1999). Regulation of intercellular adhesion molecule-1 (CD54) gene expression. *J Leukoc Biol* 66(6): 876-88.
- Roitt, I. M., J. D. Peter, J. M. Seamus, D. R. Burton and I. M. Roitt (2006). *Immunological Methods and Applications. Roitt's Essential Immunology*. Blackwell Publishing 11: 137-139.
- Romano, M., M. Sironi, C. Toniatti, N. Polentarutti, P. Fruscella, P. Ghezzi, R. Faggioni, W. Luini, V. van Hinsbergh, S. Sozzani, F. Bussolino, V. Poli, G. Ciliberto and A. Mantovani (1997). Role of IL-6 and its soluble receptor in induction of chemokines and leukocyte recruitment. *Immunity* 6(3): 315-25.

- Romeis, B. and P. Böck (1989). *Romeis-Mikroskopische Technik*. 17. Auflage, Verlag Urban & Schwarzenberg, München.
- Rose-John, S., J. Scheller, G. Elson and S. A. Jones (2006). Interleukin-6 biology is coordinated by membrane-bound and soluble receptors: role in inflammation and cancer. *J Leukoc Biol* 80(2): 227-36.
- Rosen, E. D. and B. M. Spiegelman (2000). Molecular regulation of adipogenesis. *Annu Rev Cell Dev Biol* 16: 145-71.
- Ruan, H., M. J. Zarnowski, S. W. Cushman and H. F. Lodish (2003). Standard isolation of primary adipose cells from mouse epididymal fat pads induces inflammatory mediators and down-regulates adipocyte genes. *J Biol Chem* 278(48): 47585-93.
- Rutkowski, J. M., K. E. Davis and P. E. Scherer (2009). Mechanisms of obesity and related pathologies: the macro- and microcirculation of adipose tissue. *Febs J* 276(20): 5738-46.
- Rydberg, E. K., L. Salomonsson, L. M. Hulten, K. Noren, G. Bondjers, O. Wiklund, T. Bjornheden and B. G. Ohlsson (2003). Hypoxia increases 25-hydroxycholesterol-induced interleukin-8 protein secretion in human macrophages. *Atherosclerosis* 170(2): 245-52.
- Sackett, D. L. and J. Wolff (1987). Nile red as a polarity-sensitive fluorescent probe of hydrophobic protein surfaces. *Anal Biochem* 167(2): 228-34.
- Salameh, A., M. Zinn and S. Dhein (1997). High D-glucose induces alterations of endothelial cell structure in a cell-culture model. *J Cardiovasc Pharmacol* 30(2): 182-90.
- Sapet, C., S. Simoncini, B. Lloriod, D. Puthier, J. Sampol, C. Nguyen, F. Dignat-George and F. Anfosso (2006). Thrombin-induced endothelial microparticle generation: identification of a novel pathway involving ROCK-II activation by caspase-2. *Blood* 108(6): 1868-76.
- Savale, L., L. Tu, D. Rideau, M. Izziki, B. Maitre, S. Adnot and S. Eddahibi (2009). Impact of interleukin-6 on hypoxia-induced pulmonary hypertension and lung inflammation in mice. *Respir Res* 10: 6.
- Scannell, G. (1996). Leukocyte responses to hypoxic/ischemic conditions. *New Horiz* 4(2): 179-83.
- Schaffner, W. and C. Weissmann (1973). A rapid, sensitive, and specific method for the determination of protein in dilute solution. *Anal Biochem* 56(2): 502-14.
- Scherer, P. E., S. Williams, M. Fogliano, G. Baldini and H. F. Lodish (1995). A novel serum protein similar to C1q, produced exclusively in adipocytes. *J Biol Chem* 270(45): 26746-9.
- Schlesinger, J. B., V. van Harmelen, C. E. Alberti-Huber and H. Hauner (2006). Albumin inhibits adipogenesis and stimulates cytokine release from human adipocytes. *Am J Physiol Cell Physiol* 291(1): C27-33.
- Schling, P. and G. Loffler (2002). Cross talk between adipose tissue cells: impact on pathophysiology. *News Physiol Sci* 17: 99-104.
- Schroeder, A., O. Mueller, S. Stocker, R. Salowsky, M. Leiber, M. Gassmann, S. Lightfoot, W. Menzel, M. Granzow and T. Ragg (2006). The RIN: an RNA integrity number for assigning integrity values to RNA measurements. *BMC Mol Biol* 7: 3.
- Schulte, I., H. Tammen, H. Selle and P. Schulz-Knappe (2005). Peptides in body fluids and tissues as markers of disease. *Expert Rev Mol Diagn* 5(2): 145-57.
- Schutte, B., M. M. Reynders, F. T. Bosman and G. H. Blijham (1987). Studies with anti-bromodeoxyuridine antibodies: II. Simultaneous immunocytochemical detection of antigen expression and DNA synthesis by in vivo labeling of mouse intestinal mucosa. *J Histochem Cytochem* 35(3): 371-4.

- Schutte, B., M. M. Reynders, C. L. van Assche, P. S. Hupperets, F. T. Bosman and G. H. Blijham (1987). An improved method for the immunocytochemical detection of bromodeoxyuridine labeled nuclei using flow cytometry. *Cytometry* 8(4): 372-6.
- Schwartz, M. W., S. C. Woods, D. Porte, Jr., R. J. Seeley and D. G. Baskin (2000). Central nervous system control of food intake. *Nature* 404(6778): 661-71.
- Seebach, M. E. (2006). Bachelorarbeit: Methodische Ausarbeitung eines Testverfahrens zur Adhäsion von Monozyten (U937) auf TNFalpha stimulierten humanen mikrovaskulären Endothelzellen (HMEC-1). Technische Universität München, Lehrstuhl für Ernährungsphysiologie,.
- Semenza, G. (2002). Signal transduction to hypoxia-inducible factor 1. *Biochem Pharmacol* 64(5-6): 993-8.
- Semenza, G. L. (2003). Targeting HIF-1 for cancer therapy. *Nat Rev Cancer* 3(10): 721-32.
- Shiojima, I. and K. Walsh (2002). Role of Akt signaling in vascular homeostasis and angiogenesis. *Circ Res* 90(12): 1243-50.
- Sierra-Honigmann, M. R., A. K. Nath, C. Murakami, G. Garcia-Cardena, A. Papapetropoulos, W. C. Sessa, L. A. Madge, J. S. Schechner, M. B. Schwabb, P. J. Polverini and J. R. Flores-Riveros (1998). Biological action of leptin as an angiogenic factor. *Science* 281(5383): 1683-6.
- Simons, P. J., P. S. van den Pangaart, C. P. van Roomen, J. M. Aerts and L. Boon (2005). Cytokine-mediated modulation of leptin and adiponectin secretion during in vitro adipogenesis: Evidence that tumor necrosis factor-alpha- and interleukin-1beta-treated human preadipocytes are potent leptin producers. *Cytokine* 32(2): 94-103.
- Singer, G. and D. N. Granger (2007). Inflammatory responses underlying the microvascular dysfunction associated with obesity and insulin resistance. *Microcirculation* 14(4-5): 375-87.
- Singhal, A. (2005). Endothelial dysfunction: role in obesity-related disorders and the early origins of CVD. *Proc Nutr Soc* 64(1): 15-22.
- Skilton, M. R., S. Nakhla, D. P. Sieveking, I. D. Caterson and D. S. Celmaj (2005). Pathophysiological levels of the obesity related peptides resistin and ghrelin increase adhesion molecule expression on human vascular endothelial cells. *Clin Exp Pharmacol Physiol* 32(10): 839-44.
- Skurk, T., C. Alberti-Huber, C. Herder and H. Hauner (2007). Relationship between adipocyte size and adipokine expression and secretion. *J Clin Endocrinol Metab* 92(3): 1023-33.
- Skurk, T., M. Birgel, Y. M. Lee and H. Hauner (2006). Effect of troglitazone on tumor necrosis factor alpha and transforming growth factor beta expression and action in human adipocyte precursor cells in primary culture. *Metabolism* 55(3): 309-16.
- Skurk, T., S. Ecklebe and H. Hauner (2007). A novel technique to propagate primary human preadipocytes without loss of differentiation capacity. *Obesity (Silver Spring)* 15(12): 2925-31.
- Skurk, T. and H. Hauner (2002). *Klinische Bedeutung und Pathophysiologie der Adipositas*. MVS Medizinverlage Stuttgart GmbH & Co, Stuttgart.
- Skurk, T., H. Kolb, S. Müller-Scholze, K. Rohrig, H. Hauner and C. Herder (2005). The proatherogenic cytokine interleukin-18 is secreted by human adipocytes. *Eur J Endocrinol* 152(6): 863-8.
- Skurk, T., I. Mack, K. Kempf, H. Kolb, H. Hauner and C. Herder (2009). Expression and secretion of RANTES (CCL5) in human adipocytes in response to immunological stimuli and hypoxia. *Horm Metab Res* 41(3): 183-9.
- Smith, P. J., L. S. Wise, R. Berkowitz, C. Wan and C. S. Rubin (1988). Insulin-like growth factor-I is an essential regulator of the differentiation of 3T3-L1 adipocytes. *J Biol Chem* 263(19): 9402-8.

- Smith, P. K., R. I. Krohn, G. T. Hermanson, A. K. Mallia, F. H. Gartner, M. D. Provenzano, E. K. Fujimoto, N. M. Goeke, B. J. Olson and D. C. Klenk (1985). Measurement of protein using bicinchoninic acid. *Anal Biochem* 150(1): 76-85.
- Spalding, K. L., E. Arner, P. O. Westermark, S. Bernard, B. A. Buchholz, O. Bergmann, L. Blomqvist, J. Hoffstedt, E. Naslund, T. Britton, H. Concha, M. Hassan, M. Ryden, J. Frisen and P. Arner (2008). Dynamics of fat cell turnover in humans. *Nature*.
- Spranger, J., A. Kroke, M. Mohlig, M. M. Bergmann, M. Ristow, H. Boeing and A. F. Pfeiffer (2003). Adiponectin and protection against type 2 diabetes mellitus. *Lancet* 361(9353): 226-8.
- Steinbeck, K. (2002). Obesity: the science behind the management. *Intern Med J* 32(5-6): 237-41.
- Stenina, O. I. (2005). Regulation of vascular genes by glucose. *Curr Pharm Des* 11(18): 2367-81.
- Stridsberg, M., B. Eriksson and E. T. Janson (2008). Measurements of secretogranins II, III, V and proconvertases 1/3 and 2 in plasma from patients with neuroendocrine tumours. *Regul Pept* 148(1-3): 95-8.
- Suganami, E., H. Takagi, H. Ohashi, K. Suzuma, I. Suzuma, H. Oh, D. Watanabe, T. Ojima, T. Suganami, Y. Fujio, K. Nakao, Y. Ogawa and N. Yoshimura (2004). Leptin stimulates ischemia-induced retinal neovascularization: possible role of vascular endothelial growth factor expressed in retinal endothelial cells. *Diabetes* 53(9): 2443-8.
- Suganami, T., J. Nishida and Y. Ogawa (2005). A paracrine loop between adipocytes and macrophages aggravates inflammatory changes: role of free fatty acids and tumor necrosis factor alpha. *Arterioscler Thromb Vasc Biol* 25(10): 2062-8.
- Summers, L. K. (2006). Adipose tissue metabolism, diabetes and vascular disease--lessons from in vivo studies. *Diab Vasc Dis Res* 3(1): 12-21.
- Sundstrom, C. and K. Nilsson (1976). Establishment and characterization of a human histiocytic lymphoma cell line (U-937). *Int J Cancer* 17(5): 565-77.
- Surmi, B. K. and A. H. Hasty (2008). Macrophage infiltration into adipose tissue: initiation, propagation and remodeling. *Future Lipidol* 3(5): 545-556.
- Swiersz, L. M., A. J. Giaccia and Z. Yun (2004). Oxygen-dependent regulation of adipogenesis. *Methods Enzymol* 381: 387-95.
- Takahashi, K., Y. Sawasaki, J. Hata, K. Mukai and T. Goto (1990). Spontaneous transformation and immortalization of human endothelial cells. *In Vitro Cell Dev Biol* 26(3 Pt 1): 265-74.
- Tanaka, M., K. Mizuta, F. Koba, Y. Ohira, T. Kobayashi and Y. Honda (1997). Effects of exposure to hypobaric-hypoxia on body weight, muscular and hematological characteristics, and work performance in rats. *Jpn J Physiol* 47(1): 51-7.
- Tanzi, M. C. and S. Fare (2009). Adipose tissue engineering: state of the art, recent advances and innovative approaches. *Expert Rev Med Devices* 6(5): 533-51.
- Tiller, G., P. Fischer-Posovszky, H. Laumen, A. Finck, T. Skurk, M. Keuper, U. Brinkmann, M. Wabitsch, D. Link and H. Hauner (2009). Effects of TWEAK (TNF Superfamily Member 12) on Differentiation, Metabolism, and Secretory Function of Human Primary Preadipocytes and Adipocytes. *Endocrinology*.
- Tomanek, R. J., P. J. Palmer, G. L. Peiffer, K. L. Schreiber, C. L. Eastham and M. L. Marcus (1986). Morphometry of canine coronary arteries, arterioles, and capillaries during hypertension and left ventricular hypertrophy. *Circ Res* 58(1): 38-46.
- Towbin, H., T. Staehelin and J. Gordon (1979). Electrophoretic transfer of proteins from polyacrylamide gels to nitrocellulose sheets: procedure and some applications. *Proc Natl Acad Sci U S A* 76(9): 4350-4.

- Tracey, D., L. Klareskog, E. H. Sasso, J. G. Salfeld and P. P. Tak (2008). Tumor necrosis factor antagonist mechanisms of action: a comprehensive review. *Pharmacol Ther* 117(2): 244-79.
- Trayhurn, P. (2005). Adipose tissue in obesity--an inflammatory issue. *Endocrinology* 146(3): 1003-5.
- Trayhurn, P. (2005). The biology of obesity. *Proc Nutr Soc* 64(1): 31-8.
- Trayhurn, P. and J. H. Beattie (2001). Physiological role of adipose tissue: white adipose tissue as an endocrine and secretory organ. *Proc Nutr Soc* 60(3): 329-39.
- Trayhurn, P., C. Bing and I. S. Wood (2006). Adipose tissue and adipokines--energy regulation from the human perspective. *J Nutr* 136(7 Suppl): 1935S-1939S.
- Trayhurn, P., N. Hoggard and D. V. Rayner (2001). White adipose tissue as a secretory and endocrine organ: Leptin and other secreted proteins. *Adipose Tissues*. Eureka.com / Landes Bioscience: 158-182.
- Trayhurn, P., B. Wang and I. S. Wood (2008). Hypoxia and the endocrine and signalling role of white adipose tissue. *Arch Physiol Biochem* 114(4): 267-76.
- Trayhurn, P. and I. S. Wood (2004). Adipokines: inflammation and the pleiotropic role of white adipose tissue. *Br J Nutr* 92(3): 347-55.
- Tsopanoglou, N. E. and M. E. Maragoudakis (2009). Thrombin's central role in angiogenesis and pathophysiological processes. *Eur Cytokine Netw* 20(4): 171-9.
- Tsuchiya, S., M. Yamabe, Y. Yamaguchi, Y. Kobayashi, T. Konno and K. Tada (1980). Establishment and characterization of a human acute monocytic leukemia cell line (THP-1). *Int J Cancer* 26(2): 171-6.
- Turner, L., C. Scotton, R. Negus and F. Balkwill (1999). Hypoxia inhibits macrophage migration. *Eur J Immunol* 29(7): 2280-7.
- Valet, P., G. Tavernier, I. Castan-Laurell, J. S. Saulnier-Blache and D. Langin (2002). Understanding adipose tissue development from transgenic animal models. *J Lipid Res* 43(6): 835-60.
- Van Gaal, L. F., I. L. Mertens and C. E. De Block (2006). Mechanisms linking obesity with cardiovascular disease. *Nature* 444(7121): 875-80.
- Van Harmelen, V., K. Rohrig and H. Hauner (2004). Comparison of proliferation and differentiation capacity of human adipocyte precursor cells from the omental and subcutaneous adipose tissue depot of obese subjects. *Metabolism* 53(5): 632-7.
- van Hinsbergh, V. W. (2001). The endothelium: vascular control of haemostasis. *Eur J Obstet Gynecol Reprod Biol* 95(2): 198-201.
- Van Weemen, B. K. and A. H. Schuurs (1971). Immunoassay using antigen-enzyme conjugates. *FEBS Lett* 15(3): 232-236.
- Vanecko, S. and M. Laskowski, Sr. (1961). Studies of the specificity of deoxyribonuclease I. III. Hydrolysis of chains carrying a monoesterified phosphate on carbon 5'. *J Biol Chem* 236: 3312-6.
- VanGuilder, H. D., K. E. Vrana and W. M. Freeman (2008). Twenty-five years of quantitative PCR for gene expression analysis. *Biotechniques* 44(5): 619-26.
- Varma, S., B. K. Lal, R. Zheng, J. W. Breslin, S. Saito, P. J. Pappas, R. W. Hobson, 2nd and W. N. Duran (2005). Hyperglycemia alters PI3k and Akt signaling and leads to endothelial cell proliferative dysfunction. *Am J Physiol Heart Circ Physiol* 289(4): H1744-51.
- Vestweber, D. (2000). Molecular mechanisms that control endothelial cell contacts. *J Pathol* 190(3): 281-91.
- Villena, J. A., B. Cousin, L. Penicaud and L. Casteilla (2001). Adipose tissues display differential phagocytic and microbicidal activities depending on their localization. *Int J Obes Relat Metab Disord* 25(9): 1275-80.

- Wabitsch, M., R. E. Brenner, I. Melzner, M. Braun, P. Moller, E. Heinze, K. M. Debatin and H. Hauner (2001). Characterization of a human preadipocyte cell strain with high capacity for adipose differentiation. *Int J Obes Relat Metab Disord* 25(1): 8-15.
- Wabitsch, M., P. B. Jensen, W. F. Blum, C. T. Christoffersen, P. Englaro, E. Heinze, W. Rascher, W. Teller, H. Tornqvist and H. Hauner (1996). Insulin and cortisol promote leptin production in cultured human fat cells. *Diabetes* 45(10): 1435-8.
- Wahba, I. M. and R. H. Mak (2007). Obesity and obesity-initiated metabolic syndrome: mechanistic links to chronic kidney disease. *Clin J Am Soc Nephrol* 2(3): 550-62.
- Wang, B., J. R. Jenkins and P. Trayhurn (2005). Expression and secretion of inflammation-related adipokines by human adipocytes differentiated in culture: integrated response to TNF-alpha. *Am J Physiol Endocrinol Metab* 288(4): E731-40.
- Wang, B. and P. Trayhurn (2006). Acute and prolonged effects of TNF-alpha on the expression and secretion of inflammation-related adipokines by human adipocytes differentiated in culture. *Pflugers Arch* 452(4): 418-27.
- Wang, B., I. Wood and P. Trayhurn (2008). Hypoxia induces leptin gene expression and secretion in human preadipocytes: differential effects of hypoxia on adipokine expression by preadipocytes. *J Endocrinol* 198(1): 127-134.
- Wang, B., I. S. Wood and P. Trayhurn (2007). Dysregulation of the expression and secretion of inflammation-related adipokines by hypoxia in human adipocytes. *Pflugers Arch* 455(3): 479-492.
- Wang, J. F., X. Zhang and J. E. Groopman (2004). Activation of vascular endothelial growth factor receptor-3 and its downstream signaling promote cell survival under oxidative stress. *J Biol Chem* 279(26): 27088-97.
- Watson, C., S. Whittaker, N. Smith, A. J. Vora, D. C. Dumonde and K. A. Brown (1996). IL-6 acts on endothelial cells to preferentially increase their adherence for lymphocytes. *Clin Exp Immunol* 105(1): 112-9.
- Waxman, A. B., K. Mahboubi, R. G. Knickelbein, L. L. Mantell, N. Manzo, J. S. Pober and J. A. Elias (2003). Interleukin-11 and interleukin-6 protect cultured human endothelial cells from H₂O₂-induced cell death. *Am J Respir Cell Mol Biol* 29(4): 513-22.
- Weber, C., E. Negrescu, W. Erl, A. Pietsch, M. Frankenberger, H. W. Ziegler-Heitbrock, W. Siess and P. C. Weber (1995). Inhibitors of protein tyrosine kinase suppress TNF-stimulated induction of endothelial cell adhesion molecules. *J Immunol* 155(1): 445-51.
- Weisberg, S. P., D. McCann, M. Desai, M. Rosenbaum, R. L. Leibel and A. W. Ferrante, Jr. (2003). Obesity is associated with macrophage accumulation in adipose tissue. *J Clin Invest* 112(12): 1796-808.
- Wellen, K. E. and G. S. Hotamisligil (2005). Inflammation, stress, and diabetes. *J Clin Invest* 115(5): 1111-9.
- Westphal, C. H., L. Muller, A. Zhou, X. Zhu, S. Bonner-Weir, M. Schambelan, D. F. Steiner, I. Lindberg and P. Leder (1999). The neuroendocrine protein 7B2 is required for peptide hormone processing in vivo and provides a novel mechanism for pituitary Cushing's disease. *Cell* 96(5): 689-700.
- Weyer, C., S. Snitker, C. Bogardus and E. Ravussin (1999). Energy metabolism in African Americans: potential risk factors for obesity. *Am J Clin Nutr* 70(1): 13-20.
- Whitehead, J. P., A. A. Richards, I. J. Hickman, G. A. Macdonald and J. B. Prins (2006). Adiponectin--a key adipokine in the metabolic syndrome. *Diabetes Obes Metab* 8(3): 264-80.
- Whitlock, G., S. Lewington, P. Sherliker, R. Clarke, J. Emberson, J. Halsey, N. Qizilbash, R. Collins and R. Peto (2009). Body-mass index and cause-specific mortality in 900 000 adults: collaborative analyses of 57 prospective studies. *Lancet* 373(9669): 1083-96.

- Wiernsperger, N., P. Nivoit, L. G. De Aguiar and E. Bouskela (2007). Microcirculation and the metabolic syndrome. *Microcirculation* 14(4-5): 403-38.
- Wincewicz, A., M. Sulkowska, R. Rutkowski, S. Sulkowski, B. Musiatowicz, T. Hirnle, W. Famulski, M. Koda, G. Sokol and P. Szarejko (2007). STAT1 and STAT3 as intracellular regulators of vascular remodeling. *Eur J Intern Med* 18(4): 267-71.
- Wiper-Bergeron, N., H. A. Salem, J. J. Tomlinson, D. Wu and R. J. Hache (2007). Glucocorticoid-stimulated preadipocyte differentiation is mediated through acetylation of C/EBPbeta by GCN5. *Proc Natl Acad Sci U S A* 104(8): 2703-8.
- Wirth, A. (2007). Definition, Epidemiologie und Krankheitsfolgen. *Das Metabolische Syndrom*, Urban und Vogel Verlag: 11-29.
- Wise, L. S. and H. Green (1979). Participation of one isozyme of cytosolic glycerophosphate dehydrogenase in the adipose conversion of 3T3 cells. *J Biol Chem* 254(2): 273-5.
- Wood, I. S., B. Wang, S. Lorente-Cebrian and P. Trayhurn (2007). Hypoxia increases expression of selective facilitative glucose transporters (GLUT) and 2-deoxy-D-glucose uptake in human adipocytes. *Biochem Biophys Res Commun* 361(2): 468-73.
- Wu, H., S. Ghosh, X. D. Perrard, L. Feng, G. E. Garcia, J. L. Perrard, J. F. Sweeney, L. E. Peterson, L. Chan, C. W. Smith and C. M. Ballantyne (2007). T-cell accumulation and regulated on activation, normal T cell expressed and secreted upregulation in adipose tissue in obesity. *Circulation* 115(8): 1029-38.
- Xu, H., G. T. Barnes, Q. Yang, G. Tan, D. Yang, C. J. Chou, J. Sole, A. Nichols, J. S. Ross, L. A. Tartaglia and H. Chen (2003). Chronic inflammation in fat plays a crucial role in the development of obesity-related insulin resistance. *J Clin Invest* 112(12): 1821-30.
- Yahata, Y., Y. Shirakata, S. Tokumaru, K. Yamasaki, K. Sayama, Y. Hanakawa, M. Detmar and K. Hashimoto (2003). Nuclear translocation of phosphorylated STAT3 is essential for vascular endothelial growth factor-induced human dermal microvascular endothelial cell migration and tube formation. *J Biol Chem* 278(41): 40026-31.
- Yamaji-Kegan, K., Q. Su, D. J. Angelini and R. A. Johns (2009). IL-4 is proangiogenic in the lung under hypoxic conditions. *J Immunol* 182(9): 5469-76.
- Yamauchi, T., J. Kamon, Y. Minokoshi, Y. Ito, H. Waki, S. Uchida, S. Yamashita, M. Noda, S. Kita, K. Ueki, K. Eto, Y. Akanuma, P. Froguel, F. Foufelle, P. Ferre, D. Carling, S. Kimura, R. Nagai, B. B. Kahn and T. Kadowaki (2002). Adiponectin stimulates glucose utilization and fatty-acid oxidation by activating AMP-activated protein kinase. *Nat Med* 8(11): 1288-95.
- Yan, S., X. Wang, H. Chai, H. Wang, Q. Yao and C. Chen (2006). Secretoneurin increases monolayer permeability in human coronary artery endothelial cells. *Surgery* 140(2): 243-51.
- Yao, L., T. Yokota, L. Xia, P. W. Kincade and R. P. McEver (2005). Bone marrow dysfunction in mice lacking the cytokine receptor gp130 in endothelial cells. *Blood* 106(13): 4093-101.
- Ye, J. (2009). Emerging role of adipose tissue hypoxia in obesity and insulin resistance. *Int J Obes (Lond)* 33(1): 54-66.
- Ye, J., Z. Gao, J. Yin and Q. He (2007). Hypoxia is a potential risk factor for chronic inflammation and adiponectin reduction in adipose tissue of ob/ob and dietary obese mice. *Am J Physiol Endocrinol Metab* 293(4): E1118-28.
- Yin, J., Z. Gao, Q. He, D. Zhou, Z. Guo and J. Ye (2009). Role of hypoxia in obesity-induced disorders of glucose and lipid metabolism in adipose tissue. *Am J Physiol Endocrinol Metab* 296(2): E333-42.
- Youn, B. S., S. I. Bang, N. Kloting, J. W. Park, N. Lee, J. E. Oh, K. B. Pi, T. H. Lee, K. Ruschke, M. Fasshauer, M. Stumvoll and M. Bluher (2009). Serum progranulin concentrations may be associated with macrophage infiltration into omental adipose tissue. *Diabetes* 58(3): 627-36.

- Yun, Z., H. L. Maecker, R. S. Johnson and A. J. Giaccia (2002). Inhibition of PPAR gamma 2 gene expression by the HIF-1-regulated gene DEC1/Stra13: a mechanism for regulation of adipogenesis by hypoxia. *Dev Cell* 2(3): 331-41.
- Zachary, I. and G. Gliko (2001). Signaling transduction mechanisms mediating biological actions of the vascular endothelial growth factor family. *Cardiovasc Res* 49(3): 568-81.
- Zagorska, A. and J. Dulak (2004). HIF-1: the knowns and unknowns of hypoxia sensing. *Acta Biochim Pol* 51(3): 563-85.
- Zeyda, M., D. Farmer, J. Todoric, O. Aszmann, M. Speiser, G. Gyori, G. J. Zlabinger and T. M. Stulnig (2007). Human adipose tissue macrophages are of an anti-inflammatory phenotype but capable of excessive pro-inflammatory mediator production. *Int J Obes (Lond)* 31(9): 1420-8.
- Zhang, H. and A. C. Issekutz (2002). Down-modulation of monocyte transendothelial migration and endothelial adhesion molecule expression by fibroblast growth factor: reversal by the anti-angiogenic agent SU6668. *Am J Pathol* 160(6): 2219-30.
- Zhang, Y., R. Proenca, M. Maffei, M. Barone, L. Leopold and J. M. Friedman (1994). Positional cloning of the mouse obese gene and its human homologue. *Nature* 372(6505): 425-32.
- Zhu, K., M. A. Amin, M. J. Kim, K. J. Katschke, Jr., C. C. Park and A. E. Koch (2003). A novel function for a glucose analog of blood group H antigen as a mediator of leukocyte-endothelial adhesion via intracellular adhesion molecule 1. *J Biol Chem* 278(24): 21869-77.
- Zimmerman, G. A., K. H. Albertine, H. J. Carveth, E. A. Gill, C. K. Grissom, J. R. Hoidal, T. Imaizumi, C. G. Maloney, T. M. McIntyre, J. R. Michael, J. F. Orme, S. M. Prescott and M. S. Topham (1999). Endothelial activation in ARDS. *Chest* 116(1 Suppl): 18S-24S.
- Zimmet, P., D. Magliano, Y. Matsuzawa, G. Alberti and J. Shaw (2005). The metabolic syndrome: a global public health problem and a new definition. *J Atheroscler Thromb* 12(6): 295-300.
- Zucht, H. D., J. Lamerz, V. Khamenia, C. Schiller, A. Appel, H. Tammen, R. Cramer and H. Selle (2005). Data mining methodology for LC-MALDI-MS based peptide profiling. *Comb Chem High Throughput Screen* 8(8): 717-23.

7 Appendix

7.1 List of abbreviations

7B2	Secretogranin V
ACTH	Adrenocorticotrophic hormone
Ad	Adipocyte
ADD1	Adipocyte determination and differentiation factor 1
AdipoR	Adiponectin receptor
ALBP	Adipocyte lipid binding protein
Ang	Angiopoietin
ANOVA	Analysis of variance
AP-1	Activator protein 1
aP2	Adipocyte fatty acid binding protein
APS	Acetyl peroxide solution
AT	Annealing temperature
ATF-2	Activating transcription factor 2
ATP	Adenosine triphosphate
BAT	Brown adipose tissue
BCA	Bicinchoninic acid
BMI	Body mass index
BrdU	5-bromo-2-deoxyuridine
BSA	Bovine serum albumine
C/EBP	CCAAT/ enhancer binding proteins
CaCl ₂	Calcium chloride
CAMs	Cellular adhesion molecules
cAMP	Cyclic adenosine monophosphate
CB1	Endocannabinoid receptor CB1
CCL14	Chemokine, CC motif, ligand 14
CCR	Chemokine (C-C motif) receptor
cDNA	Complementary DNA
CD99	Cluster of Differentiation 99
CDS	Protein coding sequence
CM	Conditioned medium
COX-2	Cyclooxygenase-2
CRP	C-reactive protein
Ctrl	Control
CVD	Cardiovascular disease
CXCR	CXC receptor
ddH ₂ O	Double Distilled water
DHAP	Dihydroxyacetone phosphate
DMEM/F12	Dulbecco's Modified Eagle Medium: nutrient mixture F-12
DMSO	Dimethyl sulfoxide
dNTP	Deoxynucleotide triphosphate
ds	Double-stranded

DTT	Dithiothreitol
ECM	Extracellular matrix
EDTA	Ethylenediaminetetraacetic acid
EGF	Epidermal growth factor
ELISA	Enzyme linked immunosorbent assays
ER	Endoplasmatic reticulum
ERK	Extracellular-regulated kinases
ESAM	Endothelial cell-selective adhesion molecule
EtBr	Ethidium bromide
Ets	E-twenty six
FA	Fatty acids
Fc	Constant region of an antibody
FCS	Fetal calf serum
FGF	Fibroblast growth factor
FOXC2	Forkhead box C2
GAPDH	Glyceraldehyde-3-phosphate dehydrogenase
GLUT	Glucose transporter
GPDH	Glycerinphosphate dehydrogenase
GRN	Progranulin
GRO- α	GRO protein, alpha
H ₂ O ₂	Hydrogen peroxide
H ₂ SO ₄	Sulfuric acid
H ₃ PO ₄	Phosphoric acid
HAEC	Human aortic endothelial cells
HCL	Hydrochloric acid
HDL	High-density lipoprotein
HDMEC	Human dermal microvascular endothelial cells
HIF-1 α	Hypoxia-inducible trasncription factor 1 alpha
hMADS	Human multipotent adipose-derived stem cells
hMADS	Human multipotent adipose-derived stem cells
HMEC-1	Human microvascular endothelial cells 1
HRP	Horeseradish peroxidase
HSL	Hormone-sensitive lipase
hTERT	Human telomerase reverse transcriptase
HUVEC	human umbilical vein endothelial cells
IBMX	Isobutylmethylxanthine
ICAM-1	Intercellular adhesion molecule 1
IFN- γ	Interferon gamma
Ig	Immunoglobulin
IGF-1	Insulin-like growth factor-1
IkB	Inhibitory kappa B
IKK	Inhibitory kappa B kinase
IL	Interleukin
IL-6R	IL-6 receptor
iNOS	Inducible nitric oxide synthase
IP-10	Interferon-inducible protein 10
JAK/STAT	Janus kinase signal transducer and activator of transcription

JAM	Junctional adhesion molecule
KCl	Kalium chloride
KRP	Krebs-Ringer phosphate buffer
LFA-1	Lymphocyte function-associated antigen 1
LPL	Lipoprotein lipase
LPS	Lipopolysaccharide
MAC-1	Macrophage antigen 1
MADCAM1	Mucosal vascular addressin cell-adhesion molecule 1
MAPK	Mitogen-activated protein kinase
MAPKK	MAPK kinases
MCP-1	Monocyte chemoattractant protein-1
Mg ₂ SO ₄	Magnesium sulfate
MgCL ₂	Magnesium chloride
MIF	Macrophage migratory inhibitory factor
MIP-1 α	Macrophage inflammatory protein 1 alpha
MT	Metallothionein
NaCl	Sodium chloride
NADH+H ⁺ /NAD ⁺	Nicotinamide adenine dinucleotide
NaF	Sodium fluoride
NaH ₂ PO ₄	Sodium dihydrogen phosphate
NaOH	Sodium hydroxide
NCEP/ATP III	National Cholesterol Education Program/Adult Treatment Panel III
NGF	Nerve growth factor
NF κ B	Nuclear factor kappa B
NGF	Nerve growth factor
NO	Nitric oxide
NP-40	Nonyl phenoxy polyethoxy ethanol
O ₂	Oxygen
Ob-R	Obese receptor or leptin receptor
p38 MAPK	p38 mitogen-activated protein kinase
PAGE	Polyacrylamide gel electrophoresis
PAI-1	Plasminogen activator inhibitor 1
PBMC	Peripheral blood mononuclear cell
PBS	Phosphate buffered saline
PC2	Proprotein convertase-2
PCR	Polymerase chain reaction
Pd	Preadipocyte
PE	Phycoerythrin
PECAM1	Platelet/endothelial-cell adhesion molecule 1
PEPCK	Phosphoenolpyruvate carboxykinase
PFA	Paraformaldehyde
PG	Prostaglandin
PGI ₂	Prostacyclin
PHD	Prolyl hydroxylase domain-containing enzymes
PI3K	Phosphoinositide 3-kinase
PIGF	Placenta growth factor
PKA	Protein kinase A

PKC	Protein kinase C
PLIN	Perilipin
PMSF	Phenylmethanesulfonyl-fluoride
PPAR	Peroxisome proliferators-activated receptor
PSGL1	P-selectin glycoprotein ligand 1
P-value	Probability value
PVDF	Polyvinylidene difluoride
pVHL	Von Hippel-Lindau tumor suppressor protein
qRT-PCR	Quantitative real-time PCR
RIA	Radioimmunoassays
RANTES	Regulated upon activation, normally T-expressed and presumably secreted or CCL5
RIN	RNA Integrity Number
RIPA buffer	Radioimmunoprecipitation assay buffer
RMR	Resting metabolic rate
ROS	Radical oxygen species
RPMI 1640	Roswell Park Memorial Institute 1640 medium
RT	Reverse transcriptase
RXR	Retinoic X receptor
SAA	Serum amyloid A
SAPK/JNK	Stress-activated phospho-kinases/c-Jun N-terminale Kinase
SCG2	Secretogranin II
SDF-1 α	Stromal cell-derived factor 1 alpha
SDS	Sodium dodecylsulfate
SE	Standard error
SGBS	Simpson-Golabi Behmel syndrome
S-phase	Synthesis phase
SRK-kinase	Sarcoma kinase
SREBP1	Sterol responsive element binding protein 1
ss	Single-stranded
SV 40	Simian-virus 40
SV-HCEC	Simian-virus-human cerebromicrovascular endothelial cells
T ₃	Triiodothyronine
TAG	Triacylglycerols
TAG	Triacylglycerides
TBE	Tris-Borate-EDTA
TBE buffer	Tris-borate-EDTA buffer
TCF	T-cell factor
TEMED	Tetramethylethylenediamine
TF	Tissue factor
TGF- β	Transforming growth factor beta
Th1 lymphocytes	T-helper 1 lymphocytes
TMB	Tetramethylbenzidine
TNF- α	Tumor necrosis factor alpha
TNFR	Tumor necrosis factor alpha receptor
tris-HCL	Tris-hydrochloride
VAV	VAV guanine nucleotide exchange factor

VCAM-1	Vascular cell adhesion molecule-1
VEGF	Vascular endothelial growth factor
VEGFR	Vascular endothelial growth factor receptor
VLA-4	Very late antigen 4
VLDL	Very low density lipoprotein
WAT	White adipose tissue
WHO	World Health Organisation
ZAG	Zinc- α 2-glycoprotein

7.2 List of figures

Figure 1	Secretory products of white adipose tissue.....	6
Figure 2	Monocyte infiltration into white adipose tissue.....	18
Figure 3	The leukocyte adhesion cascade	20
Figure 4	Overview of the peptide profiling process.	57
Figure 5	HMEC-1 cell proliferation.....	62
Figure 6	SGBS cell proliferation	63
Figure 7	SGBS cell differentiation capacity using different basal media	64
Figure 8	SGBS cell differentiation time course.....	66
Figure 9	HMEC-1 cell culture	67
Figure 10	Scheme of the cell culture strategy	68
Figure 11	Comparison of the preadipocyte and adipocyte gene expression and protein secretion of selected adipokines.....	72
Figure 12	Overview of the preadipocyte and adipocyte gene expression and protein secretion of IL-1 α , IL-1 β , TNF- α and IFN- γ	73
Figure 13	Adipokine release of SGBS cells cultured in the presence and.....	74
Figure 14	Comparison of the GPDH activity and adipokine secretion in SGBS preadipocytes at day 0 and 16 days culture period	75
Figure 15	U937 monocyte-HMEC-1 cell adhesion	77
Figure 16	Effect of TNF- α on microvascular endothelial cells.....	78
Figure 17	Effects of preadipocyte- and adipocyte-CM on microvascular endothelial cells .	80
Figure 18	Impact of concentrated SGBS-CM on monocyte-endothelial cell-cell adhesion .	82
Figure 19	Effects of TNF- α -stimulated preadipocytes and adipocytes on microvascular endothelial cell activation	84
Figure 20	Effects of hypoxia on HIF-1 α protein in preadipocytes and adipocytes and their CM on microvascular endothelial cell activation	89
Figure 21	Impact of hypoxia on adipokine mRNA expression and protein secretion of preadipocytes and adipocytes	91
Figure 22	Impact of CM from SGBS cells on microvascular endothelial cell NF κ B signalling pathway	95
Figure 23	Impact of CM from SGBS cells on microvascular endothelial cell MAPK and c-Jun signalling	96

Figure 24	Impact of CM from SGBS cells on microvascular endothelial cell STAT signalling	97
Figure 25	Blockade of signalling pathways in HMEC-1 cells by specific inhibitors.....	99
Figure 26	Expression analysis of leptin receptor b (Ob-Rb), VEGF receptor 2 (VEGFR-2), IL-6 receptor- α (IL-6R α) and gp130 in HMEC-1 cells and/or peripheral blood mononuclear cells (PBMC)	104
Figure 27	Impact of IL-6 on monocyte adhesion to and ICAM-1 cell surface protein expression of HMEC-1 cells.....	106
Figure 28	Proliferation analysis of HMEC-1 cells after treatment with recombinant proteins for VEGF ₁₆₅ , leptin and IL-6	107
Figure 29	Functional analysis of IL-6 in CM from normoxic and hypoxic SGBS cells on monocyte adhesion to and ICAM-1 cell surface expression of HMEC-1 cells..	108
Figure 30	Impact of IL-6 dependent on incubation time and concentration on the phosphorylations of STAT-1 and STAT-3 in HMEC-1 cells.....	111
Figure 31	Functional analysis of IL-6 in CM from normoxic and hypoxic SGBS cells on STAT-1 and STAT-3 phosphorylations in HMEC-1 cells.....	112
Figure 32	Impact of human primary mature adipocytes of different size on endothelial cell activation	115
Figure 33	Evaluation of the extent of cell lysis before and during supernatant sampling ..	118
Figure 34	Visualization of putative peptides identified by the peptidomic-technology	119
Figure 35	Validation of putative candidate peptides identified by the peptidomic-technology	123

7.3 List of tables

Table 1	Comparison of the components of DMEM/F12 and MCDB 131 medium	60
Table 2	Impact of hypoxia on adipokine gene expression and protein secretion of preadipocytes and adipocytes.....	90
Table 3	Overview of markers used for assessing the extent of cell lyses in CM of SGBS cells.....	118
Table 4	Overview of putative candidates identified by the peptidomic-technology	120

7.4 Chemicals, consumables and equipment

7.4.1 Chemicals

Chemicals	Company
100 bp DNA ladder, GeneRuler	Fermentas, St. Leon-Rot, Germany
5, 6 chloromethyl 2',7' dichlorodihydrofluorescein diacetate, acetyte ester (DCF)	Invitrogen, Karlsruhe, Germany
Acetic acid	Roth, Karlsruhe, Germany
Acrylamide	Roth, Karlsruhe, Germany
Agarose	Sigma-Aldrich, Munich, Germany
Alamar blue	eBioscience, Frankfurt, Germany
Amido black	Merck KGaA, Darmstadt, Germany
Amminocaproric acid	Merck KGaA, Darmstadt, Germany
Ammonium persulfate (APS)	Sigma-Aldrich, Munich, Germany
Biotin	Roth, Karlsruhe, Germany
Boric acid	Merck KGaA, Darmstadt, Germany
Bovine serum albumin (BSA)	Sigma-Aldrich, Munich, Germany
Bromphenol blue	Merck KGaA, Darmstadt, Germany
CaCl ₂	Merck KGaA, Darmstadt, Germany
Calcein green AM	Invitrogen, Karlsruhe, Germany
Chloroform	Roth, Karlsruhe, Germany
Collagenase 250 mg/U	Biochrom, Berlin, Germany
Complete, Mini; protease inhibitor cocktail tablets	Roche, Penzberg, Germany
Coomassie Brilliant Blue G-250	Merck KGaA, Darmstadt, Germany
Cortisol	Sigma-Aldrich, Munich, Germany
Dexamethasone	Sigma-Aldrich, Munich, Germany
Dihydroxyacetone phosphate (DHAP)	Sigma-Aldrich, Munich, Germany
Dimethylsulfoxide (DMSO)	Sigma-Aldrich, Munich, Germany
Dithiothreitol (DTT)	Omni Life Science, Hamburg, Germany
Donkey serum	Chemicon International, Hofheim, Germany
D-Pantothenat	Sigma-Aldrich, Munich, Germany
Dulbecco's Modified Eagle Medium: nutrient mixture F-12 (DMEM/F12)	Invitrogen, Karlsruhe, Germany
Ethanol	Roth, Karlsruhe, Germany
Ethidium bromide (EtBr)	Sigma-Aldrich, Munich, Germany
Ethylenediaminetetraacetate (EDTA)	Merck KGaA, Darmstadt, Germany
Fetal calf serum (FCS)	Invitrogen, Karlsruhe, Germany
Glycerol	Merck KGaA, Darmstadt, Germany
Glycin	Merck KGaA, Darmstadt, Germany
H ₂ O ₂	Sigma-Aldrich, Munich, Germany

H ₂ SO ₄	Serva, Heidelberg, Germany
H ₃ PO ₄	Serva, Heidelberg, Germany
Hank's buffered salt solution (HBSS)	Invitrogen, Karlsruhe, Germany
Hydrocortisone	Sigma-Aldrich, Munich, Germany
Insulin	Sigma-Aldrich, Munich, Germany
Isobutylmethylxanthine (IBMX)	Serva, Heidelberg, Germany
Isopropanol	Roth, Karlsruhe, Germany
KCl	Sigma-Aldrich, Munich, Germany
Mayer's Hematoxylin solution	Merck KGaA, Darmstadt, Germany
MCDB 131	Invitrogen, Karlsruhe, Germany
MCDB 131 without phenol red	PAN Biotech, Aidenbach, Germany
Mercaptoethanol	Sigma-Aldrich, Munich, Germany
Methanol	Roth, Karlsruhe, Germany
MgCl ₂	Merck KGaA, Darmstadt, Germany
MgSO ₄	Sigma-Aldrich, Munich, Germany
Molecular biology water	Sigma-Aldrich, Munich, Germany
NaCl	Sigma-Aldrich, Munich, Germany
NaH ₂ PO ₄	Sigma-Aldrich, Munich, Germany
NaOH	Sigma-Aldrich, Munich, Germany
Nicotinamideadeninucleotide (NADH)	Sigma-Aldrich, Munich, Germany
Nile Red	Invitrogen, Karlsruhe, Germany
N-Nitro-L- Arginine	Merck KGaA, Darmstadt, Germany
Nonyl enoxyl-polyethoxylethanol (NP40)	Sigma-Aldrich, Munich, Germany
Normal goat IgG	R&D Systems, Wiesbaden, Germany
Nuclease-free water	Sigma-Aldrich, Munich, Germany
Oil Red O	Sigma-Aldrich, Munich, Germany
Page ruler, prestained protein ladder	Fermentas, St. Leon-Rot, Germany
Paraformaldehyde (PFA)	Sigma-Aldrich, Munich, Germany
Penicillin/Streptomycin	Invitrogen, Karlsruhe, Germany
Phenyl methyl sulfonyl fluoride (PMSF)	Sigma-Aldrich, Munich, Germany
Phorbol 12-myristate 13-acetate	Sigma-Aldrich, Munich, Germany
Phosphate buffered saline (PBS) tablets	Sigma-Aldrich, Munich, Germany
PhosStop phosphatase inhibitor cocktail tablets	Roche, Penzberg, Germany
Ponceau S	Sigma-Aldrich, Munich, Germany
Precision plus protein standard	Bio-Rad, Munich, Germany
Primer and Probes	Applied Biosystems, Darmstadt, Germany
Rosiglitazone	Cayman, Ann Arbor, USA
Roswell Park Memorial Institute 1640 medium (RPMI)	Invitrogen, Karlsruhe, Germany
Sodium deoxycholate	Sigma-Aldrich, Munich, Germany
Sodium dodecyl sulfate (SDS)	Sigma-Aldrich, Munich, Germany
Tetramethylethylenediamin (TEMED)	Roth, Karlsruhe, Germany
Transferrin	Sigma-Aldrich, Munich, Germany
Triethanolaminhydrochlorid	Sigma-Aldrich, Munich, Germany

Triiodothyronine (T ₃)	Sigma-Aldrich, Munich, Germany
Trishydroxymethyl aminomethan hydrochlorid (Tris)	Roche, Penzberg, Germany
Trizol	Invitrogen, Karlsruhe, Germany
Trypsin/EDTA 10 x	PAA, Pasching, Austria
Tween 20	Sigma-Aldrich, Munich, Germany

Kits

Company

Bicinchoninic acid (BCA) Protein Assay Kit	Pierce, Rockford, USA
Bio-Plex Multiplex Cytokine Assay	Bio-Rad, Munich, Germany
Cell Proliferation ELISA, BrdU (colorimetric)	Roche, Penzberg, Germany
DNA-free	Ambion, Darmstadt, Germany
ECL Advance Western Blot Detection Kit	GE Healthcare, Munich, Germany
High Capacity cDNA reverse transcriptase kit	Applied Biosystems, Darmstadt, Germany
HotStarTaq DNA Polymerase kit	Qiagen, Hilden, Germany
Human Adiponektin Quantikine® ELISA	R&D Systems, Wiesbaden, Germany
Human IL-6 ELISA	eBioscience, San Diego, USA
Human Leptin Quantikine® ELISA	R&D Systems, Wiesbaden, Germany
Human MCP-1 ELISA	eBioscience, San Diego, USA
Human PAI-1 ELISA	Technoclone, Vienna, Austria
SYBR green PCR Master Mix	Applied Biosystems, Darmstadt, Germany
TaqMan Universal PCR Master Mix, No Amp Erase	Applied Biosystems, Darmstadt, Germany
UNG	Applied Biosystems, Darmstadt, Germany

Recombinant proteins

Company

Human interleukin-6 (IL-6)	R&D Systems, Wiesbaden, Germany
Human leptin	R&D Systems, Wiesbaden, Germany
Human tumor necrosis factor alpha (TNF- α)	R&D Systems, Wiesbaden, Germany
Human vascular endothelial growth factor (VEGF)	R&D Systems, Wiesbaden, Germany
Human epidermal growth factor (EGF)	Immunotools, Friesoythe, Germany

Antibodies

Primary antibodies	Catalog number	Company
Goat anti-human intercellular adhesion molecule 1 (ICAM-1)	BBA17	R&D Systems, Wiesbaden, Germany
Goat anti-human vascular cell adhesion molecule 1 (VCAM-1)	BBA19	R&D Systems, Wiesbaden, Germany New England Biolabs GmbH, Frankfurt, Germany
Rabbit anti-human β -actin	#4967	
Mouse anti-human hypoxia inducible factor alpha (HIF-1 α)	610958	BD Biosciences; Heidelberg, Germany

Mouse anti-human IL-6Ra	MAB227	R&D Systems, Wiesbaden, Germany New England Biolabs GmbH, Frankfurt, Germany
Rabbit anti-human phospho c-Jun (Ser 63)	#9164	New England Biolabs GmbH, Frankfurt, Germany
Rabbit anti-human phospho ERK1/2 (Thr202/Tyr204)	#9101	New England Biolabs GmbH, Frankfurt, Germany
Mouse anti-human phospho I κ B α (Ser 32/Ser 36)	#9246	New England Biolabs GmbH, Frankfurt, Germany
Rabbit anti-human phospho p38 MAPK (Thr180/Tyr182)	#9211	New England Biolabs GmbH, Frankfurt, Germany
Rabbit anti-human phospho Rel A (Ser536)	#3031	New England Biolabs GmbH, Frankfurt, Germany
Rabbit anti-human phospho SAPK/JNK (Thr183/Tyr185)	#9251	New England Biolabs GmbH, Frankfurt, Germany
Rabbit anti-human phospho STAT1 (Tyr 701)	#9167	New England Biolabs GmbH, Frankfurt, Germany
Rabbit anti-human phospho STAT3 (Tyr 705)	#9131	New England Biolabs GmbH, Frankfurt, Germany
Rabbit anti-human total c-Jun	#9165	New England Biolabs GmbH, Frankfurt, Germany
Rabbit anti-human total ERK1/2	#9102	New England Biolabs GmbH, Frankfurt, Germany
Rabbit anti-human total I κ B α	#9242	New England Biolabs GmbH, Frankfurt, Germany
Rabbit anti-human total p38 MAPK	#9212	New England Biolabs GmbH, Frankfurt, Germany
Rabbit anti-human total Rel A	#3034	New England Biolabs GmbH, Frankfurt, Germany
Rabbit anti-human total SAPK/JNK	#9252	New England Biolabs GmbH, Frankfurt, Germany
Rabbit anti-human total STAT1	#9175	New England Biolabs GmbH, Frankfurt, Germany
Rabbit anti-human total STAT3	#4904	New England Biolabs GmbH, Frankfurt, Germany

Secondary antibodies	Catalog number	Company
Anti-mouse IgG, horseradish peroxidase (HRP)-linked antibody	#7076	New England Biolabs
Anti-rabbit IgG, HRP-linked antibody	#7074	New England Biolabs
Donkey anti-goat IgG, HRP-linked antibody	705-035-003	Dianova, Hamburg, Germany

Antibodies used for inhibitor experiments

	Company
Enbrel®, soluble TNF- α receptor antibody	Pfizer Pharma, Berlin, Germany
Monoclonal anti human IL-6 antibody	MAB2061 R&D Systems, Wiesbaden, Germany
Mouse IgG _{2B} isotype control	MAB004 R&D Systems, Wiesbaden, Germany

Inhibitors

Company

JNK Inhibitor II	Merck KGaA, Darmstadt, Germany
SB203580	Merck KGaA, Darmstadt, Germany
JAC Inhibitor I	Merck KGaA, Darmstadt, Germany
PD98059	Merck KGaA, Darmstadt, Germany

Primer and Probes

Primer for RT-PCR

Primer pairs for RT-PCR were produced by Eurofins MWG, Ebersberg, Germany

Human target gene	Primer	T _A (°C)	Sequence
β-actin	forward	57	5' GTGGCATCCACGAAACTACCTT 3'
β-actin	reverse		5' GGACTCGTCATACTCCTGCTT 3'
gp130	forward	60	5' AGCCCAATCCGCCACATAA 3'
gp130	reverse		5' TCTTCCTTCATACAGCGAATCCTA 3'
IL-6Rα	forward	60	5' CAGGAGGAGTTCGGGCAAGG 3'
IL-6Rα	reverse		5' CCCAAAGAGTACGGCGGATG 3'
Ob-Rb	forward	55	5' AGGACGAAAGCCAGAGACAA 3'
Ob-Rb	reverse		5' AAATGCCTGGGCCTCTATCT 3'
VEGFR-2	forward	55	5' GGAAATCATTATTCTAGTAGGCACGACG 3'
VEGFR-2	reverse		5' CCTGTGGATACTTTTCGCGATG 3'

TaqMan® Primer and Probes

TaqMan® Primer and Probes were obtained from Applied Biosystems; Darmstadt, Germany

Human target gene	Primer/Probe product number
18S	Hs99999901_sl
GAPDH	Hs99999905_ml
Adiponectin	Hs00605917_ml
IL-1 α	Hs00174092_ml
IL-1 β	Hs00174097_ml
IL-4	Hs00174122_ml
IL-6	Hs00174131_ml
IL-8	Hs00174103_ml
Leptin	Hs00174877_ml
MCP-1	Hs00234140_ml
PAI-1	Hs_00167155_ml
RANTES	Hs00174575_ml
SDF-1 α	Hs00171022_ml
TNF- α	Hs99999043_ml
VEGF	Hs_00173626_ml

Primer for qRT-PCRs with SYBR® Green

Primer pairs for qRT-PCRs with SYBR® Green were produced by Eurofins MWG, Ebersberg, Germany

Human target gene	Primer	T _A (°C)	Sequence
Granulin	forward	60	5' CAACGCCACCTGCTGCTCCG 3'
Granulin	reverse		5' GCTTAGTGAGGAGGTCCGTGGTAG 3'
Secretogranin II	forward	60	5' GATCAGTGGAACCGGAGCG 3'
Secretogranin II	reverse		5' TCCCAGCACGACCAGGTGT 3'
Secretogranin V	forward	60	5' CTCCAAATCCCTGTCCTGTTG 3'
Secretogranin V	reverse		5' ACTCTCGACTGAACTCTGCAGTGT 3'

7.4.2 Consumables

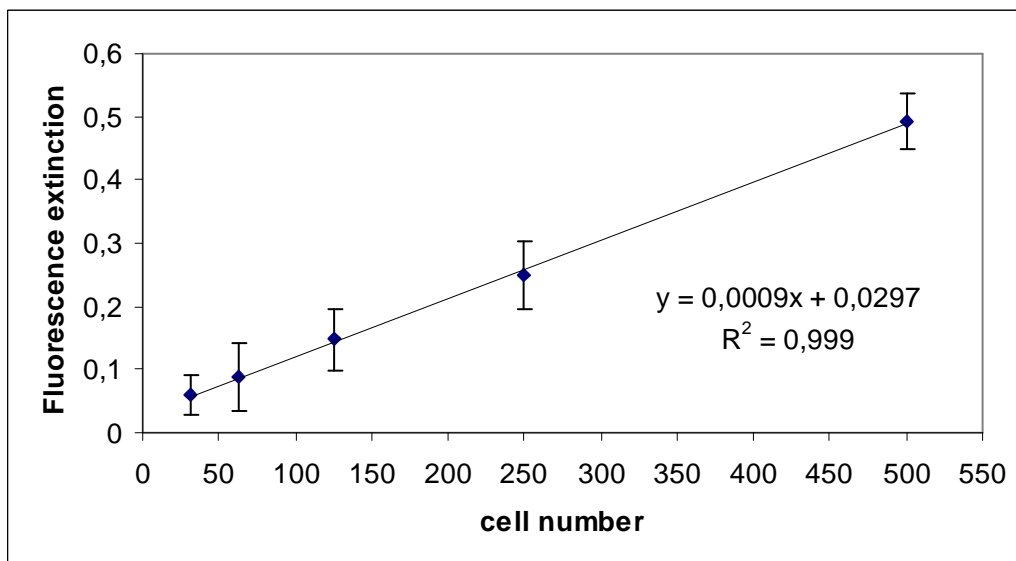
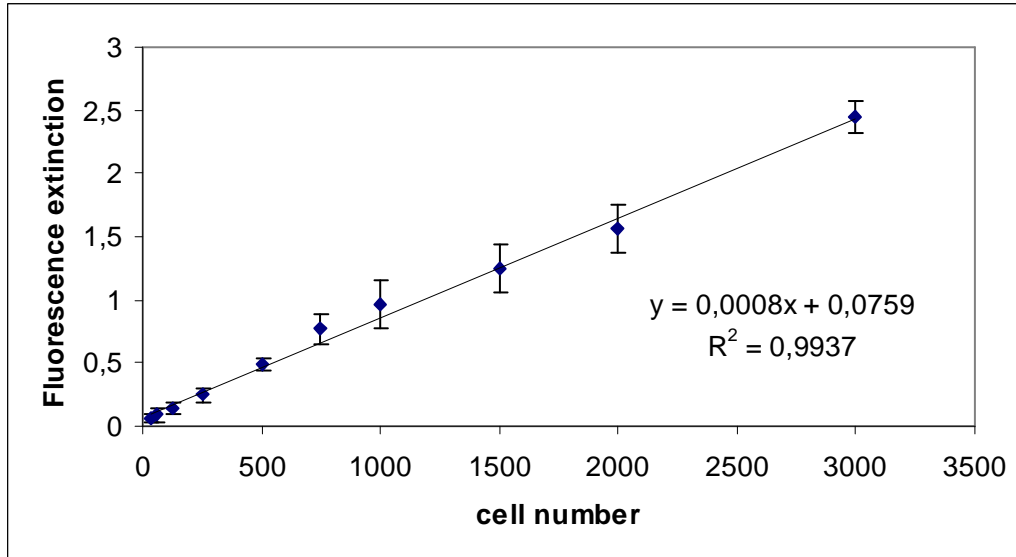
Consumables	Company
15 ml and 50 ml tubes	BD Biosciences Clontech, Heidelberg, Germany
ABsolute QPCR Seal	AB Gene, Hamburg, Germany
Amicon Ultra-15 Centrifugal Filter Units 5kDA	Millipore, Schwalbach, Germany
Baktolin wash	Bode Chemie, Hamburg, Germany
Barrycidal 36	Biohit Deutschland GmbH, Rosbach, Germany
Cell culture plates, 96-well, 6-well, 6 cm	BD Biosciences Clontech, Heidelberg, Germany
Cell Scraper	TPP, Trasadingen, Switzerland
Chromatography paper, 1mm	Whatman, Dassel, Germany
EPTwin PCR plate 96 skirted	Eppendorf, Hamburg, Germany
Gloves S, gentle skin classic	Meditrade, Kiefersfelden, Germany
Gloves S, safeskin, purple nitrile-xtra	Kimberly Clark, Koblenz-Rheinhafen, Germany
Hybond P PVDF transfer membrane	GE Healthcare, Munich, Germany
Hyperfilm ECL chemiluminescence film	GE Healthcare, Munich, Germany
Hypodermic needles	Braun, Melsungen, Germany
Korsolex Plus	Bode Chemie, Hamburg, Germany
Pasteur pipets	Corning, Kaiserslautern, Germany
Pipet tips	Brand, Wertheim, Germany
Pipet tips	Gilson, Limburg-Offheim, Germany
Pipet tips, filtered	Biozym Scientific GmbH, Hess. Oldendorf, Germany
Pipet tips, filtered	Molecular BioProducts, Fisher Scientific GmbH, Schwerte, Germany
Plastic disposable serological pipets	Corning, Kaiserslautern, Germany
Reaction tubes, 0.2 ml, 0.5 ml, 1.5 ml, 2.0 ml	Eppendorf, Hamburg, Germany
Reaction tubes, 1.5 ml, 2.0 ml	Zefa, Harthausen, Germany
Single use syringe filter, 0.2 µm	Sartorius AG, Goettingen, Germany
Sterile insulin syringe, micro-fine plus (29 G)	BD Biosciences Clontech, Heidelberg, Germany
Sterilium	Bode Chemie, Hamburg, Germany
Sterivex sterile filter unit 0.22 µm	Millipore, Schwalbach, Germany
Syringes	BD Biosciences Clontech, Heidelberg, Germany
Taktosan	Stockhausen, Krefeld, Germany

7.4.3 Equipment

Equipment	Company
Biophotometer	Eppendorf, Hamburg, Germany
Bio-Plex Suspension array system	Bio-Rad, Munich, Germany
Centrifuge 5415R, 5430 and 5810	Eppendorf, Hamburg, Germany
CO2-Incubator CB210	Binder, Tuttlingen, Germany
CO2-Incubator HERAcell 150	Thermo Scientific, Schwerte, Germany
Dewar flasks	Nalgene, Hereford, England
Fastblot, semi-dry blotting unit	Biometra, Goettingen, Germany
Fluorescence microscope DMIL and camera DC300	Leica Microsystems, Wetzlar, Germany
Freezer, -86°C ULT	Thermo Scientific, Schwerte, Germany
Freezer, HERAfreeze	Thermo Scientific, Schwerte, Germany
Freezer, VIP Series -86°C	Sanyo, Munich, Germany
Glass ware	Schott GmbH, Mainz, Germany
Heidolph Polymax wave platform shaker 1040	Schuett, Göttingen, Germany
Horizontal electrophoresis units	Biorad, Munich, Germany
Hypoxia workstation, InVivo O2 400	IUL Instruments, Koenigswinter, Germany
Inolab pH meter	WTW, Weilheim, Germany
Laboratory balance	Denver Instruments, Goettingen, Germany
Mastercycler gradient	Eppendorf, Hamburg, Germany
Mastercycler® ep realplex	Eppendorf, Hamburg, Germany
Microscope, Axiovert 40C	Zeiss, Jena, Germany
Mini centrifuge, model GMC-060	LMS Consult, Brigachtal, Germany
Minigel-Twin, vertical electrophoresis units	Biometra, Goettingen, Germany
MultiScreen Separations System 96-well suction	Millipore, Schwalbach, Germany
Neubauer Chamber	Brand, Wertheim, Germany
Pipettes	Eppendorf, Hamburg, Germany
Pipetting Aid	Gilson, Limburg-Offheim, Germany
Power Pack P25T	Biometra, Goettingen, Germany
Scissors, forceps	VWR, Darmstadt, Germany
Spectrophotometer with cuvette holder, DU 800	Beckman Coulter, Krefeld, Germany
Sterile workbench, HERAsafe	Thermo Scientific, Schwerte, Germany
Tecan Safire multiwell photo- and fluorometer	Tecan, Crailsheim, Germany
Thermomixer confort for 1.5 ml and 2.0 ml tubes	Eppendorf, Hamburg, Germany
Transferpette 12 multichannel pipettes	Brand, Wertheim, Germany
Typhoon TRIO+, variable mode imager	GE Healthcare, Munich, Germany
Ultrasound homogenator Sonopuls HD 2070	Bandelin, Berlin, Germany
UV transilluminator and camera, INTAS UV Systeme	Intas Science Imaging Instruments, Göttingen, Germany
Vacu hand control	Vacuubrand, Wertheim, Germany
Vacuum pump unit, PC 2004 Vario	Vacuubrand, Wertheim, Germany
Varioskan multiwell photo- and fluorometer	Thermo Scientific, Schwerte, Germany
Vortex gene 2	Scientific Industries, Bohemia, USA
Water bath with heating circulator TW20	Julabo, Seelbach, Germany

7.5 Monocyte-endothelial cell-cell adhesion assay

7.5.1 Quantitation of *Calcein green AM* labelled U937 cells



U937 cells were labelled with *Calcein green AM*, counted and diluted to the indicated cell numbers and transferred as 100 μ l cell suspension to the designated wells of a 96-well cell culture plate. After cell lysis and centrifugation the fluorescence signal was detected at 494 and 517 nm using the Varioskan multiwell photo- and fluorometer (Thermo Scientific; n=3).

7.5.2 Example for the analysis of the monocyte-endothelial cell-cell adhesion assay data

An example for the analysis of the monocyte-endothelial cell-cell adhesion assay data is given below. HMEC-1 cells were treated with control MCDB 131 medium, preadipocyte-CM (Pd-CM), adipocyte-CM (Ad-CM) and TNF- α as positive control. Next, the monocyte-endothelial cell-cell adhesion assay was carried out as described in chapter 2.1.6. The fluorescence signal was detected at 494 and 517 nm using the Varioskan multiwell photo- and fluorometer (Thermo Scientific)

Raw data (optical density) of one single experiment with at least four replicates:

Control	Pd16-CM	Ad16-CM	TNF alpha 25 ng/ml	Blank
0,3325	0,4246	0,3753	1,509	0,09424
0,227	0,5197	0,3217	1,27	0,08868
0,3507	0,4436	0,3021	1,349	
0,359	0,458	0,3643	1,104	
	0,4291	0,3157	1,161	
	0,509	0,4352	0,9523	

Mean of the blank:	
	0,09424
	0,08868
Mean	0,09146

Raw data minus mean of the blank:			
Control	Pd16-CM	Ad16-CM	TNF alpha 25 ng/ml
0,24104	0,33314	0,28384	1,41754
0,13554	0,42824	0,23024	1,17854
0,25924	0,35214	0,21064	1,25754
0,26754	0,36654	0,27284	1,01254
	0,33764	0,22424	1,06954
	0,41754	0,34374	0,86084

Mean of the replicates of the control:	
	Control
	0,24104
	0,13554
	0,25924
	0,26754
Mean	0,22584

The mean value of the control replicates was considered as 1 in order to obtain the relative values in fold for the other groups for comparison. $0,22584 = 1$

Relative values:			
Control	Pd16-CM	Ad16-CM	TNF alpha 25 ng/ml
1	1,47511513	1,25681899	6,2767446
	1,89620971	1,01948282	5,21847326
	1,55924548	0,93269571	5,56827843
	1,62300744	1,20811194	4,4834396
	1,49504074	0,99291534	4,73583068
	1,84883103	1,52205101	3,81172512

Relative mean values of all replicates:			
Control	Pd16-CM	Ad16-CM	TNF alpha 25 ng/ml
1	1,47511513	1,25681899	6,2767446
	1,89620971	1,01948282	5,21847326
	1,55924548	0,93269571	5,56827843
	1,62300744	1,20811194	4,4834396
	1,49504074	0,99291534	4,73583068
	1,84883103	1,52205101	3,81172512
Mean	1	1,64957492	1,15534597
			5,01574861

In order to combine the results of independent experiments for analysis, the relative mean values of all replicates of each experiment were used to calculate the final mean values and standard deviations.

	Treatment	Relative mean values of all replicates		Treatment	Relative mean values of all replicates
Independent experiment 1	Control	1,00	Independent experiment 3	Control	1,00
	Pd16-CM	1,65		Pd16-CM	1,47
	Ad16-CM	1,16		Ad16-CM	1,18
	TNF alpha	5,02		TNF alpha	5,00
Independent experiment 2	Control	1,00	Independent experiment 4	Control	1,00
	Pd16-CM	1,82		Pd16-CM	1,82
	Ad16-CM	1,20		Ad16-CM	1,20
	TNF alpha	8,08		TNF alpha	3,74

	Control	Pd16-CM	Ad16-CM	TNF alpha	
Experiment 1	1,00	1,65	1,16	5,02	
Experiment 2	1,00	1,82	1,20	8,08	
Experiment 3	1,00	1,47	1,18	5,00	
Experiment 4	1,00	1,82	1,20	3,74	
	1	1,69	1,18	5,46	Mean
		0,17	0,02	1,85	Standard deviation

7.6 Acknowledgements

I like to thank the following people for their assistance in completing this work:

Prof. Dr. Hans Hauner¹ for providing the required resources and discussion during the practical and written part of this thesis. Also, for giving me the possibility to do a variety of scientific activities and advanced trainings having not always been directly associated with the thesis.

Dr. Bernhard L. Bader¹ for unlimited supervision, discussion, advice, reliability and patience during the practical and written part of the thesis.

Prof. Dr. Agnes Görlach² for discussion, support and the opportunity to perform experiments in her laboratory over a period of four years.

Talija Djordjevic² and Siham Bel Aiba² for advice, valuable discussion and teaching me the handling of HMEC-1 cells.

Gabriele Tiller¹ and Thomas Skurk¹ for advice, valuable discussion and teaching me the preparation of human primary preadipocytes and adipocytes.

Elisabeth Seebach for practical support during her Bachelor thesis.

Lissi Hofmair¹ for helping me with Western blots during my pregnancy.

Patricia Dietl¹ for the kind donation of RNA and protein from peripheral blood mononuclear cells.

Christoph Dahlhoff⁴ for valuable discussion, technical advice and support, especially during my pregnancy.

Tobias Ludwig¹ for technical support during my pregnancy and providing me during the written part of the thesis with literature.

Lydia Gerke¹, Manuela Hubersberger¹, Jana Kolew¹, Silke Ecklebe¹, Nico Gebhardt³, Ingrid Schmöllner³ and Kerstin Diemer² for their practical support and advice.

Christiane Vollhardt¹ for valuable discussion and motivation.

Eva-Maria Sedlmeier¹ for help and support.

Christoph Hoffmann⁵ for teaching me the EMSA technique.

Simone Matthä¹ for the kind donation of RNA and protein from HepG2 cells.

Dr. Helmut Laumen¹, Dr. Alexander Tups, Dr. Michael Helwig⁵, Florian Bolze⁵ and Dr. Tobias Fromme⁵, Prof. Dr. Dirk Haller³, Prof. Dr. Martin Klingenspor⁵, Prof. Dr. Michael Ristow⁶ and Prof. Dr. Paul Trayhurn⁷ for discussion.

Prof. Dr. Hannelore Daniel⁴ for use of facilities at her department and discussion.

Bill Taylor for personal support, discussion and correcting the thesis.

Sylvie Heinrich¹ for her assistance with administrative work.

My husband Andi for continued unlimited personal support, advice, patience and motivation.

Mum and dad, my parents-in-law and friends for their personal support and advice.

The Eli Lilly International Foundation and Else Kröner-Fresenius-Stiftung, Bad Homburg, for funding me and the project.

¹Else Kröner-Fresenius-Center for Nutritional Medicine, Research Center for Nutrition and Food Science, Nutritional Medicine Unit, Technische Universität München, Freising/Weihenstephan, Germany;

²Experimental Pediatric Cardiology, Department of Pediatric Cardiology and Congenital Heart Disease, German Heart-Center Munich, Technische Universität München, Munich, Germany;

³Research Center for Nutrition and Food Science, Biofunctionality Unit, Technische Universität München, Freising/Weihenstephan, Germany;

⁴Else Kröner-Fresenius-Center for Nutritional Medicine, Research Center for Nutrition and Food Science, Molecular Nutrition Unit, Technische Universität München, Freising/Weihenstephan, Germany;

⁵Research Center for Nutrition and Food Science, Molecular Nutrition Medicine, Technische Universität München, Freising/Weihenstephan, Germany;

⁶Institute of Nutrition, Department of Human Nutrition, University of Jena, Jena, Germany;

⁷Obesity Biology Research Unit, School of Clinical Sciences, University of Liverpool, Liverpool, UK.

7.7 Curriculum Vitae

Name	Isabelle Mack geb. Eisele
Geburtsdatum	23.05.1980
Geburtsort	Fribourg (Schweiz)
Staatsangehörigkeit	Deutsch
E-mail	isabelle.mack@wzw.tum.de isa.mack@gmx.net

Ausbildung

09.2005 – 08.2010	Doktorarbeit zur Erlangung des Dr. rer. nat. am Lehrstuhl für Ernährungsmedizin der Technischen Universität München, Freising/Weihenstephan
05.2004 – 08.2004	Laborpraktikum in der Abteilung für Klinische Ernährung am Deutschen Institut für Ernährungsforschung (DifE), Potsdam-Rehbrücke
10.1999 – 06.2004	Studium der Ernährungswissenschaft an der Universität Potsdam, Potsdam Abschluss: Diplom Ernährungswissenschaftlerin Notendurchschnitt: 1.1, Note der Diplomarbeit: 1.0. Die Diplomarbeit wurde an der University of Liverpool, Liverpool Centre for Nutritional Genomics, Liverpool, England durchgeführt. Titel: “Adipokine gene expression in companion animals”
01.1991 – 06.1999	Wilhelmsgymnasium, Kassel, Deutschland Abschluss: Allgemeine Hochschulreife, Notendurchschnitt: 1.8.
01.1988 – 01.1991	Deutsche Internationale Schule Johannesburg, Johannesburg, Südafrika
09.1986 – 09.1987	Textorschule Frankfurt, Frankfurt am Main, Deutschland

Auszeichnungen

2008	Posterpreis mit dem Titel: “Analyse der molekularen und zellulären Interaktionen zwischen Adipozyten und Endothelzellen“ verliehen durch die Deutsche Adipositasgesellschaft
------	--

Stipendien

2003	Reisestipendium von der European Foundation for the Study of Diabetes/ Merck & Co. Inc
------	---

Publikationen

Wissenschaftliche
Artikel

Mack I, BelAiba RS, Djordjevic T, Gorlach A, Hauner H and Bader BL: Functional analyses reveal the greater potency of preadipocytes compared with adipocytes as endothelial cell activator under normoxia, hypoxia and TNF alpha exposure. *Am J Physiol Endocrinol Metab* 297(3): E735-748, 2009

Skurk T, **Mack I**, Kempf K, Kolb K, Hauner H, Herder C: Expression and secretion of RANTES (CCL5) in human adipocytes in response to immunological stimuli and hypoxia. *Horm Metab Res* 41(3): 183-189, 2009

Eisele I, Wood IS, German AJ, Hunter L, Trayhurn P: Adipokine gene expression in dog adipose tissues and dog white adipocytes differentiated in primary culture. *Horm Metab Res* 37(8): 474-481, 2005

Wissenschaftliche
Übersichtsartikel

Mack I, Hauner H: Low Carb - Kohlenhydratarme Kostformen unter die Lupe genommen. *Ernährungsumschau* 12: 720-726, 2007

Eisele I, Hauner H: Gewichtsabnahme ohne Jojo-Effekt ist keine Utopie. *Ärztzeitung, Forschung und Praxis* 25: 8-12, 2006

Publizierte
Zusammenfassungen

Mack I, Bader BL, Gorlach A, Hauner H: Analysis of the molecular and cellular cross-talk between preadipocytes/adipocytes and microvascular endothelial cells. *International Journal of Obesity* 32: 42, 2008

Mack I, Bader BL, Gorlach A, Hauner H: Einfluss von Normoxie und Hypoxie auf humane Präadipozyten und Adipozyten mit Folgewirkungen für mikrovaskuläre Endothelzellen. *Diabetologie und Stoffwechsel, Supplement* 3: 47, 2008

Mack I, Bader BL, Hauner H: Analyse der molekularen und zellulären Interaktionen zwischen Adipozyten und Endothelzellen. *Aktuelle Ernährungsmedizin* 32: 269, 2007

Mack I, Bader BL, Gorlach A, Hauner H: Analysis of the molecular and cellular cross-talk between adipocytes and endothelial cells. *Fourth European Nutrigenomics Conference, abstract collection* 4: 70, 2007

Eisele I, Wood IS, German A, Hunter L, Trayhurn P: Expression of adipokine genes in dog adipose tissue. *International Journal of Obesity* 28: 93, 2004

Genbankdateneinträge

Eisele I, Wood I.S, German A, Hunter L, and Trayhurn P:
- Felis catus partial mRNA for hormone sensitive lipase
GenBank AJ639862 (19-APR-2004)
- Felis catus partial mRNA for adiponectin
GenBank AJ639861 (19-APR-2004)
- Felis catus partial mRNA for nerve growth factor beta
Genbank AJ639860 (19-APR-2004)
- Canis familiaris partial mRNA for nerve growth factor beta
GenBank AJ626845 (04-FEB-2004)